

# Worldline instantons

and the Sauter-Schwinger effect.



PhD Thesis  
Christian Schneider



# Worldline instantons

and the Sauter-Schwinger effect.

Dissertation  
presented to the

Faculty of Physics,  
Universität Duisburg-Essen

to obtain the degree of  
*Dr. rer. nat.*

by

Christian Schneider  
from Duisburg,

September 2018.

Defended on 21 February 2019,

refereed by

Prof. Dr. Ralf Schützhold,  
Prof. Dr. Holger Gies, and  
Prof. Dr. Jürgen König.

Produced using L<sup>A</sup>T<sub>E</sub>X 2<sub>ε</sub>, biber and the Xe<sub>L</sub>A<sub>T</sub>E<sub>X</sub> engine. Based on the KOMA-Script book class. Main text and math set in Robert Slimbach's *Minion Pro*, headings and captions set in ParaType's *PT Sans*, with advanced typographic features provided by the fontspec package. Computer code set in Paul D. Hunt's *Source Code Pro*. Title and chapter numbers set in Julieta Ulanovsky's *Montserrat*. Cover and most figures created using the *TikZ* package.

©2018 Christian Schneider

Printed by:  
BoD – Books on Demand, Norderstedt

# Contents

Abstract . . . . .	v
List of publications . . . . .	vii
Acknowledgments . . . . .	ix
<b>I. Background and methods</b>	<b>1</b>
<b>1. History and classic results</b>	<b>3</b>
1.1. Early quantum mechanics . . . . .	3
1.2. Spin and special relativity . . . . .	5
1.3. Dirac's quantum theory of the electron . . . . .	6
1.4. Sauter-Schwinger pair production . . . . .	8
1.5. Worldline instantons . . . . .	9
<b>2. Mathematical preliminaries</b>	<b>11</b>
2.1. Conventions and notation . . . . .	11
2.2. Quantum mechanical path integral . . . . .	13
2.3. Gaussian integrals . . . . .	16
2.4. Laplace's method . . . . .	17
2.5. Analytic continuation . . . . .	19
2.6. Zero- and negative modes . . . . .	20
2.7. Determinants of differential operators . . . . .	23
2.8. Gelfand-Yaglom formula . . . . .	24
<b>3. Riccati formalism</b>	<b>27</b>
3.1. Introduction . . . . .	27
3.2. Derivation of the Riccati formalism . . . . .	27
3.3. Numerical evaluation . . . . .	29
<b>4. Worldline instanton method</b>	<b>33</b>
4.1. Physical model . . . . .	33
4.2. Worldline path integral . . . . .	40
4.3. Saddle point approximation . . . . .	47
4.4. Discretized worldline instantons . . . . .	49
4.5. Prefactor in the continuous case . . . . .	51
<b>5. Numerical instanton finding</b>	<b>55</b>
5.1. Shooting method . . . . .	55
5.2. Discrete instanton finding . . . . .	56
5.3. Numerical continuation . . . . .	57

<b>II. Applications</b>	<b>61</b>
<b>6. Example fields</b>	<b>63</b>
6.1. Constant electric fields . . . . .	63
6.2. One-dimensional field inhomogeneities . . . . .	68
6.3. Multidimensional field inhomogeneities . . . . .	77
6.4. Transversal field dependences . . . . .	81
6.5. Spin and magnetic effects . . . . .	82
<b>7. Dynamically assisted Sauter-Schwinger effect</b>	<b>87</b>
7.1. Introduction . . . . .	87
7.2. Inhomogeneous background field . . . . .	88
7.3. Pulse shape dependence . . . . .	92
7.4. Momentum spectra and dominant order . . . . .	95
7.5. Assistance by a plane wave . . . . .	98
<b>8. Code user's manual</b>	<b>103</b>
8.1. Riccati equation . . . . .	103
8.2. Discrete worldline instantons . . . . .	106
<b>III. Conclusions</b>	<b>111</b>
<b>IV. Appendix</b>	<b>117</b>
<b>A. Source code listings</b>	<b>119</b>
A.1. Riccati equation . . . . .	119
A.2. Discrete worldline instantons . . . . .	123
<b>Bibliography</b>	<b>131</b>

## Abstract

The Sauter-Schwinger effect, that is, electron-positron pair creation from the vacuum due to a strong electric field, was predicted only shortly after the foundations of quantum mechanics were first laid out. But even today, many years later, although the existence of the effect follows straightforwardly from a relativistic quantum description of the electron and can be motivated quite intuitively by a tunneling picture, our understanding is far from complete.

First of all, it has not yet been experimentally verified due to the extremely large field strength required to obtain a detectable pair creation probability. A theoretical treatment is difficult as well, since it is a nonperturbative effect so the usual toolkit of perturbation theory does not apply. In general, to calculate the pair production probability for a non-static or spatially inhomogeneous electric field, we need to solve the Dirac equation exactly for that background field.

Only recently progress has been made both in terms of computational methods, numerical and analytical, and in terms of insight on how more complicated field profiles affect the pair production rate. A method well suited to study the Sauter-Schwinger effect in inhomogeneous fields is the *worldline instanton* method. Worldline instantons provide a semiclassical approximation that is valid in many field configurations of interest. Although the computational problem of the worldline instanton method can be stated very succinctly for arbitrary background fields, actually *finding* instantons is still rather complicated for general fields.

This thesis has three main goals: 1. to give a complete, self-contained derivation of the worldline instanton method suitable for a reader new to the topic, 2. to introduce a completely general numerical scheme to robustly find instantons in arbitrary background fields, and 3. to build some intuition by analytically calculating results for several fields and using the numerical method to show how they qualitatively carry over to more complex and realistic scenarios that are inaccessible to other approaches. We will especially focus on the dynamically assisted Sauter-Schwinger effect here.

Apart from the worldline instanton method this thesis also introduces a scheme to numerically integrate the Riccati equation, an exact formulation of the pair production problem, with high precision, to obtain exact (up to tunable numerical errors) results for time dependent fields.

## Zusammenfassung

Der Sauter-Schwinger-Effekt, also Elektron-Positron-Paarerzeugung aus dem Vakuum durch ein starkes elektrisches Feld, wurde bereits kurz nach der Begründung der Quantenmechanik vorhergesagt. Aber selbst heute, viele Jahre später, und obwohl das Auftreten des Effekts unmittelbar aus einer relativistischen Beschreibung des Elektrons folgt und recht intuitiv durch ein Tunnelbild motiviert werden kann, ist unser Verständnis noch unvollständig.

Zunächst einmal wurde der Effekt noch nicht experimentell bestätigt, aufgrund der extrem hohen Feldstärke die nötig ist um eine beobachtbare Teilchenerzeugungswahrscheinlichkeit zu erhalten. Auch eine theoretische Beschreibung ist schwierig, da es sich um einen nichtperturbativen Effekt handelt und die üblichen Werkzeuge der Störungsrechnung nicht anwendbar sind. Im Allgemeinen müssen exakte Lösungen der Dirac-Gleichung in einem Hintergrundfeld gefunden werden, um die Paarerzeugungswahrscheinlichkeit durch dieses Feld zu berechnen.

Erst vor vergleichsweise kurzer Zeit gab es Fortschritte, sowohl bei numerischen und analytischen Methoden, als auch beim Verständnis wie sich kompliziertere Feldprofile auf die Paarerzeugungsrate auswirken. Eine Methode die sich gut zur Untersuchung des Sauter-Schwinger-Effekts eignet ist die *Worldline-Instanton*-Methode. Worldline-Instantonen liefern eine semiklassische Näherung, die in vielen relevanten Feldkonfigurationen anwendbar ist. Auch wenn die in der Worldline-Instanton-Methode letztendlich zu berechnenden Ausdrücke für beliebige Hintergrundfelder einfach formuliert werden können, ist es immer noch recht kompliziert die nötigen Instantonen zu *finden*.

Diese Arbeit hat drei Hauptziele: 1. Eine vollständige, in sich geschlossene Herleitung der Worldline-Instanton-Methode zu geben, die für einen Einsteiger des Themas geeignet ist, 2. einen vollständig allgemeinen numerischen Ansatz einzuführen, zuverlässig Instantonen in beliebigen Hintergrundfeldern zu finden und 3. durch analytische Ergebnisse für einige Felder Intuition zu entwickeln und mit der numerischen Methode zu zeigen wie diese Ergebnisse qualitativ auch in komplexeren, realistischen Szenarios wiederzufinden sind, die anderen Methoden nicht zugänglich sind. Hierbei werden wir uns vor allem auf den dynamisch assistierten Sauter-Schwinger-Effekt konzentrieren.

Neben der Worldline-Instanton-Methode beschreibt die Arbeit noch einen Ansatz die Riccati-Gleichung, eine exakte Formulierung des Paarerzeugungsproblems, mit hoher Genauigkeit numerisch zu integrieren, um exakte (bis auf anpassbare numerische Fehler) Ergebnisse für zeitabhängige Felder zu erhalten.

## List of publications

These are the publications that resulted from the research performed during the preparation of this PhD thesis, and the contribution the thesis author has made to each. In all cases every author gave their input on the final text, this will not be noted explicitly.

**[Lin+15]** Malte F. Linder, Christian Schneider, Joachim Sicking, Nikodem Szpak, and Ralf Schützhold. “Pulse shape dependence in the dynamically assisted Sauter-Schwinger effect.” In: *Physical Review D* 92 (Oct. 2015), p. 085009.

*Contributions:* Sections describing and applying the worldline instanton method.

**[SS16a]** Christian Schneider and Ralf Schützhold. “Dynamically assisted Sauter-Schwinger effect in inhomogeneous electric fields.” In: *Journal of High Energy Physics* 2016.2 (2016).

*Contributions:* All analytical and numerical calculations.

**[SS16b]** Christian Schneider and Ralf Schützhold. “Prefactor in the dynamically assisted Sauter-Schwinger effect.” In: *Phys. Rev. D* 94 (Oct. 2016), p. 085015.

*Contributions:* All analytical and numerical calculations.

**[Tor+17]** Greger Torgrimsson, Christian Schneider, Johannes Oertel, and Ralf Schützhold. “Dynamically assisted Sauter-Schwinger effect — non-perturbative versus perturbative aspects.” In: *Journal of High Energy Physics* 2017.6 (2017).

*Contributions:* Numerical solutions of the Riccati equation.

**[TSS18]** Greger Torgrimsson, Christian Schneider, and Ralf Schützhold. “Sauter-Schwinger pair creation dynamically assisted by a plane wave.” In: *Physical Review D* 97 (2018), p. 096004.

*Contributions:* Section on worldline instantons, numerical calculations.

**[STS19]** Christian Schneider, Greger Torgrimsson, and Ralf Schützhold. “Discrete worldline instantons.” In: *Physical Review D* 98 (2019), p. 085009.

*Contributions:* Development of the discrete formalism and generation of numerical data. The regularization approach and input on many aspects provided by GT.

Sections of the thesis that take content from one of these publications will be marked with the citation key.



## Acknowledgments

I want to express my gratitude to all the people who made this thesis possible and the whole process a thoroughly enjoyable experience.

First of all I want to thank my advisor Ralf Schützhold for giving me the opportunity to work on this topic and providing guidance along the way. Without his physical intuition and at times incredible accuracy in predicting results not yet found I surely would not have seen the paths to reach them.

For his invaluable scientific input I would like to thank Dr. Greger Torgrimson, who never failed to find the mistakes I made, and also how to correct them.

Special thanks go to Friedemann Queisser, Malte Linder and Nicolai ten Brinke for the fun we had both on- and off-topic, and especially Johannes Oertel for obsessing with me over software, programming and typographic details more than any sane person ever should.

I would also like to thank all other group members, past and present, for the wonderful atmosphere and uncountable pleasant discussions, no matter if scientific, historic, linguistic, or of entirely different nature. Lunch and coffee would have been severely lacking without all of you.

This thesis would not have been possible without the lasting support of my family and friends, thanks for everything!

Last, and very far from least, I want to thank my wife for her patience and un-failing support in all matters during this time.



## **Part I.**

# **Background and methods**



## 1

## History and classic results

*This first chapter will briefly retrace the steps that have led from the beginnings of quantum mechanics to the prediction of the Sauter-Schwinger effect and laid the theoretical groundwork for all further calculations.*

### 1.1. Early quantum mechanics

Quantum theory, in the sense that some physical quantities are restricted to integer multiples of some smallest quantity, first emerged in 1900 with Max Planck's law of radiation [Pla00b]. To derive the spectral properties of a black body of given temperature, he proposed a thermodynamic approach of distributing a fixed amount of energy over a large number of monochromatic oscillators in the radiating body. The relative amount of energy given to oscillators of a specific frequency would follow from combinatorics, by maximizing what Boltzmann called *Complexion*, essentially the number of microstates of equal energy. Classically, energy is continuous, so there are infinitely many ways to distribute it over the oscillators. To solve this problem, Planck simply assumed that each oscillator of frequency  $\nu$  could only hold energy in multiples of  $h\nu$ , where  $h$  is the constant he deduced from measurements of the exponent in Wien's law [Pla00a]. From this, it is possible to calculate the number of ways to assign  $n_\nu$  energy quanta  $h\nu$  to  $N_\nu$  oscillators, finally leading to his law of radiation that explained experimental results to high accuracy.

[Pla00b] Planck. *Verhandl. Dtsch. Phys. Ges.* (1900)

[Pla00a] Planck. *Ann. Phys.* (1900)

In Planck's model the quantization of energies is a property of the radiating body, a view that was changed by Albert Einstein in 1905, when he described the photoelectric effect in terms of quantization of light [Ein05].

[Ein05] Einstein. *Ann. Phys.* (1905)

From 1913 on early quantum mechanics was mainly concerned with the emission spectra of atoms. Nils Bohr applied Planck's idea of discrete energy states to the hydrogen system of an electron orbiting a proton, by relating the energy quanta with classical, circular orbits of given energy [Boh13]. Calculating the frequencies of transitions between different orbits he reproduced the (heuristically known) formula for the Balmer series, providing a theoretical value for the Rydberg constant.

[Boh13] Bohr. *Science* (1913)

Bohr's approach was significantly generalized by Arnold Sommerfeld, who objected that the restriction to circular orbits worked for hydrogen only, and that elliptical orbits had to be considered in general as well [Som16]. His quantization condition was to require the action of classical orbits to be an integer multiple of  $h$ , which he thus named the quantum of action (*Wirkungsquantum*). This allowed him to extend Bohr's analysis to elliptical orbits, introducing a second quantum

[Som16] Sommerfeld. *Ann. Phys.* (1916)

number to label the possible ellipticities. In the unperturbed hydrogen atom this gives no different energy levels than before, adding relativistic corrections however slightly splits these levels. Sommerfeld applied these corrections to the classical Kepler problem, using his quantization condition on the perturbed solutions. The resulting spectrum correctly described the *fine structure* splitting of the hydrogen emission lines that has been experimentally observed, defining the fine structure constant  $\alpha = e^2/\hbar c$  that governs the strength of the corrections. The remarkable agreement with experiments has to be regarded as a coincidence however: Sommerfeld knew nothing about the electron spin, which is essential in the correct treatment. Furthermore, his approach of incorporating relativistic corrections is incorrect. Apparently these errors cancel, giving the correct analytic result exactly.

A separate prediction of Sommerfeld's method is that of a quantized orientation of the orbits (*Richtungsquantelung*). This does not enter the energy spectra, but nevertheless restricts the observable values of the electrons angular momentum projected onto a given direction. Otto Stern imagined a setup to experimentally test this prediction [Ste21], conclusively verifying the splitting of a beam of silver atoms together with Walther Gerlach [GS22]. In hindsight, although they did demonstrate some quantum effect, it is actually the spin of the unpaired electron that provides the quantized magnetic moment, not angular momentum.

In 1925 Werner Heisenberg began a new formulation of quantum mechanics [Hei25]. Instead of integrating classical equations of motion and then imposing heuristic quantization conditions, he proposed a method to formulate equations of motion for quantum observables directly. He concluded that classical observables are represented by objects that, in general, do not commute. Shortly afterwards, Born and Jordan provided the necessary theory in [BJ25], where they explain that mathematicians, in fact, know of such non-commuting objects, which are called matrices – from then on Heisenberg's approach would be called *matrix mechanics*. They also introduce the fundamental commutation relations and equation of motion for operators as they are known today. In parallel, Dirac expanded on Heisenberg's paper in [Dir25], relating the quantum commutator to the classical Poisson bracket (without expressing observables as matrices, he just noted that the  $p_i$  and  $q_i$  do not commute, more in line with the modern formulation using operators). Some of Dirac's conclusions were also found (again, simultaneously) by Born, Jordan and Heisenberg in [BHJ26], who furthermore related the physical spectrum of a system with the mathematical spectrum of matrices, finding the eigenvalues of a matrix by diagonalization. In 1926 Pauli applied the newly developed method to rederive the hydrogen spectrum, reproducing the Balmer series without having to apply any heuristics or arbitrarily exclude solutions as Sommerfeld did [Pau26].

In a series of publications in 1926, Erwin Schrödinger introduced a different method of quantization, by inserting an Ansatz in terms of the function  $\psi$  into the classical Hamilton-Jacobi equation and postulating a variational problem [Sch26a]. This method, applied to the hydrogen system, again produced the known results (after matching an unknown constant in his Ansatz), quantization now stemming from boundary conditions imposed on his wave function, similar to the modes of an oscillating string. In [Sch26b] he produced results for

[Ste21] Stern. *Z. Phys.* (1921)

[GS22] Gerlach and Stern. *Z. Phys.* (1922)

[Hei25] Heisenberg. *Z. Phys.* (1925)

[BJ25] Born and Jordan. *Z. Phys.* (1925)

[Dir25] Dirac. *Proc. R. Soc. A* (1925)

[BHJ26] Born, Heisenberg, and Jordan. *Z. Phys.* (1926)

[Pau26] Pauli. *Z. Phys.* (1926)

[Sch26a] Schrödinger. *Ann. Phys.* (1926)

[Sch26b] Schrödinger. *Ann. Phys.* (1926)

further simple systems. The Equation he used for these calculations is the *stationary* Schrödinger equation, the full time dependence was added in [Sch26c]. There, he also provided an interpretation of the wave function  $\psi$ , claiming  $\psi^*\psi$  represented a *weight function* in configuration space. In [Sch26d] Schrödinger provided a proof that his method and Heisenberg's matrix mechanics are, in fact, equivalent.

[Sch26c] Schrödinger. *Ann. Phys.* (1926)

[Sch26d] Schrödinger. *Ann. Phys.* (1926)

## 1.2. Spin and special relativity

Despite the success of the “new quantum theory” in explaining atomic spectra, key ingredients were still missing. Although some level splitting was understood to be caused by relativistic effects, some other magnetic effect had to be responsible for the levels in an atom subject to a strong magnetic field (the *anomalous Zeeman effect* [Zee97; Lor09]).

[Zee97] Zeeman. *Science* (1897)

[Lor09] Lorentz. *Columbia University Press* (1909)

Besides the known quantum numbers that describe the energy level, angular momentum and the projection of angular momentum in a specified direction, a fourth number was needed to consistently enumerate all the experimentally observed lines, especially in the Zeeman effect [Lan21]. This was suspected to be a property of the atomic rest (which remains when removing the most weakly bound electron). Further complications arose in the structure of the periodic table of elements. The *Aufbauprinzip* [Boh21] could explain many observed properties, however the rules appeared to be inconsistent in allowing multiple electrons in some seemingly equivalent configurations (that is, having the same three electronic quantum numbers) but not in others.

[Lan21] Landé. *Z. Phys.* (1921)

[Boh21] Bohr. *Nature* (1921)

In 1925 Pauli discovered that if the fourth quantum number were a property of the electron as well, then the structure of atoms and the period lengths follow from the simple rule that no two electrons may ever have the same *four* quantum numbers in an atom [Pau25]. He did however not have an explanation where this *exclusion principle* should come from.

[Pau25] Pauli. *Z. Phys.* (1925)

To find a simpler organization scheme of spectral lines, Samuel Goudsmit recommended a different combination of quantum numbers [Gou25], whereafter he and George Uhlenbeck predicted the additional magnetic property of the electron to be an intrinsic angular momentum [UG25]. In [UG26] they explained how this model is able to describe the hydrogen fine structure due to *spin-orbit-coupling* which, in contrast to Sommerfeld's relativistic explanation, was consistent with all other observations, including the Zeeman effect — as long as the connection between the magnetic moment and the angular momentum is given by a Landé factor (as introduced in [Lan21]) of  $g = 2$ .

[Gou25] Goudsmit. *Z. Phys.* (1925)

[UG25] Uhlenbeck and Goudsmit. *Naturwissenschaften* (1925)

[UG26] Uhlenbeck and Goudsmit. *Nature* (1926)

Equipped with this new model, Heisenberg and Jordan performed a quantitative calculation to verify that it correctly reproduces all previously known effects, which it did [HJ26].

[HJ26] Heisenberg and Jordan. *Z. Phys.* (1926)

Early attempts to incorporate the electron spin in Schrödinger's wave mechanics led to technical difficulties, so some intermediate steps were necessary.

The first step appeared in [Hei26] where Heisenberg considered a system of multiple electrons. He noticed that the indistinguishability of electrons leads to a multitude of different configurations, of which one would automatically include Pauli's exclusion principle, so this would have to be the realization found in na-

[Hei26] Heisenberg. *Z. Phys.* (1926)

ture. Dirac made this more precise, determining that the many body wave function of a system of indistinguishable particles has to be either totally symmetric or totally antisymmetric under exchange of particles [Dir26]. He also explicitly calculated the thermodynamic energy distribution of particles with antisymmetric wave functions, resulting in the *Fermi-Dirac distribution* (which Enrico Fermi derived independently [Fer26a; Fer26b]) while symmetric wave functions lead to Bose-Einstein statistics.

The second step was a more general formulation of the fundamental laws of quantum mechanics, including interpretation of squares of wave functions in terms of probabilities, composition of probability amplitudes, observables as hermitian operators, and a general scheme to transform between different representations, developed simultaneously by Jordan [Jor27] and Dirac [Dir27].

Using this new, more general formulation, Pauli was able to find a description of the electron that combined Schrödinger's spatial wave function with a single, two-fold degree of freedom for the  $z$ -component of spin [Pau27]. To ensure that the spin degree of freedom obeys the correct relations, he introduced a set of three  $2 \times 2$ -matrices with the respective commutation relations, that operate on a two-component wavefunction.

As a major shortcoming of both his theory and the results of Heisenberg and Jordan's matrix mechanics Pauli notes that they are still not formulated in a relativistically invariant way.

In the last of his introductory papers [Sch26c] Schrödinger attempted to find a relativistic equation to describe the electron, which he however dismisses because it failed to incorporate spin. The same equation was proposed independently by Gordon [Gor26], Fock [Foc26], and Klein [Kle27] and is now typically known as *Klein-Gordon equation*.

### 1.3. Dirac's quantum theory of the electron

In 1928 Dirac succeeded in combining both relativistic invariance and the electrons's spin in a single wave equation [Dir28]. In fact, he even shows that the inclusion of spin follows necessarily<sup>1</sup> from the requirements that

1. the equation is linear in  $\partial_t$  so his and Jordan's general transformation theory can be applied,
2. the classical limit reproduces the relativistic energy-momentum relation.

Because Lorentz transformations mix time and spatial coordinates, (1.) also restricts the equation to be linear in the momenta. He thus formed a general linear combination of  $\partial_t$  and the  $\partial_{x_i}$  and concluded that to fulfill the energy-momentum relation the coefficients had to be matrices. The resulting wave equation is<sup>2</sup>

$$(i\hbar\gamma^\mu\partial_\mu - mc)\psi = 0 \quad (1.1)$$

where the  $\gamma^\mu$  are matrices obeying the relations

$$\{\gamma^\mu, \gamma^\nu\} = 2g^{\mu\nu}. \quad (1.2)$$

[Dir26] Dirac. *Proc. R. Soc. A* (1926)

[Fer26a] Fermi. *Rend. Lincei* (1926)

[Fer26b] Fermi. *Z. Phys.* (1926)

[Jor27] Jordan. *Z. Phys.* (1927)

[Dir27] Dirac. *Proc. R. Soc. A* (1927)

[Pau27] Pauli. *Z. Phys.* (1927)

[Gor26] Gordon. *Z. Phys.* (1926)

[Foc26] Fock. *Z. Phys.* (1926)

[Kle27] Klein. *Z. Phys.* (1927)

[Dir28] Dirac. *Proc. R. Soc. A* (1928)

<sup>1</sup> We know today that consistent relativistic scalar fields do exist (e.g., the Higgs field). It is his first requirement that is overly restrictive.

<sup>2</sup> In modern notation. More about our conventions in Section 2.1.

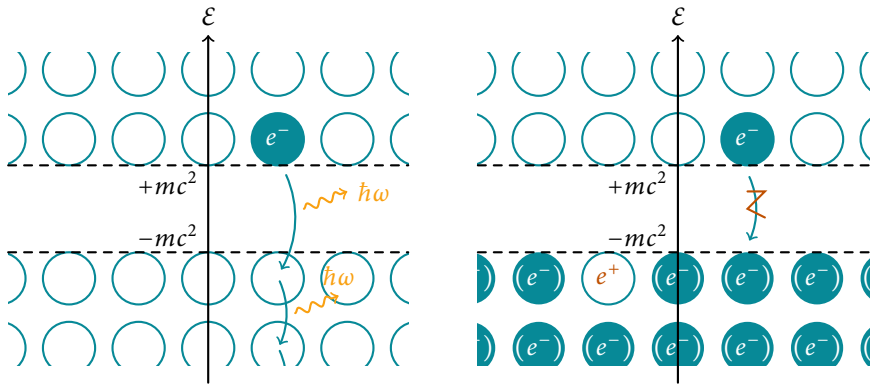


Figure 1.1.: Qualitative sketch of the energy landscape of QED with a single electron (left), jumping to negative energy states it would radiate energy forever. Dirac's solution (right), where all negative energy states are occupied. An electron missing from such a state would appear as a positron.

Coupled to an arbitrary electromagnetic field, the Dirac equation also correctly predicts the fact that the spin magnetic moment is twice that corresponding to orbital angular momentum, that is,  $g_s = 2$ .

Still, his equation is troubled by the same problems that he criticized about the Klein-Gordon equation: To any solution with energy  $E = mc^2 + \text{kinetic energy}$ , it admits a solution with energy  $-E$ . In a purely classical theory these supposedly unphysical states could just be ignored, but in a quantum theory transitions between these states would be possible, accompanied by electromagnetic radiation (see Figure 1.1, left). This is a serious issue, as the negative energy states are unbounded from below.

In [Dir30a] Dirac proposed a solution to this difficulty. The crucial ingredient is Pauli's exclusion principle: If all negative energy states were occupied, an electron could no longer transition to a state of negative energy (Figure 1.1, right). If this infinite distribution were exactly uniform, it could be consistent with our observations, he argued. Furthermore, a single unoccupied state in the negative continuum would be expected to behave like a particle with positive charge, a picture that already worked to describe vacancies in atoms created by X-ray radiation.

At that point, the only known particle with a positive charge of the same magnitude as the electron's was the proton. Thus, despite the problem of differing masses, Dirac proposed the proton to be described by holes in the negative continuum. He then proceeded to calculate the probability of electron-proton annihilation, corresponding to an electron recombining with an unoccupied negative energy state [Dir30b].

This model was however quickly disputed, because the rate of annihilation is too high compared with our observations and Weyl demonstrating that the positive particle would necessarily have the same mass as the electron. In [Dir31] Dirac then concluded that the anti-electron, as he calls it, has to be some as yet unknown particle, while the proton would have its own anti-proton.

Indeed, in 1932, Carl Anderson noticed tracks in a cloud chamber that appeared to stem from a positive particle with mass comparable to the electron mass [And32]. He gave several possible explanations at first, finally concluding that the existence of a positive electron is the most probable one [And33]. In [And33] the editor suggested the name *positron* for the newly discovered particle, which held on<sup>3</sup>.

[Dir30a] Dirac. *Proc. R. Soc. A* (1930)

[Dir30b] Dirac. *Proc. R. Soc. A* (1930)

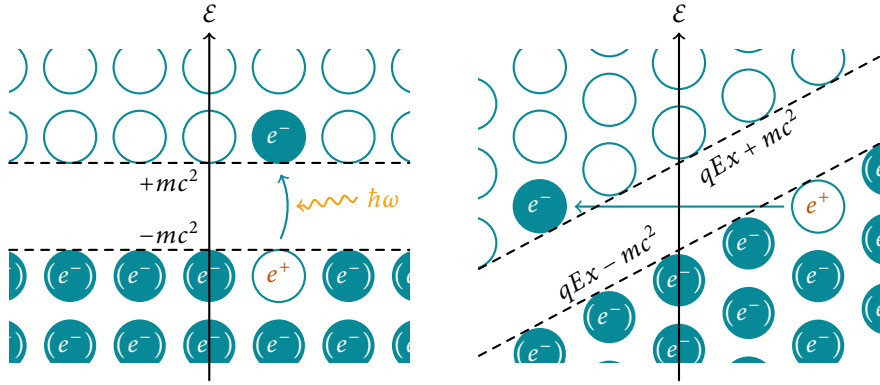
[Dir31] Dirac. *Proc. R. Soc. A* (1931)

[And32] Anderson. *Science* (1932)

[And33] Anderson. *Phys. Rev.* (1933)

<sup>3</sup> The proposed renaming of the original electron to *negatron* however, did not.

Figure 1.2.: Qualitative picture for perturbative (left) and non-perturbative (right) pair creation.



## 1.4. Sauter-Schwinger pair production

Apart from the process depicted in Figure 1.2 on the left, which is analogous to excitations in atomic systems, there is a second process that can produce electron-positron pairs. A static, homogeneous electric field oriented in the  $x$ -direction yields a potential energy of  $qEx$  for the electrons, both in the positive and the negative continuum (Figure 1.2). An electron in a negative energy state can then tunnel to a positive energy state, producing a pair as well. We can roughly estimate the probability for this process using the WKB formula for nonrelativistic tunneling, the barrier being the upper “triangle” in Figure 1.2 on the right. We then have  $V(x) = qEx$ , and get the width by demanding  $2mc^2 \stackrel{!}{=} V(L) \leadsto L = 2mc^2/qE$  and thus

$$|T|^2 \approx \exp\left(-2 \int_0^L dx \sqrt{2 \frac{m}{\hbar^2} V(x)}\right) = \exp\left(-A \frac{c^3 m^2}{\hbar qE}\right), \quad (1.3)$$

with some numeric factor  $A$ . Although this is only a rough qualitative picture, apart from the value of  $A$  the exponential dependence agrees with the correct result. The expression (1.3) already highlights an important property of this process: the probability can not be expanded as a perturbation series in  $q$  (or equivalently in  $\alpha$ ), it is consequently called *nonperturbative*. This has serious technical implications, as most mathematical methods for quantum electrodynamics are perturbative in nature.

The first sign of this effect appeared already in 1929 when Klein calculated the transmission and reflection probabilities at a potential step using the Dirac equation [Kle29]. For small potential steps he obtained the same qualitative results one would expect for a nonrelativistic treatment, partial transmission when the electron’s kinetic energy is greater than the height of the step and total reflection below. If the potential step exceeds the kinetic energy by more than  $2mc^2$  however, transmission is again possible, which is called *Klein’s Paradox*. Furthermore he found that the group velocity of the transmitted wave in this case is opposite to its momentum, which hints at antiparticle production.

Some remained skeptical, as a discontinuous potential step corresponds to an infinite electric field over a vanishing spatial region. Sauter performed the calculation for a piecewise linear potential which describes a constant, finite electric field over a finite length [Sau31]. He arrived at the same qualitative conclusions as

[Kle29] Klein. *Z. Phys.* (1929)

[Sau31] Sauter. *Z. Phys.* (1931)

Klein before, obtaining the transmission coefficient

$$|T|^2 = \exp\left(-\pi \frac{c^3 m^2}{\hbar qE}\right). \quad (1.4)$$

Shortly afterwards he extended his results to a completely smooth potential with the same general shape, corresponding to an electric field of the form  $\cosh^{-2}(kx)$ , which we will in the following call a *Sauter profile* [Sau32]. A detailed interpretation of Klein's paradox in terms of pair production was performed in 1941 by Hund [Hun41] where he concluded that pair production happens even without an initial, incoming matter wave (which was needed for the tunneling setup Klein and Sauter considered).

[Sau32] Sauter. *Z. Phys.* (1932)

[Hun41] Hund. *Z. Phys.* (1941)

In 1936 Heisenberg and Euler used Dirac's theory for a slightly different goal, deriving the modifications of Maxwell's theory in vacuum due to the possibility of (virtual) pair creation, yielding an *effective* Lagrangian for the electromagnetic fields [HE36]. There they also presented the exponential probability for pair creation as  $\exp(-\pi E_{\text{cr}}/E)$ , with the critical field strength  $E_{\text{cr}} := c^3 m^2 / \hbar q \approx 1.32 \times 10^{18}$  V/m, now commonly known as the *Schwinger limit*. The point of view of observing how the electromagnetic vacuum changes due to interaction with virtual electrons and positrons is actually very close to our derivation in Chapter 4.

[HE36] Heisenberg and Euler. *Z. Phys.* (1936)

The approach most in line with modern calculations came in 1951 from Julian Schwinger [Sch51]. In contrast to the single-particle tunneling picture from before he gave a proper multiparticle treatment, starting from the vacuum expectation value of the current operator. From this he deduced the rate of pair production<sup>4</sup> per unit volume and time in terms of the imaginary part of the effective Lagrangian (in units with  $\hbar = c = 1$ ),

[Sch51] Schwinger. *Phys. Rev.* (1951)

<sup>4</sup> Or rather the rate of vacuum decay, more on this distinction in Section 4.2.

$$\Im \mathcal{L} = \frac{(qE)^2}{(2\pi)^3} \sum_{n=1}^{\infty} \frac{1}{n^2} \exp\left(-n\pi \frac{m^2}{qE}\right). \quad (1.5)$$

Due to [Sch51] this nonperturbative pair production process is commonly denoted *Schwinger effect* or *Schwinger pair production*, although many more names could be attached. Because something along the lines of *Dirac-Klein-Sauter-Heisenberg-Euler-Hund-Schwinger effect* would be unwieldy, we will however settle on *Sauter-Schwinger effect*.

## 1.5. Worldline instantons

The concept of instantons first appeared in Yang-Mills theory [YM54], when Belavin, Polyakov, Schwartz and Tyupkin obtained a classical solution to the Euclidean field equations with finite action and nontrivial topology [Bel+75], today called the *BPST instanton*. Belavin, Polyakov [BP77] and 't Hooft [t H76] noticed how such solutions give important contributions to the vacuum structure of Yang-Mills theory, and thus quantum chromodynamics (a specific type of Yang-Mills that was found to be a good candidate to describe the strong interaction in the standard model [FGL73]). As solutions of definite action instead of energy, Polyakov proposed to call them *pseudoparticles*, while 't Hooft preferred the name

[YM54] Yang and Mills. *Phys. Rev.* (1954)

[Bel+75] Belavin, Polyakov, Schwartz, and Tyupkin. *Phys. Lett. B* (1975)

[BP77] Belavin and Polyakov. *Nucl. Phys. B* (1977)

[t H76] 't Hooft. *Phys. Rev. Lett.* (1976)

[FGL73] Fritzsch, Gell-Mann, and Leutwyler. *Phys. Lett. B* (1973)

*instanton*. The suffix “-on” indicates a “particle-like,” (spatially localized) excitation, while “instant” suggests localization in time.

Finding nontrivial solutions to (possibly nonlinear) field equations is in general very difficult. Luckily the instantons we are concerned with in the following are much simpler – despite describing an effect of quantum electrodynamics, we only need nonrelativistic quantum mechanical instantons as used by Polyakov as a toy example of his approach [Pol77]. This is made possible by the *worldline* representation of QED.

[Pol77] Polyakov. *Nucl. Phys. B* (1977)

It was Vladimir Fock who first demonstrated that solutions of the Dirac equation can be obtained from solutions of a four-dimensional Schrödinger-type equation with  $\mathbf{r}$  and  $t$  all parametrized by an additional parameter  $\tau$ , identified with the proper time of a propagating particle [Foc37]. Richard Feynman, developing his Path integral approach for nonrelativistic quantum mechanics,<sup>5</sup> mentioned that a relativistic Klein-Gordon or Dirac particle could be described by four coordinates, introducing an additional parametrization parameter, however he dismissed this approach as “add[ing] nothing to the understanding of these equations” [Fey48]. Only after Yōichirō Nambu expanded on Fock’s representation and emphasized how beneficial this point of view would be in the path integral approach [Nam50], Feynman used it in an appendix to derive a propagator (albeit for the Klein-Gordon equation) in terms of a single-particle path integral in four dimensions [Fey50], and finally for the Dirac equation in [Fey51]. In parallel, in the work that gave the nonperturbative pair production effect its name, Schwinger used a similar representation that is now often, like the effect, attributed to him only. As the path  $(\mathbf{r}(\tau), t(\tau))$  of a particle traced by its proper time is its worldline, this is called *worldline representation*.

[Foc37] Fock. *Phys. Z. Sowjetunion* (1937)

<sup>5</sup> More details in Section 2.2.

[Fey48] Feynman. *Rev. Mod. Phys.* (1948)

[Nam50] Nambu. *Prog. Theor. Phys.* (1950)

[Fey50] Feynman. *Phys. Rev.* (1950)

[Fey51] Feynman. *Phys. Rev.* (1951)

Although both Feynman and Schwinger already mentioned the equations of motion of the fictional four-dimensional particle in the classical limit, the first explicit mention of an instanton technique was in 1982 by Affleck, Alvarez and Manton [AAM82]. There, they gave a derivation of the pair production rate in a constant, homogeneous electric field that is essentially identical to the way used today. It has the great advantage of being readily generalized to more complicated background fields, and made possible most results presented in this thesis. Because the classical solutions in this case are those of the worldline path integral, they are called *worldline instantons*. We will derive the method in detail in Chapter 4 and give applications in Part II.

[AAM82] Affleck, Alvarez, and Manton. *Nucl. Phys. B* (1982)

## 2

**Mathematical preliminaries**

*This chapter contains notational conventions and some of the mathematical tools needed in the following.*

**2.1. Conventions and notation**

There are many different conventions regarding the presentation of vectors and tensors, so the present chapter introduces all notation used in this thesis.

**Spatial vectors and matrices**

Spatial, that is 3-component-, vectors will be typeset in bold italic. Their components are subscripted using Latin indices. Unit vectors carry a circumflex, and summation over repeated indices in a term is understood (*Einstein's summation convention*):

$$\mathbf{a} = (a_1, a_2, a_3)^T = a_i \hat{\mathbf{e}}_i. \quad (2.1)$$

In some cases, where the geometry is to be emphasized, components will be denoted using  $x$ ,  $y$  and  $z$ :

$$\mathbf{r} = (x, y, z)^T, \quad \mathbf{v} = (v_x, v_y, v_z)^T. \quad (2.2)$$

Multiplication by a scalar will be denoted by juxtaposition, dot and cross products by a centered dot and a cross, respectively:

$$c\mathbf{a}, \quad \mathbf{a} \cdot \mathbf{b}, \quad \mathbf{a} \times \mathbf{b}. \quad (2.3)$$

Matrices are typeset in upright bold:

$$\mathbf{M} = \begin{pmatrix} m_{11} & m_{12} & m_{13} \\ m_{21} & m_{22} & m_{23} \\ m_{31} & m_{32} & m_{33} \end{pmatrix}. \quad (2.4)$$

In general, we will also use lowercase symbols for vectors and uppercase symbols for matrices. Exceptions include the electromagnetic fields  $\mathbf{E}$  and  $\mathbf{B}$ .<sup>6</sup>

We will in some places encounter general  $N$ -tuples and matrices with no immediate connection to geometry, these will be bold as well.

Never will a multiplication symbol be used for scalar-vector or scalar-scalar multiplication, with the exception of a product between numerical quantities, for example

$$2 \times 2 = 4, \quad \hbar \approx 1.055 \times 10^{-34} \text{ kg m}^2/\text{s}. \quad (2.5)$$

<sup>6</sup> Being vectors, they are still italic. In contrast, there could be matrices  $\mathbf{E}$  and  $\mathbf{B}$ , although we will always avoid such clashes in notation where possible.

### Four-vectors and tensors

Working exclusively in flat space, the only metric we will be concerned with is the Minkowskian metric in the *mostly minus*-convention<sup>7</sup>

<sup>7</sup> Often,  $g_{\mu\nu}$  describes a generic metric, while the Minkowskian metric is  $\eta_{\mu\nu}$ . Because no other metric tensors appear in this thesis,  $\eta$  is reserved for different use.

$$(g_{\mu\nu}) = \text{diag}(1, -1, -1, -1) = \begin{pmatrix} 1 & 0 & 0 & 0 \\ 0 & -1 & 0 & 0 \\ 0 & 0 & -1 & 0 \\ 0 & 0 & 0 & -1 \end{pmatrix}. \quad (2.6)$$

The metric tensor gives a one-to-one correspondence between contravariant vectors carrying upper Greek indices (for example the spacetime position  $x^\mu$ )<sup>8</sup> and covariant vectors (for example the 4-gradient  $\partial_\mu$ ):

$$a_\mu = g_{\mu\nu} a^\nu, \quad (2.7)$$

<sup>8</sup> Here *contravariant* can be readily understood as *counteracting* changes in the coordinate system. If we scale an axis by a factor of 10, we have to reduce the corresponding component of a vector to 1/10.

so the same physical object can be represented both using upper or lower indices, only the spatial components change sign, for example:

$$x^\mu = (ct, x, y, z)^\top \quad (2.8)$$

$$\simeq x_\mu = g_{\mu\nu} x^\nu = (ct, -x, -y, -z)^\top.$$

Tensor operations like the dot product will be typeset using regular italic symbols:

$$a \cdot b := a^\mu g_{\mu\nu} a^\nu. \quad (2.9)$$

There should never be any ambiguity between scalars and four-vectors, because the latter will either carry an index, or be included in a dot product or matrix-vector multiplication.

<sup>9</sup> See Chapter 4. In the worldline instanton formalism we work in Euclidean spacetime, by performing a Wick rotation to imaginary time<sup>9</sup>. Because the metric is proportional to the identity in this case, we will not distinguish between co- and contravariant vectors, usually keeping indices as subscripts. By convention, the time component of a Minkowski vector has index 0, while it has index 4 in Euclidean spacetime.

### Spinors

We will at a few points briefly encounter spinorial objects, these will be highlighted in bold typeface like spatial vectors and matrices. It will always be made clear from the context which type of quantities are involved in expressions.

### Units

In the following, we will always use a system of units where  $\hbar = c = 1$  (called *natural units*). Thus, only one physical dimension remains, which is usually taken to be a length or an energy:<sup>10</sup>

<sup>10</sup> The brackets mean *dimension of*.

$$[x^\mu] = [t] = L = E^{-1}, \quad [v] = 1, \quad [p_\mu] = [m] = [A_\mu] = L^{-1} = E. \quad (2.10)$$

This way it is possible to express masses and frequencies using energies, which is often convenient.

## Conventions for the electromagnetic potential

During our calculations it will be beneficial to work with dimensionless quantities, for numerical computations it is even necessary. We note down our conventions here for reference, they will be properly introduced on page 47:

$$\tilde{x}_\mu = x_\mu \frac{qE}{m}, \quad \tilde{F}_{\mu\nu} = F_{\mu\nu} \frac{1}{E}, \quad \tilde{A}_\mu = \frac{qE}{m} \frac{1}{E} A_\mu. \quad (2.11)$$

Here,  $E$  is some reference field strength,  $q$  the elementary charge and  $m$  the electron mass. We will sometimes denote by  $A_\mu$  the potential with physical dimensions and by  $\tilde{A}_\mu$  the dimensionless version, but mostly drop the tilde in sections that deal with the dimensionless field only, to reduce clutter in the equations<sup>11</sup>. To refer to dimensionful quantities we then employ a superscript of  $A_\mu^{\text{dim.}}$ . The meaning of  $A_\mu$  should mostly be clear from the context, but we will also add reminders which conventions are active in a given section. The marker  $[\mathbf{A}] = \mathbf{L}^{-1}$  will mean that quantities without decorations carry physical dimensions,<sup>12</sup>  $[\mathbf{A}] = \mathbf{1}$  that they do not.

Similarly, we sometimes deal with both Minkowskian and Euclidean quantities. Our choice of Euclidean four-potential is

$$A_4^{\text{E}}(x_\mu) = \frac{1}{i} A_0(t = -ix_4, \mathbf{x}), \quad \mathbf{A}^{\text{E}}(x_\mu) = \mathbf{A}(t = -ix_4, \mathbf{x}), \quad (2.12)$$

it will be introduced on page 42. For convenience, only one or the other will be marked by a superscript. There will also be reminders if quantities without any decorations are Minkowskian ( $\mathbf{x}_i = -\mathbf{x}^i$ ) or Euclidean ( $\mathbf{x}_i = \mathbf{x}^i$ ).

## 2.2. Quantum mechanical path integral

The key mathematical tool for the worldline instanton formalism is the quantum mechanical *path integral*, which is yet another alternative formulation of quantum mechanics. In contrast to the operator or wavefunction formalism, it does not rely on a Hamiltonian formulation, but uses the Lagrangian  $L$  of a system. This was first discussed in 1933, and 1945 again in more detail by Dirac [Dir33; Dir45], where he argued that the time evolution of a quantum system could be expressed by small time increments, each generated by factors related to the classical action along a small path.

This was made more precise in 1948 by Feynman [Fey48], who also demonstrated that the approach is equivalent to the existing methods. There are several ways to introduce the method, either postulating the form of the path integral and then showing that it implies the Schrödinger equation as Feynman did, amounting to a new *definition* of quantum mechanics, or deriving the path integral from the quantum mechanical time evolution operator.

We will quickly sketch the latter approach, following Zee's textbook [Zee10], as this immediately yields the correct normalization factors for the discretized path integral. We consider a one-dimensional, nonrelativistic particle of mass  $m$  in some potential  $V(x)$ . The Hamiltonian of this system is

$$\hat{H} = \frac{\hat{p}^2}{2m} + V(\hat{x}), \quad (2.13)$$

<sup>11</sup> The same holds for other quantities, most notably the coordinates  $x_\mu$ .

<sup>12</sup> We still set  $\hbar = c = 1$ , though.

[Dir33] Dirac. *Phys. Z. Sowjetunion* (1933)

[Dir45] Dirac. *Rev. Mod. Phys.* (1945)

[Fey48] Feynman. *Rev. Mod. Phys.* (1948)

[Zee10] Zee. *Princeton University Press* (2010)

[Sak94] Sakurai.  
Addison-Wesley (1994)

and the probability amplitude to find the particle, initially positioned at  $x_I$ , at the final position  $x_F$  after a time of  $T$  is given by (see, e.g., [Sak94])

$$\langle x_F | e^{-i\hat{H}T} | x_I \rangle. \quad (2.14)$$

We now split the time evolution into  $N \gg 1$  slices of length  $\delta t = T/N$ , and insert a decomposition of the identity operator into a complete set of position eigenstates  $\mathbb{1} = \int dx_k |x_k\rangle \langle x_k|$  between each slice,

$$\begin{aligned} \langle x_F | e^{-i\hat{H}T} | x_I \rangle &= \int d^N x \left( \langle x_F | e^{-i\hat{H}\delta t} | x_{N-1} \rangle \langle x_{N-1} | e^{-i\hat{H}\delta t} | x_{N-2} \rangle \right. \\ &\quad \left. \dots \langle x_2 | e^{-i\hat{H}\delta t} | x_1 \rangle \langle x_1 | e^{-i\hat{H}\delta t} | x_I \rangle \right). \end{aligned} \quad (2.15)$$

This is just Feynman's postulate that to obtain the amplitude for a process (in this case propagation from  $x_I$  to  $x_F$  in time  $T$ ), we have to sum over all possible intermediate states (first propagating to some  $x_1$  after  $\delta t$ , then to some  $x_2$  after  $2\delta t$  and so on). Let us pick one of the slices, from  $x_k$  to  $x_{k+1}$ :

$$\langle x_{k+1} | e^{-i\hat{H}\delta t} | x_k \rangle = \langle x_{k+1} | e^{-i(\frac{\hat{p}^2}{2m} + V(\hat{x}))\delta t} | x_k \rangle. \quad (2.16)$$

We would like to apply the operator  $\hat{x}$  to the state  $|x_k\rangle$ . Since  $\delta t$  is small, violating the *Baker-Campbell-Hausdorff*-formula  $e^{\hat{A}+\hat{B}} = e^{\hat{A}}e^{\hat{B}}(1 - \frac{1}{2}[\hat{A},\hat{B}] + \dots)$  is a good approximation here,<sup>13</sup> and we get

$$\begin{aligned} \langle x_{k+1} | e^{-i(\frac{\hat{p}^2}{2m} + V(\hat{x}))\delta t} | x_k \rangle &= \\ \langle x_{k+1} | e^{-i\frac{\hat{p}^2}{2m}\delta t} e^{-iV(x_k)\delta t} | x_k \rangle (1 + O(\delta t^2)) & \\ \approx \int_{-\infty}^{\infty} dp \langle x_{k+1} | e^{-i\frac{p^2}{2m}\delta t} | p \rangle \langle p | e^{-iV(x_k)\delta t} | x_k \rangle & \\ = e^{-iV(x_k)\delta t} \int_{-\infty}^{\infty} \frac{dp}{2\pi} e^{-i\frac{p^2}{2m}\delta t} e^{-ip(x_{k+1}-x_k)} & \\ = \sqrt{\frac{m}{i2\pi\delta t}} \exp \left[ i \left( \frac{m}{2} \left( \frac{x_{k+1}-x_k}{\delta t} \right)^2 - V(x_k) \right) \delta t \right], & \end{aligned} \quad (2.17)$$

where we have dropped the second order terms that vanish in the limit  $\delta t \rightarrow 0$ , inserted a complete set of momentum eigenstates and used the relation

$$\langle p | x \rangle = \frac{1}{\sqrt{2\pi}} e^{-ipx} \quad (2.18)$$

and the integral (see sections 2.3 and 2.6)

$$\int_{-\infty}^{\infty} dx e^{-i(ax^2+bx)} = \sqrt{\frac{\pi}{ia}} e^{i\frac{b^2}{4a}}. \quad (2.19)$$

<sup>13</sup> In fact, for operators that are bounded from below, it is exact in the limit  $\delta t \rightarrow 0$  that we wish to do in the end.

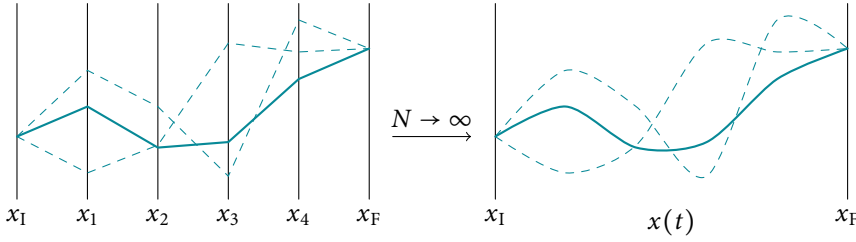


Figure 2.1.: Left: Integration over  $N = 4$  intermediate points, right: integration over  $N \rightarrow \infty$  intermediate points, i.e. continuous paths.

In the limit  $\delta t \rightarrow 0$ , using the finite difference expression of the velocity, we can identify the exponent in (2.17) as  $iL(\dot{x}(k\delta t), x(k\delta t))\delta t$ , where  $L$  is the classical Lagrangian for a particle of mass  $m$  in the potential  $V(x)$  evaluated at  $t = k\delta t$ . Inserting (2.17) into (2.15) we obtain

$$\langle x_F | e^{-i\hat{H}T} | x_I \rangle = \int d^N x \left( \frac{m}{i2\pi\delta t} \right)^{N/2} \exp \left( i \sum_{k=0}^N \delta t L_k \right). \quad (2.20)$$

If we now perform the (formal) limit  $\delta t \rightarrow 0$  or respectively  $N \rightarrow \infty$ , the sum in the exponent of (2.20) tends to the classical action  $\mathcal{S}$ ,

$$\lim_{N \rightarrow \infty} \sum_{k=0}^N \frac{T}{N} L_k = \int_0^T dt L(\dot{x}(t), x(t)) =: \mathcal{S}[x], \quad (2.21)$$

where the square brackets denote a functional, i.e. an object depending on a function  $x(t)$ . The integrals over ever more intermediate points  $x_k$  effectively turn into an integration over all possible paths  $x(t)$  connecting  $x_I$  and  $x_F$  (see Figure 2.1), which will be denoted  $\int \mathcal{D}x$ .

The prefactor in (2.20) is of course hopelessly divergent for  $N \rightarrow \infty$ , however it does not depend on the coordinates, so it can be seen as an infinite normalization constant that cancels when taking ratios.<sup>14</sup>

Finally, the path integral expression for the probability amplitude of a particle to travel from  $x_I$  to  $x_F$  in time  $T$  is thus given by

$$\langle x_F | e^{-i\hat{H}T} | x_I \rangle = \int_{x(0)=x_I}^{x(T)=x_F} \mathcal{D}x(t) e^{i\mathcal{S}[x]}, \quad (2.22)$$

where the action  $\mathcal{S}$  is evaluated using the Lagrangian corresponding to the Hamiltonian  $\hat{H}$ . This definition works for a particle in  $d$  dimensions as well, we just replace each intermediate integration by  $d$  integrations.

We can use the normalization constant we found in this derivation to define the path integral for an arbitrary integration over  $d$ -dimensional paths with integrand  $f[x]$ , by

$$\int \mathcal{D}x(t) f[x(t)] = \left( \prod_{k=0}^{N-1} \int d^d x^k \left( \frac{mN}{2\pi iT} \right)^{d/2} \right) f[x_\mu^l], \quad (2.23)$$

where  $f[x_\mu^l]$  is an appropriate discretization of the integrand. In this case the square brackets denote dependence on all points  $l = 1, 2, \dots, N$ .

<sup>14</sup> More properly, one has to evaluate the integrals for some finite  $N$ , cancel the normalization constant in the ratio and then take the limit  $N \rightarrow \infty$ .

One great advantage of (2.22) is that it immediately generalizes to propagators in field theories, by integrating over all field configurations. In particular, we obtain the *vacuum persistence amplitude*, i.e. the transition amplitude between an initially vacuum state to stay vacuum after an infinite amount of time:

$$\lim_{T \rightarrow \infty} \langle 0 | e^{-i\hat{H}T} | 0 \rangle = \int \mathcal{D}\phi(x^\mu) e^{iS[\phi]}, \quad S[\phi] = \int d^4x \mathcal{L}(\partial_\mu \phi, \phi). \quad (2.24)$$

## 2.3. Gaußian integrals

The by far most important definite (improper) integral in the following is the *Gaußian integral*<sup>15</sup>

<sup>15</sup> It is easily computed by evaluating the square of the integral and transforming to polar coordinates.

$$\int_{-\infty}^{\infty} dx e^{-x^2} = \sqrt{\pi}, \quad (2.25)$$

or by substitution and shifting the region of integration

$$\int_{-\infty}^{\infty} dx e^{-\frac{1}{2}a(x-x_0)^2} = \sqrt{\frac{2\pi}{a}}. \quad (2.26)$$

An important generalization of (2.26) is the multivariate Gaußian. Consider the  $N$ -dimensional integral

$$\int_{\mathbb{R}^N} d^N x e^{-\frac{1}{2} \mathbf{x}^\top \cdot \mathbf{A} \cdot \mathbf{x}} \quad (2.27)$$

with real, symmetric and positive definite  $N \times N$  matrix  $\mathbf{A}$ . Because it is symmetric and positive definite, we can find an orthogonal matrix  $\mathbf{X}$  (so  $\mathbf{X}^{-1} = \mathbf{X}^\top$ ) that diagonalizes  $\mathbf{A}$ ,

$$\mathbf{A} = \mathbf{X}^\top \cdot \mathbf{D} \cdot \mathbf{X}, \quad \mathbf{D} = \text{diag}(\lambda_1, \lambda_2, \dots, \lambda_N), \quad (2.28)$$

where the  $\lambda_i$  are the eigenvalues of  $\mathbf{A}$ . Let us change variables to

$$\mathbf{y} = \mathbf{X} \cdot \mathbf{x}, \quad \curvearrowright \quad d^N y = \det \mathbf{X} d^N x = d^N x, \quad (2.29)$$

so that the exponent separates into a sum over eigenvalues

$$\mathbf{x}^\top \cdot \mathbf{A} \cdot \mathbf{x} = \mathbf{y}^\top \cdot \mathbf{D} \cdot \mathbf{y} = \sum_{k=1}^N \lambda_k y_k^2 \quad (2.30)$$

and the whole integral factors into  $N$  separate parts

$$\int_{\mathbb{R}^N} d^N x e^{-\frac{1}{2} \mathbf{x}^\top \cdot \mathbf{A} \cdot \mathbf{x}} = \prod_{i=1}^N \int_{-\infty}^{\infty} dy_i e^{-\frac{1}{2} \lambda_i y_i^2} = \prod_{i=1}^N \sqrt{\frac{2\pi}{\lambda_i}} = \sqrt{\frac{(2\pi)^N}{\det \mathbf{A}}}. \quad (2.31)$$

We can expand this result to integration over complex variables, with  $\mathbf{M}$  now a positive definite hermitian matrix,

$$\int_{\mathbb{R}^{2N}} d^N z^* d^N z e^{-\frac{1}{2} \mathbf{z}^\dagger \cdot \mathbf{M} \cdot \mathbf{z}}, \quad (2.32)$$

where the slightly peculiar integration measure means we consider the variable  $z$  and its complex conjugate  $z^*$  to be independent degrees of freedom. In practice

this means we integrate over its real and imaginary parts from  $-\infty$  to  $\infty$ , hence the range  $\mathbb{R}^{2N}$ . We can now, with a few modifications, perform the same steps as before,  $\mathbf{M}$  is now diagonalized by a unitary matrix  $\mathbf{U}$  (so  $\mathbf{U}^{-1} = \mathbf{U}^\dagger$ )

$$\mathbf{M} = \mathbf{U}^\dagger \cdot \mathbf{D} \cdot \mathbf{U}, \quad \mathbf{D} = \text{diag}(\lambda_1, \lambda_2, \dots, \lambda_N), \quad (2.33)$$

and we again change variables for  $z$  and  $z^*$

$$\mathbf{y} = \mathbf{U} \cdot \mathbf{z}, \quad \mathbf{y}^\dagger = \mathbf{z}^\dagger \cdot \mathbf{U}^\dagger \rightsquigarrow \text{d}^N y^* \text{d}^N y = \det \mathbf{U}^\dagger \det \mathbf{U} \text{d}^N z^* \text{d}^N z = \text{d}^N z^* \text{d}^N z, \quad (2.34)$$

so the exponent separates once more

$$\mathbf{z}^\dagger \cdot \mathbf{M} \cdot \mathbf{z} = \mathbf{y}^\dagger \cdot \mathbf{D} \cdot \mathbf{y} = \sum_{k=1}^N \lambda_k |y_k|^2 = \sum_{k=1}^N \lambda_k (u_k^2 + v_k^2) \quad (2.35)$$

with  $y_k = u_k + iv_k$ . We again arrive at a product of one-dimensional Gaussian integrations, this time twice as many

$$\begin{aligned} \int_{\mathbb{R}^{2N}} \text{d}^N z^* \text{d}^N z e^{-\frac{1}{2} \mathbf{z}^\dagger \cdot \mathbf{M} \cdot \mathbf{z}} &= \prod_{k=1}^N \int_{-\infty}^{\infty} \text{d}u_k \int_{-\infty}^{\infty} \text{d}v_k e^{-\frac{1}{2} \lambda_k (u_k^2 + v_k^2)} \\ &= \prod_{k=1}^N \sqrt{\frac{2\pi}{\lambda_k}} \sqrt{\frac{2\pi}{\lambda_k}} = \frac{(2\pi)^N}{\det \mathbf{M}}. \end{aligned} \quad (2.36)$$

The last two examples can also be generalized to an infinite number of dimensions, that is, path integration. The  $N$ -dimensional integrals are replaced by functional integrals over paths  $x(t)$  and the matrix  $\mathbf{A}$  by some positive definite linear differential operator  $\hat{A}$ . It is then again possible to change variables to eigenfunctions of  $\hat{A}$ , giving a product of (in general infinitely many) simple Gaussian integrals. Again denoting the product of eigenvalues by  $\text{Det } \hat{A}$ <sup>16</sup>, we have

$$\int \mathcal{D}x e^{-\frac{1}{2} \int \text{d}t x(t) \hat{A} x(t)} \sim \frac{1}{\sqrt{\text{Det } \hat{A}}}, \quad (2.37)$$

and in the complex form

$$\int \mathcal{D}z^* \mathcal{D}z e^{-\frac{1}{2} \int \text{d}t z^*(t) \hat{A} z(t)} \sim \frac{1}{\text{Det } \hat{A}}. \quad (2.38)$$

It is obvious that some care has to be taken to define (2.37) and (2.38), as both the factor  $(2\pi)^N$  and in general the operator determinant (naïvely defined as the infinite product of its eigenvalues) diverge as  $N \rightarrow \infty$ . We will come back to this issue in Section 2.7.

## 2.4. Laplace's method

It is possible to approximate integrals of the form

$$\int_{-\infty}^{\infty} \text{d}x h(x) e^{-Mf(x)} \quad (2.39)$$

<sup>16</sup> A capital D is used to distinguish the functional determinant from the regular one.

<sup>17</sup> Often called *method of steepest descent*, *stationary phase* or *saddle point method* in the literature, although these actually refer to an extension of Laplace's method for line integrals in the complex plane.

where  $M$  is large using *Laplace's method*.<sup>17</sup>

Assume  $f(x)$  in (2.39) has a global minimum at  $x_0$ . Then, because  $M$  is large, the integral is dominated by contributions around  $x_0$  (see Figure 2.2). Let us expand  $f(x)$  to quadratic order around  $x_0$  (the linear term vanishes due to the assumption of  $x_0$  being a minimum).

$$f(x) \approx f(x_0) + \frac{1}{2}f''(x_0)(x - x_0)^2, \quad (2.40)$$

and insert into (2.39).

$$\begin{aligned} \int_{-\infty}^{\infty} dx h(x) e^{-Mf(x)} &\approx h(x_0) e^{-Mf(x_0)} \int_{-\infty}^{\infty} dx e^{-\frac{1}{2}Mf''(x_0)(x-x_0)^2} \\ &= h(x_0) e^{-Mf(x_0)} \sqrt{\frac{2\pi}{Mf''(x_0)}}, \end{aligned} \quad (2.41)$$

because  $f''(x_0) > 0$  again since  $f$  has a minimum at  $x_0$ . Since  $M$  is large,  $h(x)$  is essentially constant over the interval of significant support, or more precisely

$$\frac{h'(x_0)}{h(x_0)} \ll \sqrt{Mf''(x_0)}, \quad (2.42)$$

so we can take it out of the integration.

It is easy to extend Laplace's method to a multivariate setting. Consider the Integral

$$\int d^N x h(\mathbf{x}) e^{-Mf(\mathbf{x})}, \quad (2.43)$$

where we again expand  $f$  around the minimum  $\mathbf{x}_0$ ,

$$f(\mathbf{x}) \approx f(\mathbf{x}_0) + \frac{1}{2}(\mathbf{x} - \mathbf{x}_0) \cdot \mathbf{H}_f(\mathbf{x}_0) \cdot (\mathbf{x} - \mathbf{x}_0), \quad (2.44)$$

with the *Hessian* of  $f$  at  $\mathbf{x}_0$

$$(\mathbf{H}_f(\mathbf{x}_0))_{ij} = \left. \frac{\partial}{\partial x_i} \frac{\partial}{\partial x_j} f(\mathbf{x}) \right|_{\mathbf{x}=\mathbf{x}_0} \quad (2.45)$$

giving an  $N$ -dimensional Gaussian integral that converges, because  $\mathbf{x}_0$  being a minimum of  $f$  makes  $\mathbf{H}_f(\mathbf{x}_0)$  positive definite,

$$\begin{aligned} \int d^N x h(\mathbf{x}) e^{-Mf(\mathbf{x})} &\approx h(\mathbf{x}_0) e^{-Mf(\mathbf{x}_0)} \int d^N x e^{-\frac{1}{2}M(\mathbf{x}-\mathbf{x}_0) \cdot \mathbf{H}_f(\mathbf{x}_0) \cdot (\mathbf{x}-\mathbf{x}_0)} \\ &= h(\mathbf{x}_0) e^{-Mf(\mathbf{x}_0)} \sqrt{\frac{(2\pi)^N}{M^N \det(\mathbf{H}_f(\mathbf{x}_0))}}. \end{aligned} \quad (2.46)$$

Equation (2.46) can again be extended to path integrals. Instead of the minimum of a function we have to minimize a functional. Consider

$$\int \mathcal{D}x h[x] e^{-M\mathcal{A}[x]}, \quad \mathcal{A}[x] = \int dt L(\dot{x}(t), x(t), t), \quad (2.47)$$

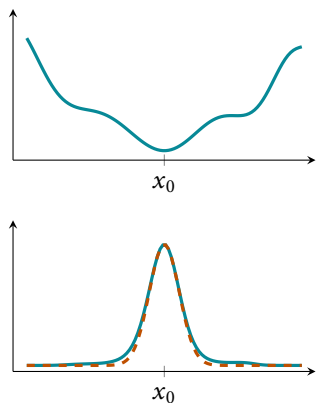


Figure 2.2.: Top: Some function  $f(x)$ . Bottom:  $e^{-10f(x)}$  (solid) and the Gaussian approximation (dashed).

the extremum in this case is a solution to the classical equations of motion of a particle with Lagrange function  $L$ , denoted by  $x^{\text{cl}}(t)$ . We can then expand the functional around the classical solution

$$\mathcal{A}[x] \approx \mathcal{A}[x^{\text{cl}}] + \frac{1}{2} \int dt \eta(t) \Lambda(x^{\text{cl}}) \eta(t), \quad \eta(t) = x(t) - x^{\text{cl}}(t), \quad (2.48)$$

where the operator  $\Lambda$  is determined by taking the second variation of  $\mathcal{A}$  and integrating by parts. According to (2.37), we arrive at the approximation

$$\begin{aligned} \int \mathcal{D}x h[x] e^{-M\mathcal{A}[x]} &\approx h[x^{\text{cl}}] e^{-M\mathcal{A}[x^{\text{cl}}]} \int \mathcal{D}x e^{-\frac{1}{2} M \int dt \eta(t) \Lambda(x^{\text{cl}}) \eta(t)} \\ &\sim \frac{h[x^{\text{cl}}]}{\sqrt{\text{Det } \Lambda(x^{\text{cl}})}} e^{-M\mathcal{A}[x^{\text{cl}}]}. \end{aligned} \quad (2.49)$$

In any setting, if the exponent has multiple minima that are well separated, we can split the integration into multiple parts that each include one minimum. The approximation to the full integral is then the sum of the single approximations.

## 2.5. Analytic continuation

An important tool in the following will be *analytic continuation*. Consider two functions  $f_A(z)$  and  $f_B(z)$  that are analytic on subsets  $A$  and  $B$  of the complex plane respectively with  $A \subset B$  (see Figure 2.3) and  $f_A(z) = f_B(z)$  for  $z \in A$ . Then  $f_B$  is an analytic continuation of  $f_A$  over  $B$ . The important point is that this continuation is unique, because if we have another  $\tilde{f}_B(z)$  defined over  $B$  with  $f_A(z) = \tilde{f}_B(z)$  for  $z \in A$ , then  $f_B(z) - \tilde{f}_B(z) = 0$  for all  $z \in A$  and thus  $f_B(z) - \tilde{f}_B(z) = 0$  everywhere in  $B$ .<sup>18</sup> It is thus possible to speak of *the* analytic continuation of an expression.

In practice, this means we can use analytic continuation to extend the domain of validity of expressions, for example convergence of series. Consider the sum

$$1 + 2 + 3 + \dots = \sum_{n=1}^{\infty} n. \quad (2.50)$$

Obviously, this does not converge. But what if the expression were to come up in a physical calculation<sup>19</sup>, in that case we would have to find a way to extract the physical information from the divergent quantity.

To do so, we can use the *Riemann Zeta function*, defined by [BO99; Olv+10]

$$\zeta(s) = \sum_{n=1}^{\infty} n^{-s}, \quad (2.51)$$

for  $\Re(s) > 1$  (e.g.  $\zeta(2) = \sum 1/n^2 = \pi^2/6$ ). As it turns out,  $\zeta(s)$  can be extended to the whole complex plane with a pole at  $s = 1$ . In particular it is defined for  $s = -1$ , which makes (2.51) formally equal to (2.50). Using the functional relation [Rie59]

$$\zeta(s) = 2^s \pi^{s-1} \sin\left(\frac{\pi s}{2}\right) \Gamma(1-s) \zeta(1-s) \quad (2.52)$$

we can see that

$$\zeta(-1) = \frac{1}{2\pi^2} \sin\left(-\frac{\pi}{2}\right) \Gamma(2) \zeta(2) = -\frac{1}{12}, \quad (2.53)$$

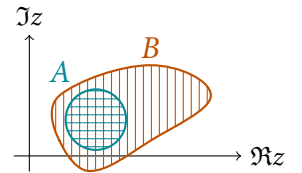


Figure 2.3.: Two subsets  $A \subset B$  of the complex plane.

<sup>18</sup> Sums of analytic functions are analytic and either have isolated zeros or are constant.

<sup>19</sup> It actually does in the calculation of the QED Casimir energy.

[BO99] Bender and Orszag. *Springer* (1999)

[Olv+10] Olver, Lozier, Boisvert, and Clark. *Cambridge University Press* (2010)

[Rie59] Riemann. *Ber. Akad. Wiss. Berlin* (1859)

so we use this to associate with our sum the value

$$1 + 2 + 3 + \dots \stackrel{“=”}{=} \zeta(-1) = -\frac{1}{12}. \tag{2.54}$$

While this is obviously not a valid equation, it extracts the unique, finite, physically relevant part. We will use a similar method in Section 2.7 to define the determinant of a differential operator.

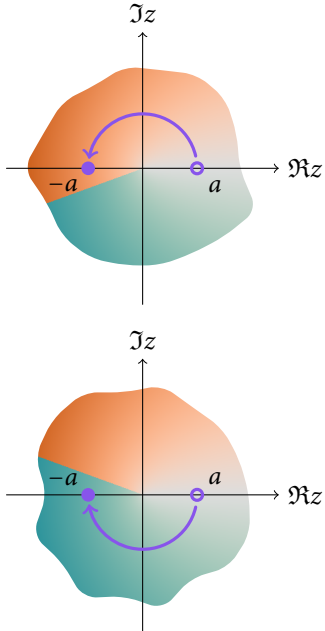


Figure 2.4.: The two ways of analytically continuing the square root to negative arguments given different branch cut choices. Color encodes the imaginary part of  $\sqrt{z}$ , blue is negative, red is positive.

## 2.6. Zero- and negative modes

In sections 2.3 and 2.4 we have assumed the matrix  $\mathbf{A}$  or operator  $A$  to be positive definite, corresponding to a true minimum in the saddle point approximation (where the Hessian is positive definite). But what if this constraint is not satisfied and one or several eigenvalues are zero or negative? The Gaussian integrals would diverge, so in the spirit of the last section we can only hope to obtain a result anyway using analytic continuation.

In fact, concerning negative eigenvalues we are done already: In the relation

$$\int_{-\infty}^{\infty} dx e^{-\frac{1}{2}ax^2} = \sqrt{\frac{2\pi}{a}} \tag{2.55}$$

the left hand side is analytic in  $a$  and converges for  $\Re a > 0$ , whereas the right hand side is analytic on the whole complex plane with a branch cut from 0 to  $\infty$ . It can thus in particular be continued to imaginary or negative real values of  $a$ , up to the ambiguity of continuing above or below zero (corresponding to branch cut choices along negative or positive imaginary parts, see Figure 2.4). Which choice is appropriate depends on the given situation, just as the solutions to a squared equation have to be checked for applicability to the original problem. In our case, the imaginary part of such an analytically continued Gaussian integral will be shown to give the rate of pair creation in an external field—we will therefore choose the branch cut to obtain a positive imaginary part.

A different problem is that of zero modes, occurring in Laplace’s method when the minimum of the function in the exponent is not a single point but, for example, a valley (see Figure 2.5). Here, the gradient of the two dimensional function vanishes everywhere along the dashed line. Laplace’s method will fail in this case, as the Hessian has a zero eigenvalue corresponding to the direction along the valley.

This difficulty arises in even simpler cases, for example rotationally symmetric integrals like

$$\mathcal{I} = \iint dx dy e^{-M(x^2+y^2)(x^2+y^2-2)} \left( = \frac{1}{2} \sqrt{\frac{\pi^3}{M}} \left( 1 + \operatorname{erf}(\sqrt{M}) \right) e^M \right). \tag{2.56}$$

Of course, we could immediately go over to polar coordinates, but let us for the moment pretend we did not know how to perform such a change of coordinates, only that there is some sort of transformation that leaves the integral invariant. Let us first try to naively perform Laplace’s method. Setting the gradient of the exponent in (2.56) to zero we find a maximum at  $x^2 + y^2 = 0$  and a collection of

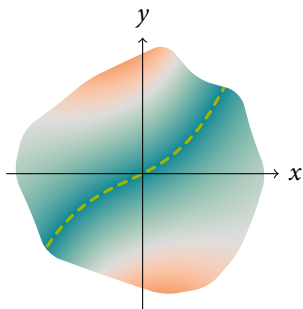


Figure 2.5.: A function  $f(x, y)$  with a valley, values increase from blue to red. Along the dashed line  $f(x, y)$  attains a minimum.

minima at  $x^2 + y^2 = 1$ . Substituting these minima into the exponent we obtain the correct exponential dependence ( $e^M$ ), so let us see if we can find an approximation to the prefactor as well. The Hessian is readily found from the second derivatives of the exponent but, alas, one of its eigenvalues (and thus its determinant) is  $4(x^2 + y^2 - 1) = 0$  at the minimum, so Laplace's method gives infinity. The corresponding eigenvector is  $\hat{e}_\phi$ , which is intuitively the invariant direction.

We can use the *Faddeev-Popov*-method [FP67] to separate the integration over this invariant direction from the rest. First, note the identity

$$1 = \frac{1}{w} \int d\phi \delta(\chi(\phi)) |\chi'(\phi)|, \quad (2.57)$$

where  $w$  is the number of real solutions  $\phi$  to  $\chi(\phi) = 0$ . The idea is now to choose a function  $\chi(x, y, \phi)$  where the condition  $\chi = 0$  fixes the zero mode in our original integral and  $\phi$  parametrizes the different ways to do so. Let  $f(x, y)$  denote a rotationally invariant function (as in (2.56)), so

$$\begin{aligned} \mathcal{I} &= \iint dx dy e^{-Mf(x,y)} \\ &= \frac{1}{w} \iint dx dy \int d\phi \delta(\chi(x, y, \phi)) |\chi'(x, y, \phi)| e^{-Mf(x,y)}, \end{aligned} \quad (2.58)$$

where  $\chi'(x, y, \phi)$  means the  $\phi$ -derivative. Now, by definition,  $f$  does not depend on  $\phi$ <sup>20</sup> so for every choice of  $\phi$  we can counteract this transformation by a change of coordinates to  $(x', y')$  so that  $\chi(x, y, \phi) = \chi(x', y', \phi_0)$ , making the  $\phi$ -integration trivial,

$$\begin{aligned} \mathcal{I} &= \frac{1}{w} \int d\phi \iint dx' dy' \delta(\chi(x', y', \phi_0)) |\chi'(x', y', \phi_0)| e^{-Mf(x',y')} \\ &= \frac{V_\phi}{w} \iint dx dy \delta(\chi(x, y, \phi_0)) |\chi'(x, y, \phi_0)| e^{-Mf(x,y)}, \end{aligned} \quad (2.59)$$

where  $V_\phi$  is the volume of the  $\phi$  integration range and we have relabeled  $(x', y')$  to  $(x, y)$  again.<sup>21</sup> For the case of rotational symmetry we can choose  $\chi = \sin(\phi)x + \cos(\phi)y$ , which restricts the region of integration to a line in the  $x - y$ -plane. For any given point  $(x, y)$ , if it lies on the  $\phi = \phi_0$  line it is also included in the line  $\phi = \phi_0 + \pi$ , so either we restrict the  $\phi$ -integration to  $[0, \pi)$  with  $w = 1$  or let it range over  $[0, 2\pi)$  with  $w = 2$ , in any case  $V_\phi/w = \pi$  (which makes the meaning of  $w$  clear, it compensates for over counting). Let us simply choose  $\phi_0 = 0$ . Then

$$\mathcal{I} = \pi \iint dx dy \delta(y) |x| e^{-Mf(x,y)} = \pi \int_{-\infty}^{\infty} dx |x| e^{-Mf(x,0)} = 2\pi \int_0^{\infty} dx x e^{-Mf(x,0)}, \quad (2.60)$$

renaming  $x$  to  $r$  we have successfully recovered integration in polar coordinates! In this case we were able to trivially perform one of the coordinate integrals due to the delta distribution, but in more complicated situations this is not necessarily true—usually the argument of the delta distribution is a function of many coordinates and it is not obvious how this cancels one integration. For a numerical treatment we can use a Gaussian limit representation of the delta distribution,

$$\delta(x) = \lim_{\varepsilon \rightarrow 0} \sqrt{\frac{M}{\varepsilon}} e^{-\pi \frac{M}{\varepsilon} x^2}, \quad (2.61)$$

[FP67] Faddeev and Popov. *Phys. Lett.* (1967)

<sup>20</sup> In the sense that the transform parametrized by  $\phi$  in the fixing condition leaves the integrand invariant.

<sup>21</sup> Remember that the form of  $f(x, y)$  did not change under the change of variables.

which can simply be included when performing Laplace's method. Of course, numerically taking the limit  $\varepsilon \rightarrow 0$  is not viable either, but as it turns out, for Laplace's method we do not have to. Using (2.61) in (2.59) the exponent gains an additional term proportional to  $\chi^2$

$$\mathcal{I} = \frac{V_\phi}{w} \iint dx dy \lim_{\varepsilon \rightarrow 0} \sqrt{\frac{M}{\varepsilon}} |\chi'(x, y, \phi_0)| e^{-M((f(x, y) + \frac{\pi}{\varepsilon} \chi^2(x, y, \phi_0)))}, \quad (2.62)$$

which is minimized when  $\chi = 0$ , so this implements fixing of the symmetry. Further note that if  $\chi = 0$  fixes the symmetry, then the vector  $\nabla \chi$  points in the invariant direction. Let us now check how this modifies the Hessian at the minimum.

$$\begin{aligned} \mathbf{H}(x_0, y_0) &= \mathbf{H}_f(x_0, y_0) + \frac{\pi}{\varepsilon} \nabla(\nabla \chi^2)|_{x_0, y_0} \\ &= \mathbf{H}_f(x_0, y_0) + 2\frac{\pi}{\varepsilon} (\nabla \chi \otimes \nabla \chi + \chi \nabla(\nabla \chi))|_{x_0, y_0}, \end{aligned} \quad (2.63)$$

where the second summand is zero at the minimum (because  $\chi = 0$ ). Now we can represent any diagonalizable matrix using its eigenvectors and  $\lambda$ -values, so writing  $\hat{\mathbf{e}}_i$  for the eigenvectors of  $\mathbf{H}_f$  and  $\lambda_i$  for its eigenvalues<sup>22</sup>

$$\begin{aligned} \mathbf{H}(x_0, y_0) &= \sum_i \lambda_i \hat{\mathbf{e}}_i \otimes \hat{\mathbf{e}}_i + 2\frac{\pi}{\varepsilon} \nabla \chi \otimes \nabla \chi|_{x_0, y_0} \\ &= \sum_{i>0} \lambda_i \hat{\mathbf{e}}_i \otimes \hat{\mathbf{e}}_i + (0 + 2\frac{\pi}{\varepsilon} |\nabla \chi|^2) \hat{\mathbf{e}}_0 \otimes \hat{\mathbf{e}}_0, \end{aligned} \quad (2.64)$$

where we have used that  $\nabla \chi$  is parallel to the eigenvector corresponding to the zero eigenvalue.<sup>23</sup> This shows that all other eigenvalues remain untouched, only the zero eigenvalue is replaced by a finite value. This can also be turned around to find a suitable choice of  $\chi$  if the zero mode is known,  $\chi(\phi, \mathbf{r}) = \hat{\mathbf{e}}_0(\phi) \cdot \mathbf{r}$ .

If we now take the determinant of the corrected Hessian we have

$$\det \mathbf{H}(x_0, y_0) = \frac{2\pi}{\varepsilon} |\nabla \chi|^2 \det^* \mathbf{H}_f(x_0, y_0) \quad (2.65)$$

where  $\det^*$  means the determinant omitting the zero mode. Inserting this determinant into Laplace's formula, the factor of  $\sqrt{\varepsilon}$  cancels, which means we can just set  $\varepsilon = 1$ . In practice, we neither need to explicitly remove the zero eigenvalue from the determinant nor compute  $|\nabla \chi|$ , we just apply Laplace's method to (2.62). For our toy example we again choose  $\chi(\phi) = \sin(\phi)x + \cos(\phi)y$  with  $\phi_0 = 0$ , so we need to minimize  $(x^2 + y^2)(x^2 + y^2 - 2) + \pi y^2$ . This now has the two solutions  $y = 0, x = \pm 1$ , both with value  $-1$ . The determinant of  $\mathbf{H}$  in both cases is  $16\pi$ ,  $V_\phi/w = \pi$  and  $|\chi| = 1$ . Because we have two equal contributions from each minimum, we obtain a factor of 2. The approximation to our integral is thus

$$\mathcal{I} \approx 2\pi \sqrt{M} \sqrt{\frac{(2\pi)^2}{M^2 16\pi}} e^M = \sqrt{\frac{\pi^3}{M}} e^M. \quad (2.66)$$

Indeed, comparing to (2.56), we see that

$$1 - \frac{\mathcal{I}}{\mathcal{I}_\infty} = \frac{1}{2} \left(1 - \operatorname{erf}(\sqrt{M})\right) \xrightarrow{M \rightarrow \infty} 0 \quad (2.67)$$

exponentially.

<sup>22</sup> In our toy example there are only two eigenvectors of course, but this immediately generalizes to any dimension, hence the notation.

<sup>23</sup> But not necessarily normalized, hence the norm squared.

## 2.7. Determinants of differential operators

In multiple contexts it is necessary to evaluate determinants of differential operators, for example in (2.49). Let  $L$  be some linear differential operator acting on the space of sufficiently smooth functions on the interval  $[0, 1]$ . Then the determinant of this operator can formally be expressed as

$$\text{Det}(L) = \prod_i \lambda_i, \quad (2.68)$$

$\lambda_i$  denoting the eigenvalues of  $L$ .

Usually however, (2.68) is ill-defined, as the  $\lambda_i$  grow unbounded and the product does not converge. To cope with these infinities, most of the time only ratios between determinants are computed, for example

$$\frac{\text{Det}(L)}{\text{Det}(L_0)}, \quad (2.69)$$

where  $L_0$  denotes some sort of *trivial* or *known* variant of  $L$ . In quantum field theory  $L$  could be a field operator in the presence of a background, while  $L_0$  describes the free theory. The reasoning for (2.69) is that the asymptotic behavior of the eigenvalues  $\lambda_i$  and  $\lambda_{0,i}$  is the same and cancels in the ratio.

This does not immediately help to actually calculate (2.69), as there is no obvious way to separate the *interesting* part from the divergent part that cancels in the ratio. In physical theories, the process of removing such divergent contributions is called *regularization*.

### Zeta function regularization

One such method to make sense of the expression (2.69) is *zeta function regularization*. We can use a method similar to the one in Section 2.5 to define the functional determinant by analytic continuation. First, we define the *operator zeta function* of  $L$  as

$$\zeta_L(s) := \sum_i \lambda_i^{-s}, \quad (2.70)$$

for  $\Re(s)$  sufficiently large,  $\lambda_i$  again denoting the eigenvalues of  $L$ . It can also be analytically continued, allowing us to *define* the functional determinant as

$$\text{Det}(L) = \exp(-\zeta'_L(0)), \quad (2.71)$$

or, for a ratio of determinants

$$\frac{\text{Det}(L)}{\text{Det}(L_0)} = \exp(-(\zeta'_L(0) - \zeta'_{L_0}(0))). \quad (2.72)$$

The motivation for this definition can be seen by formally evaluating

$$\exp(-\zeta'_L(0)) \stackrel{“=”}{=} \exp\left(-\sum_i \frac{-\log \lambda_i}{\lambda_i^s}\right) \Big|_{s=0} = \prod_i \lambda_i. \quad (2.73)$$

## 2.8. Gel'fand-Yaglom formula

There is a beautiful, and not at all obvious, way to reduce the calculation of an operator determinant to a finite determinant over solutions of an ordinary differential equation. This method is due to Gel'fand and Yaglom [GY60], who introduced it by discretizing the operator, finding a difference equation for the  $N$ -dimensional determinant that turns into a differential equation in the limit  $N \rightarrow \infty$ . A similar approach is detailed in [Kle09]. We will however quickly sketch an alternative derivation following the very clear approach by Kirsten and McKane [KM03] that uses the operator zeta function defined in the last section.

Assume that  $L$  is a second order differential operator over the interval  $[0, 1]$  with strictly positive eigenvalues. Let  $\eta_k$  be the (unique) solution to the initial value problem

$$(L - k^2)\eta_k(x) = 0, \quad \eta_k(0) = 0, \quad \eta'_k(0) = 1, \quad (2.74)$$

with complex parameter  $k$ . Demanding that  $\eta_k(1) \stackrel{!}{=} 0$  then fixes the eigenvalues  $\lambda_i = k_i^2$  of the operator. Let us consider  $f(k) := \eta_k(1)$  as a function of the complex variable  $k$ . Then its logarithmic derivative  $\frac{d}{dk} \ln(f(k))$  has simple poles for all  $k_i$  that satisfy the eigenvalue condition. Thus, for any smooth function  $g(k)$  we have

$$\int_{\gamma} dk g(k) \frac{d}{dk} \ln(f(k)) = 2\pi i \sum_i g(k_i), \quad (2.75)$$

for a curve  $\gamma$  that includes all eigenvalues  $k_i$  in counter-clockwise orientation (see Figure 2.6). In particular, we can use this to write the operator zeta function as

$$\zeta_L(s) = \sum_i (k_i^2)^{-s} = \frac{1}{2\pi i} \int_{\gamma} dk k^{-2s} \frac{d}{dk} \ln(\eta_k(1)), \quad (2.76)$$

and the difference

$$\zeta_L(s) - \zeta_{L_0}(s) = \frac{1}{2\pi i} \int_{\gamma} dk k^{-2s} \frac{d}{dk} \ln \left( \frac{\eta_k(1)}{\eta_{0,k}(1)} \right). \quad (2.77)$$

We now assume, as mentioned before, that the asymptotic behavior of the operators  $L$  and  $L_0$  is the same, so that

$$\frac{d}{dk} \ln \left( \frac{\eta_k(1)}{\eta_{0,k}(1)} \right) \rightarrow 0, \quad \text{for } |k| \rightarrow \infty, \quad (2.78)$$

and we can “bend open” the integration path  $\gamma$  in Figure 2.6 to range from  $+\infty$  to

[GY60] Gel'fand and Yaglom. *J. Math. Phys.* (1960)

[Kle09] Kleinert. *World Scientific* (2009)

[KM03] Kirsten and McKane. *Ann. Phys.* (2003)

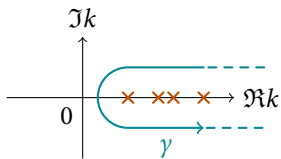


Figure 2.6.: Integration curve in the complex plane that includes all eigenvalues of the operator  $L$ .

–∞ along the imaginary axis to give

$$\begin{aligned}
 \zeta_L(s) - \zeta_{L_0}(s) &= \frac{1}{2\pi i} \int_{-\infty}^{\infty} dk (ik)^{-2s} \frac{d}{dk} \ln \left( \frac{\eta_{ik}(1)}{\eta_{0,ik}(1)} \right) \\
 &= \frac{1}{2\pi i} \left( - \int_0^{\infty} \frac{dk}{(ik)^{2s}} + \int_0^{-\infty} \frac{dk}{(ik)^{2s}} \right) \frac{d}{dk} \ln \left( \frac{\eta_{ik}(1)}{\eta_{0,ik}(1)} \right) \\
 &= \frac{1}{2\pi i} (-i^{-2s} + (-i)^{-2s}) \int_0^{\infty} \frac{dk}{k^{2s}} \frac{d}{dk} \ln \left( \frac{\eta_{ik}(1)}{\eta_{0,ik}(1)} \right) \\
 &= \frac{\sin(\pi s)}{\pi} \int_0^{\infty} \frac{dk}{k^{2s}} \frac{d}{dk} \ln \left( \frac{\eta_{ik}(1)}{\eta_{0,ik}(1)} \right), \tag{2.79}
 \end{aligned}$$

where in the third line we have used that the eigenvalue equation (2.74) is invariant under the replacement  $ik \rightarrow -ik$ , so  $\eta_{-ik}(x) = \eta_{ik}(x)$  because the solution is unique. According to (2.72) we need the  $s$ -derivative evaluated at  $s = 0$ , so

$$\begin{aligned}
 \zeta'_L(0) - \zeta'_{L_0}(0) &= \cos(0) \int_0^{\infty} dk \frac{d}{dk} \ln \left( \frac{\eta_{ik}(1)}{\eta_{0,ik}(1)} \right) + \frac{\sin(0)}{\pi} \times \dots \\
 &= \ln \left( \frac{\eta_{ik}(1)}{\eta_{0,ik}(1)} \right) \Big|_0^{\infty} = \ln \left( \frac{\eta_{k=0}(1)}{\eta_{0,k=0}(1)} \right), \tag{2.80}
 \end{aligned}$$

where we have again used that the  $k \rightarrow \infty$  behavior of  $\eta$  and  $\eta_0$  is the same. The final result is thus

$$\frac{\text{Det}(L)}{\text{Det}(L_0)} = \exp(-(\zeta'_L(0) - \zeta'_{L_0}(0))) = \frac{\eta(1)}{\eta_0(1)}, \tag{2.81a}$$

where

$$L\eta(x) = 0, \quad \eta(0) = 0, \quad \eta'(0) = 1, \tag{2.81b}$$

and the same for  $L_0$  and  $\eta_0$ . If the interval is not  $[0, 1]$ , a simple rescaling of  $x$  shows that the result is the same, with the solution  $\eta$  evaluated at the end of the interval. Equation (2.81) is called *Gel'fand-Yaglom formula*. In [KM04] Kirsten and McKane also show how to extend these results to other boundary conditions and multidimensional operators. We will just state the result, the derivation is similar to the one above but more cumbersome. For matrix-valued operators  $\Lambda_{\mu\nu}$  the determinant is given by

$$\frac{\text{Det}(\Lambda_{\mu\nu})}{\text{Det}(\Lambda_{0,\mu\nu})} = \frac{\det(\eta_{\mu}^{(v)}(1))}{\det(\eta_{0,\mu}^{(v)}(1))}, \tag{2.82a}$$

where the finite dimensional determinant is performed with respect to the indices  $\mu$  and  $\nu$  and

$$\Lambda_{\mu\nu}\eta_{\nu}(x) = 0, \quad \eta_{\mu}^{(v)}(0) = 0, \quad \eta_{\mu}^{(v)'}(0) = \delta_{\mu\nu}. \tag{2.82b}$$

[KM04] Kirsten and McKane. *J. Phys. A* (2004)

<sup>24</sup> It is related to the partition function of a quantum harmonic oscillator, although the context does not matter for this example.

Let us now apply the one-dimensional result to a toy example, the following ratio of determinants<sup>24</sup>

$$\frac{\text{Det}(-\partial_\tau^2 + \omega^2)}{\text{Det}(-\partial_\tau^2)}, \quad 0 \leq \tau \leq \beta. \quad (2.83)$$

We first compute the ratio explicitly. We need to find all eigenfunctions vanishing for  $\tau = 0$  and  $\tau = \beta$ , so

$$\begin{aligned} (-\partial_\tau^2 + \omega^2)f_\lambda(\tau) = \lambda f_\lambda(\tau) &\Leftrightarrow \ddot{f}_\lambda(\tau) = -(\lambda - \omega^2)f_\lambda(\tau) \\ \simeq f_\lambda(\tau) = \sin(\sqrt{\lambda - \omega^2}\tau), \quad 0 \stackrel{!}{=} f_\lambda(\beta) &\rightarrow \lambda_n = \omega^2 + \left(\frac{\pi n}{\beta}\right)^2. \end{aligned} \quad (2.84)$$

The ratio of determinants is thus

$$\frac{\text{Det}(-\partial_\tau^2 + \omega^2)}{\text{Det}(-\partial_\tau^2)} = \prod_{n=1}^{\infty} \frac{\omega^2 + \left(\frac{\pi n}{\beta}\right)^2}{0 + \left(\frac{\pi n}{\beta}\right)^2} = \prod_{n=1}^{\infty} \left(1 + \left(\frac{\omega\beta}{\pi n}\right)^2\right) = \frac{\sinh(\omega\beta)}{\omega\beta}. \quad (2.85)$$

Let us now apply (2.81) instead. We need to find the solution to

$$(-\partial_\tau^2 + \omega^2)\eta(\tau) = 0, \quad \eta(0) = 0, \quad \dot{\eta}(0) = 1, \quad (2.86)$$

which is given by  $\eta(\tau) = \sinh(\omega\tau)/\omega$ . The solution for the denominator,

$$-\partial_\tau^2\eta_0(\tau) = 0, \quad \eta_0(0) = 0, \quad \dot{\eta}_0(0) = 1, \quad (2.87)$$

is just  $\eta_0(\tau) = \tau$ . We immediately recover the same ratio

$$\frac{\text{Det}(-\partial_\tau^2 + \omega^2)}{\text{Det}(-\partial_\tau^2)} = \frac{\eta(\beta)}{\eta_0(\beta)} = \frac{\sinh(\omega\beta)}{\omega\beta}. \quad (2.88)$$

In general, it is usually much easier to find a single solution to (2.81) than to find the whole spectrum of the operator and perform the infinite product.

# 3

## Riccati formalism

*This chapter contains a derivation of the Riccati formalism for pair production, which is an exact method starting from a mode decomposition of the field equations. We will use numerical solutions to the Riccati equation as references in future chapters to check different approximations.*

### 3.1. Introduction

Although the main focus of this thesis are the titular worldline instantons, we will first introduce a different approach to calculate the pair production rate for spatially homogeneous, time dependent electric fields. The first advantage of the *Riccati equation* derived in the following section is that it is closer in spirit to the qualitative picture of pair creation given in Section 1.4. The second advantage is that it can be numerically integrated without resorting to approximations,<sup>25</sup> which will be explained in Section 3.3. This way we can use numerical solutions of the Riccati equation as a baseline to compare other solutions to.

The main idea of the method is to consider electric background fields that vanish for  $t \rightarrow \pm\infty$ , expand the field operators describing the electrons and positrons into one set of single particle solutions for the distant past, and another set in the distant future, after the electric field was switched on and off again. We then find a way to determine the time evolution of the expansion coefficients interpolating between these sets, which tell us if an initial negative energy state turns into a mixture of positive and negative energy states due to the interaction with the electric background field. This corresponds to an electron tunneling through the forbidden region creating an electron-positron pair.

### 3.2. Derivation of the Riccati formalism

Because we will only consider spatially homogeneous background fields, we can work in  $1 + 1$  spacetime dimensions which simplifies the derivation. The starting point is the Dirac equation coupled to a classical potential<sup>26</sup> (bold type denoting spinorial objects)

$$(i\boldsymbol{\gamma}^\mu(\partial_\mu + iqA_\mu(t, x)) - m\mathbb{1}) \cdot \boldsymbol{\psi}(t, x) = 0, \quad \mu \in \{0, 1\}. \quad (3.1)$$

In this case, we only need two  $2 \times 2$  matrices for the  $\boldsymbol{\gamma}^\mu$  and we choose

$$\boldsymbol{\gamma}^0 = \sigma_z, \quad \boldsymbol{\gamma}^1 = i\sigma_y. \quad (3.2)$$

<sup>25</sup> Apart from the numerical discretization of course, but this can be, in principle, made arbitrarily precise.

**[A]** =  $\mathbf{L}^{-1}$ ,  $\mathbf{x}_i = -\mathbf{x}^i$   
(see page 13).

<sup>26</sup> We simply assume right now that this describes the physics we are interested in, more detail on the physical model will be given in Section 4.1

We also use temporal gauge for the vector potential and assume it to be spatially homogeneous, that is<sup>27</sup>

$$E(t) = \partial_t A^1(t) =: \partial_t A(t), \quad A^0 = 0. \quad (3.3)$$

Thus, multiplying by  $\gamma^0 = \sigma_z$ , the Dirac equation reads

$$i\partial_t \psi(t, x) = (-i\sigma_x(\partial_x + iqA(t)) + m\sigma_z) \cdot \psi(t, x). \quad (3.4)$$

Because the electric field is spatially homogeneous, we can expand the spinor  $\psi(t, x)$  into Fourier modes:

$$\psi(t, x) = \int_{-\infty}^{\infty} \frac{dk}{2\pi} \phi_k(t) e^{ikx}, \quad (3.5)$$

leading to<sup>28</sup>

$$i\partial_t \phi_k(t) = ((k + qA(t))\sigma_x + m\sigma_z) \cdot \phi_k(t) = \mathbf{M}_k(t) \cdot \phi_k(t) \quad (3.6)$$

with the spinor matrix

$$\mathbf{M}_k(t) = \begin{pmatrix} m & k + qA(t) \\ k + qA(t) & -m \end{pmatrix}. \quad (3.7)$$

We can decouple (3.6) by diagonalizing the Matrix  $\mathbf{M}_k$ . Its eigenvalues and (normalized) eigenvectors are

$$\mathbf{M}_k(t) \cdot \mathbf{u}_k(t) = +\Omega_k(t) \mathbf{u}_k(t), \quad (3.8)$$

$$\mathbf{M}_k(t) \cdot \mathbf{v}_k(t) = -\Omega_k(t) \mathbf{v}_k(t),$$

with

$$\Omega_k(t) = \sqrt{m^2 + (k + qA(t))^2},$$

$$\mathbf{u}_k = \frac{1}{\sqrt{1 + \xi_k^2}} \begin{pmatrix} 1 \\ \xi_k \end{pmatrix}, \quad \xi_k = \frac{k + qA(t)}{m + \Omega_k(t)}, \quad (3.9)$$

$$\mathbf{v}_k = \frac{1}{\sqrt{1 + \xi_k^2}} \begin{pmatrix} -\xi_k \\ 1 \end{pmatrix}.$$

Using these eigenvectors we can now construct an *Ansatz* for (3.6)

$$\phi_k = \alpha_k(t) \mathbf{u}_k(t) e^{-iS_k(t)} + \beta_k(t) \mathbf{v}_k(t) e^{+iS_k(t)}, \quad S_k(t) = \int_{-\infty}^t dt' \Omega_k(t'), \quad (3.10)$$

where we have separated the phase  $S_k(t)$ . In the absence of an electric field, the phase is just that of a single, free particle of definite energy,  $S_k(t) = \Omega_k t$ . The coefficient  $\alpha_k(t)$  thus gives the positive energy part,  $\beta_k(t)$  the negative energy part of the spinor. This identification is only possible when no field is present, so it is important that  $E(t = -\infty) = 0$  to construct an initial state with positive

<sup>27</sup> Note that the “vector potential”  $A(t)$  and the electric field are scalar here, as there is only one spatial dimension.

<sup>28</sup> Note that  $k$  is a label of momentum modes, not an index that is summed over.

energy only, and  $E(t = \infty) = 0$  to interpret the final state. By demanding that  $\phi_k$  be normalized, it follows that  $|\alpha_k(t)|^2 + |\beta_k(t)|^2 = 1$ .

Inserting the Ansatz into (3.6) and projecting either onto  $\mathbf{u}_k$  or onto  $\mathbf{v}_k$  we get the following system of differential equations for the coefficients  $\alpha_k$  and  $\beta_k$ :

$$\begin{aligned}\dot{\alpha}_k(t) &= +\Xi_k(t)\beta_k(t)e^{+2iS_k(t)}, \\ \dot{\beta}_k(t) &= -\Xi_k(t)\alpha_k(t)e^{-2iS_k(t)},\end{aligned}\tag{3.11}$$

using the abbreviation

$$\Xi_k(t) = \dot{\mathbf{u}}_k \cdot \mathbf{v}_k = -\dot{\mathbf{v}}_k \cdot \mathbf{u}_k = \frac{mq\dot{A}(t)}{2\Omega_k(t)^2}.\tag{3.12}$$

While we could directly integrate the system of equations (3.11), we do not need  $\alpha_k$  and  $\beta_k$  separately. We instead consider the ratio  $R_k(t) := \alpha_k(t)/\beta_k(t)$ , so that

$$\dot{R}_k(t) = \frac{\dot{\alpha}_k(t)}{\beta_k(t)} - \frac{\alpha_k(t)\dot{\beta}_k(t)}{\beta_k^2(t)} = \Xi_k(t) \left( e^{+2iS_k(t)} + R_k^2(t)e^{-2iS_k(t)} \right).\tag{3.13}$$

In principle, all equations of the type

$$\dot{y}(t) = f(t) + g(t)y(t) + h(t)y^2(t),\tag{3.14}$$

i.e. first order differential equations that are quadratic in the unknown, are called Riccati equations. In the context of pair creation however, (3.13) is generally referred to as *the* Riccati equation.

If we now consider a state in mode  $k$  with negative energy initially, that is  $\alpha_k(-\infty) = 0$ ,  $\beta_k(-\infty) = 1$ , so  $R_k(-\infty) = 0$  and evolve  $R_k$  according to (3.13), we can read off the pair production probability as

$$|\alpha_k(\infty)|^2 = \frac{|R_k(\infty)|^2}{1 + |R_k(\infty)|^2} \approx |R_k(\infty)|^2,\tag{3.15}$$

because we expect  $|R_k(\infty)|^2$  to be small. There are now two approaches to tackle (3.13), either by neglecting the term proportional to  $R_k^2(t)$ , which means the solution is immediately given as an ordinary integral that can be approximated analytically using methods of complex analysis, or by numerically solving the full equation. We will only consider the latter here.

### 3.3. Numerical evaluation

To numerically integrate the Riccati equation (3.13), we first have to bring all quantities into dimensionless forms. We choose to represent the time dependent vector potential using a dimensionless function  $f$ :

$$A(t) = \frac{E}{\omega}f(\omega t), \quad \dot{A}(t) = Ef'(\omega t),\tag{3.16}$$

with a scaling frequency  $\omega$ . Using this definition:

$$\Omega_k(t) = m\sqrt{1 + \left( \frac{k}{m} + \frac{qE}{m\omega}f(\omega t) \right)^2},\tag{3.17}$$

which motivates letting

$$p = \frac{k}{m}, \quad \gamma = \frac{m\omega}{qE}, \quad \tau = \frac{tqE}{m}. \quad (3.18)$$

[Kel65] Keldysh. *J. Exp. Theor. Phys.* (1965)

The quantity  $\gamma$  is known as the *Keldysh parameter* [Kel65], and as it turns out it is a natural parameter to describe the dependence of pair production on the timescale of a field varying with time. Consequently,

$$S_p(\tau) = \frac{m^2}{qE} \int_{-\infty}^{\tau} d\tau' \sqrt{1 + (p + f(\gamma\tau')/\gamma)^2}, \quad (3.19)$$

where we can now express the electric field strength via the critical Schwinger field:

$$\frac{E}{E_S} = \frac{qE}{m^2}. \quad (3.20)$$

Using the same substitutions for  $\Xi$  we arrive at the dimensionless Riccati equation

$$\begin{aligned} \dot{R}_p(\tau) = & \frac{\frac{E}{E_S} f'(\gamma\tau)}{2 \left( 1 + \left( p + \frac{f(\gamma\tau)}{\gamma} \right)^2 \right)} \\ & \times \left( \exp \left( i \frac{E_S}{E} 2\varphi_p(\tau) \right) + R_p^2(\tau) \exp \left( -i \frac{E_S}{E} 2\varphi_p(\tau) \right) \right), \end{aligned} \quad (3.21a)$$

$$\dot{\varphi}_p(\tau) = \sqrt{1 + \left( p + \frac{f(\gamma\tau)}{\gamma} \right)^2}, \quad (3.21b)$$

where the dot now denotes a derivative with respect to  $\tau$ .

While the solution for  $\varphi_p = \frac{E}{E_S} S_p$  in (3.21) could be immediately expressed as an integral, this is not optimal for the numerical solution. Because the integral can in general only be evaluated numerically, this would have to be done at each integration step of  $R(\tau)$ <sup>29</sup>. Therefore it is far more efficient to solve the system of differential equations (3.21) for  $R$  and  $\varphi$  in lockstep.

Usually, numerically solving an initial value problem like (3.21) is simple enough and many general purpose algorithms exist. The problem however is that the coefficients, and consequently the solution, oscillate at a frequency of order  $\frac{E_S}{E}$ . This means a small step size has to be chosen to correctly capture the solution's behavior. On the other hand, we wish to integrate from  $\tau = -\infty$  to  $\tau = \infty$ , which of course is not possible in practice, so we have to choose an integration range  $\tau \in [-T/2, T/2]$  with  $T$  sufficiently large. The combination of ever smaller time steps and large integration range means that even for high order numerical schemes, rounding errors quickly become dominant. This has limited numerical results using the Riccati equation, or equivalently the quantum kinetic equation [Sch+98], to field strengths above  $E \approx E_S/10$ , e.g. in [OHA11; DD11; Koh+13].

A simple solution to the problem is to just use higher precision in the calculation. A standard library for arbitrary precision arithmetic is the GNU MPFR package [Fou+07], which implements elementary arithmetic operations on floating point numbers with a user specified number of bits, only limited by computer

<sup>29</sup> Alternatively, it could be pre-computed for different values of  $\tau$ , however due to the adaptive integration algorithm for  $\dot{R}$  it is not known beforehand which values of  $\tau$  are actually needed. Consequently, either performance or accuracy (or both in different regions) suffers.

[Sch+98] Schmidt et al. *Int. J. Mod. Phys. E* (1998)

[OHA11] Orthaber, Hebenstreit, and Alkofer. *Phys. Lett. B* (2011)

[DD11] Dumlu and Dunne. *Phys. Rev. D* (2011)

[Koh+13] Kohlfürst, Mitter, Von Winckel, Hebenstreit, and Alkofer. *Phys. Rev. D* (2013)

[Fou+07] Fousse, Hanrot, Lefèvre, Pélissier, and Zimmermann. *ACM Trans. Math. Softw.* (2007)

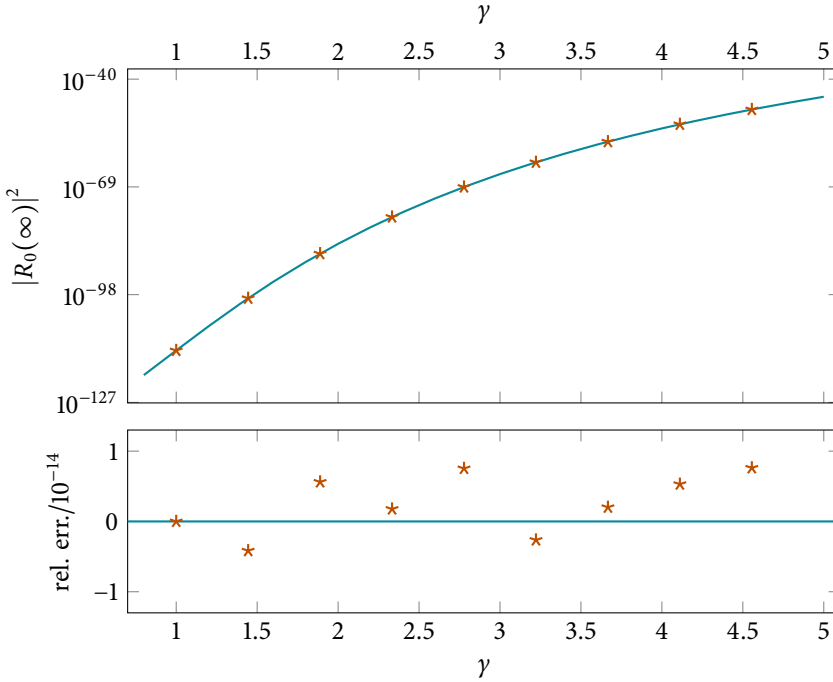


Figure 3.1.: Comparison of the numerical calculation to the exactly known result (3.23) for the Sauter pulse (3.22) for  $E = 10^{-2}m^2/q$ . The top panel shows the resulting pair creation while the bottom panel contains the residual numerical error (less than one part in  $10^{14}$ ).

memory. A software implementation of the Taylor series method for ordinary differential equations that employs MPFR is the freely available TIDES [Aba+12]. Originally devised for the study of unstable orbits and chaotic systems [ABD11; Den+12], it consists of a Mathematica package to preprocess the differential equations and a C library to perform the integration.

To check the accuracy of the numerical implementation we turn to a simple example, the single temporal pulse (we can not compare to a static field, because we need the field to vanish for large positive and negative time)

$$f(\gamma\tau) = \tanh(\gamma\tau) \quad \rightsquigarrow \quad \mathbf{E} = E \cosh^{-2}(\omega t) \mathbf{e}_z. \quad (3.22)$$

In analogy to the spatial profile he considered in [Sau32] we call this field a *Sauter pulse*. The pair production rate can be obtained analytically in this case (as Sauter did for the spatial profile), for a derivation see [Heb11]. The analytical result for the mode  $p = 0$  reads

$$|R_0(\infty)|^2 = \frac{\sinh^2\left(\frac{\pi m^2}{qE} \frac{1}{\gamma^2}\right)}{\sinh^2\left(\frac{\pi m^2}{qE} \frac{\sqrt{1+\gamma^2}}{\gamma^2}\right)}. \quad (3.23)$$

We use TIDES to integrate (3.21) for the field (3.22) and multiple choices of  $\gamma$  from  $\tau = -100$  to  $\tau = 100$  using 100 digits of precision. Figure 3.1 shows this data and the analytical expression (3.23). Even for this weak field strength (and thus very low pair creation probability) the results agree to high precision. If we were to choose an even weaker field strength we would have to increase the number of digits in the calculation, which increases the (moderate) runtime and memory usage, but there is no other limit in principle.

Further (more interesting) applications will be presented in chapters 6 and 7.

[Aba+12] Abad, Barrio, Blesa, and Rodríguez. *ACM Trans. Math. Softw.* (2012)

[ABD11] Abad, Barrio, and Dena. *Phys. Rev. E* (2011)

[Den+12] Dena, Rodríguez, Ser-rano, and Barrio. *Abstr. Appl. Anal.* (2012)

[Sau32] Sauter. *Z. Phys.* (1932)

[Heb11] Hebenstreit. *PhD thesis* (2011)



## 4

## Worldline instanton method

This chapter contains a derivation of the worldline path integral and the worldline instanton approximation. It also describes a discretization scheme that lends itself well to numerical computation.

## 4.1. Physical model

To keep the derivation in this chapter as self-contained as possible, we will first discuss two physical models (scalar and spinor quantum electrodynamics) in canonical quantization. This helps to motivate why the mathematical objects we work on actually describe the physical effects we are interested in. The derivation in this section mostly follows [PS95].

We start with the simplest possible case, a real scalar field. The central object defining the physical theory is the Lagrangian density, in this case

$$\mathcal{L} = \frac{1}{2}(\partial_\mu\phi)(\partial^\mu\phi) - \frac{1}{2}m^2\phi^2, \quad (4.1)$$

where  $\phi$  is a field depending on space and time and  $m$  simply some parameter (for now). Deriving the Euler-Lagrange equations for this Lagrangian,<sup>30</sup>

$$0 = \partial_\mu \frac{\partial\mathcal{L}}{\partial(\partial_\mu\phi)} - \frac{\partial\mathcal{L}}{\partial\phi} = (\partial_\mu\partial^\mu + m^2)\phi, \quad (4.2)$$

we obtain the Klein-Gordon equation mentioned before. We can immediately write down plane wave solutions

$$\phi_p = \exp(ip_\mu x^\mu), \quad \text{with } p_\mu p^\mu = m^2. \quad (4.3)$$

The restriction on  $p_\mu$  can be rewritten as  $p_0 = \pm\sqrt{m^2 + \mathbf{p}^2}$ , which already looks a whole lot like the relativistic energy-momentum relation, except for the unintuitive solutions of negative energy.

We can learn something more about this classical system using *Noether's theorem* [Noe18]. For any infinitesimal transformation of the field that changes the Lagrangian up to a divergence only (and thus does not affect the action)

$$\phi \rightarrow \phi + \varepsilon\Delta\phi, \quad \mathcal{L} \rightarrow \mathcal{L} + \varepsilon\partial_\mu J^\mu \quad (4.4)$$

we have a corresponding conserved current<sup>31</sup>

$$\partial_\mu j^\mu = 0, \quad j^\mu = \frac{\partial\mathcal{L}}{\partial(\partial_\mu\phi)}\Delta\phi - J^\mu. \quad (4.5)$$

[PS95] Peskin and Schroeder. *Westview Press* (1995)

[A] =  $\mathbf{L}^{-1}$ ,  $\mathbf{x}_i = -\mathbf{x}^i$   
(see page 13).

<sup>30</sup> Although slightly imprecise, we mostly use the terms *La-grangian* and *Lagrangian density* interchangeably.

[Noe18] Noether. *Nachr. d. Königl. Gesellsch. d. Wiss. zu Göttingen, Math-Phys. Klasse* (1918)

<sup>31</sup> If the transformation affects multiple fields in the Lagrangian, they have to be summed over.

The Klein-Gordon Lagrangian (4.1) does not explicitly depend on spacetime, so we can find conserved currents corresponding to spacetime translations:<sup>32</sup>

$$\phi(x^\mu) \rightarrow \phi(x^\mu + \varepsilon^\mu) = \phi + \varepsilon^\nu \partial_\nu \phi(x^\mu) + O(\varepsilon^2) \quad (4.6)$$

for infinitesimal  $\varepsilon^\mu$ <sup>33</sup>, and the same in the Lagrangian density

$$\mathcal{L} \rightarrow \mathcal{L} + \varepsilon^\nu \partial_\nu \mathcal{L} = \mathcal{L} + \varepsilon^\nu \partial_\mu (\delta^\mu_\nu \mathcal{L}), \quad (4.7)$$

where we used the last step to write the change as a proper four-divergence for each component of  $\varepsilon^\nu$ . The four conserved currents from spacetime translations taken together form the *energy-momentum-tensor*

$$T^\mu_\nu = \frac{\partial \mathcal{L}}{\partial (\partial_\mu \phi)} \partial_\nu \phi - \delta^\mu_\nu \mathcal{L}. \quad (4.8)$$

The conserved charge corresponding to time translations is the Hamiltonian,

$$H = \int d^3x \mathcal{H} = \int d^3x T^{00}, \quad (4.9)$$

so the Hamiltonian density is given by

$$\mathcal{H} = T^{00} = \pi \dot{\phi} - \mathcal{L} = \frac{1}{2} \pi^2 + \frac{1}{2} (\nabla \phi)^2 + \frac{1}{2} m^2 \phi^2, \quad (4.10)$$

using the definition of the canonical momentum

$$\pi := \frac{\partial \mathcal{L}}{\partial \dot{\phi}} = \dot{\phi}, \quad (4.11)$$

in this case. The charge corresponding to spatial translations is the total momentum<sup>34</sup>

$$P^i = \int d^3x \mathcal{P}^i = \int d^3x T^{0i} \quad (4.12)$$

so

$$P^i = T^{0i} = -T^0_i = -\pi \partial_i \phi. \quad (4.13)$$

We can now begin to build a quantum theory, by promoting the fields  $\phi$  and  $\pi$  (and thus also the Hamiltonian) to quantum mechanical operators and imposing the canonical commutation relations<sup>35</sup>

$$[\hat{\phi}(\mathbf{x}), \hat{\pi}(\mathbf{y})] = i\delta^3(\mathbf{x} - \mathbf{y}), \quad [\hat{\phi}(\mathbf{x}), \hat{\phi}(\mathbf{y})] = [\hat{\pi}(\mathbf{x}), \hat{\pi}(\mathbf{y})] = 0. \quad (4.14)$$

Let us now try to find the spectrum of our Hamiltonian operator. Guided by the solutions of the Klein-Gordon equation we try expanding the operators into plane waves

$$\hat{\phi}(\mathbf{x}) = \int \frac{d^3p}{(2\pi)^3} \frac{1}{\sqrt{2\omega_p}} (\hat{a}_p e^{i\mathbf{p}\cdot\mathbf{x}} + \hat{a}_p^\dagger e^{-i\mathbf{p}\cdot\mathbf{x}}), \quad (4.15a)$$

$$\hat{\pi}(\mathbf{x}) = \int \frac{d^3p}{(2\pi)^3} (-i) \sqrt{\frac{\omega_p}{2}} (\hat{a}_p e^{i\mathbf{p}\cdot\mathbf{x}} - \hat{a}_p^\dagger e^{-i\mathbf{p}\cdot\mathbf{x}}), \quad (4.15b)$$

<sup>32</sup> For the rest of the section we will drop the symbol denoting higher order terms. All equalities are to be understood as valid to first order in  $\varepsilon$ .

<sup>33</sup> These are four separate transformations, leading to four separate conserved currents.

<sup>34</sup> The *physical* momentum, in contrast to the *canonical* momentum.

<sup>35</sup> In direct analogy to the non-relativistic case with  $\hat{x}$  and  $\hat{p}$ .

with some clever normalization and  $\omega_{\mathbf{p}} = \sqrt{m^2 + \mathbf{p}^2}$ . We can invert these definitions to obtain the operator  $\hat{a}_{\mathbf{p}}$  and its adjoint  $\hat{a}_{\mathbf{p}}^\dagger$ . The following combination does the trick:

$$\begin{aligned} & \int d^3x \sqrt{\frac{\omega_{\mathbf{k}}}{2}} \left( \hat{\phi}(\mathbf{x}) + \frac{i}{\omega_{\mathbf{k}}} \hat{\pi}(\mathbf{x}) \right) e^{-i\mathbf{k}\cdot\mathbf{x}} \\ &= \int d^3p \underbrace{\int \frac{d^3x}{(2\pi)^3} e^{i(\mathbf{p}-\mathbf{k})\cdot\mathbf{x}}}_{\delta^3(\mathbf{p}-\mathbf{k})} \sqrt{\frac{\omega_{\mathbf{k}}}{2}} \left[ \frac{\hat{a}_{\mathbf{p}} + \hat{a}_{-\mathbf{p}}^\dagger}{\sqrt{2\omega_{\mathbf{p}}}} + \sqrt{\frac{\omega_{\mathbf{p}}}{2}} \frac{\hat{a}_{\mathbf{p}} - \hat{a}_{-\mathbf{p}}^\dagger}{\omega_{\mathbf{k}}} \right] \\ &= \hat{a}_{\mathbf{k}} \end{aligned} \quad (4.16)$$

and the corresponding expression for the adjoint,

$$\hat{a}_{\mathbf{k}}^\dagger = \int d^3x \sqrt{\frac{\omega_{\mathbf{k}}}{2}} \left( \hat{\phi}(\mathbf{x}) - \frac{i}{\omega_{\mathbf{k}}} \hat{\pi}(\mathbf{x}) \right) e^{+i\mathbf{k}\cdot\mathbf{x}}. \quad (4.17)$$

We can now check the commutator between  $\hat{a}_{\mathbf{p}}$  and  $\hat{a}_{\mathbf{p}'}^\dagger$ :

$$\begin{aligned} [\hat{a}_{\mathbf{p}}, \hat{a}_{\mathbf{p}'}^\dagger] &= \int d^3x \int d^3x' e^{i(\mathbf{p}'\cdot\mathbf{x}' - \mathbf{p}\cdot\mathbf{x})} \\ &\quad \times \left[ \sqrt{\frac{\omega_{\mathbf{p}}}{2}} \left( \hat{\phi}(\mathbf{x}) + \frac{i\hat{\pi}(\mathbf{x})}{\omega_{\mathbf{p}}} \right), \sqrt{\frac{\omega_{\mathbf{p}'}}{2}} \left( \hat{\phi}(\mathbf{x}') - \frac{i\hat{\pi}(\mathbf{x}')}{\omega_{\mathbf{p}'}} \right) \right] \\ &= \int d^3x \int d^3x' e^{i(\mathbf{p}'\cdot\mathbf{x}' - \mathbf{p}\cdot\mathbf{x})} \\ &\quad \times \frac{\sqrt{\omega_{\mathbf{p}}\omega_{\mathbf{p}'}}}{2} \left( -\frac{i}{\omega_{\mathbf{p}'}} \underbrace{[\hat{\phi}(\mathbf{x}), \hat{\pi}(\mathbf{x}')]_{i\delta^3(\mathbf{x}-\mathbf{x}')}} + \frac{i}{\omega_{\mathbf{p}}} \underbrace{[\hat{\pi}(\mathbf{x}), \hat{\phi}(\mathbf{x}')]_{-i\delta^3(\mathbf{x}-\mathbf{x}')}} \right) \\ &= \int d^3x e^{i(\mathbf{p}'-\mathbf{p})\cdot\mathbf{x}} \frac{\sqrt{\omega_{\mathbf{p}}\omega_{\mathbf{p}'}}}{2} \left( \frac{1}{\omega_{\mathbf{p}'}} + \frac{1}{\omega_{\mathbf{p}}} \right) = (2\pi)^3 \delta^3(\mathbf{p} - \mathbf{p}'). \end{aligned} \quad (4.18)$$

This is the field equivalent of the commutator between the ladder operators known from the quantum harmonic oscillator. We use this equivalence to define the vacuum of our quantum theory to be the state that is annihilated by  $\hat{a}_{\mathbf{p}}$ . We now try to express the Hamiltonian and total momentum using these operators.

Inserting the expressions (4.15) into the Hamiltonian, we arrive at

$$\begin{aligned}
 \hat{H} &= \int d^3x \iint \frac{d^3p d^3p'}{(2\pi)^3(2\pi)^3} \frac{1}{2} \left( -\frac{\sqrt{\omega_p \omega_{p'}}}{2} (\hat{a}_p - \hat{a}_{-p}^\dagger)(\hat{a}_{p'} - \hat{a}_{-p'}^\dagger) \right. \\
 &\quad \left. + \frac{-\mathbf{p} \cdot \mathbf{p}' + m^2}{2\sqrt{\omega_p \omega_{p'}}} (\hat{a}_p + \hat{a}_{-p}^\dagger)(\hat{a}_{p'} + \hat{a}_{-p'}^\dagger) \right) e^{i(\mathbf{p}+\mathbf{p}') \cdot \mathbf{x}} \\
 &= \int \frac{d^3p}{(2\pi)^3} \int d^3p' \int \frac{d^3x}{(2\pi)^3} \underbrace{e^{i(\mathbf{p}+\mathbf{p}') \cdot \mathbf{x}} \frac{1}{2} (\dots)}_{\delta^3(\mathbf{p}+\mathbf{p}')} \\
 &= \int \frac{d^3p}{(2\pi)^3} \omega_p \left( \hat{a}_p^\dagger \hat{a}_p + \frac{1}{2} \underbrace{[\hat{a}_p, \hat{a}_p^\dagger]}_{\sim \delta^3(0)} \right).
 \end{aligned} \tag{4.19}$$

To get to the last line we used that the integrand is even, so we could exchange  $\mathbf{p} \rightarrow -\mathbf{p}$  in some of the terms. The term proportional to  $\delta^3(0)$  is infinite, which seems troubling. In the case of the Hamiltonian we could argue that we only measure differences in energy, so a constant (even an infinite one) should not matter. This is the symptom of a more general problem though, which is ordering ambiguity. In the classical theory the order in which fields appear in observables has no meaning, so there are different quantum theories corresponding to different ways the fields can be arranged before promoting them to operators. In this sense we have multiple quantum theories to choose from, and one way to make this choice is the process of *normal ordering*. By a normal ordered product of creation and annihilation operators, denoted by  $: \hat{O} :$ , we mean that we reorder the terms until all creation operators are “on the left” of all annihilation operators. This makes the vacuum expectation value of  $: \hat{O} :$  vanish, which in the case of the Hamiltonian means we set the energy scale to be zero in the vacuum state. Indeed,

$$: \hat{H} := \int \frac{d^3p}{(2\pi)^3} \omega_p \hat{a}_p^\dagger \hat{a}_p. \tag{4.20}$$

Since we know that  $\hat{a}_p$  and  $\hat{a}_p^\dagger$  obey the commutation relations of a harmonic oscillator’s ladder operators, we can interpret the spectrum of  $\hat{H}$  as discrete excitations for each value of  $\mathbf{p}$  that carry the energy  $\omega_p$ . Furthermore, we can check the total momentum  $\hat{\mathbf{P}}$ :

$$\begin{aligned}
 : \hat{\mathbf{P}} : &:= - \int d^3x \pi \nabla \phi : \\
 &:= \int \frac{d^3p}{(2\pi)^3} \int d^3p' \int \frac{d^3x}{(2\pi)^3} \underbrace{e^{i(\mathbf{p}+\mathbf{p}') \cdot \mathbf{x}} (-i) \mathbf{p}' (\hat{a}_p - \hat{a}_{-p})(\hat{a}_{p'} + \hat{a}_{-p'})}_{\delta^3(\mathbf{p}+\mathbf{p}')} : \\
 &= \int \frac{d^3p}{(2\pi)^3} \mathbf{p} \hat{a}_p^\dagger \hat{a}_p.
 \end{aligned} \tag{4.21}$$

To summarize, the quantum theory arising from the Lagrangian density (4.1) describes discrete excitations parametrized by a label  $\mathbf{p}$ , that each contribute  $\mathbf{p}$  to the total momentum and  $\omega_{\mathbf{p}} = \sqrt{m^2 + \mathbf{p}^2}$  to the total energy. This way, we can conclude that the Klein-Gordon Lagrangian describes relativistic, massive particles.

To study pair creation, some key ingredients are still missing. The particles have no charge so far, and the electromagnetic background field is missing as well. We take a small step forward and consider a complex scalar field,

$$\mathcal{L} = (\partial_\mu \phi^*)(\partial^\mu \phi) - m^2 \phi^* \phi, \quad (4.22)$$

where instead of the real and imaginary part we consider  $\phi$  and its complex conjugate  $\phi^*$  to be the independent degrees of freedom. Varying  $\mathcal{L}$  with regard to  $\phi^*$  or  $\phi$  gives the Klein-Gordon equation for  $\phi$  and  $\phi^*$  respectively. The theory is still invariant under spacetime translations (of both fields at the same time), with the Hamiltonian density

$$\mathcal{H} = T^{00} = \pi \dot{\phi} + \pi^* \dot{\phi}^* - \mathcal{L} = \pi^* \pi + (\nabla \phi^*)(\nabla \phi) + m^2 \phi^* \phi, \quad (4.23)$$

and the momentum density

$$\mathcal{P}^i = -T^0_i = -\pi \partial_i \phi - \pi^* \partial_i \phi^*. \quad (4.24)$$

We again promote the fields to operators and expand in plane waves. We now get four distinct operators, and since the fields are not real, the operator-valued expansion coefficients are not the adjoint of each other,

$$\hat{\phi}(\mathbf{x}) = \int \frac{d^3 p}{(2\pi)^3} \frac{1}{\sqrt{2\omega_{\mathbf{p}}}} (\hat{a}_{\mathbf{p}} e^{i\mathbf{p}\cdot\mathbf{x}} + \hat{b}_{\mathbf{p}}^\dagger e^{-i\mathbf{p}\cdot\mathbf{x}}), \quad (4.25a)$$

$$\hat{\pi}(\mathbf{x})^\dagger = \int \frac{d^3 p}{(2\pi)^3} (-i) \sqrt{\frac{\omega_{\mathbf{p}}}{2}} (\hat{a}_{\mathbf{p}} e^{i\mathbf{p}\cdot\mathbf{x}} - \hat{b}_{\mathbf{p}}^\dagger e^{-i\mathbf{p}\cdot\mathbf{x}}), \quad (4.25b)$$

$$\hat{\phi}(\mathbf{x})^\dagger = \int \frac{d^3 p}{(2\pi)^3} \frac{1}{\sqrt{2\omega_{\mathbf{p}}}} (\hat{a}_{\mathbf{p}}^\dagger e^{-i\mathbf{p}\cdot\mathbf{x}} + \hat{b}_{\mathbf{p}} e^{i\mathbf{p}\cdot\mathbf{x}}), \quad (4.25c)$$

$$\hat{\pi}(\mathbf{x}) = \int \frac{d^3 p}{(2\pi)^3} i \sqrt{\frac{\omega_{\mathbf{p}}}{2}} (\hat{a}_{\mathbf{p}}^\dagger e^{-i\mathbf{p}\cdot\mathbf{x}} - \hat{b}_{\mathbf{p}} e^{i\mathbf{p}\cdot\mathbf{x}}). \quad (4.25d)$$

We can now use (4.25) to derive the commutation relations for  $\hat{a}_{\mathbf{p}}$ ,  $\hat{a}_{\mathbf{p}}^\dagger$ ,  $\hat{b}_{\mathbf{p}}$  and  $\hat{b}_{\mathbf{p}}^\dagger$  as well as the (normal ordered) Hamiltonian and total momentum. We find (via essentially the same calculation as before)

$$[\hat{a}_{\mathbf{p}}, \hat{a}_{\mathbf{p}'}^\dagger] = [\hat{b}_{\mathbf{p}}, \hat{b}_{\mathbf{p}'}^\dagger] = (2\pi)^3 \delta^3(\mathbf{p} - \mathbf{p}') \quad (4.26)$$

with all other combinations zero, and

$$:\hat{H} := \int \frac{d^3 p}{(2\pi)^3} \omega_{\mathbf{p}} (\hat{a}_{\mathbf{p}}^\dagger \hat{a}_{\mathbf{p}} + \hat{b}_{\mathbf{p}}^\dagger \hat{b}_{\mathbf{p}}), \quad : \hat{\mathbf{P}} := \int \frac{d^3 p}{(2\pi)^3} \mathbf{p} (\hat{a}_{\mathbf{p}}^\dagger \hat{a}_{\mathbf{p}} + \hat{b}_{\mathbf{p}}^\dagger \hat{b}_{\mathbf{p}}). \quad (4.27)$$

It looks like the complex scalar field theory (4.22) simply contains two copies of the same relativistic particle with mass  $m$ . We do however have a new symmetry now,<sup>36</sup>

<sup>36</sup> Which is physically plausible, we should not be able to detect complex phases.

$$\phi \rightarrow e^{-iq\varepsilon} \phi = \phi + \varepsilon(-iq\phi), \quad \simeq \quad \phi^* \rightarrow e^{iq\varepsilon} \phi^* = \phi + \varepsilon iq\phi^*, \quad (4.28)$$

which keeps the Lagrangian invariant, so  $\Delta\mathcal{L} = 0$  and we obtain the conserved current

$$j^\mu = iq(\phi^* \partial^\mu \phi - \phi \partial^\mu \phi^*). \quad (4.29)$$

<sup>37</sup> The calculations works just as the one for the Hamiltonian and momentum.

Let us find the quantum operator corresponding to  $j^0$  and  $\mathbf{j}$ ,<sup>37</sup>

$$:\hat{Q}: =: \int d^3x \hat{j}^0 := \int \frac{d^3p}{(2\pi)^3} q (\hat{a}_p^\dagger \hat{a}_p - \hat{b}_p^\dagger \hat{b}_p) \quad (4.30a)$$

$$:\hat{\mathbf{J}}: =: \int d^3x \hat{\mathbf{j}} := \int \frac{d^3p}{(2\pi)^3} \underbrace{\frac{q\mathbf{p}}{\omega_p}}_{q\mathbf{v}} (\hat{a}_p^\dagger \hat{a}_p - \hat{b}_p^\dagger \hat{b}_p). \quad (4.30b)$$

While they have the same mass, the two species of particles have another property in which they differ by a sign – of course this will turn out to be the electric charge, so they are antiparticles of each other. Each particle carries the charge  $q$  or  $-q$ , and the electric current  $q\mathbf{v}$  or  $-q\mathbf{v}$  respectively. To actually see any effect of this charge we need some electromagnetic field to couple to. In fact, it emerges naturally when we demand a little more symmetry from our Lagrangian. The transformation (4.28) is called a *global gauge transformation*, because we add a constant phase to the fields at each point in spacetime. Maybe our theory is invariant under a *local* gauge transformation too, with the phase in the transformation varying over spacetime

$$\phi \rightarrow e^{-iq\lambda(x^\mu)} \phi, \quad \simeq \quad \phi^* \rightarrow e^{iq\lambda(x^\mu)} \phi^*. \quad (4.31)$$

In the global case (4.28) the phase factors of the transformed  $\phi$  and  $\phi^*$  cancel immediately. In the local transformation the same happens in the term proportional to  $m^2$ , but the derivative terms cause trouble:

$$\partial_\mu \phi \rightarrow \partial_\mu e^{-iq\lambda(x^\mu)} \phi = e^{-iq\lambda(x^\mu)} (\partial_\mu \phi - iq\partial_\mu \lambda(x^\mu) \phi), \quad (4.32)$$

so we can not just “pull out” the phase factor and cancel it against the one from  $\phi^*$ . Let’s see if we can somehow enforce local gauge invariance by a minimal modification. The derivative causes problems, so we replace  $\partial_\mu$  by the *covariant derivative*

$$D_\mu := \partial_\mu + iqA_\mu(x^\nu), \quad (4.33)$$

which is nothing but a *very* educated guess for now,  $A_\mu$  being some arbitrary function of spacetime. Then the local gauge transformation reads

$$\begin{aligned} D_\mu \phi &\rightarrow (\partial_\mu + iqA_\mu) e^{-iq\lambda(x^\mu)} \phi \\ &= e^{-iq\lambda(x^\mu)} (\partial_\mu \phi - iq\partial_\mu \lambda(x^\mu) \phi + iqA_\mu \phi) \\ &= e^{-iq\lambda(x^\mu)} (\partial_\mu + iq(A_\mu - (\partial_\mu \lambda))) \phi, \end{aligned} \quad (4.34)$$

so we can obtain a locally gauge invariant theory by replacing  $\partial_\mu$  by  $D_\mu$ , provided we look at the *combined* gauge transformation

$$\phi \rightarrow e^{-iq\lambda(x^\mu)}\phi, \quad A_\mu \rightarrow A_\mu + \partial_\mu\lambda. \quad (4.35)$$

Now, if we take  $A_\mu$  to be the four-potential known from classical electrodynamics this combined invariance appears very sensible, as we do not expect to be able to detect complex phases and we already know that classical electrodynamics does not change if we add a total derivative to the potential. So let us add to our complex Klein-Gordon Lagrangian with modified derivatives the Lagrangian of the electromagnetic field,

$$\mathcal{L} = (D^\mu\phi)^* D_\mu\phi - m^2\phi^*\phi - \frac{1}{4}F^{\mu\nu}F_{\mu\nu}, \quad F^{\mu\nu} = \partial^\mu A^\nu - \partial^\nu A^\mu. \quad (4.36)$$

Taking the Euler-Lagrange equations with regard to the field  $A_\mu$ , we get

$$\begin{aligned} 0 &= \partial_\mu \frac{\partial\mathcal{L}}{\partial(\partial_\mu A_\nu)} - \frac{\partial\mathcal{L}}{\partial A_\nu} \\ &= \partial_\mu(-F^{\mu\nu}) - (iq(D^\nu\phi)^*\phi - iq\phi^*(D^\nu\phi)) \end{aligned} \quad (4.37)$$

$$\Leftrightarrow \partial_\mu F^{\mu\nu} = j^\nu, \quad j^\nu = iq(\phi^* D^\nu\phi - (D^\nu\phi)^*\phi),$$

which are Maxwell's equations in the presence of a charge density  $j^0$  and current density  $\mathbf{j}$ .

We conclude that the Lagrangian (4.36) describes two species of relativistic particles of mass  $m$ , coupling to Maxwell's equations by each carrying a charge  $q$  or  $-q$  and producing an electrical current  $qv$  or  $-qv$ . This is *almost* quantum electrodynamics, which contains the electromagnetic field, electrons and positrons. The difference is that we still model our charged particles with a scalar field, which does not account for the spin degree of freedom. This theory is consequently called *scalar* quantum electrodynamics.

To bring spin into the picture, we have to turn to the Dirac equation. The corresponding Lagrangian density is<sup>38</sup>

$$\mathcal{L} = \bar{\psi} \cdot (i\boldsymbol{\gamma}^\mu \partial_\mu - m\mathbb{1}) \cdot \psi, \quad (4.38)$$

where  $\psi$  is a four-component spinor,  $\mathbb{1}$  the four-by-four identity matrix,  $\boldsymbol{\gamma}^\mu$  is any set of four-by-four matrices that obey the anticommutation relations

$$\{\boldsymbol{\gamma}^\mu, \boldsymbol{\gamma}^\nu\} = 2g^{\mu\nu}\mathbb{1}, \quad (4.39)$$

and the Dirac adjoint  $\bar{\psi} = \psi^\dagger \cdot \boldsymbol{\gamma}^0$ . Taking the Euler-Lagrange equations with regard to  $\bar{\psi}$  yields the Dirac equation for  $\psi$ , the other way around the adjoint of the Dirac equation for  $\bar{\psi}$ .

The Dirac equation admits plane wave solutions as well, and we can again use these to expand the field operators into creation and annihilation operators to quantize the system. The only difference to the complex scalar field above is that each plane wave is spinor valued and we have to assume anticommutation relations for the operator coefficients to obtain a sensible theory.

<sup>38</sup> There are now multiple types of vector-like objects. Spinors and spinorial matrices are typeset in bold and use operations like the dot product, vector components will be written using indices only.

<sup>39</sup> They are explained in detail in [PS95]

We do not perform all the steps from before explicitly, since we will not work with spinors at all in the following and the derivations are not any more illuminating than the ones we already did.<sup>39</sup> Expressing the conserved charges corresponding to translation invariance in terms of creation and annihilation operators we again find discrete excitations of two different species, each obeying the relativistic energy-momentum relation. Global gauge invariance once more shows that these differ in charge, while we can also obtain local gauge invariance (and coupling to the electromagnetic field) by replacing the partial derivative with the covariant derivative as before,

$$\mathcal{L} = \bar{\psi} \cdot (i\gamma^\mu D_\mu - m\mathbb{1}) \cdot \psi - \frac{1}{4} F^{\mu\nu} F_{\mu\nu}, \quad (4.40)$$

which is the Lagrangian for quantum electrodynamics proper.

The only new result is that it now in fact describes spin- $\frac{1}{2}$  particles. Looking at the conserved charge due to rotations of spacetime, it contains a term due to mechanical angular momentum, but also an additional term due to the spin degree of freedom.

## 4.2. Worldline path integral

We will now turn away from the canonical quantization picture from last section and instead work with the path integral for fields (2.24). For the scalar electrodynamics Lagrangian (4.36), the vacuum persistence amplitude is

$$[\mathbf{A}] = \mathbf{L}^{-1}, \quad \mathbf{x}_i = -\mathbf{x}^i$$

(see page 13).

$$\langle 0_{\text{out}} | 0_{\text{in}} \rangle = \iiint \mathcal{D}\phi \mathcal{D}\phi^* \mathcal{D}A_\mu e^{iS[\phi, \phi^*, A_\mu]}, \quad S[\phi, \phi^*, A_\mu] = \int d^4x \mathcal{L}. \quad (4.41)$$

We can split the action into a part not including  $\phi$  or  $\phi^*$  and the rest, rearranging the integrations

$$\iiint \mathcal{D}\phi \mathcal{D}\phi^* \mathcal{D}A_\mu e^{iS[\phi, \phi^*, A_\mu]} = \int \mathcal{D}A_\mu e^{i(S_A[A_\mu] + \Gamma[A_\mu])}, \quad (4.42)$$

which now looks like a theory containing the electromagnetic field  $A_\mu$  only, using the definitions

$$S_A[A_\mu] = \int d^4x \left( -\frac{1}{4} F^{\mu\nu} F_{\mu\nu} \right) \quad (4.43a)$$

$$e^{i\Gamma[A_\mu]} = \iint \mathcal{D}\phi \mathcal{D}\phi^* e^{iS_\phi[\phi, \phi^*, A_\mu]} \quad (4.43b)$$

$$S_\phi[\phi, \phi^*, A_\mu] = \int d^4x \left( (D^\mu \phi)^* D_\mu \phi - m^2 \phi^* \phi \right). \quad (4.43c)$$

This way, all interaction with the scalar particle field is “integrated out” and included in the (possibly very complicated) functional  $\Gamma[A_\mu]$ , which we consequently call *effective action* for the electromagnetic field.<sup>40</sup> If we could actually derive this effective action explicitly, it would give corrections to Maxwell’s equations due to interactions with virtual charged particles.

<sup>40</sup> We do not include the Maxwell part  $S_A$  of the action, so  $\Gamma$  is not what is usually called effective action in the literature, but only its one-loop approximation.

In the situation we are interested in we consider a fixed, strong, classical electromagnetic potential  $A_\mu$ . We thus do not integrate over  $A_\mu$  in the vacuum persistence amplitude, instead regarding it as an external parameter,

$$\langle 0_{\text{out}} | 0_{\text{in}} \rangle [A_\mu] = \iint \mathcal{D}\phi \mathcal{D}\phi^* e^{iS_\phi[\phi, \phi^*, A_\mu]} = e^{i\Gamma[A_\mu]}. \quad (4.44)$$

This means we neglect any quantum effects of the electromagnetic field and also any fields emitted by the created electron-positron pairs. This is a good approximation here, as the field strengths necessary to observe any pair creation are so high that quantum fluctuations in the background field should be negligible, and backreactions from the produced pairs have no sizable influence either as their expected density is very low.

Our approach to extract the pair production rate is now straightforward, the process of particle production is intuitively the complement of the vacuum remaining vacuum so we have

$$P^{e^+e^-} = 1 - P^{\text{Vac.}} = 1 - |\langle 0_{\text{out}} | 0_{\text{in}} \rangle|^2 = 1 - |e^{i\Gamma[A_\mu]}|^2 \approx 2\mathcal{J}\Gamma[A_\mu]. \quad (4.45)$$

This relation is not completely correct however. Apart from the creation of an electron-positron pair, there is also the possibility of coherent creation of two, or even more pairs. All these processes destroy the vacuum, but each produces a different number of particles. Due to this distinction, what we calculate is not exactly the number of created pairs, a detailed discussion of this is given in [CM08]. Because the rates in the cases we consider are very small, and the probabilities of creating multiple pairs at once are exponentially smaller still, there will be no practical difference, and we will keep referring to (4.45) as the pair production probability.

[CM08] Cohen and McGady. *Phys. Rev. D* (2008)

The main problem to solve is now the calculation of the imaginary part of the effective action for a given background field  $A_\mu$ . The exponent in (4.43b) can be brought into Gaussian form using integration by parts,

$$\begin{aligned} S_\phi &= \int d^4x \left( ((\partial^\mu + iqA^\mu)\phi)^* (\partial_\mu + iqA_\mu)\phi - m^2\phi^*\phi \right) \\ &= \int d^4x \left( (\partial^\mu - iqA^\mu)\phi^* (\partial_\mu + iqA_\mu)\phi - m^2\phi^*\phi \right) \\ &= \int d^4x \left( \phi^* (-\partial^\mu - iqA^\mu)(\partial_\mu + iqA_\mu)\phi - m^2\phi^*\phi \right) \\ &= - \int d^4x \phi^* (D^\mu D_\mu + m^2) \phi. \end{aligned} \quad (4.46)$$

To make the oscillatory integral in (4.43b) converge, we analytically continue the time integral in the action to imaginary values, in particular we make the replacement  $x_4 := it$

$$\int d^4x = \int d^3x dt = -i \int d^3x dx_4 =: -i \int d^4x^E, \quad (4.47)$$

the superscript <sup>E</sup> standing for *Euclidean*, because under the replacement  $t \rightarrow x_4 := it$  the Minkowski metric turns into the Euclidean metric. We will immediately

drop this superscript though, and never use  $\int d^4x$  for the combination  $\int d^3x dt$  again, which is arguably more confusing anyway. We still have to do the same replacements for  $t$  in the integrand as well, in particular

$$\begin{aligned}
D^\mu D_\mu &= (\partial_t + iqA_0(t))^2 - (\nabla + iq\mathbf{A}(t))^2 \\
&= (i\partial_{x_4} + iqA_0(-ix_4))^2 - (\nabla + iq\mathbf{A}(t))^2 \\
&= -(\partial_{x_4} + iq\frac{1}{i}A_0(-ix_4))^2 - (\nabla + iq\mathbf{A}(t))^2 \\
&= -(\partial_\mu + iqA_\mu^E)^2 =: -\square_A
\end{aligned} \tag{4.48}$$

with the definition of the Euclidean four-potential

$$A_4^E(x_\mu) = \frac{1}{i}A_0(t = -ix_4, \mathbf{x}), \quad \mathbf{A}^E(x_\mu) = \mathbf{A}(t = -ix_4, \mathbf{x}). \tag{4.49}$$

Now we can perform the path integral (4.43b) using (2.38),

$$\begin{aligned}
e^{i\Gamma[A_\mu]} &= \iint \mathcal{D}\phi \mathcal{D}\phi^* e^{i\mathcal{S}_\phi[\phi, \phi^*, A_\mu]} \\
&= \iint \mathcal{D}\phi \mathcal{D}\phi^* \exp\left(-\int d^4x \phi^* (-\square_A + m^2)\phi\right) \\
&\sim \frac{1}{\text{Det}(-\square_A + m^2)}.
\end{aligned} \tag{4.50}$$

As discussed in Section 2.7, it is not exactly clear how to define this operator determinant. We instead consider the ratio of Determinants

$$e^{i\Gamma[A_\mu]} = \frac{\text{Det}(-\square_0 + m^2)}{\text{Det}(-\square_A + m^2)} e^{i\Gamma[0]} \tag{4.51}$$

where  $\Gamma[0]$  can only be an irrelevant phase, because the vacuum is stable when there is no electromagnetic field present. As this phase does not contribute to the absolute value that gives the pair production rate we set it to zero and solve for the effective action  $\Gamma$ ,

$$\Gamma[A_\mu] = i \log\left(\frac{\text{Det}(-\square_A + m^2)}{\text{Det}(-\square_0 + m^2)}\right). \tag{4.52}$$

In analogy to how the exponent in (4.50) changed from  $i\mathcal{S}_\phi$  to  $-\mathcal{S}_\phi^E$ , we introduce the Euclidean effective action

$$\Gamma^E[A_\mu] = -i\Gamma[A_\mu] = \log\left(\frac{\text{Det}(-\square_A + m^2)}{\text{Det}(-\square_0 + m^2)}\right), \tag{4.53}$$

so that the pair production probability, that is the imaginary part of the effective action, is given by

$$\Im\Gamma[A_\mu] = \Im\Gamma^E[A_\mu]. \tag{4.54}$$

We will now find a way to express the effective action as an ordinary quantum mechanical path integral. The first step is a formal manipulation of the ratio of

determinants,

$$\begin{aligned}\Gamma^E &= \log \left( \frac{\text{Det}(-\square_A + m^2)}{\text{Det}(-\square_0 + m^2)} \right) = \log \text{Det} \left( \frac{-\square_A + m^2}{-\square_0 + m^2} \right) \\ &= \text{Tr} \log \left( \frac{-\square_A + m^2}{-\square_0 + m^2} \right).\end{aligned}\tag{4.55}$$

We can use a special case of the theorem of Frullani [Fru28], the definite integral

[Fru28] Frullani. *Memorie Mat. Fis. Soc. ital. Sci.* (1828)

$$-\log \left( \frac{a}{b} \right) = \int_0^\infty dT \frac{e^{-aT} - e^{-bT}}{T}.\tag{4.56}$$

The lower limit of the integration looks problematic due to the factor of  $T$  in the denominator, but the small- $T$  behavior of the numerator cancels the divergence. Applying this to the expression for the effective action we get

$$\begin{aligned}\Gamma^E &= -\text{Tr} \int_0^\infty \frac{dT}{T} \left( e^{-(\square_A + m^2)T} - e^{-(\square_0 + m^2)T} \right) \\ &= -\int_0^\infty \frac{dT}{T} \left( \text{Tr} e^{-(\square_A + m^2)T} - \text{Tr} e^{-(\square_0 + m^2)T} \right).\end{aligned}\tag{4.57}$$

Some physical reasoning enables us to simplify this further. The second term that does not include the background field can not contribute to the pair production probability in a meaningful way, in particular it can not introduce the imaginary part of the effective action. If we were to just discard it however, the integral would not converge anymore due to the  $1/T$  divergence. We can instead replace the lower integration limit by a finite UV-cutoff  $\Lambda^{-2}$  which makes the integral finite, but cutoff-dependent. Appropriate counter terms can then be added to obtain finite results in the limit  $\Lambda \rightarrow \infty$  with the proper renormalization for physical quantities, as for example in [GL02; GLM03]. Since we will evaluate the  $T$ -Integral using Laplace's method later, an exact treatment of the low- $T$  behavior is not necessary, we only need to know that it is possible and the integration finite. What remains is

[GL02] Gies and Langfeld. *Int. J. Mod. Phys. A* (2002)

[GLM03] Gies, Langfeld, and Moyaerts. *JHEP* (2003)

$$\Gamma^E = -\int_0^\infty \frac{dT}{T} \text{Tr} e^{-(\square_A + m^2)T},\tag{4.58}$$

where the proper, careful treatment of the lower integration limit is implied.

The next step is the evaluation of the functional trace. We can perform it by analogy. First, the trace of an operator can be written as a sum over diagonal elements in any complete basis,

$$\text{Tr} \hat{O} = \sum_\psi \langle \psi | \hat{O} | \psi \rangle.\tag{4.59}$$

We can interpret the derivative operator  $\partial_\mu$  in  $\square_A$  as the position base representation of the quantum mechanical momentum operator,  $\hat{\mathbf{p}} = -i\nabla$ , only in four

instead of three spatial dimensions. We thus write the trace as a sum over position eigenstates in four spatial dimensions,

$$\Gamma^{\text{E}} = - \int_0^{\infty} \frac{dT}{T} \text{Tr} e^{-(\square_A + m^2)T} = - \int_0^{\infty} \frac{dT}{T} \int d^4x \langle x | e^{-(\square_A + m^2)T} | x \rangle. \quad (4.60)$$

Now with a few replacements the diagonal elements can be turned into path integrals by comparing to (2.22). In particular

$$\langle x | e^{-i\hat{H}T} | x \rangle \rightarrow \langle x | e^{-(\square_A + m^2)T} | x \rangle \quad (4.61)$$

when we perform the replacements

$$iT \rightarrow T, \quad it \rightarrow \tau, \quad \hat{H} \rightarrow \frac{(\hat{p}_\mu + qA_\mu^{\text{E}})^2}{2\tilde{m}} + m^2, \quad \tilde{m} = \frac{1}{2} \quad (4.62)$$

The Hamiltonian corresponds to a charged particle of mass  $\tilde{m}$  moving in an electromagnetic field  $A_\mu$  with an additional potential energy of  $m^2$ . The corresponding classical Lagrangian is

$$L = \frac{1}{2} \tilde{m} \left( \frac{dx_\mu}{dt} \right)^2 - q \frac{dx_\mu}{dt} A_\mu^{\text{E}} - m^2 = -\frac{1}{4} \left( \frac{dx_\mu}{d\tau} \right)^2 - iq \frac{dx_\mu}{d\tau} A_\mu^{\text{E}} - m^2, \quad (4.63)$$

so we arrive at the path integral representation

$$\langle x | e^{-(\square_A + m^2)T} | x \rangle = \int_{x(T)=x(0)=x} \mathcal{D}x(\tau) \exp \left( - \int_0^T d\tau \left( \frac{\dot{x}^2}{4} + iq\dot{x} \cdot A^{\text{E}} + m^2 \right) \right). \quad (4.64)$$

We can resubstitute this expression into the effective action now,

$$\Gamma^{\text{E}} = - \int_0^{\infty} \frac{dT}{T} \int d^4x \int_{x(T)=x(0)=x} \mathcal{D}x(\tau) \exp \left( - \int_0^T d\tau \left( \frac{\dot{x}^2}{4} + iq\dot{x} \cdot A^{\text{E}} + m^2 \right) \right). \quad (4.65)$$

We now rescale  $T \rightarrow \frac{T}{2}$ ,  $\tau \rightarrow \frac{\tau}{2}$  for reasons of convention, combine

$$\int_{x(T)=x(0)=x} d^4x \int_{x(T)=x(0)} \mathcal{D}x(\tau) = \int_{x(T)=x(0)} \mathcal{D}x(\tau), \quad (4.66)$$

and drop all superscripts of  $^{\text{E}}$  to arrive at the worldline path integral representation of the Euclidean effective action in scalar QED,

$$\Gamma = - \int_0^{\infty} \frac{dT}{T} e^{-\frac{m^2}{2}T} \int_{x(T)=x(0)} \mathcal{D}x(\tau) e^{-\int_0^T d\tau \left( \frac{\dot{x}^2}{2} + iq\dot{x} \cdot A(x) \right)}. \quad (4.67)$$

The step from scalar to full spinor QED needs some technical details in the derivation, but surprisingly the end result differs very little from (4.67). First of all, we want to express the vacuum persistence amplitude as a path integral over fields. Since the spinor fields are supposed to anticommute, we need some way to encode this in the path integral formulation that knows nothing of operator ordering. The solution is to represent  $\psi$  and  $\psi^\dagger$  as *Grassmann number*-valued fields.

These type of numbers were first introduced by Hermann Graßmann in [Gra44] in a geometric context, with the basic property that for  $\theta, \eta$  Graßmann numbers, [Gra44] Graßmann. *Otto Wigand* (1844)

$$\theta\eta = -\eta\theta. \quad (4.68)$$

This has some immediate consequences. First of all

$$\theta\theta = -\theta\theta = 0, \quad (4.69)$$

so any general function of  $\theta$  that can be expressed as a Taylor series has the simple form

$$f(\theta) = a + b\theta, \quad (4.70)$$

for real or complex  $a$  and  $b$ , as any higher order terms vanish identically.

The concept of integration over Graßmann numbers was formalized by Felix Berezin [Ber66], by demanding just a few properties.<sup>41</sup> We only consider definite integrals over the whole space, and these should be

[Ber66] Berezin. *Academic Press* (1966)

- linear, i.e.

$$\int d\theta (af(\theta) + bg(\theta)) = a \int d\theta f(\theta) + b \int d\theta g(\theta) \quad (4.71)$$

- translation invariant

$$\int d\theta f(\theta + \theta_0) = \int d\theta f(\theta) \quad (4.72)$$

- and not depend on the integration variable anymore.

A moment of experimentation shows that the only way to satisfy these properties is the definition

$$\int d\theta f(\theta) = \int d\theta (a + b\theta) := b, \quad (4.73)$$

up to a global normalization factor, conventionally chosen to be one. In particular this means that

$$\int d\theta \theta = 1, \quad \int d\theta = 0. \quad (4.74)$$

For multiple integrals there is an ambiguity in the order they are evaluated, we decide to perform the innermost integral first, that is

$$\int d\eta \int d\theta \theta\eta = +1. \quad (4.75)$$

We can now calculate the Berezin analog of the complex Gaussian integral. Let  $\theta = (\theta_0 + i\theta_1)/\sqrt{2}$  and  $\theta^* = (\theta_0 - i\theta_1)/\sqrt{2}$  be the independent degrees of freedom, then

$$\int d\theta^* \int d\theta e^{-\theta^* a \theta} = \int d\theta^* \int d\theta (1 - \theta^* a \theta) \quad (4.76)$$

$$= \int d\theta^* \int d\theta (1 + a\theta\theta^*) = a. \quad (4.77)$$

and in the  $n$ -dimensional case

$$\int d^N \theta^* \int d^N \theta \exp(-\theta_i^* A_{ij} \theta_j) = \det A, \quad (4.78)$$

<sup>41</sup> He went on to generalize this to spaces with elements having both regular commuting and anticommuting components, known today as *superspaces* that form the basis for supersymmetry.

with the determinant in the numerator instead of the denominator as for the regular Gaußian. This can then again be generalized to functional integrals and operators, so we can formally evaluate the fermionic path integral for spinor QED,

$$e^{i\Gamma} = \iint \mathcal{D}\psi^\dagger \mathcal{D}\psi \exp\left(i \int d^4x \bar{\psi} \cdot (i\boldsymbol{\gamma}^\mu D_\mu - m\mathbb{1}) \cdot \psi\right) \quad (4.79)$$

$$\sim \text{Det}(i\boldsymbol{\gamma}^\mu D_\mu - m\mathbb{1}). \quad (4.80)$$

Using properties of the determinant and the gamma matrices this can be manipulated into a form that more closely resembles the expression obtained in the scalar case,

$$\begin{aligned} \log \text{Det}(i\boldsymbol{\gamma}^\mu D_\mu - m\mathbb{1}) &= \frac{1}{2} \log \text{Det}\left((\boldsymbol{\gamma}^\mu D_\mu)^2 + m^2\mathbb{1}\right) \\ &= \frac{1}{2} \log \text{Det}\left((D^\mu D_\mu + m^2)\mathbb{1} + \frac{q}{2}\boldsymbol{\sigma}^{\mu\nu}F_{\mu\nu}\right), \end{aligned} \quad (4.81)$$

with

$$\boldsymbol{\sigma}_{\mu\nu} = \frac{1}{2} [\boldsymbol{\gamma}_\mu, \boldsymbol{\gamma}_\nu]. \quad (4.82)$$

Unfortunately, it is not as easy as in the scalar case to turn this into a worldline path integral by analogy. Instead, after writing the logarithm using the  $T$ -integral and continuation to imaginary times,

$$\begin{aligned} \Gamma^{\text{Spin}} &= \frac{1}{2} \int_0^\infty \frac{dT}{T} \text{Tr} \exp\left(-T\left((-\square_A + m^2)\mathbb{1} + \frac{iq}{2}\boldsymbol{\sigma}_{\mu\nu}F_{\mu\nu}\right)\right) \\ &= \frac{1}{2} \int_0^\infty \frac{dT}{T} \int d^4x \text{tr} \langle x | \exp\left(-T\left((-\square_A + m^2)\mathbb{1} + \frac{iq}{2}\boldsymbol{\sigma}_{\mu\nu}F_{\mu\nu}\right)\right) | x \rangle, \end{aligned} \quad (4.83)$$

we have to retrace the steps in the derivation of the path integral in Section 2.2. This works essentially the same way as before, only that the terms containing  $\boldsymbol{\sigma}_{\mu\nu}$  do not commute, so when we perform the  $N \rightarrow \infty$  limit the slices have to retain their order.

We finally arrive at

$$\Gamma^{\text{Spin}} = \int_0^\infty \frac{dT}{T} e^{-\frac{m^2}{2}T} \int_{x(T)=x(0)} \mathcal{D}x(\tau) \Phi[x] e^{-\int_0^T d\tau \left(\frac{\dot{x}^2}{2} + iq\dot{x} \cdot A(x)\right)}, \quad (4.84)$$

which differs from (4.67) in a global sign and the inclusion of the *spin factor*<sup>42</sup>

$$\Phi[x] = \frac{1}{2} \text{tr} \mathcal{P} \exp\left(\frac{i}{4} q \int_0^T d\tau \boldsymbol{\sigma}_{\mu\nu} F_{\mu\nu}(x(\tau))\right). \quad (4.85)$$

The trace is with regard to the spinor indices in  $\boldsymbol{\sigma}^{\mu\nu}$ , the symbol  $\mathcal{P}$  denotes the *path ordered exponential*. It is to be understood like the time ordered solution of the matrix differential equation

$$\dot{\mathbf{A}} = \mathbf{M}(t) \cdot \mathbf{A} \quad \rightsquigarrow \quad \mathbf{A}(t) = T \exp\left(\int_0^t dt' \mathbf{M}(t')\right), \quad (4.86)$$

<sup>42</sup> The factor of  $\frac{1}{2}$  is not usually included in the spin factor, we do so for notational convenience.

in this case now ordered along the path  $x(\tau)$ . This expression was already given by Feynman in [Fey51]. A more modern way to represent this spin factor is using additional Graßmann-valued integrals, derived in [Sch01] for example.

[Fey51] Feynman. *Phys. Rev.* (1951)

[Sch01] Schubert. *Phys. Rep.* (2001)

### 4.3. Saddle point approximation

We can perform both the  $T$ -integral and the path integral in (4.84) using Laplace's method. We want the approximation to be valid for fields below the critical field strength  $E_{\text{crit}} = m^2/q$ , so the large parameter in Laplace's method is  $m^2/qE$ , where  $E$  is the peak value of the electric field in consideration. Let us thus first express all quantities as dimensionless ratios. We choose<sup>43</sup>

$$\tilde{x}_\mu = x_\mu \frac{qE}{m}, \quad \tilde{F}_{\mu\nu} = F_{\mu\nu} \frac{1}{E}, \quad \tilde{A}_\mu = \frac{qE}{m} \frac{1}{E} A_\mu, \quad (4.87)$$

and rescale the integration variables as<sup>44</sup>

$$\tilde{T} = qET, \quad u = \frac{1}{\tilde{T}} \tau = \frac{qE}{\tilde{T}} \tau, \quad \curvearrowright \frac{\partial}{\partial u} = \frac{\tilde{T}}{qE} \frac{\partial}{\partial \tau}. \quad (4.88)$$

Inserting these definitions into (4.84) and rearranging the order of integration we arrive at<sup>45</sup>

$$\Gamma = \int_{\tilde{x}(1)=\tilde{x}(0)} \mathcal{D}\tilde{x}(u) \int_0^\infty \frac{d\tilde{T}}{\tilde{T}} \Phi[\tilde{x}] e^{-\frac{m^2}{qE} \left( \frac{\tilde{T}}{2} + \int_0^1 du \left( \frac{1}{2} \dot{\tilde{x}}^2 + i \dot{\tilde{x}} \cdot \tilde{A}(\tilde{x}) \right) \right)}. \quad (4.89)$$

with

$$\Phi[\tilde{x}] = \frac{1}{2} \text{tr} \mathcal{P} e^{\frac{\tilde{T}}{4} \int_0^1 du \sigma_{\mu\nu} i \tilde{F}_{\mu\nu}(x)} \quad (4.90)$$

For a given path, the  $\tilde{T}$ -integration in equation (4.89) now has the form<sup>46</sup>

$$I := \int_0^\infty d\tilde{T} g(\tilde{T}) e^{-\frac{m^2}{qE} f(\tilde{T})}, \quad (4.91)$$

with  $f$  and  $g$  dimensionless, smooth functions of  $\tilde{T}$ .

Let us proceed to find the minimum  $\tilde{T}_0$  of  $f$ ,

$$0 \stackrel{!}{=} \left. \frac{df}{d\tilde{T}} \right|_{\tilde{T}=\tilde{T}_0} = \frac{1}{2} - \frac{1}{2\tilde{T}_0^2} \int_0^1 du \dot{\tilde{x}}^2 \quad (4.92)$$

$$\curvearrowright \tilde{T}_0 = \sqrt{\int_0^1 du \dot{\tilde{x}}^2} =: a[\tilde{x}],$$

and the second derivative at the minimum

$$f''(\tilde{T}_0) = \frac{1}{\tilde{T}_0^3} \int_0^1 du \dot{\tilde{x}}^2 = \frac{1}{a[\tilde{x}]} > 0, \quad (4.93)$$

Collecting the pieces, we find

$$I \approx g(\tilde{T}_0) \sqrt{\frac{2\pi}{\frac{m^2}{qE} f''(\tilde{T}_0)}} e^{-\frac{m^2}{qE} f(\tilde{T}_0)} = \sqrt{\frac{2\pi}{a[\tilde{x}]} \frac{qE}{m^2}} \Phi[\tilde{x}] e^{-\frac{m^2}{qE} \mathcal{A}[\tilde{x}]}, \quad (4.94)$$

$[\mathbf{A}] = \mathbf{L}^{-1}$ ,  $\mathbf{x}_i = \mathbf{x}^i$   
(see page 13).

<sup>43</sup> We could have used powers of the electron mass alone, however the incorporation of the electric field will prove useful in the following.

<sup>44</sup> Note that the *proper time parameter*  $T$  does not actually have the dimension of time.

<sup>45</sup> Note that there is a subtlety in the change in the path integration measure. We will come back to this in Section 4.4.

<sup>46</sup> Note that that the spin factor is part of  $g$  since it does not include the large parameter in the exponent.

with the non-local (due to  $a[\tilde{x}]$ ) action

$$\mathcal{A}[\tilde{x}] = a[\tilde{x}] + \int_0^1 du \dot{\tilde{x}} \cdot i\tilde{A}(\tilde{x}), \quad (4.95)$$

and the spin factor

$$\Phi[\tilde{x}] = \frac{1}{2} \text{tr} \mathcal{P} \exp \left( \frac{a[\tilde{x}]}{4} \int_0^1 du \sigma_{\mu\nu} i\tilde{F}_{\mu\nu}(\tilde{x}) \right). \quad (4.96)$$

The remaining path integral is thus

$$\Gamma \approx \int_{\tilde{x}(1)=\tilde{x}(0)} \mathcal{D}\tilde{x}(\tau) \sqrt{\frac{2\pi}{a[\tilde{x}]} \frac{qE}{m^2}} \Phi[\tilde{x}] e^{-\frac{m^2}{qE} \mathcal{A}[\tilde{x}]}. \quad (4.97)$$

We can again apply Laplace's method now, which in this case means finding the periodic path  $\tilde{x}(u)$  that minimizes the functional  $\mathcal{A}[\tilde{x}]$ <sup>47</sup>. Demanding the variational derivative of  $\mathcal{A}[\tilde{x}]$  to vanish yields the *instanton equations of motion*

$$\frac{\ddot{\tilde{x}}_\mu(u)}{a[\tilde{x}]} = i\tilde{F}_{\mu\nu}(\tilde{x}(u))\dot{\tilde{x}}_\nu(u). \quad (4.98)$$

Since  $a[\tilde{x}]$  depends on the integral over  $\tilde{x}_\mu$ , this is an integro-differential equation. We do, however, immediately learn a property of the solutions  $\tilde{x}_\mu(u)$  by contracting (4.98) with  $\dot{\tilde{x}}_\mu$ :

$$\frac{\dot{\tilde{x}}_\mu \ddot{\tilde{x}}_\mu}{a[\tilde{x}]} = \frac{1}{a[\tilde{x}]} \frac{1}{2} \frac{d}{du} \dot{\tilde{x}}^2 = i\dot{\tilde{x}}_\mu \tilde{F}_{\mu\nu} \dot{\tilde{x}}_\nu = 0, \quad (4.99)$$

where the last equality follows because  $\tilde{F}_{\mu\nu}$  is an antisymmetric tensor. This implies that

$$\dot{\tilde{x}}^2 = \text{const.} =: a, \quad (4.100)$$

simplifying the instanton equations of motion to<sup>48</sup>

$$\ddot{\tilde{x}}_\mu(u) = ia\tilde{F}_{\mu\nu}(\tilde{x}(u))\dot{\tilde{x}}_\nu(u). \quad (4.101)$$

A solution to these equations of motion with the periodicity constraint  $\tilde{x}_\mu(1) = \tilde{x}_\mu(0)$  is called a worldline instanton and usually denoted with the superscript <sup>cl</sup>, for *classical trajectory*. Evaluating the action  $\mathcal{A}[\tilde{x}_\mu^{\text{cl}}]$  on this solution gives the exponent of the effective action in units of  $m^2/qE$ , and thus the leading contribution to the pair production probability.

Although (4.101) looks rather simple, remember that  $\tilde{F}_{\mu\nu}$  may in general, for spacetime dependent fields, depend on  $\tilde{x}_\mu$  in an arbitrarily complex way, turning the equations of motion into a system of coupled, nonlinear boundary value problems. While they can be solved analytically in a few special cases,<sup>49</sup> in general we have to resort to numerical methods, outlined in Chapter 5.

Having found an instanton, that is, a critical point of the exponent, we have to evaluate the fluctuation prefactor. There are some subtleties involved in this and we will postpone its discussion for the continuous path integral, looking at a discretized version first.

<sup>47</sup> Again, we do not consider the exponent of the spin factor to be part of this action, as it is slowly varying (it does not include the large parameter).

<sup>48</sup> The parameter  $a$  still has to be chosen to fulfill the periodicity constraint, but it does not depend on the trajectory in a non-local way anymore.

<sup>49</sup> See Chapter 6.

## 4.4. Discretized worldline instantons [STS19]

Equation (2.23) tells us how to discretize the path integral in (4.97). The normalization constant depends on the parametrization of the paths, specifically the time period between the first and last points, so to read off the prefactor we need to reinstate the original path integration measure, with the dimensionful coordinates  $x_\mu$  parametrized by  $0 < \tau < T$ .

We do have to slightly modify the normalization in (2.23). First of all the period  $T$  does not have the dimension of time, but  $mT$  does. Furthermore we have to analytically continue to Euclidean time, that is  $iT \rightarrow T$ . We thus arrive at the discretized version of the worldline path integral (the square brackets now denoting dependence on all  $N$  points along the trajectory),

$$\begin{aligned} \Gamma &\approx \left( \prod_{k=0}^{N-1} \int d^d x^k \left( \frac{N}{2\pi T_0} \right)^{d/2} \right) \sqrt{\frac{2\pi}{a[\tilde{x}_\mu^l]} \frac{qE}{m^2}} \Phi[\tilde{x}_\mu^l] e^{-\frac{m^2}{qE} \mathcal{A}[\tilde{x}_\mu^l]} \\ &= \left( \prod_{k=0}^{N-1} \int d^d \tilde{x}^k \right) \left( \frac{m^2}{qE} \frac{N}{2\pi a[\tilde{x}_\mu^l]} \right)^{Nd/2} \sqrt{\frac{2\pi}{a[\tilde{x}_\mu^l]} \frac{qE}{m^2}} \Phi[\tilde{x}_\mu^l] e^{-\frac{m^2}{qE} \mathcal{A}[\tilde{x}_\mu^l]}. \end{aligned} \quad (4.102)$$

Note that we have now expressed everything in terms of dimensionless variables. We will from now on only consider these, so we will drop the tilde. To explicitly refer to the original, dimensionful quantities we will add a superscript  $\text{dim}$ .

We obtain discrete expressions for  $a$ ,  $\Phi$  and  $\mathcal{A}$  by approximating derivatives by forward differences and integrals by Riemann sums, which is valid for large  $N$ . More precisely, we need to undo the steps that lead to the continuous path integral (2.22), or rather keep the result with finite  $N$  without performing the symbolic limit. This distinction is important in the case of the term containing  $A_\mu$ , we obtain

$$a[x_\mu^l] := \sqrt{N \sum_{k=0}^{N-1} (x_v^{k+1} - x_v^k)^2} \quad (4.103)$$

$$\mathcal{A}[x_\mu^l] := a[x_\mu^l] + \sum_{k=0}^{N-1} \left( \frac{A_v(x_\mu^{k+1}) + A_v(x_\mu^k)}{2} \right) (x_v^{k+1} - x_v^k). \quad (4.104)$$

Other discretizations for the gauge term would lead to the same classical continuum limit, for example simply taking the potential at one point  $A_v(x_\mu^k)$ . This is not what we get from the derivation however, and can even be shown to give wrong results, see [RF95; Gav+04].

Special care has to be taken to implement path ordering for  $\Phi$  as well; we can not just perform the Riemann sum and then exponentiate. Instead, we use the product representation of the exponential function (again, valid for large  $N$ ) which is automatically path ordered

$$\Phi[x_\lambda^l] := \frac{1}{2} \text{tr} \left[ \prod_{k=0}^{N-1} \left( \mathbb{1} + \frac{a[x_\lambda^l]}{4N} \sigma_{\mu\nu} iF_{\mu\nu}(x_\lambda^k) \right) \right]. \quad (4.105)$$

At this point we have to perform the  $N \times d$ -dimensional integral over all points

**[A] =  $L^{-1}$ ,  $x_i = x^i$**   
(see page 13).

**[A] =  $\mathbf{1}$**  (see page 13).

[RF95] Rabello and Farina. *Phys. Rev. A* (1995)

[Gav+04] Gaveau, Mihóková, Roncadelli, and Schulman. *Am. J. Phys.* (2004)

on the trajectory. Using Laplace's method for the multivariate case (2.46), we get

$$\begin{aligned}\Gamma &\approx \sqrt{\frac{2\pi}{a^{\text{cl}}}} \frac{qE}{m^2} \left( \frac{m^2}{qE} \frac{N}{2\pi a^{\text{cl}}} \right)^{Nd/2} \sqrt{\frac{(2\pi)^{Nd}}{\left(\frac{m^2}{qE}\right)^{Nd} \det \mathbf{H}[x_\mu^{\text{cl},l}]}} \Phi[x_\mu^{\text{cl},l}] e^{-\frac{m^2}{qE} \mathcal{A}[x_\mu^{\text{cl},l}]} \\ &= \sqrt{\frac{2\pi}{a^{\text{cl}}}} \frac{qE}{m^2} \left( \frac{N}{a^{\text{cl}}} \right)^{Nd/2} \frac{\Phi[x_\mu^{\text{cl},l}]}{\sqrt{\det \mathbf{H}[x_\mu^{\text{cl},l}]}} e^{-\frac{m^2}{qE} \mathcal{A}[x_\mu^{\text{cl},l}]},\end{aligned}\quad (4.106)$$

where the collection of points  $x_\mu^{\text{cl},l}$ , a *discretized instanton*, is the solution to the discrete equations of motion, which are just the condition of an extremal point of the  $N \times d$ -dimensional function  $\mathcal{A}$ ,

$$\left. \frac{\partial}{\partial x_\mu^l} \mathcal{A}[x_\mu^l] \right|_{x_\mu^l = x_\mu^{\text{cl},l}} = 0. \quad (4.107)$$

The Hessian  $\mathbf{H}$  is comprised of all second derivatives of the action  $\mathcal{A}$  and  $a^{\text{cl}} := a[x_\mu^{\text{cl},l}]$ .

The biggest complication arising in this scheme is that of zero modes. Since only the periodicity of the trajectory is fixed, an overall shift of the proper time parameter  $u$  does not change anything. In the discretized version this means moving the points (which are labeled by the index  $l$  corresponding to  $u = l/N$ ) along the trajectory. We can fix this using the Faddeev-Popov method from Section 2.6. The parameter of the symmetry is the amount of reparametrization  $\Delta u$ , the volume  $V_{\Delta u} = 1$ , the eigenvector the classical velocity  $\dot{x}_\mu^{\text{cl},l}$ . Taking a step back to the continuous situation we can choose<sup>50</sup>

$$\chi_u[x_\mu](\Delta u) = \frac{2}{(a^{\text{cl}})^2} \int_0^1 du \dot{x}_v^{\text{cl}}(u) x_v(u + \Delta u). \quad (4.108)$$

This gives  $w = 2$  and the prefactors are chosen so that

$$\frac{1}{w} |\chi_u[x_\mu]'(0)| = \frac{1}{2} \frac{2}{(a^{\text{cl}})^2} \int_0^1 du \dot{x}_v^{\text{cl}}(u) \dot{x}_v(u) \stackrel{x=x^{\text{cl}}}{=} 1, \quad (4.109)$$

at the saddle point. This means we only have to introduce  $\pi \chi_u^2$  in the exponent of (4.106) and a prefactor of  $\sqrt{m^2/qE}$  (corresponding to  $\sqrt{M}$ ) as in (2.62). Discretized,  $\chi_u$  reads

$$\chi_u[x_\mu^l] = \frac{2}{(a^{\text{cl}})^2} \sum_{k=0}^{N-1} \dot{x}_v^{\text{cl},k} x_v^k. \quad (4.110)$$

If the electromagnetic field does not depend on time or a spatial coordinate additional zero modes arise. These are in principle easier to deal with, we can immediately replace integrations in the corresponding directions with volume factors representing the spatial volume or time period under consideration. In practice however, selectively suppressing some of the integrations automatically is more complicated than just adding additional terms  $\pi \chi_{x_v}^2$ .

The zero eigenvalue in a field not depending on coordinate  $x_v$  is just the vector in the  $\mu$ -direction at every point of the trajectory, so

$$\chi_{x_v}[x_\mu^l] = \frac{1}{N} \sum_{k=0}^{N-1} x_v^k. \quad (4.111)$$

<sup>50</sup> The dot product replaced by integration.

Each coordinate held fixed gives again a factor of  $\sqrt{m^2/qE}$  and a volume factor  $L_\mu$ . Note however that this volume factor is given in terms of the dimensionless coordinates that include the electric field, so in terms of dimensionful scales  $L_\mu^{\text{dim}}$  we have

$$L_\mu \sqrt{\frac{m^2}{qE}} = L_\mu^{\text{dim}} \sqrt{qE} \quad (4.112)$$

per invariant direction, consistent with the  $(qE)^2$ -dependence in the case of a constant homogeneous field.

In summary, the computational strategy is now to find a solution to (4.107) for a given background field and evaluate the fluctuation prefactor as well as the spin factor (if desired). The Euclidean effective action can then be assembled as

$$\Gamma = V_{N_0} (qE)^{N_0/2} \sqrt{\frac{2\pi}{a^{\text{cl}}}} \left(\frac{N}{a^{\text{cl}}}\right)^{Nd/2} \frac{\Phi[x_\mu^{\text{cl},l}]}{\sqrt{\det \mathbf{H}[x_\mu^{\text{cl},l}]}} e^{-\frac{m^2}{qE} \mathcal{A}[x_\mu^{\text{cl},l}]}, \quad (4.113)$$

where  $N_0$  is the number of translational zero modes. How to implement this scheme in practice will be discussed in Chapter 5.

## 4.5. Prefactor in the continuous case

To calculate the prefactor in the functional setting without resorting to discretization we need to take a few steps back again. The formalism to compute the necessary determinants using the Gel'fand-Yaglom formula is not applicable to non-local operators, so we can not use it for the path integral after having performed the  $T$ -integral before. Instead we write down the full expression again, with all quantities replaced by their dimensionless versions. We also keep the initial point fixed, which avoids zero modes in the path integral.

**[A] = 1,  $\mathbf{x}_j = \mathbf{x}^j$**   
(see page 13).

$$\Gamma = \int_0^\infty \frac{dT}{T} e^{-\frac{m^2}{qE} \frac{T}{2}} \int d^4 x^0 \int_{x(1)=x(0)=x^0} \mathcal{D}x(u) \Phi[x] e^{-\frac{m^2}{qE} S} \quad (4.114)$$

with the action<sup>51</sup>

$$S = \int_0^1 du L = \int_0^1 du \left( \frac{\dot{x}^2}{2T} + i\dot{x} \cdot A(x) \right). \quad (4.115)$$

<sup>51</sup> We use the different symbol  $S$  instead of  $\mathcal{A}$  here, as  $\mathcal{A}$  includes the saddle point value of  $T/2$  which is kept apart here.

The Euler-Lagrange equations look similar to before,

$$\ddot{x}_\mu(u) = T i F_{\mu\nu}(x(u)) \dot{x}_\nu(u), \quad (4.116)$$

only that  $T$  is a free integration parameter now, instead of the saddle point value  $T = a[x]$ .

Let us assume we have found a solution of the equations of motion that we call  $x^{\text{cl}}$  (for *classical*). We then need the second variation, by expanding  $x(u) =$

$x^{\text{cl}}(u) + \eta(u)$  (but drop the  $\text{cl}$  for brevity):

$$\begin{aligned}
\delta^2 \mathcal{S} &= \int_0^1 du \left( \frac{\partial^2 L}{\partial \dot{x}_\mu \partial \dot{x}_\nu} \dot{\eta}_\mu \dot{\eta}_\nu + \frac{\partial^2 L}{\partial x_\mu \partial \dot{x}_\nu} \eta_\mu \dot{\eta}_\nu \right. \\
&\quad \left. + \frac{\partial^2 L}{\partial \dot{x}_\mu \partial x_\nu} \dot{\eta}_\mu \eta_\nu + \frac{\partial^2 L}{\partial x_\mu \partial x_\nu} \eta_\mu \eta_\nu \right) \\
&= \int_0^1 du \eta_\mu \left( -\frac{\partial^2 L}{\partial \dot{x}_\mu \partial \dot{x}_\nu} \frac{\partial^2}{\partial u^2} + \frac{\partial^2 L}{\partial x_\mu \partial \dot{x}_\nu} \frac{\partial}{\partial u} - \frac{\partial}{\partial u} \frac{\partial^2 L}{\partial \dot{x}_\mu \partial x_\nu} + \frac{\partial^2 L}{\partial x_\mu \partial x_\nu} \right) \eta_\nu \\
&= \int_0^1 du \eta_\mu \Lambda_{\mu\nu} \eta_\nu
\end{aligned} \tag{4.117}$$

Where we have performed integration by parts on the first and third term (the boundary terms do not contribute, as the variations  $\eta$  vanish at 0 and 1), and defined

$$\Lambda_{\mu\nu} = -\frac{\delta_{\mu\nu}}{T} \frac{\partial^2}{\partial u^2} + Q_{\mu\nu} \frac{\partial}{\partial u} - \frac{\partial}{\partial u} Q_{\nu\mu} + R_{\mu\nu} \tag{4.118}$$

with

$$Q_{\mu\nu} = \frac{\partial^2 L}{\partial x_\mu \partial \dot{x}_\nu} = i \frac{\partial A_\nu}{\partial x_\mu} \quad \text{and} \quad R_{\mu\nu} = \frac{\partial^2 L}{\partial x_\mu \partial x_\nu} = i \frac{\partial^2 A}{\partial x_\mu \partial x_\nu} \cdot \dot{x}. \tag{4.119}$$

As described before, the path integral over the fluctuations is Gaussian, so it is given by the determinant of  $\Lambda_{\mu\nu}$ . Since by itself it is divergent, we have to instead consider a ratio, in particular relate it to some quantity we know. Fortunately, we can evaluate the path integral in the free ( $A_\mu = 0$ ) case by using the correctly normalized, discrete formulation (2.23) (for one dimension):

$$\begin{aligned}
I^{\text{Free}} &= \int_{x(1)=x(0)} \mathcal{D}x \exp \left( -\frac{m^2}{qE} \int_0^1 du \frac{\dot{x}^2}{2T} \right) \\
&= \left( \prod_{k=0}^{N-1} \int dx_k \sqrt{\frac{m^2}{qE} \frac{N}{2\pi T}} \right) \exp \left( -\frac{m^2}{qE} \frac{N}{2T} \sum_{k=0}^{N-1} (x_{k+1} - x_k)^2 \right) \\
&=: \mathcal{N} \int dx_0 \dots dx_{N-1} \exp \left( -\xi \sum_{k=0}^{N-1} (x_{k+1} - x_k)^2 \right),
\end{aligned} \tag{4.120}$$

<sup>52</sup> Torgrimsson, *personal communication*.

with  $x_N \equiv x_0$ . There is a neat trick to evaluate this integral<sup>52</sup>. We introduce an additional integral over  $x_N$  but keep  $x_N = x_0$  using a Dirac delta that we represent

using an oscillatory integral,

$$\begin{aligned} I^{\text{Free}} &= \mathcal{N} \int dx_0 \dots dx_{N-1} \exp\left(-\xi \sum_{k=0}^{N-1} (x_{k+1} - x_k)^2\right) \\ &= \mathcal{N} \int \frac{d\zeta}{2\pi} \int dx_0 \dots dx_N e^{i\zeta(x_0 - x_N)} \exp\left(-\xi \sum_{k=0}^{N-1} (x_{k+1} - x_k)^2\right). \end{aligned} \quad (4.121)$$

Now we shift the integrations one by one, e.g.  $y_0 = x_0 - x_1$ ,

$$\begin{aligned} I^{\text{Free}} &= \mathcal{N} \int \frac{d\zeta}{2\pi} \int dy_0 dx_1 \dots dx_N \\ &\quad \times \exp\left(i\zeta(y_0 + x_1 - x_N) - \xi y_0^2 - \xi \sum_{k=1}^{N-1} (x_{k+1} - x_k)^2\right) \\ &= \mathcal{N} \int \frac{d\zeta}{2\pi} \int dx_1 \dots dx_N \sqrt{\frac{\pi}{\xi}} \\ &\quad \times \exp\left(-\frac{\zeta^2}{4\xi} + i\zeta(x_1 - x_N) - \xi \sum_{k=1}^{N-1} (x_{k+1} - x_k)^2\right) \\ &= \mathcal{N} \int \frac{d\zeta}{2\pi} \int dx_N \left(\frac{\pi}{\xi}\right)^{\frac{N}{2}} \exp\left(-N \frac{\zeta^2}{4\xi}\right) \\ &= \int dx_N \frac{1}{2\pi} \sqrt{\frac{\pi 4\xi}{N}} \left(\frac{\pi}{\xi}\right)^{\frac{N}{2}} = V \sqrt{\frac{m^2}{qE} \frac{1}{2\pi T}}. \end{aligned} \quad (4.122)$$

For the known, free part of the fluctuation prefactor we get this factor for each spatial dimension (without the volume factor  $V$  because we keep the loop's starting point fixed),

$$\text{Pref.} = (I^{\text{Free}})^4 \sqrt{\frac{\text{Det}(\Lambda_{\mu\nu}^{\text{Free}})}{\text{Det}(\Lambda_{\mu\nu})}} = \left(\frac{m^2/qE}{2\pi T}\right)^2 \sqrt{\frac{\text{Det}(\Lambda_{\mu\nu}^{\text{Free}})}{\text{Det}(\Lambda_{\mu\nu})}} \quad (4.123)$$

We can now tackle the ratio of determinants using the Gelfand-Yaglom method from section 2.8:

$$\frac{\text{Det}(\Lambda_{\mu\nu}^{\text{Free}})}{\text{Det}(\Lambda_{\mu\nu})} = \frac{\det(\eta_{\mu}^{(v),\text{Free}}(1))}{\det(\eta_{\mu}^{(v)}(1))}, \quad (4.124)$$

with

$$\Lambda_{\mu\nu} \eta_{\nu}(u) = 0, \quad \eta_{\mu}^{(v)}(0) = 0, \quad \dot{\eta}_{\mu}^{(v)}(0) = \delta_{\mu\nu}. \quad (4.125)$$

The free case is very simple, it is just

$$0 = \Lambda_{\mu\nu}^{\text{Free}} \eta_{\nu}(u) = -\frac{1}{T} \ddot{\eta}_{\mu} \quad (4.126)$$

So the solutions satisfying the initial conditions are

$$\eta_{\mu}^{(v),\text{Free}} = \delta_{\mu\nu} u, \quad (4.127)$$

and thus

$$\det(\eta_{\mu}^{(v),\text{Free}}(1)) = 1. \quad (4.128)$$

Assembling the parts we arrive at

$$\Gamma \approx \int d^4 x^0 \int \frac{dT}{T} e^{-\frac{m^2}{qE} \frac{T}{2}} \left( \frac{m^2/qE}{2\pi T} \right)^2 \frac{\Phi[x] e^{-\frac{m^2}{qE} S(T)}}{\sqrt{\det(\eta_\mu^{(\nu)}(1))}}. \quad (4.129)$$

The big complication is now that the action  $S$  depends on  $T$  not only explicitly, but also via the instanton. This means we can not, in general, just perform Laplace's method as before. The saddle point value for the  $T$ -integral actually does come out as  $a$  again, the fluctuation around this value depends non-trivially on the instanton though. We will thus postpone any actual evaluation until Chapter 6.2 where we will calculate (4.129) for background fields depending on one coordinate only.

## 5

## Numerical instanton finding

This chapter introduces the methods used to numerically solve the instanton equations of motion, as well as continuation algorithms to trace solution sets with regard to a physical parameter.

## 5.1. Shooting method

On first sight, numerically finding worldline instantons for a given electromagnetic field appears simple enough, after all we only have to deal with a system of ordinary differential equations:

$$\ddot{x}_\mu(u) = iaF_{\mu\nu}\dot{x}_\nu(u). \quad (5.1)$$

Of course, given some initial conditions, we can easily integrate (5.1) using standard numerical methods. This is, however, not what we want, as we need solutions that satisfy the periodic boundary conditions  $x_\mu(1) = x_\mu(0)$  and we do not know in advance which initial conditions lead to periodic solutions. *Boundary value problems* like this are in general much harder to study and fewer general purpose algorithms exist.<sup>53</sup>

The method presented here is the *shooting method*, which is very simple conceptually, but works reasonably well for simple problems. Let us for now consider a general system of  $N$  first order differential equations with periodic boundary conditions

$$\dot{\mathbf{y}}(t) = \mathbf{f}(y_i(t), t), \quad \mathbf{y}(1) = \mathbf{y}(0). \quad (5.2)$$

To find a periodic solution, we just start with some initial conditions  $y_i(0) = y_i^0$ , “shoot” a trajectory (numerically integrate (5.2) from  $t = 0$  to  $t = 1$ ) and check if the solution  $\mathbf{y}(t)$  is periodic. If it is, all is well and we are done. If it is not, we have to improve our aim, by adjusting the initial conditions  $y_i^0$ . We could, in principle, do so by hand, however a better strategy is to use a nonlinear root finding algorithm.

Introducing the function

$$\mathbf{r}(y_i^0) = \mathbf{y}(1) - \mathbf{y}^0, \quad (5.3)$$

where  $\mathbf{y}(1)$  is obtained by numerically solving 5.2, finding a periodic solution is reduced to finding an  $N$ -dimensional zero of the  $N$ -dimensional function  $\mathbf{r}$ . This is a well understood problem and many algorithms exist to solve it, mostly variants of the *Newton-Raphson* scheme, which iteratively adjusts a trial point using the inverse of the Jacobian  $\mathbf{J}^r$ .

[A] = 1,  $\mathbf{x}_i = \mathbf{x}^i$   
(see page 13).

<sup>53</sup> They are also more complicated from an analytic point of view. For initial value problems the *Peano theorem* proves existence, and the *Picard-Lindelöf theorem* even guarantees uniqueness of solutions under some mild assumptions. For boundary value problems there are only results for specific differential equations that are, e.g., linear or have strictly positive right hand sides.

[Aba+12] Abad, Barrio, Blesa, and Rodríguez. *ACM Trans. Math. Softw.* (2012)

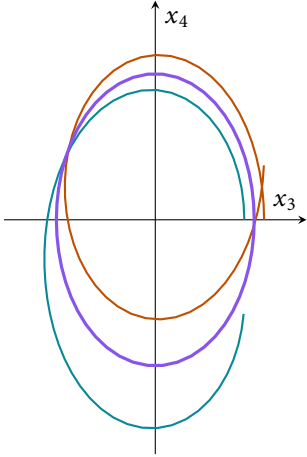


Figure 5.1.: Shooting method for a spatial Sauter profile. The purple trajectory is the instanton, the blue trajectory has  $x_3(0)$  chosen 10% too small, while it is 10% too large for the red trajectory.

In many cases, the entries of  $\mathbf{J}^r$  are expensive to compute or no partial derivatives are accessible at all, in which case it has to be approximated (e.g. using finite difference schemes). There are, however, methods of integrating ordinary differential equations that do provide us with these derivatives of the solution with regard to the initial values. In Mathematica the function `ParametricNDSolve[]` can compute these derivatives using sensitivity methods, while the software package `TIDES` [Aba+12], which uses the Taylor series method, can efficiently compute partial derivatives of the solution with regard to initial conditions and parameters using automatic differentiation.

Taking  $J_{ij}^{y^{(1)}} = \frac{\partial y_i(1)}{\partial y_j^0}$  from one of these methods, we can assemble the Jacobian needed for root finding:

$$\mathbf{J}^r(y_i^0) = \mathbf{J}^{y^{(1)}}(y_i^0) - \mathbf{1}. \quad (5.4)$$

In our case, the instanton equations of motion are a system of four second order differential equations, so we need eight initial conditions. Instead of specifying the initial velocity's four components, we usually use  $a = |\dot{x}_\mu(0)|$  and three angles.

In many cases the symmetry of the instanton can be predicted from the field or by playing around with the initial conditions by hand. This reduces the number of parameters that need to be adjusted by the shooting method, and keeping one component of the initial point static fixes the reparametrization invariance. For a linearly polarized field, depending on one coordinate/time only, with time reversal/reflection symmetry (for example a Sauter- or Gaussian pulse or a sinusoidal profile), we only need to vary  $a$  and one initial position component, see Figure 5.1.

## 5.2. Discrete instanton finding

[STS19]

There is a second approach to find worldline instantons numerically. Instead of deriving the continuous instanton equations and solving them algorithmically, we can use the discretized path integral, that is, solve the nonlinear algebraic equations in  $N \times d$  unknowns (4.107), where  $d = 4$  in general and  $N$  is the number of points in the discretization. This can then again be solved using a standard root finding algorithm.

At first it might seem strange to trade the root finding problem of at most eight unknowns for the shooting method against one for several hundred or even thousands of unknowns. The crucial problem of the shooting method is that the point  $x_\mu(1)$  depends on the initial conditions very sensitively, to the point that the smallest possible change<sup>54</sup> produces a jump in the end position so large that it is not possible to close the trajectory. This amounts to the target function  $r(y_i)$  effectively jumping over zero in a discontinuous way, making locating the root impossible.

In contrast, by moving all points simultaneously the root function, albeit high-dimensional, varies far more smoothly. Especially in combination with the continuation methods introduced in the next subsection this makes for a robust numerical scheme. Some details have to be taken care of however. In this approach

<sup>54</sup> Due to the finite precision of floating point arithmetic.

the velocity  $a$  can be solved for immediately,

$$a[x_\mu^l] = \sqrt{N \sum_{k=0}^{N-1} (x_v^{k+1} - x_v^k)^2}, \tag{5.5}$$

which can be substituted into the other equations. This however means that every coordinate  $x_\mu^l$  couples to every other. This leads to a densely populated Jacobian, depicted in Figure 5.2. We do know that at the root, i.e. the solution of the instanton equations,  $a$  is constant. We can thus replace the integral over the velocity in (5.5) with the instantaneous value

$$a_k[x_\mu^l] = \sqrt{N^2 (x_v^{k+1} - x_v^k)^2}, \tag{5.6}$$

Now all components couple to a few nearest neighbors only, giving the sparse structure of the Jacobian seen in Figure 5.3. While it is possible to compute the entries analytically, it is most performant in the Mathematica implementation to instruct the root finding algorithm to approximate the Jacobian by finite differences, but at the same time passing the locations of nonzero entries using the `SparsityPattern` option.

We still need to take care of zero modes. The most elegant way to keep a translational zero mode fixed would be hold the average of this direction constant (which is precisely what happens by adding  $\chi_{x_v}$  from (4.111) to the action), but this would again couple all points. Instead we just keep the respective coordinate of the first point fixed, by replacing the right hand side of the respective equation by a constant (usually zero)<sup>55</sup>.

### 5.3. Numerical continuation

[STS19]

The strategies outlined in the last two subsections both have one practical flaw – Newton-like algorithms are highly dependent on finding a good initial guess for the root. This is especially true for our  $r(y_i^0)$ , since nonlinear differential equations tend to depend on initial conditions very sensitively. If we try to choose good starting guesses by hand, we are not much better off than trying to find the periodic solutions directly.

Also in most of our further studies we are not only interested in a single world-line instanton, but in a whole family of solutions, depending on one or more parameters.<sup>56</sup> We can actually use this to our benefit, by means of *Numerical continuation* methods [AG03]. The basic idea of continuation is to take a system of equations we can easily solve and slowly deform it into the systems we are interested in.<sup>57</sup>

Let us, for definiteness, say our system of equations above depends on a parameter  $\lambda$ , so

$$\dot{y}(t) = f(\lambda, y_i(t), t), \quad r(\lambda, y_i^0) = y_\lambda(1) - y^0. \tag{5.7}$$

Now, the function  $r$  from (5.7) is an  $N$ -dimensional function of  $N + 1$  variables, so the condition  $r = \mathbf{0}$  fixes a one-dimensional manifold in the space  $\{\lambda, y^0\}$ . The continuation algorithm then consists of starting at a known point of this manifold and somehow stepping along it.

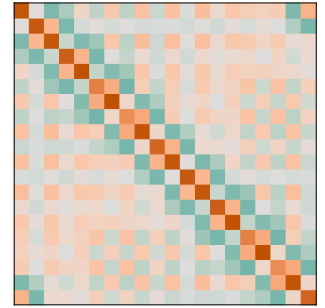


Figure 5.2.: Jacobian of the root function in a simple field with  $a$  replaced by (5.5), showing how all variables couple. Blue entries are negative, red entries are positive – the main point being that all entries are nonzero in general.

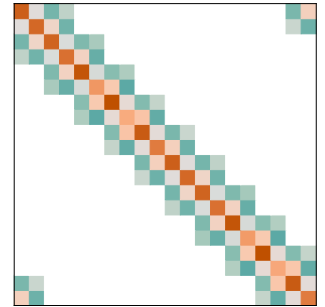


Figure 5.3.: Jacobian of the root function with  $a$  replaced by the local velocity (5.6), giving a sparse banded structure, zero entries displayed in white.

<sup>55</sup> Of course it is trivial after finding a solution to center the instanton by removing the average in the invariant direction, for example for visualization.

<sup>56</sup> For example the Keldysh parameter for time dependent fields. [AG03] Allgower and Georg. *Society for Industrial and Applied Mathematics* (2003)

<sup>57</sup> Continuation is also called *homotopy method*, due to this homotopy deformation.

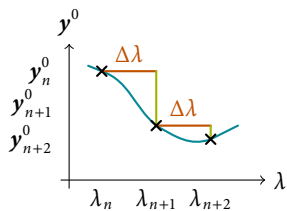


Figure 5.4.: Predictor (red) and corrector (green) steps in natural parameter continuation. The blue line depicts the true solution curve.

Assume we know that for  $\lambda = \lambda_n$ , the vector  $\mathbf{y}_n^0$  is a solution. We can then use a *predictor-corrector* scheme to find the next point on the solution manifold. The predictor step provides a guess for the next solution  $\mathbf{y}_{n+1}^{0*}$  for  $\lambda_{n+1}$  and the corrector step uses these as starting point for the root finding procedure to determine  $\mathbf{y}_{n+1}^0$ .

The easiest, trivial to implement variant of predictor leads to the *natural parameter continuation* method. We simply set  $\lambda_{n+1} = \lambda_n + \Delta\lambda$  and  $\mathbf{y}_{n+1}^{0*} = \mathbf{y}_n^0$ , for some fixed value of  $\Delta\lambda$ . As long as the change in initial conditions needed to maintain periodic solutions is fairly smooth and  $\Delta\lambda$  is chosen small enough, the following corrector step is able to “pull” the predicted values back onto the solution manifold. This procedure is qualitatively shown in Figure 5.4. The predictor step of natural parameter continuation could be called “zeroth order,” because it does not actually predict anything. Of course, the admissible value of  $\Delta\lambda$  strongly varies with the dependence of  $\mathbf{y}^0$  on  $\lambda$  (the slope in Figure 5.4). This means, a fixed choice of  $\Delta\lambda$  will likely either be too large in some regions, leading to deviations the corrector step cannot accommodate, or too small in other regions, wasting computing power. We could just ignore the latter problem and trade off some efficiency for the simplicity of the algorithm, but there are cases where natural parameter continuation fails completely.

We have implicitly assumed that it is possible to parametrize the solution manifold as  $\mathbf{y}^0(\lambda)$ , which may not actually be true everywhere. We could have values of  $\lambda$  where the slope grows infinite, or there could be turning points in  $\lambda$ , so that  $\mathbf{y}^0(\lambda)$  is not single valued anymore.

This motivates a different kind of parametrization of the solution curve, which leads to *pseudo-arclength* continuation. Let us introduce the  $N + 1$ -dimensional parametrization

$$\mathbf{c}(u) = \begin{pmatrix} \mathbf{y}^0(u) \\ \lambda(u) \end{pmatrix}. \quad (5.8)$$

Now we can take the total derivative of the periodicity condition:

$$\mathbf{0} = \frac{d}{du} \mathbf{r}(y_i^0(u), \lambda) = \frac{d}{du} \mathbf{r}(\mathbf{c}(u)) = \mathbf{J}^r(\mathbf{c}(u)) \cdot \dot{\mathbf{c}}(u), \quad (5.9)$$

where the dot denotes differentiation with regard to  $u$ . Note that the Jacobian  $\mathbf{J}^r$  is now an  $N \times (N + 1)$  matrix, containing the  $\lambda$ -derivatives as well. Equation (5.9) is intuitively clear, if  $\mathbf{c}(u)$  is a zero of  $\mathbf{r}$  then the solution curve flows orthogonal to the change of  $\mathbf{r}$ , because we want it to remain zero.

$\dot{\mathbf{c}}$  is not completely determined, though. We only know that  $\dot{\mathbf{c}}$  is orthogonal to  $\mathbf{J}^r$ , so we still have to fix its magnitude and orientation. The nicest choice of normalization would be parametrization by arclength, so that  $\|\dot{\mathbf{c}}\| = 1$ . Actually enforcing this constraint in the numerical scheme is difficult, but we can at least do the predictor step using a fixed arclength. The corrector step that follows will then change this length (which is why it is called *pseudo-arclength*), but not substantially. We first define the  $(N + 1) \times (N + 1)$  *augmented Jacobian*

$$\tilde{\mathbf{J}}^r = \begin{pmatrix} \mathbf{J}^r \\ \dot{\mathbf{c}}^\top \end{pmatrix}, \quad (5.10)$$

so that both the orthogonality and the arclength condition are encoded in the

equation

$$\tilde{\mathbf{J}}^r \cdot \dot{\mathbf{c}} = \begin{pmatrix} \mathbf{0} \\ 1 \end{pmatrix}. \tag{5.11}$$

This equation is quadratic in  $\dot{\mathbf{c}}$ , so we get two solutions  $\dot{\mathbf{c}}^\pm$  (corresponding to the two possible orientations). We can finally fix the direction by demanding

$$\det \tilde{\mathbf{J}}^r > 0. \tag{5.12}$$

We can now summarize the pseudo-arclength algorithm. We start with an approximately known zero  $\mathbf{c}_n^*$ . The corrector step provides us with  $\mathbf{c}_n$  and  $\mathbf{J}^r(\mathbf{c}_n)$ . We then solve (5.11) for  $\dot{\mathbf{c}}_n^\pm$ , and choose the  $\dot{\mathbf{c}}_n$  that gives  $\det \tilde{\mathbf{J}}^r > 0$ . We can finally do our prediction step  $\mathbf{c}_{n+1}^* = \mathbf{c}_n + \Delta u \dot{\mathbf{c}}_n$ . A variant of this approach was introduced in 1953 by Davidenko to solve a variety of problems starting with [Dav53], because of this we also use *Davidenko continuation* synonymously with pseudo-arclength continuation.

Compared to natural parameter continuation the pseudo-arclength method has several advantages. First of all, it is applicable to solution sets that can not be parametrized by the physical parameter, that is, solutions that have a turning point in  $\lambda$  or diverge in some direction, by tracing some curve in  $N + 1$ -dimensional space. There are dynamical systems with such properties, however they will not appear in our context. The more important property is that pseudo-arclength continuation provides a much better guess for the subsequent root finding process. Especially in spatially inhomogeneous fields, if the initial configuration is not very close to the solution, root finding quickly wanders off. In these cases, natural parameter continuation would need prohibitively small steps, while pseudo-arclength continuation predicts the solution well enough for far larger steps. Furthermore, it is actually possible to do multiple steps according to (5.11) before running the root finding procedure again. This way a fine tradeoff between evaluations of the Jacobian and performance of root finding can be chosen, by varying the step width  $\Delta u$  and the number of predictor steps taken before the next corrector step.

Solving (5.11) requires that the Jacobian is invertible. Fortunately, if we use the Hessian<sup>58</sup> including the Faddev-Popov fixing terms from section 4.4, the zero modes that would cause  $\tilde{\mathbf{J}}^r$  not to be invertible are removed already.

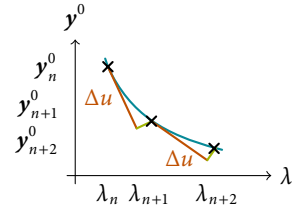


Figure 5.5.: Predictor (red) and corrector (green) steps in pseudo-arclength continuation. The blue line depicts the true solution curve.

[Dav53] Davidenko. *Dokl. Akad. Nauk SSSR* (1953)

<sup>58</sup> We called it the Hessian because it includes the second derivatives of the action. Interpreting the gradient of the action as an  $N$ -dimensional root function, the Hessian of the action is the Jacobian of the root function.



**Part II.**

## **Applications**



# 6

## Example fields

Having introduced several methods to calculate pair production probabilities, we will now apply these to some example fields and compare the results.

### 6.1. Constant electric fields

The scenario that started it all is that of pair creation in a constant, homogeneous, purely electric field. This case is fairly tractable using multiple methods, so we will rederive the classic result, at first for scalar QED only, using the different methods introduced in the first part.

For reference, the real part of the Euclidean effective action of scalar QED, which is the imaginary part of the Minkowski variant, in a constant electric field reads

$$\frac{\Re\Gamma}{V_4} = \frac{(qE)^2}{2(2\pi)^3} \sum_{n=1}^{\infty} \frac{(-1)^{n+1}}{n^2} \exp\left(-n\pi \frac{m^2}{qE}\right), \quad (6.1)$$

with the instantaneous pair production rate given by the first term in the series and  $V_4$  a volume factor (otherwise the pair production rate would be infinite). We can now reproduce this result using our different methods.

First of all we can start with the derivation of the worldline path integral in Section 4.2, but instead of expressing the trace as a path integral we directly evaluate the diagonal elements and perform the integral. We pick up from<sup>59</sup>

$$\Gamma = - \int_0^{\infty} \frac{dT}{T} \int d^4x \langle x | e^{-(\square_A + m^2)T} | x \rangle \quad (6.2)$$

and proceed like [BI70]. Similarly to the derivation in 4.2 we take the partial derivatives to be the coordinate representation of the momentum operator in ordinary quantum mechanics, then

$$\square_A = (\partial_\mu + iqA_\mu)^2 = - \underbrace{\left( \frac{1}{i} \partial_\mu + qA_\mu \right)^2}_{\hat{p}_\mu}. \quad (6.3)$$

To represent the constant, homogeneous electric field we choose the Euclidean four-potential

$$A_3 = ix_4 E, \quad (6.4)$$

and expand the operator  $\square_A$ ,

$$-\square_A = (\hat{p}_\mu + qA_\mu(\hat{x}))^2 = \hat{p}_1^2 + (\hat{p}_3 + iqE\hat{x}_4)^2 + \hat{p}_4^2, \quad (6.5)$$

**[A] = L<sup>-1</sup>, x<sub>i</sub> = x<sup>i</sup>**  
(see page 13).

<sup>59</sup> We perform this derivation, up to eq. (6.18), using the original dimensionful variables.

[BI70] Brézin and Itzykson. *Phys. Rev. D* (1970)

where  $\hat{p}_\perp$  means the 1- and 2-components of the momentum operator. To evaluate the trace, we introduce decompositions of unity in terms of momentum operators in front of and behind the exponential. The term with  $m^2$  is just a number so we can take it out of the expectation value. what remains is

$$\langle x | e^{\square_A T} | x \rangle = \int d^4 p \int d^4 p' \times \langle x | p \rangle \langle p | \exp \left( -(\hat{p}_\perp^2 + (\hat{p}_3 + iqE\hat{x}_4)^2 + \hat{p}_4^2) T \right) | p' \rangle \langle p' | x \rangle \quad (6.6)$$

The operator  $\hat{p}_\perp$  commutes with the other operators in the exponent so we can pull it out and have it operate either on  $|p'\rangle$  to the right or  $\langle p|$  on the left, we will see in a moment that which one does not matter. We can not immediately have the other operators operate on the states around them though, as  $\hat{x}_4$  and  $\hat{p}_4$  do not commute. We can disentangle the exponent a bit using the quantum mechanical translation operator,

$$f(\hat{x} + \hat{y}) = \hat{T}^{-1}(\hat{y}) f(\hat{x}) \hat{T}(\hat{y}) := \exp(i\hat{y}\hat{p}_x) f(\hat{x}) \exp(-i\hat{y}\hat{p}_x) \quad (6.7)$$

in our case with  $\hat{y} = \hat{p}_3/iqE$ . For the amplitude we thus get

$$\begin{aligned} \langle p | \exp \left( -(\hat{p}_\perp^2 + (\hat{p}_3 + iqE\hat{x}_4)^2 + \hat{p}_4^2) T \right) | p' \rangle &= e^{-p_\perp^2 T} \langle p | \exp \left( \frac{\hat{p}_3}{qE} \hat{p}_4 \right) \exp \left( -T \left( -(qE)^2 \hat{x}_4^2 + \hat{p}_4^2 \right) \right) \exp \left( -\frac{\hat{p}_3}{qE} \hat{p}_4 \right) | p' \rangle \\ &= e^{-p_\perp^2 T} \exp \left( \frac{p_3 p_4 - p'_3 p'_4}{qE} \right) \langle p | \exp \left( -T \left( -(qE)^2 \hat{x}_4^2 + \hat{p}_4^2 \right) \right) | p' \rangle \\ &= e^{-p_\perp^2 T} \exp \frac{p_3 p_4 - p'_3 p'_4}{qE} \langle p_{1,2,3} | p'_{1,2,3} \rangle \langle p_4 | \exp \left( -T \left( -(qE)^2 \hat{x}_4^2 + \hat{p}_4^2 \right) \right) | p'_4 \rangle, \end{aligned} \quad (6.8)$$

where, in the last line, we used that the operator in the exponent acts on the 4-subspace only. Now we use

$$\langle p_{1,2,3} | p'_{1,2,3} \rangle = \delta^3(p_{1,2,3} - p'_{1,2,3}) \quad (6.9)$$

so we can immediately perform three of the  $p'_\mu$  integrations, and

$$\begin{aligned} \int d^3 p' \langle x | p \rangle \delta^3(p_{1,2,3} - p'_{1,2,3}) \langle p' | x \rangle &= |\langle x_{1,2,3} | p_{1,2,3} \rangle|^2 \langle x_4 | p_4 \rangle \langle p'_4 | x_4 \rangle = \frac{1}{(2\pi)^3} \frac{1}{2\pi} e^{ix_4(p_4 - p'_4)}. \end{aligned} \quad (6.10)$$

Resubstituting this into the expression for the propagator we have

$$\begin{aligned} \langle x | e^{\square_A T} | x \rangle &= \frac{1}{(2\pi)^4} \int d^3 p \int dp_4 \int dp'_4 \\ &\times e^{-p_\perp^2 T} e^{ix_4(p_4 - p'_4)} e^{i(p_4 - p'_4)p_3/iqE} \langle p_4 | e^{-T(\hat{p}_4^2 - (qE)^2 \hat{x}_4^2)} | p'_4 \rangle. \end{aligned} \quad (6.11)$$

We can easily perform the  $p_1$  and  $p_2$  integrals,

$$\int d^2 p_\perp e^{-p_\perp^2 T} = \frac{\pi}{T}, \quad (6.12)$$

and the  $p_3$ -integral by rotating it into the complex plane as  $\xi = \frac{p_3}{iqE}$ , so

$$\int dp_3 e^{i(p_4 - p'_4)p_3/iqE} = iqE \int d\xi e^{i\xi(p_4 - p'_4)} = iqE 2\pi \delta(p_4 - p'_4). \quad (6.13)$$

With this Dirac delta we can now perform the  $p'_4$ -integral, so we arrive at

$$\langle x | e^{\square_A T} | x \rangle = \frac{iqE}{(2\pi)^3} \frac{\pi}{T} \int dp_4 \langle p_4 | e^{-2T \left( \frac{p_4^2}{2} - (qE)^2 \frac{x_4^2}{2} \right)} | p_4 \rangle. \quad (6.14)$$

The remaining integral and expectation value have exactly the form of the quantum partition function  $Z$  of a harmonic oscillator with frequency  $\omega = iqE$  at inverse temperature  $\beta = 2T$ , which is easily found by summing over the energy eigenvalues,

$$\begin{aligned} Z &= \text{tr} \left( e^{-\beta \hat{H}} \right) = \sum_{n=0}^{\infty} e^{-\beta \omega (n+1/2)} = e^{-\beta \omega / 2} \sum_{n=0}^{\infty} (e^{-\beta \omega})^n = \frac{e^{-\beta \omega / 2}}{1 - e^{-\beta \omega}} \\ &= \frac{1}{e^{\beta \omega / 2} - e^{-\beta \omega / 2}} = \frac{1}{2 \sinh(\beta \omega / 2)} = \frac{1}{2i \sin(qET)}. \end{aligned} \quad (6.15)$$

We have now fully evaluated  $\langle x | e^{\square_A T} | x \rangle$ , which does not depend on  $x_\mu$  anymore. The  $d^4 x$ -integration thus gives a volume factor as expected. This is in Euclidean space though, so to compare to a physical, Minkowskian volume we have to replace  $dx_4 = idt$  again, so that  $\int d^4 x = iV_4$ .

Taking these results back to the expression for the Euclidean effective action we have

$$\begin{aligned} \Gamma &= - \int_0^\infty \frac{dT}{T} \int d^4 x \langle x | e^{-(\square_A + m^2)T} | x \rangle \\ &= - \int_0^\infty \frac{dT}{T} iV_4 \frac{iqE}{(2\pi)^3} \frac{\pi}{T} e^{-m^2 T} \frac{1}{2i \sin(qET)} \\ &= -iV_4 \frac{(qE)^2}{2(2\pi)^3} \int_0^\infty \frac{ds}{s^2} e^{-s\pi \frac{m^2}{qE}} \frac{1}{\sin(\pi s)} \end{aligned} \quad (6.16)$$

using the substitution  $s = qET/\pi$  in the last step. Since we need the real part of the Euclidean effective action, we are interested in the imaginary part of the  $s$ -integral. We now see why we do not need to explicitly regularize the lower limit of the integration, the divergence there is purely real. The imaginary contributions come from the poles of  $\sin^{-1}(\pi s)$  on the real axis at  $s = n \in \{1, 2, 3, \dots\}$  with residue  $(-1)^{n+1}/\pi$ . With a suitable choice of  $i\varepsilon$ -prescription, we pick up for each  $s_n = n$  the term

$$i\pi \text{Res}(\dots)|_{s=s_n} = i\pi \frac{1}{n^2} e^{-n\pi \frac{m^2}{qE}} \frac{(-1)^{n+1}}{\pi} \quad (6.17)$$

so finally we arrive at the expression noted in the beginning of this section

$$\Re\Gamma = V_4 \frac{(qE)^2}{2(2\pi)^3} \sum_{n=1}^{\infty} \frac{(-1)^{n+1}}{n^2} e^{-n\pi \frac{m^2}{qE}}. \quad (6.18)$$

We will see what changes in the spinor case in Section 6.5.

Obtaining this result, at least the exponential dependence, is much more straightforward in the worldline instanton formalism. If we want to calculate the prefactor using the Gel'fand-Yaglom method as outlined in Section 4.5, we need to perform the path integral first with  $T$  variable, and then perform the  $T$ -integral afterwards. Unfortunately this does not work in the constant, homogeneous field case as we will see in a moment.

[A] = 1 (see page 13).

We take the same potential as before,  $A_3 = ix_4$  (in dimensionless units again), so the only non-zero components of the field tensor are  $iF_{34} = -iF_{43} = 1$  and the instanton equations read

$$\ddot{x}_3 = T\dot{x}_4, \quad (6.19)$$

$$\ddot{x}_4 = -T\dot{x}_3,$$

for some fixed value of  $T$ . Now it is easy to see that these equations of motion are solved by

$$x_3(u) = \frac{a}{T} \sin(Tu), \quad x_4(u) = \frac{a}{T} \cos(Tu), \quad (6.20)$$

where  $a$  is again the constant velocity  $a^2 = \dot{x}^2$ . This solution lacks the freedom to satisfy the periodicity constraint for different values of  $T$ , only the choices  $T_n = 2\pi n$  are admissible. This prevents us from performing the remaining  $T$  integral.

So let us start over and solve the instanton equations of motion (4.101) after the  $T$  integration has been performed by Laplace's method, which are then

$$\ddot{x}_3 = a\dot{x}_4, \quad (6.21)$$

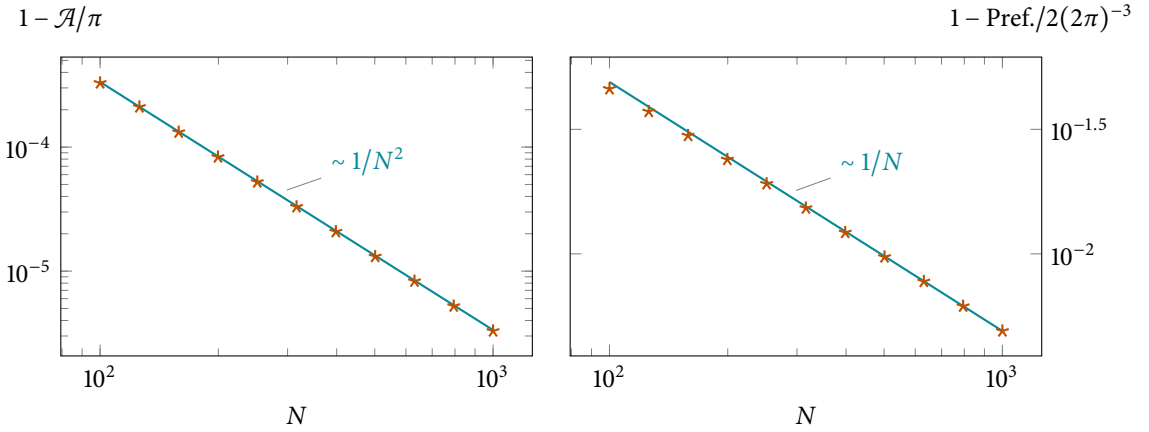
$$\ddot{x}_4 = -a\dot{x}_3,$$

and the solutions are

$$x_3(u) = \sin(au), \quad x_4(u) = \cos(au), \quad (6.22)$$

where the periodicity is satisfied by  $a_n = 2\pi n$ . This is perfectly fine this time and every choice is an instanton, because  $a$  is a parameter of the solution, not something that is specified beforehand. We can now obtain the exponent of the effective action using (4.95),

$$\begin{aligned} \mathcal{A} &= a + \int_0^1 du \dot{x} \cdot iA(x) = 2\pi n + \int_0^1 du \dot{x}_3(-x_4) \\ &= 2\pi n - 2\pi n \int_0^1 du \cos^2(2\pi nu) = \pi n. \end{aligned} \quad (6.23)$$



Since we have found multiple instantons, the full result is a sum over the individual contributions,

$$\Re\Gamma = \sum_{n=1}^{\infty} C_n e^{-\frac{m^2}{qE} \mathcal{A}_n} = \sum_{n=1}^{\infty} C_n e^{-n\pi \frac{m^2}{qE}}. \quad (6.24)$$

To find the prefactors  $C_n$  we would now have to explicitly perform the integrals over quadratic fluctuations around the instanton in the nonlocal action  $\mathcal{A}$ . While this is possible by expanding the fluctuations in Fourier series and then integrating over the expansion coefficients (as done in [AAM82] for the first term of the series, for example), it is tedious and not very illuminating. We will instead postpone the analytical fluctuation prefactor until next section where we will derive it for one-dimensional field inhomogeneities.

Although we can easily solve the instanton equations of motion analytically, we can also employ the discrete instanton approach. Of course, a circular trajectory as an initial guess works very well, and solutions are found almost instantly. Note that these are not trivial discretizations of the unit circle, they are slightly larger for small  $N$ . Figure 6.1 shows the deviation of both the exponent and the prefactor from the exact result for the first term of the series.<sup>60</sup> As expected, the error decreases with a larger number of points  $N$ , in the case of the prefactor as  $\frac{1}{N}$ . For the exponent it decreases even faster, because a first order variation in the trajectory, by definition of a classical solution, does not change the action. Even better accuracy could be obtained by using higher order schemes in the discretization of the action.

We can also try to use a numeric solution of the Riccati equation to get to the same result. It can not produce the whole effective action, only the pair production rate (the first term of the series). This is not straightforward either though, as our numerical approach needs the electric field to vanish for large negative and positive times. We thus construct a field that is approximately constant for a specified time duration and vanishes rapidly before and after. We choose the function  $f$  in the potential to be

$$f(\gamma\tau) = \frac{1}{2} \left( \log \cosh \left( \gamma\tau + \gamma \frac{T}{2} \right) - \log \cosh \left( \gamma\tau - \gamma \frac{T}{2} \right) \right) \quad (6.25)$$

representing the electric field profile (see Figure 6.3)

Figure 6.1.: Accuracy of the method for a constant, homogeneous field. The error of the prefactor decreases as  $1/N$  (the first order discretization error), the error of the action as  $1/N^2$  (because the action has an extremum at that point).

[AAM82] Affleck, Alvarez, and Manton. *Nucl. Phys. B* (1982)

<sup>60</sup> The higher order terms can be obtained by starting with an initial guess that winds around the origin  $n$  times.

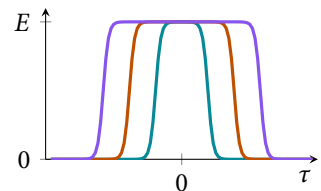
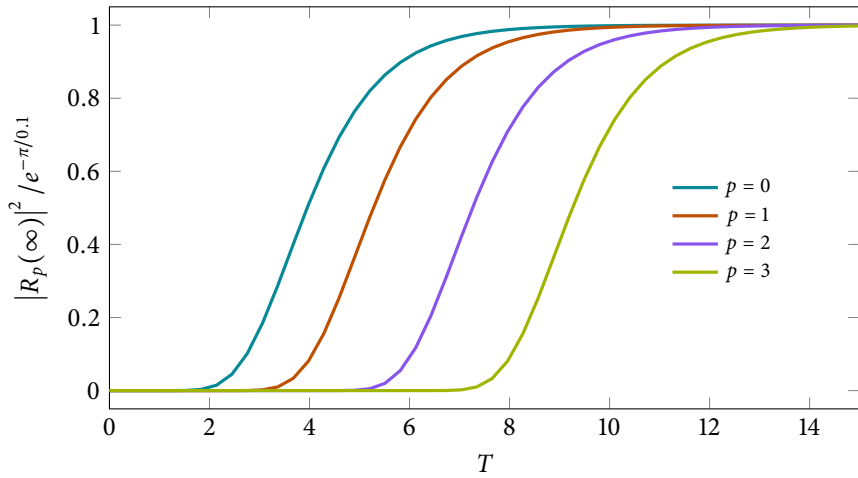


Figure 6.3.: The electric field (6.26) for different values of  $T$ .

Figure 6.2.: Pair production rate in different momentum modes for varying time durations of the field (6.26) with field strength  $qE/m^2 = 0.1$ .



$$E(\tau) = \frac{E}{2} \left( \tanh\left(\gamma\tau + \gamma\frac{T}{2}\right) - \tanh\left(\gamma\tau - \gamma\frac{T}{2}\right) \right) \quad (6.26)$$

and set the duration  $T$  to be *long enough*. One could imagine a larger value of  $T$ , so the electric field is present for a longer time, to lead to a larger value of  $|R_p(\infty)|^2$ . This is not the case however, as the produced pairs are accelerated as long as the electric field is switched on, so for longer  $T$  higher and higher momentum modes get populated. As long as  $T$  is large enough,  $|R_p(\infty)|^2$  tends to the value  $\exp(-\pi m^2/qE)$  for each  $p$ . Figure 6.2 shows this for the example case  $\frac{qE}{m^2} = 0.1$  and different momenta  $p$ . In this description the prefactor arises from the momentum integrals to obtain the total pair creation rate.

The constant homogeneous field results can be used to roughly approximate the pair production probability for inhomogeneous or time dependent fields by assuming that at every spacetime point the constant field result holds and integrate over all spatial components and time, that is

$$\Re\Gamma^{\text{LCFA}} = \int d^4x \frac{q^2 |\mathbf{E}(t, \mathbf{r})|^2}{2(2\pi)^3} \exp\left(-\pi \frac{m^2}{q|\mathbf{E}(t, \mathbf{r})|}\right). \quad (6.27)$$

This is called *locally constant field approximation*. Since many fields of interest are strongly peaked, (6.27) can often be approximated using the saddle point method.

## 6.2. One-dimensional field inhomogeneities

Let us now consider fields that depend on time, but are still spatially homogeneous. The main results of this section were derived in [DS05; Dun+06], however using slightly different conventions and skipping over parts of the calculation, especially concerning the prefactor. We thus give a more detailed derivation with some minor differences using our conventions.

$$[\mathbf{A}] = \mathbf{1}, \quad \mathbf{x}_i = \mathbf{x}^i$$

(see page 13).

We represent the homogeneous, time dependent fields using the four-potential

$$iA_3 = -f(\gamma x_4)/\gamma \quad (6.28)$$

resulting in the electric field

$$\mathbf{E} = E f'(\omega it) \hat{\mathbf{e}}_z \quad (6.29)$$

[DS05] Dunne and Schubert. *Phys. Rev. D* (2005)

[Dun+06] Dunne, Wang, Gies, and Schubert. *Phys. Rev. D* (2006)

with the Keldysh parameter  $\gamma = m\omega/qE$ . Since we want to find the full pair creation rate including the prefactor we need to proceed as outlined in Section 4.5 and solve the instanton equations of motion with variable  $T$ . With this choice of potential the instanton equations are<sup>61</sup>

$$\ddot{x}_3 = T f'(\gamma x_4) \dot{x}_4, \quad (6.30a)$$

$$\ddot{x}_4 = -T f'(\gamma x_4) \dot{x}_3. \quad (6.30b)$$

Equation (6.30a) can immediately be integrated once, giving

$$\dot{x}_3 = \frac{T}{\gamma} f(\gamma x_4), \quad (6.31)$$

so, using the fact that the velocity of an instanton is constant with  $(\dot{x}_\mu)^2 = a^2$ , we arrive at a relation closed in  $x_4$ ,

$$\dot{x}_4^2 + \left( \frac{T}{\gamma} f(\gamma x_4) \right)^2 = a^2. \quad (6.32)$$

This has the form of *kinetic energy + potential energy = const*. If we assume  $f$  to be an odd function that grows unbounded for large  $|x_4|$  (this is the case for the time dependent profiles we consider in the following), then periodic solutions of  $x_4(u)$  for all  $T$ ,  $a$  and  $\gamma$  are possible.<sup>62</sup> Also the resulting instantons are symmetric under  $x_4 \rightarrow -x_4$ , have  $\dot{x}_4 = \pm a$  for  $x_4 = 0$  and thus  $\dot{x}_3(x_4 = 0) = 0$ . From this it immediately follows that the instantons have the symmetry  $x_3 \rightarrow -x_3$  as well. We will use these properties in a moment.

First, we solve (6.32) for  $\dot{x}_4$ ,

$$\frac{dx_4}{du} = \pm \sqrt{a^2 - T^2 (f(\gamma x_4)/\gamma)^2} = \pm T \sqrt{\alpha^2 - (f(\gamma x_4)/\gamma)^2}, \quad (6.33)$$

with  $\alpha = a/T$ . The two branches  $\pm$  correspond to the two “sides” of the instanton with  $x_3 \lesseqgtr 0$ . Demanding that the instantons are periodic with period 1 fixes  $a$  (or  $\alpha$ ) for a given value of  $T$ . We choose a quarter of the trajectory, say the one with  $x_4 > 0$  and  $\dot{x}_4 > 0$ , set  $x_4(0) = 0$  and integrate

$$\begin{aligned} \int_0^{1/4} du &\stackrel{!}{=} \int_0^{x_4^*} \frac{dx_4}{T \sqrt{\alpha^2 - (f(\gamma x_4)/\gamma)^2}} \\ &\simeq T \stackrel{!}{=} 4 \int_0^{x_4^*} \frac{dx_4}{\sqrt{\alpha^2 - (f(\gamma x_4)/\gamma)^2}} =: \pi P(\alpha, \gamma), \end{aligned} \quad (6.34)$$

with the turning point

$$x_4^* = f^{-1}(\gamma \alpha)/\gamma. \quad (6.35)$$

The factor of  $\pi$  in the definition of  $P(\alpha, \gamma)$  is added for convenience later.

We can express the instanton action using a similar integral. Remember we want to evaluate (4.129), that is (without the spin factor for now)

$$\Gamma = \int d^4 x^0 \int \frac{dT}{T} \left( \frac{m^2/qE}{2\pi T} \right)^2 \frac{e^{-\frac{m^2}{qE} \mathcal{A}(T)}}{\sqrt{\det(\eta_\mu^{(v)}(1))}} \quad (6.36)$$

<sup>61</sup> Whenever we use the trajectories  $x_3, x_4$  from now on we assume that they satisfy these equations of motion and not bother to explicitly mark them using <sup>cl</sup>.

<sup>62</sup> Of course, in general, to have a periodicity of 1, the value of  $a$  has to be tuned appropriately.

<sup>63</sup> After finding the saddle point value of  $T$  this coincides with the nonlocal  $\mathcal{A}$  from before, hence the use of this symbol.

where we have combined the action  $S$  with the  $T/2$  in the exponent to give<sup>63</sup>

$$\mathcal{A}(T) = \frac{T}{2} + S(T) = \frac{T}{2} + \int_0^1 du \left( \frac{\dot{x}^2}{2T} + i\dot{x} \cdot A(x) \right). \quad (6.37)$$

We will now insert our choice of potential,  $iA_3 = -f(\gamma x_4)/\gamma$ , and use  $\dot{x}^2 = a^2$ ,

$$\begin{aligned} \mathcal{A} &= \frac{T}{2} + \frac{a^2}{2T} - \int_0^1 du \dot{x}_3 \frac{f(\gamma x_4)}{\gamma} = \frac{T}{2} (1 + \alpha^2) - \frac{1}{T} \int_0^1 du \dot{x}_3^2 \\ &= \frac{T}{2} (1 + \alpha^2) - \frac{a^2}{T} + \frac{1}{T} \int_0^1 du \dot{x}_4^2 = \frac{T}{2} (1 - \alpha^2) + \frac{1}{T} \int_0^1 du \frac{dx_4}{du} \dot{x}_4 \end{aligned} \quad (6.38)$$

Where we have used (6.31) in the first step. For the integral we can again exploit the instanton's symmetry and integrate over a quarter of the trajectory, so

$$\mathcal{A} = \frac{T}{2} (1 - \alpha^2) + \pi g(\alpha, \gamma) \quad (6.39)$$

where we defined the important function

$$g(\alpha, \gamma) := \frac{4}{\pi} \int_0^{x_4^*} dx_4 \sqrt{\alpha^2 - (f(\gamma x_4)/\gamma)^2}, \quad (6.40)$$

the factor of  $\pi$  included for convenience again. We can immediately note that

$$\frac{d}{d\alpha} g(\alpha, \gamma) = \alpha P(\alpha, \gamma). \quad (6.41)$$

To apply Laplace's method to the  $T$ -integration we need to find the extremum of the exponent. The function  $g$  depends on  $T$  via  $\alpha(T)$  where  $\alpha(T)$  is determined implicitly by

$$P(\alpha, \gamma) = \frac{T}{\pi}. \quad (6.42)$$

The  $T$ -derivative of  $g$  is thus given by

$$\frac{d}{dT} g(\alpha, \gamma) = \frac{d\alpha}{dT} \frac{d}{d\alpha} g(\alpha, \gamma) = \frac{d\alpha}{dT} \alpha P(\alpha, \gamma) = \frac{d\alpha}{dT} \alpha \frac{T}{\pi}. \quad (6.43)$$

To extremize the exponent with respect to  $T$  we demand

$$\begin{aligned} 0 &\stackrel{\dagger}{=} \frac{d}{dT} \mathcal{A} = \frac{1}{2} (1 - \alpha^2) - T\alpha \frac{d\alpha}{dT} + \pi \frac{d}{dT} g(\alpha, \gamma) \\ &= \frac{1}{2} (1 - \alpha^2) - T\alpha \frac{d\alpha}{dT} + T\alpha \frac{d\alpha}{dT} = \frac{1}{2} (1 - \alpha^2), \end{aligned} \quad (6.44)$$

so the saddle is simply given by  $\alpha = 1$ , that is  $T = a$ , just like before when we performed the  $T$ -integration first and the path integral later. The fluctuation around this value is non-trivial though, to calculate it we need the second derivative of the exponent. First we take the  $T$  derivative on both sides of (6.42),

$$\frac{d\alpha}{dT} \frac{d}{d\alpha} P(\alpha, \gamma) = \frac{1}{\pi} \quad \rightsquigarrow \quad \frac{d\alpha}{dT} = \left( \pi \frac{d}{d\alpha} P(\alpha, \gamma) \right)^{-1}. \quad (6.45)$$

We now find

$$\frac{d^2}{dT^2} \mathcal{A} = -\alpha \frac{d\alpha}{dT} = -\alpha \left( \pi \frac{d}{d\alpha} P(\alpha, \gamma) \right)^{-1}. \quad (6.46)$$

We still need to find the determinant of solutions to the fluctuation equations  $\det(\eta_\mu^{(v)})$  where

$$\Lambda_{\mu\nu} \eta_\nu(u) = 0, \quad \eta_\mu^{(v)}(0) = 0, \quad \dot{\eta}_\mu^{(v)}(0) = \delta_{\mu\nu}. \quad (6.47)$$

For our potential  $iA_3(x_4)$  the fluctuation operator in the  $x_1$ - $x_2$  subspace is just the free case, which gives 1 using our normalization. The  $x_3$ - $x_4$  subspace gives the operator

$$\begin{aligned} (\Lambda_{\mu\nu}) &= \begin{pmatrix} -\frac{\partial_u^2}{T} & \gamma f''(\gamma x_4) \dot{x}_4 + f'(\gamma x_4) \partial_u \\ -f'(\gamma x_4) \partial_u & -\frac{\partial_u^2}{T} - \gamma f''(\gamma x_4) \dot{x}_3 \end{pmatrix} \\ &= \frac{1}{T} \begin{pmatrix} -\partial_u^2 & -\left(\partial_u \frac{\ddot{x}_4}{\dot{x}_3}\right) - \frac{\ddot{x}_4}{\dot{x}_3} \partial_u \\ \frac{\ddot{x}_4}{\dot{x}_3} \partial_u & -\partial_u^2 + \frac{\dot{x}_3}{\dot{x}_4} \left(\partial_u \frac{\ddot{x}_4}{\dot{x}_3}\right) \end{pmatrix}. \end{aligned} \quad (6.48)$$

The global factor of  $T$  does not affect the solutions, as the equation is homogeneous and we can just multiply it by  $T$ . We will omit this factor in the following.

Since  $\Lambda$  is now a two-dimensional, second order differential operator there are four independent solutions to  $\Lambda_{\mu\nu} \eta_\nu = 0$ . Two of these are fairly easy to guess, first of all  $\phi^{(1)} = (1, 0)^\top$ , corresponding to translation in  $x_3$ -direction which our field does not depend on, and secondly  $\phi^{(2)} = (\dot{x}_3, \dot{x}_4)^\top$ , corresponding to reparametrization along the instanton. That  $\phi^{(2)}$  is a solution to the fluctuation equations may not be obvious, but is easy to check. First, using the instanton equations we find

$$\ddot{x}_3 \dot{x}_3 = -\dot{x}_4 \dot{x}_3 \quad \rightsquigarrow \quad \ddot{x}_3 = -\frac{\dot{x}_4}{\dot{x}_3} \dot{x}_4. \quad (6.49)$$

We can use this to find  $\Lambda_{33} \phi_3^{(2)} = -\ddot{x}_3$ ,

$$-\ddot{x}_3 = -\partial_u \dot{x}_3 = \partial_u \frac{\dot{x}_4}{\dot{x}_3} \dot{x}_4 = \left( \partial_u \frac{\ddot{x}_4}{\dot{x}_3} \right) \dot{x}_4 + \frac{\ddot{x}_4}{\dot{x}_3} \partial_u \dot{x}_4, \quad (6.50)$$

which is exactly  $-\Lambda_{34} \phi_4^{(2)}$ , so the first component of the equation is satisfied. The second component works analogously.

Unfortunately, these two solutions do not help us to construct solutions satisfying the initial conditions

$$\eta_\mu^{(v)}(0) = 0, \quad \dot{\eta}_\mu^{(v)}(0) = \delta_{\mu\nu}, \quad (6.51)$$

and the other two solutions are far less obvious. They are

$$\phi^{(3)} = \begin{pmatrix} \dot{x}_3 h(u) - \tilde{h}(u) \\ \dot{x}_4 h(u) \end{pmatrix}, \quad \phi^{(4)} = \begin{pmatrix} \dot{x}_3 \tilde{h}(u) - a^2 h(u) \\ \dot{x}_4 \tilde{h}(u) \end{pmatrix}, \quad (6.52)$$

with the two functions

$$h(u) := \int_0^u du' \frac{1}{\dot{x}_4^2(u')}, \quad \tilde{h}(u) := \int_0^u du' \frac{\dot{x}_3(u')}{\dot{x}_4^2(u')}. \quad (6.53)$$

Even just validating that  $\phi^{(3)}$  and  $\phi^{(4)}$  are solutions is tedious, but works similarly to how we checked  $\phi^{(2)}$ . Using  $\phi^{(3)}$  and  $\phi^{(4)}$  we can now construct  $\eta^{(3)}$  and  $\eta^{(4)}$  that obey the correct initial conditions,

$$\eta^{(3)} = \dot{x}_3(0)\phi^{(3)} - \phi^{(4)}, \quad \eta^{(4)} = \dot{x}_4(0)\phi^{(3)}. \quad (6.54)$$

We finally have to compute the  $2 \times 2$  determinant of these solutions evaluated at  $u = 1$ . Since we know that the instanton is periodic we can use  $\dot{x}_\mu(1) = \dot{x}_\mu(0)$ , and also  $\tilde{h}(1) = 0$ , since  $\dot{x}_3(u')/\dot{x}_4^2(u')$  is positive over one half of the period and negative on the other half. Thus,

$$\begin{aligned} \det(\eta_\mu^{(v)}(1)) &= \det(\eta^{(3)}(1), \eta^{(4)}(1)) \\ &= \det \begin{pmatrix} \dot{x}_3(0)^2 h(1) + a^2 h(1) & \dot{x}_4(0)\dot{x}_3(0)h(1) \\ \dot{x}_3(0)\dot{x}_4(0)h(1) & \dot{x}_4(0)^2 h(1) \end{pmatrix} \\ &= h(1)^2 ((\dot{x}_3(0)^2 + a^2)\dot{x}_4(0)^2 - \dot{x}_3(0)^2\dot{x}_4(0)^2) \\ &= a^2\dot{x}_4(0)^2 h(1)^2. \end{aligned} \quad (6.55)$$

Just like  $g$  and  $P$  before, we can rewrite  $h(1)$  as an integral over  $f(\gamma x_4)$ , specifically

$$\begin{aligned} ah(1) &= a \int_0^1 du \frac{1}{\dot{x}_4^2} = a \int_0^1 du \frac{\dot{x}_4}{\dot{x}_4^3} = 4a \int_0^{x_4^*} \frac{dx_4}{T^3 (\alpha^2 - (f(\gamma x_4)/\gamma)^2)^{3/2}} \\ &= -\frac{\pi}{T^2} \frac{d}{d\alpha} P(\alpha, \gamma), \end{aligned} \quad (6.56)$$

so the fluctuation factor is

$$\frac{1}{\sqrt{\det(\eta_\mu^{(v)}(1))}} = \frac{1}{\dot{x}_4(0)ah(1)} = \frac{T^2}{\dot{x}_4(0)} \left( -\pi \frac{d}{d\alpha} P(\alpha, \gamma) \right)^{-1}. \quad (6.57)$$

We are almost done now, the last ingredient is the integral over the starting point of the instanton. As our field does not depend on the spatial coordinates, we can move the starting point in these directions and the instanton “rigidly” follows, so these integrations yield volume factors. They are given in terms of the dimensionless coordinates, so to obtain the physical volume factor each coordinate gives a contribution of  $qE/m$ . The whole instanton is fixed in  $x_4$ -direction though, so  $x_4^0$  really can only follow the trajectory. This means we can turn the  $x_4^0$ -integration into a  $u$ -integration from the lower to the upper limit of the instanton, that is

$$\int d^4 x^0 = V_3 \left( \frac{qE}{m} \right)^3 \int_{x_4^{\min}}^{x_4^{\max}} dx_4^0 = V_3 \left( \frac{qE}{m} \right)^3 \int_{-1/4}^{1/4} du \dot{x}_4(0) = \frac{V_3}{2} \left( \frac{qE}{m} \right)^3 \dot{x}_4(0). \quad (6.58)$$

We can finally put everything together:

$$\begin{aligned}
\Gamma &= \int d^4 x^0 \int \frac{dT}{T} \left( \frac{m^2/qE}{2\pi T} \right)^2 \frac{e^{-\frac{m^2}{qE} \mathcal{A}(T)}}{\sqrt{\det(\eta_\mu^{(\nu)}(1))}} \\
&= \frac{V_3}{2} \left( \frac{qE}{m} \right)^3 \dot{x}_4(0) \frac{1}{T} \sqrt{\frac{2\pi}{\frac{m^2}{qE} \frac{d^2}{dT^2} \mathcal{A}}} \left( \frac{m^2/qE}{2\pi T} \right)^2 \frac{T^2 e^{-\frac{m^2}{qE} \pi g(\alpha, \gamma)}}{\dot{x}_4(0) \left( -\pi \frac{d}{d\alpha} P(\alpha, \gamma) \right)} \Bigg|_{\alpha=1} \quad (6.59) \\
&= V_3 m^3 \frac{\sqrt{2} (qE/m^2)^{3/2}}{(2\pi)^3} \frac{e^{-\frac{m^2}{qE} \pi g(\alpha, \gamma)}}{P(\alpha, \gamma) \sqrt{-\frac{d}{d\alpha} P(\alpha, \gamma)}} \Bigg|_{\alpha=1}.
\end{aligned}$$

We can still improve on this expression. Right now we need  $P(\alpha, \gamma)$  with arbitrary  $\alpha$  to find the derivative before setting  $\alpha = 1$ . Also, if we want to obtain  $P$  as the derivative of  $g(\alpha, \gamma)$  we need that with variable  $\alpha$  too. There is a different way to represent these derivatives, first we rewrite the integral expression for  $g$

$$\begin{aligned}
g(\alpha, \gamma) &= \frac{4}{\pi} \int_0^{x_4^*} dx_4 \sqrt{\alpha^2 - (f(\gamma x_4)/\gamma)^2} \\
&= \alpha \frac{4}{\pi} \int_0^{x_4^*} dx_4 \sqrt{1 - \left( \frac{f(\gamma x_4)}{\alpha \gamma} \right)^2}. \quad (6.60)
\end{aligned}$$

we now substitute

$$y = \frac{f(\gamma x_4)}{\alpha \gamma} \quad \rightsquigarrow \quad dy = \frac{1}{\alpha} f'(\gamma x_4) dx_4 \quad (6.61)$$

so

$$g(\alpha, \gamma) = \alpha^2 \frac{4}{\pi} \int_0^1 dy \frac{\sqrt{1-y^2}}{f'(f^{-1}(\alpha \gamma y))} =: \alpha^2 \tilde{g}(\tilde{\gamma}), \quad (6.62)$$

where we have defined  $\tilde{\gamma} := \alpha \gamma$ . Now we can rewrite the  $\alpha$ -derivatives as  $\tilde{\gamma}$ -derivatives, which are just  $\gamma$ -derivatives after setting  $\alpha = 1$ . Let us first determine  $P(\alpha, \gamma)$ ,

$$P(\alpha, \gamma) = \frac{1}{\alpha} \frac{d}{d\alpha} g(\alpha, \gamma) = 2\tilde{g}(\tilde{\gamma}) + \tilde{\gamma} \frac{d}{d\tilde{\gamma}} \tilde{g}(\tilde{\gamma}) = 2 \frac{d}{d\tilde{\gamma}^2} \tilde{\gamma}^2 \tilde{g}(\tilde{\gamma}) =: \tilde{P}(\tilde{\gamma}). \quad (6.63)$$

Now that  $\tilde{P}$  depends on  $\alpha$  only via  $\tilde{\gamma}$  we have

$$\frac{d}{d\alpha} P(\alpha, \gamma) = \gamma \frac{d}{d\tilde{\gamma}} \tilde{P}(\tilde{\gamma}) = 4\gamma \tilde{\gamma} \frac{d^2}{d(\tilde{\gamma}^2)^2} \tilde{\gamma}^2 \tilde{g}(\tilde{\gamma}). \quad (6.64)$$

Now that there are no  $\alpha$ -derivatives left we can set  $\alpha = 1$  without problems and thus drop the tilde over all quantities. Replacing these expressions into our result for the effective action we get

$$\Gamma = V_3 m^3 \frac{\sqrt{2} (qE/m^2)^{3/2}}{4(2\pi)^3 \gamma} \frac{\exp\left(-\frac{m^2}{qE} \pi g(\gamma)\right)}{\left(\frac{d}{d\tilde{\gamma}^2} \tilde{\gamma}^2 g(\gamma)\right) \sqrt{-\frac{d^2}{d(\tilde{\gamma}^2)^2} \tilde{\gamma}^2 g(\gamma)}}. \quad (6.65)$$

In conclusion, the worldline instanton result for a background field depending on time only is completely determined by the single function  $g(\gamma)$  and its first two derivatives.

Let us look at an example now, the Sauter pulse again. we have

$$f(x) = \tan(x), \quad f' = 1 + \tan^2(x), \quad f'(f^{-1}(\gamma)) = 1 + \gamma^2 \gamma^2, \quad (6.66)$$

so we can calculate the function  $g$  (and thus the exponent of the effective action),

$$g(\gamma) = \frac{4}{\pi} \int_0^1 dy \frac{\sqrt{1-y^2}}{1+\gamma^2 y^2} = \frac{2}{1+\sqrt{1+\gamma^2}}. \quad (6.67)$$

The prefactor is only two derivatives away as well, we have

$$\frac{d}{d\gamma^2} \gamma^2 g(\gamma) = \frac{d}{d\gamma^2} \gamma^2 \frac{2}{1+\sqrt{1+\gamma^2}} = \frac{1}{\sqrt{1+\gamma^2}} \quad (6.68)$$

and

$$-\frac{d^2}{d(\gamma^2)^2} \gamma^2 g(\gamma) = -\frac{d}{d\gamma^2} \frac{1}{\sqrt{1+\gamma^2}} = \frac{1}{2} \frac{1}{(1+\gamma^2)^{3/2}}. \quad (6.69)$$

The full worldline instanton result for a temporal Sauter pulse is then

$$\Gamma = V_3 m^3 \frac{(qE/m^2)^{3/2}}{2(2\pi)^3} \frac{(1+\gamma^2)^{5/4}}{\gamma} \exp\left(-\frac{m^2}{qE} \frac{2\pi}{1+\sqrt{1+\gamma^2}}\right). \quad (6.70)$$

With a bit of care we can use (6.65) for fields depending on  $z$  too. Nowhere in the derivation did we use that  $x_4$  is related to time, the distinction stems solely from the different prescriptions to turn the Minkowskian four-potential into the Euclidean version. For a time dependent field

$$\mathbf{E}(t) = f'(\omega t) \hat{\mathbf{e}}_z \rightsquigarrow A_3^M = -f(\omega t)/\omega \rightsquigarrow iA_3 = -if(\omega(-i)x_4)/\omega \quad (6.71)$$

and for a spatially inhomogeneous field

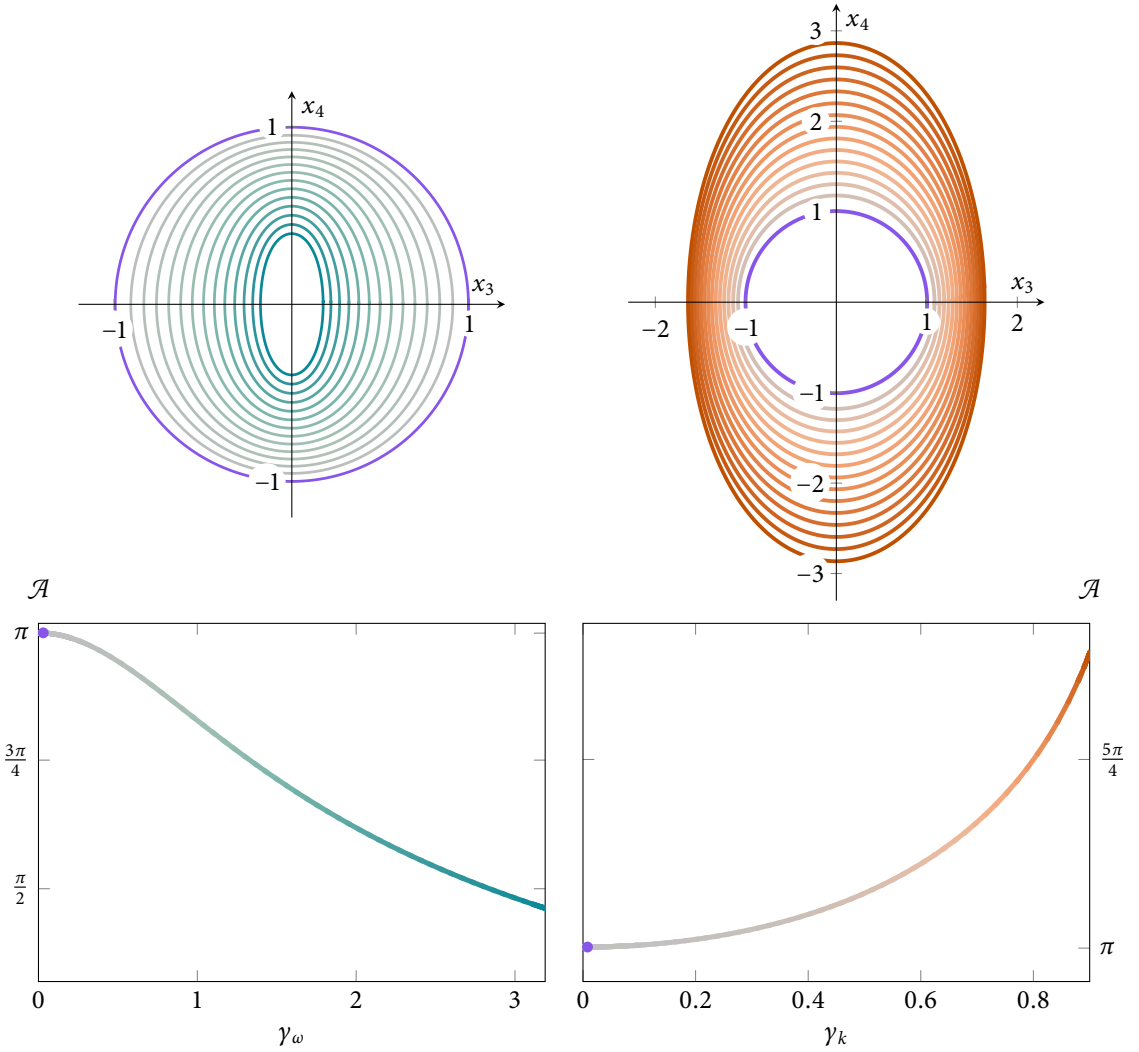
$$\mathbf{E}(z) = f'(kz) \hat{\mathbf{e}}_z \rightsquigarrow A_0^M = -f(kz)/k \rightsquigarrow iA_4 = f(kx_3)/k. \quad (6.72)$$

Up to the meaningless distinction between  $x_3$  and  $x_4$  the two cases are related by  $k = -i\omega$ , or  $\gamma_k = -i\gamma_\omega$  where we distinguish the temporal and spatial Keldysh parameters

$$\gamma_\omega = \frac{m\omega}{qE}, \quad \gamma_k = \frac{mk}{qE}. \quad (6.73)$$

The only other modification is that, since the field does not depend on time anymore, one of the volume factors now means the temporal extent of the field and has to be rotated back to physical time,  $V_{x_4} = iV_t$ . The factor of  $i$  cancels against the factor from  $\gamma_\omega = i\gamma_k$  in the denominator of (6.65), so the result for a time dependent field can immediately be transferred to a corresponding spatially inhomogeneous one. For a spatial Sauter profile we get by replacing  $\gamma = i\gamma_k$  in (6.70)

$$\Gamma = V_2 V_t m^3 \frac{(qE/m^2)^{3/2}}{2(2\pi)^3} \frac{(1-\gamma_k^2)^{5/4}}{\gamma_k} \exp\left(-\frac{m^2}{qE} \frac{2\pi}{1+\sqrt{1-\gamma_k^2}}\right). \quad (6.74)$$



In contrast to the time dependent case (6.70) where pair production is enhanced for higher values of  $\gamma_\omega$ , pair production is reduced for higher values of  $\gamma_k$ , vanishing exactly for  $\gamma_k \rightarrow 1$ . This is, in fact, a general property of time dependent or inhomogeneous fields of the form just described. First of all consider a spatially inhomogeneous field profile with its maximum of strength  $E$  at  $z = 0$ . Then  $f'(0) = 1$ , and  $f'(z) < 1$  elsewhere. This immediately means that

$$g(\gamma_k) = \frac{4}{\pi} \int_0^1 dy \frac{\sqrt{1-y^2}}{f'(f^{-1}(\gamma_k y))} > \frac{4}{\pi} \int_0^1 dy \frac{\sqrt{1-y^2}}{1} = 1, \quad (6.75)$$

so pair production is always reduced. Furthermore for peaked electric fields,  $f'(x)$  is smaller for larger  $x$ , so every increase in  $\gamma_k$  means a larger range of  $x$  in  $f'(x)$  are included in the integration, leading to larger  $g(\gamma_k)$ . Even more importantly, if the energy of the field profile is to be finite, the function  $f$  has to be bounded,  $|f(\gamma_k x_3)| < M$  for all  $x_3$ . This has the consequence that the inverse

Figure 6.4.: Top: Instantons for a temporal Sauter pulse (left) and a spatial Sauter profile (right) for various values of  $\gamma_\omega$  or  $\gamma_k$ . The purple trajectories belong to the limit  $\gamma_{\omega/k} \rightarrow 0$ , blue colors denote decrease in action, red colors an increase. Bottom: Corresponding actions with the same color coding.

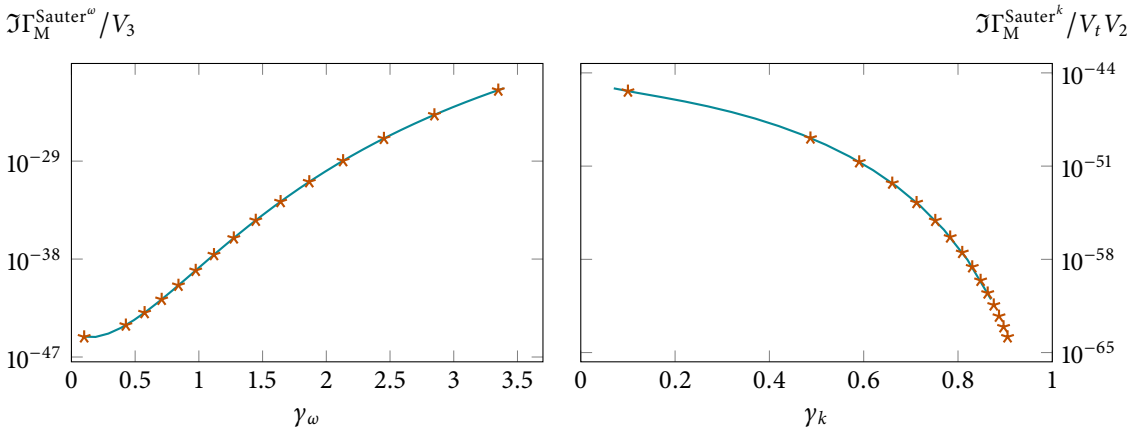


Figure 6.5.: Imaginary part of the Minkowskian effective action (i.e. the pair production rate) for  $E = 0.033m^2/q$ . Left: temporal Sauter pulse, right: spatial Sauter profile. Numerical results are given by markers and the analytic expressions (6.70) and (6.74) by lines. Note the spacing of markers in the spatial case, the step length decreases to keep the overall arclength  $\Delta s$  constant.

function  $f^{-1}$  diverges for  $\gamma_k y \rightarrow M$ , and thus

$$f'(f^{-1}(\gamma_k y)) \rightarrow 0 \quad \leadsto \quad g(\gamma_k) \rightarrow \infty \text{ for } \gamma_k \rightarrow M. \quad (6.76)$$

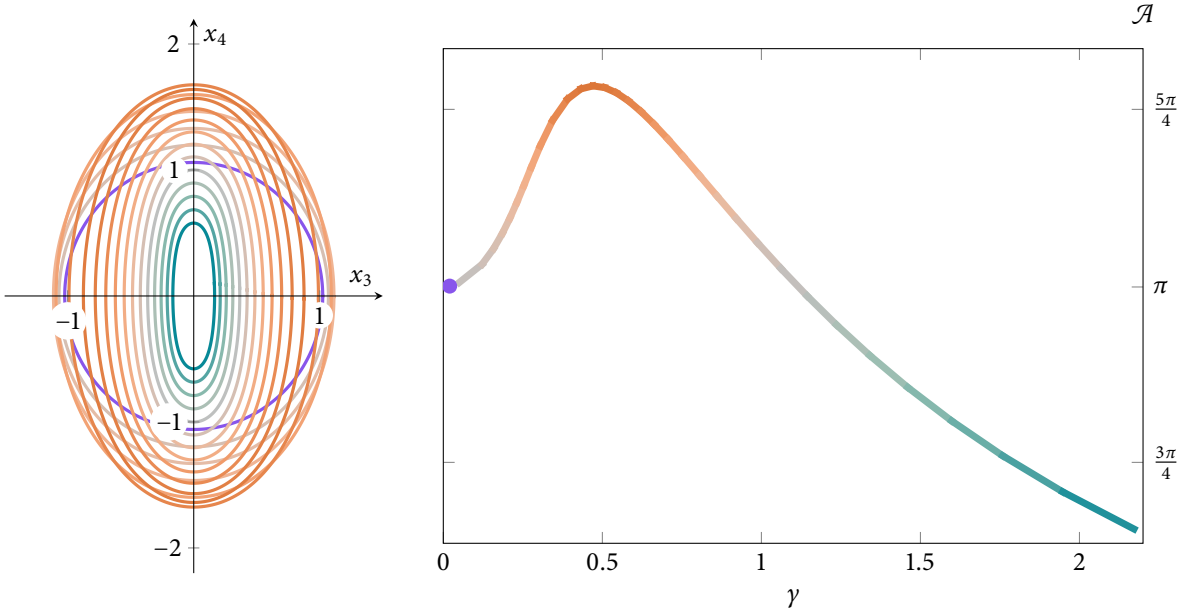
This is what happens in the case of the Sauter profile with  $f = \tanh$  for  $\gamma_k \rightarrow 1$ .

That the same does not hold for a time dependent field is a consequence of the analytic continuation to imaginary times and can again be understood quite generally. The electric field pulse should still be finite, so the Minkowskian potential is bounded again. We however assume that the potential is analytic, and any analytic function bounded in the complex plane is constant. Since this contradicts our choice, the potential must be unbounded when analytically continued into the complex plane. In the case of the Sauter pulse we have  $f = \tan(\gamma_\omega x_4)$  instead of  $f = \tanh(\gamma_k x_3)$ , for example.

These qualitative differences can not only be observed in the definition of  $g$ , but also geometrically from the instanton equations. Locally, the instanton equations describe a circular trajectory with curvature  $\sim f'$ , closed solutions being centered around the field maximum. Now spatial inhomogeneities decrease the curvature further from the maximum, leading to larger instantons, up to the limit where the curvature is too small to produce closed solutions at all ( $\gamma_k \rightarrow 1$  for the Sauter profile). In contrast, for time dependent fields  $f'$ , and thus curvature, increases for larger  $x_4$ , so the instantons shrink.

Figure 6.4 shows a family of instantons for the two cases of a time dependent Sauter pulse and a spatial Sauter profile, found using the numerical approach of Section 5.2. While the instanton trajectories can be found in analytical form for these fields, they are visually indistinguishable from the numerical results, and calculating the action and prefactor is much easier using the approach above, so there is no benefit in analytically obtaining the instanton.

By using the pseudo-arclength continuation method the instantons in Figure 6.4 do not correspond to fixed steps in  $\gamma_\omega/\gamma_k$ , but instead are chosen to keep the mean distance between instantons constant. The effect can be seen clearly in Figure 6.5 which shows the full effective action for both the numerical evaluation and the analytic expressions (6.70) and (6.74) at a field strength of  $E = 0.033 \frac{m^2}{qE}$ . For the time dependent pulse the steps in  $\gamma_\omega$  are fairly evenly spaced, but for the



inhomogeneous profile the step width decreases for larger  $\gamma_k$ , since the instantons grow quickly.

Figure 6.6.: Left: Instantons for the field (6.77) with varying  $\gamma$ . Right: Corresponding action.

### 6.3. Multidimensional field inhomogeneities [STS19]

Although the analytic treatment of last section works for one-dimensional field dependences only, the numerical instanton approach can be applied to arbitrary fields. The qualitative results that time dependence increases pair production while spatial inhomogeneity reduces it still holds for more complicated scenarios though. As a simple example to study the interplay between both effects let us consider the product of a temporal and a spatial Sauter profile, that is

$$E = E \cosh^{-2}(\omega t) \cosh^{-2}(kz) \hat{e}_z, \quad (6.77)$$

for a fixed relation  $mk/qE = 3m\omega/qE = \gamma$ . This might represent a very crude approximation to a localized profile created by colliding laser pulses, but should rather be seen as a technical example only. We use the four-potential

$$iA_3 = \cosh^{-2}(3\gamma x_3) \tan(\gamma x_4)/\gamma, \quad (6.78)$$

which now depends on  $x_3$  and  $x_4$  so we can not integrate the instanton equations analytically like we did before. We can however find discrete instantons and evaluate their action and prefactor.

Figure 6.6 shows these instantons obtained using numerical continuation starting from the homogeneous limit  $\gamma \rightarrow 0$ . First, The spatial inhomogeneity dominates and leads to an increase in action (visualized as red color), but after  $\gamma \approx \frac{1}{2}$  the time dependence takes over and leads to reduced action. Figure 6.8 shows the full pair production rate for  $E = 0.033 \frac{m^2}{qE}$ , where the adaptive step width of the continuation algorithm is visible again.

**[A] = 1,  $x_i = x^i$**   
(see page 13).

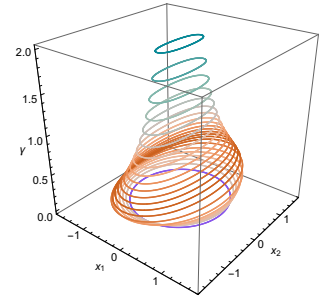
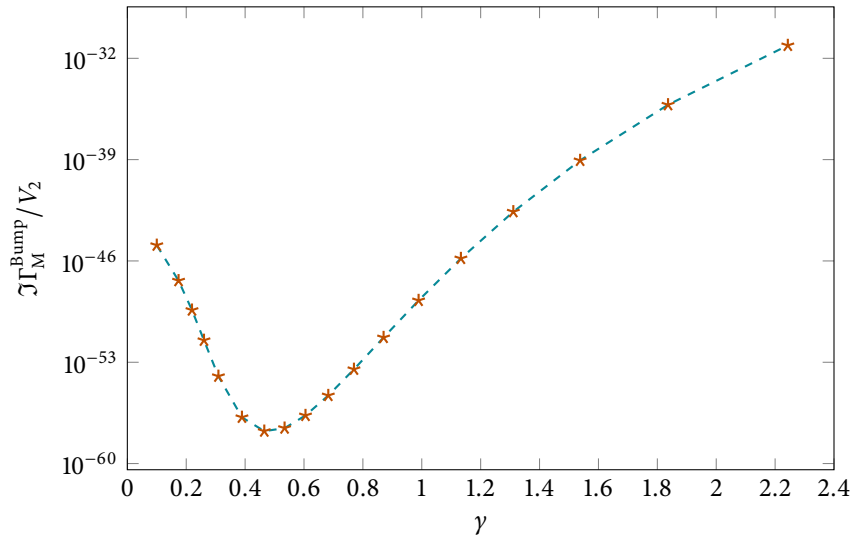


Figure 6.7.: The same worldline instantons as in Figure 6.6, but stacked, with the  $z$ -coordinate given by the parameter  $\gamma$ . This presentation makes it easier to correlate the instantons' change in shape with the parameter.

Figure 6.8.: Imaginary part of the Minkowskian effective action for the spacetime bump profile  $E = E \cosh^{-2}(\omega t) \cosh^{-2}(kz) e_z$  with  $k = 3\omega$  and  $E = 0.033m^2/q$ . Here (and in the following cases) there are no analytical results to compare with, so we just add the connecting dashed lines as a guide to the eye.



[DW06] Dunne and Wang. *Phys. Rev. D* (2006)

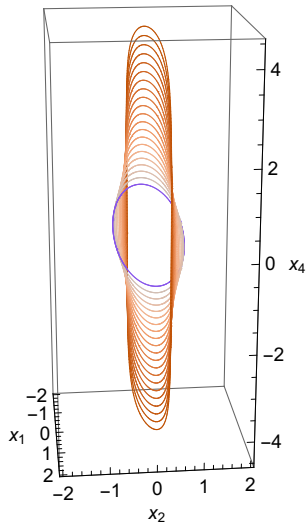


Figure 6.9.: Worldline instantons for the four-potential (6.79).

As before, stronger inhomogeneity stretches the instantons (in a more complicated way than for the one-dimensional fields) and increases the action.

[Bas86] Bassett. (1986)

[Gon+12] Gonoskov, Aiello, Heugel, and Leuchs. *Phys. Rev. A* (2012)

<sup>64</sup> A pure dipole field would diverge at the origin.

[Gon+13] Gonoskov et al. *Phys. Rev. Lett.* (2013)

For planar instantons like those in Figure 6.6 a different visualization is possible as shown in Figure 6.7. There, the instantons are placed in the three-dimensional space  $(x_3, x_4, \gamma)$ , which more closely shows the relation between the Keldysh parameter and the shape of closed trajectories.

More complicated higher dimensional instantons have been considered in [DW06] using the shooting method. In this case, even though the instantons are found using numerical integration of the instanton equations, some considerable analytical effort is needed to obtain the fluctuation prefactor. In contrast, using the discretized formulation we immediately obtain the exponent and prefactor without any further work.

As one example, we choose the potential

$$iA_4 = \frac{1}{\sqrt{2}\gamma_k} \frac{\tanh(\gamma_k x_1 + \gamma_k x_2)}{1 + (\gamma_k x_1)^2 + 10(\gamma_k x_2)^2} \quad (6.79)$$

from Figure 1 in [DW06], dividing by a factor of  $\sqrt{2}$  to make the peak field strength  $E$ . Starting from the homogeneous limit  $\gamma_k \rightarrow 0$ , the continuation method yields instantons for a range of inhomogeneities  $\gamma_k$ . These instantons are shown in a three-dimensional plot in Figure 6.9, and projected onto the coordinate planes in Figure 6.10. Just as in the one-dimensional case, stronger inhomogeneity leads to larger instantons and reduced pair probability. The full effective action is depicted in Figure 6.11.

As a final, highly nontrivial example for this section, we consider an  $e$ -dipole field. These are a class of field profiles that are vacuum solutions of Maxwell's equation, of finite spatial and temporal extent and highly focused. There is a limit in the attainable field amplitude from a pulse with given laser power [Bas86], and these fields saturate this upper bound [Gon+12]. They are structurally similar to the radiation field of a dipole varying with time, but with finite energy. <sup>64</sup>

An  $e$ -dipole field can be represented using an auxiliary vector field [Gon+13]

$$\mathbf{Z} = \hat{\mathbf{e}}_z \frac{d}{|r|} \left( \xi(t + |r|) - \xi(t - |r|) \right), \quad (6.80)$$

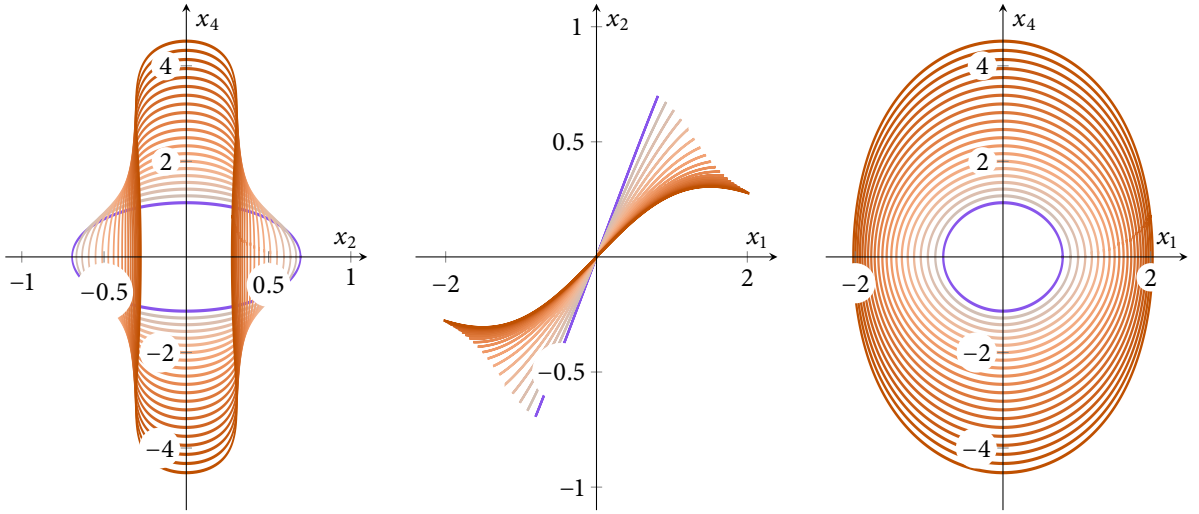


Figure 6.10.: The same world-line instantons as in Figure 6.9, projected onto the coordinate planes.

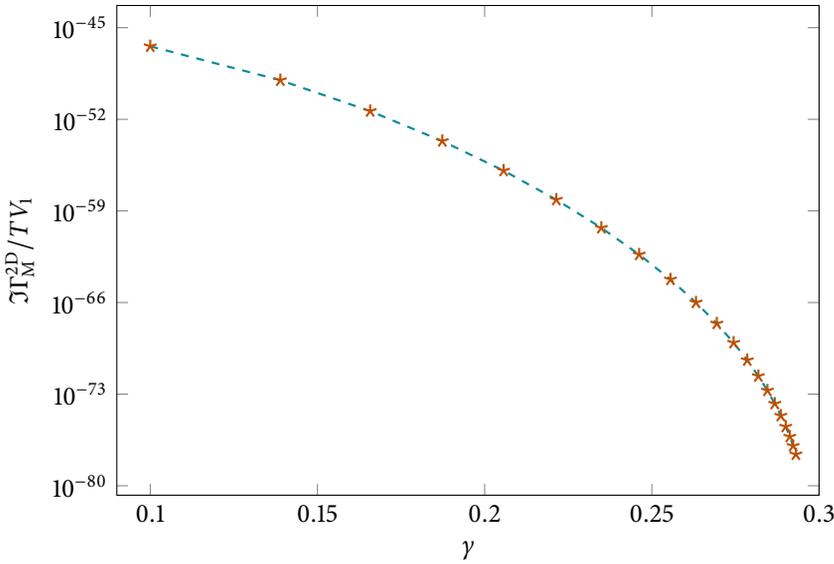


Figure 6.11.: Imaginary part of the effective action for the multidimensional field (6.79) from [DW06] for  $E = 0.033m^2/q$ , the dashed line added as visual aid again.

with some choice of “driving function”  $\xi$  and virtual dipole moment  $d$ . The electromagnetic fields are then given by

$$\mathbf{E} = -\nabla \times (\nabla \times \mathbf{Z}), \quad \mathbf{B} = -\nabla \times \dot{\mathbf{Z}}. \quad (6.81)$$

At the origin the magnetic field vanishes and the electric field is given by

$$\mathbf{E}(t, \mathbf{r} = 0) = \frac{4}{3} d \overset{\dots}{\xi}(t) \hat{\mathbf{e}}_z, \quad (6.82)$$

so by setting  $d = 3E/4$  and choosing an appropriate function  $\xi$  we can study a time dependent field in a physically realistic context.

The problem is now that we defined the field in terms of the vector  $\mathbf{Z}$ , but not an actual four-potential. To apply the worldline instanton method we first have to obtain an expression for  $A_\mu$  from the electromagnetic field. We can calculate it in coordinate gauge  $A \cdot x = 0$  using the integral [Shi80]

[Shi80] Shifman. *Nucl. Phys. B* (1980)

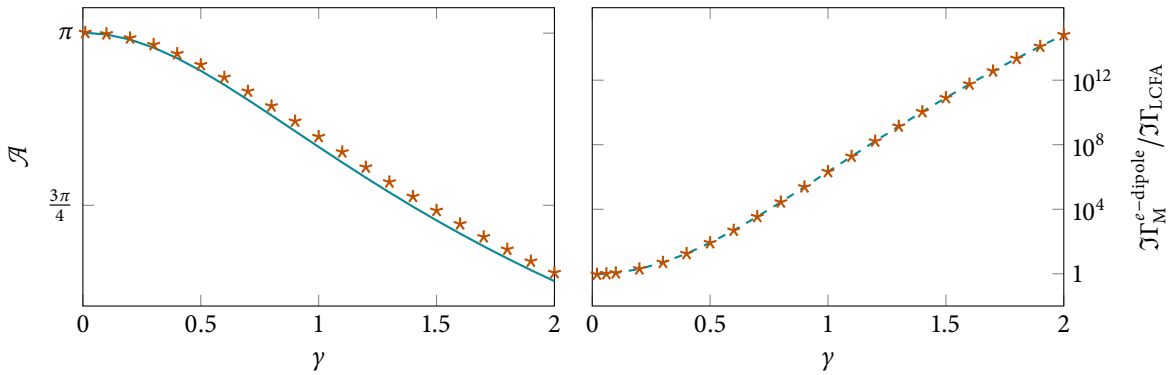


Figure 6.12.: Left: Instanton action for the  $e$ -dipole field (markers) and for a homogeneous field with Gaussian time dependence (line). Right: Ratio of the full effective action and the locally constant field approximation, with dashed connecting lines.

$$A_{\mu}^{\text{M}} = \int_0^1 d\alpha F_{\mu\nu}^{\text{M}}(\alpha x) \alpha x^{\nu}. \quad (6.83)$$

For the  $e$ -dipole field this gives a rather lengthy expression, but after transforming to the Euclidean potential we can apply the discrete worldline instanton method.

To describe an approximately Gaussian pulse we choose

$$\xi(t) = \frac{t}{4\omega^2} e^{-\omega^2 t^2} + \frac{\sqrt{\pi}}{8\omega^3} (1 + 2\omega^2 t^2) \text{erf}(\omega t), \quad (6.84)$$

so at the origin

$$\mathbf{E}(t, \mathbf{r} = 0) = E \ddot{\xi}(t) \hat{\mathbf{e}}_z = E e^{-\omega^2 t^2} \hat{\mathbf{e}}_z. \quad (6.85)$$

Although this field profile can in principle be treated numerically just like the other fields before, it does need some care in the practical execution. For  $\gamma \rightarrow 0$  the  $e$ -dipole pulse is approximately static and homogeneous around the origin so one might try to start with a circular trajectory as the initial guess in this limit. Unfortunately the instanton is only weakly confined for small frequencies so root finding converges slowly. This is not a problem for simpler fields, where the root finding algorithm simply takes more steps, but for the potential above each evaluation is a lot more costly. Instead we craft the initial guess by hand: We first construct a simple field (a sum of temporal and spatial pulses) that matches the curvature of the  $e$ -dipole pulse around the origin for  $\gamma = 1$ , find an instanton, and use that as an initial guess for the actual field. We then perform numerical continuation in both directions to higher  $\gamma$  and to smaller  $\gamma$ .

Figure 6.12 shows the result. The left plot compares the instanton action (exponent of the pair production rate) to that of a homogeneous field with Gaussian time dependence, obtained by numerically performing the integral for  $g(\gamma)$ . As expected, the spatial inhomogeneity of the  $e$ -dipole pulse slightly increases the action (decreasing the pair production rate), but not significantly. The right plot shows the ratio of the imaginary part of the effective action to the locally constant field approximation, in this case (calculated using the saddle point method)

$$\Re\Gamma_{\text{LCFA}}^{e\text{-dipole}} \approx \frac{5\sqrt{5}}{2(2\pi)^3 \gamma^4} \exp\left(-\pi \frac{m^2}{qE}\right). \quad (6.86)$$

As expected, the ratio tends to unity for small values of  $\gamma$  (where the approximation works well), but grows exponentially larger for higher frequencies.

From this we can conclude that the  $e$ -dipole pulse might be a good candidate for an experimental setup to observe nonperturbative pair production.

## 6.4. Transversal field dependences

A special case of multidimensional inhomogeneity is the addition of a purely transversal spatial dependence.

Let us consider a linearly polarized field (in  $z$ -direction) that depends on time and a transversal coordinate ( $x$ ). We choose the Euclidean four-potential

$$iA_3 = -f(\gamma_\omega x_4, \gamma_k x_1)/\gamma_\omega, \quad (6.87)$$

so the non-vanishing components of the field tensor are

$$iF_{34} = -iF_{43} = \dot{f}(\gamma_\omega x_4, \gamma_k x_1), \quad (6.88a)$$

$$iF_{31} = -iF_{13} = \frac{\gamma_k}{\gamma_\omega} f'(\gamma_\omega x_4, \gamma_k x_1), \quad (6.88b)$$

a dot denoting the derivative with regard to the temporal dependence of  $f$  and a prime with regard to the spatial one. This gives the instanton equations of motion

$$\ddot{x}_1 = -T \frac{\gamma_k}{\gamma_\omega} f'(\gamma_\omega x_4, \gamma_k x_1) \dot{x}_3, \quad (6.89a)$$

$$\ddot{x}_3 = T \frac{\gamma_k}{\gamma_\omega} f'(\gamma_\omega x_4, \gamma_k x_1) \dot{x}_1 + T \dot{f}(\gamma_\omega x_4, \gamma_k x_1) \dot{x}_4 \quad (6.89b)$$

$$\ddot{x}_4 = -T \dot{f}(\gamma_\omega x_4, \gamma_k x_1) \dot{x}_3. \quad (6.89c)$$

If the  $x_1$ -derivative of  $f$  vanishes somewhere (i.e. it has a spatial maximum) independent of time,  $f'(\gamma_\omega x_4, \gamma_k x_1^*) = 0$ , then  $x_1(u) \equiv x_1^* = \text{const.}$  is a solution to (6.89a) and the equations for the other components reduce to

$$\ddot{x}_3 = T \dot{f}(\gamma_\omega x_4) \dot{x}_4 \quad (6.90a)$$

$$\ddot{x}_4 = -T \dot{f}(\gamma_\omega x_4) \dot{x}_3, \quad (6.90b)$$

where we have defined  $f(\gamma_\omega x_4) := f(\gamma_\omega x_4, \gamma_k x_1^*)$ . These equations are identical to the one-dimensional case from Section 6.2, so the inhomogeneity has no effect on the instanton solutions and by extension on the exponent of the pair production rate. The prefactor does change however, and unfortunately it's not as easy to see how. The fluctuation operator even separates into block-diagonal parts for the  $x_3 - x_4$  and the  $x_1$  components evaluated at the instanton, so it's possible to calculate the additional part due to the transversal field dependence. We still need to perform the integration over the starting point of the instanton though, and it's not obvious how to do the  $x_1(0)$  integral. It might be possible to approximate the solution of the instanton equations for small nonzero  $x_1 - x_1^*$  and perform the  $x_1(0)$  integral using Laplace's method around  $x_1^*$ , this could be an area of future studies.

**[A] = 1,  $x_j = x^i$**   
(see page 13).

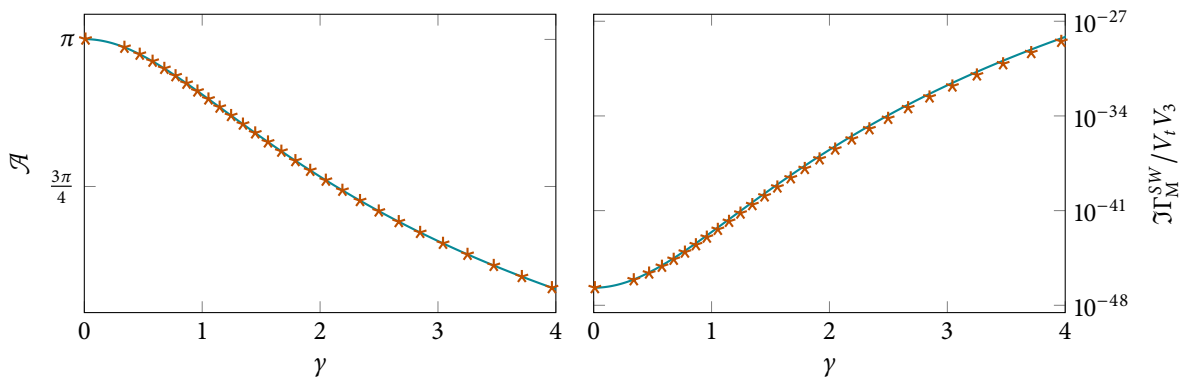


Figure 6.13.: Left: Instanton action for a standing wave (markers) and for a homogeneous field with sinusoidal time dependence (line). Right: Imaginary part of the effective action for the standing wave (markers) and the homogeneous, time dependent field (line).

An example for the configuration shown above would be a superposition of two counter-propagating plane waves,

$$E = E \frac{1}{2} (\cos(\omega t + kx) + \cos(\omega t - kx)) \hat{\mathbf{e}}_z = E \cos(\omega t) \cos(kx) \hat{\mathbf{e}}_z. \quad (6.91)$$

Figure 6.13 Shows the instanton action and pair production rate for a standing wave (with  $\omega = k = \gamma q E / m$ ) obtained using the discrete instanton method and compares it to the result for a homogeneous field with sinusoidal time dependence.

## 6.5. Spin and magnetic effects

Up to now we have only considered purely (or predominantly) *electric* fields for *scalar* quantum electrodynamics. In the worldline instanton formalism the only difference for spinor QED is a global sign and the inclusion of the spin factor (see Section 4.2)

$$[\mathbf{A}] = \mathbf{1}, \quad \mathbf{x}_i = \mathbf{x}^i \quad (\text{see page 13}).$$

$$\Phi[x] = \frac{1}{2} \text{tr} \mathcal{P} \exp \left( \frac{a}{4} \int_0^1 du \sigma_{\mu\nu} i F_{\mu\nu}(x(u)) \right). \quad (6.92)$$

For the Euclidean gamma matrices we choose<sup>65</sup>

$$\gamma_k = i \begin{pmatrix} \mathbf{0} & \sigma_k \\ -\sigma_k & \mathbf{0} \end{pmatrix}, \quad \gamma_4 = \begin{pmatrix} \mathbf{0} & \mathbf{1} \\ \mathbf{1} & \mathbf{0} \end{pmatrix}. \quad (6.93)$$

Let us first evaluate  $\Phi$  for the case of a constant homogeneous electric field.

Remember we have

$$iA_3 = -x_4 \quad \rightsquigarrow \quad iF_{34} = -iF_{43} = 1, \quad (6.94)$$

so the integrand in the spin factor is

$$\sigma_{\mu\nu} iF_{\mu\nu} = \sigma_{34} iF_{34} + \sigma_{43} iF_{43} = 2\sigma_{34} \quad (6.95)$$

because both  $\sigma_{\mu\nu}$  and  $F_{\mu\nu}$  are antisymmetric. Now we just need some matrix multiplication

$$\sigma_{34} = \gamma_3 \gamma_4 - \gamma_4 \gamma_3 = 2 \begin{pmatrix} 1 & 0 & 0 & 0 \\ 0 & -1 & 0 & 0 \\ 0 & 0 & -1 & 0 \\ 0 & 0 & 0 & 1 \end{pmatrix}. \quad (6.96)$$

<sup>65</sup> These do not actually satisfy the Clifford algebra (4.39): Due to our choice of metric signature, after Wick rotation we end up with  $(g_{\mu\nu}) = -\mathbf{1}$ . For the choice (6.93) we would have to redefine the Euclidean metric to be  $(g_{\mu\nu}) = \mathbf{1}$ , which would not affect the final results, however.

Since the matrix in the exponent is diagonal path ordering has no effect and we can immediately perform the integral, which gives 1 as the integrand does not depend on  $u$  at all. The spin factor is then

$$\Phi = \frac{1}{2} \text{tr} \exp\left(i \frac{a}{2} \text{diag}(1, -1, -1, 1)\right) = \frac{1}{2} (2e^{ia/2} + 2e^{-ia/2}) = 2 \cos\left(\frac{a}{2}\right). \quad (6.97)$$

Now, since for the instantons in a constant electric field we have  $a = 2\pi n$ , this gives

$$\Phi = 2 \cos\left(\frac{2\pi n}{2}\right) = 2(-1)^n = -2(-1)^{n+1}, \quad (6.98)$$

so resubstituted into the effective action the alternating sign cancels in the sum, the negative sign in front cancels the global sign and the factor of 2 survives,

$$\frac{\Re \Gamma^{\text{Spinor}}}{V_4} = \frac{(qE)^2}{(2\pi)^3} \sum_{n=1}^{\infty} \frac{1}{n^2} \exp\left(-n\pi \frac{m^2}{qE}\right). \quad (6.99)$$

For the pair production rate (the first term) this only amounts to a factor of 2.

Remarkably, the same applies to the one-dimensional inhomogeneities of Section 6.2. Instead of  $iF_{34} = 1$  we have  $iF_{34} = f'(\gamma x_4)$ , but the matrix structure in the exponent is still the same, so the terms along the path commute and we can just perform the integral,

$$\Phi = \frac{1}{2} \text{tr} \exp(i\mathcal{T} \text{diag}(1, -1, -1, 1)) \quad (6.100)$$

with

$$\mathcal{T} = \frac{a}{2} \int_0^1 du f'(\gamma x_4). \quad (6.101)$$

Now we can transform the integral in a similar way to before, by substituting

$$y = f(\gamma x_4)/\gamma, \quad \simeq \quad dy = \dot{x}_4 f'(\gamma x_4) du. \quad (6.102)$$

We again restrict the integration to a quarter of the trajectory with  $\dot{x}_4 > 0$ , which is traversed  $n$  times in total for an instanton with winding number  $n$ , so

$$\mathcal{T} = \frac{a}{2} 4n \int_0^1 dy \frac{1}{\dot{x}_4|_y} = \frac{a}{2} \frac{4n}{a} \int_0^1 dy \frac{1}{\sqrt{1-y^2}} = n\pi \quad (6.103)$$

which gives then the same spin factor

$$\Phi = 2 \cos(\pi n) = -2(-1)^{n+1}, \quad (6.104)$$

or simply a global factor of 2 for the pair creation rate.

As could be anticipated, things get more interesting in the presence of a magnetic field. We have to discern between two cases. If the magnetic field is perpendicular to the electric field the invariant  $\mathbf{E} \cdot \mathbf{B} = 0$  and there is an inertial frame with either  $\mathbf{E} = 0$  (if  $|\mathbf{B}| > |\mathbf{E}|$ ) with no pair production at all, or with  $\mathbf{B} = 0$  so nothing new happens, the effective electric field is simply reduced. If the fields are parallel however, there is no frame with either vanishing. We represent the sum of (possibly time dependent) electric and constant magnetic fields as

$$iA_3 = -f(\gamma x_4)/\gamma, \quad iA_2 = ibx_1, \quad b := \frac{B}{E}. \quad (6.105)$$

The instanton equations for this combination read

$$\ddot{x}_1 = ibT\dot{x}_2, \quad \ddot{x}_2 = -ibT\dot{x}_1, \quad (6.106a)$$

$$\ddot{x}_3 = Tf'(\gamma x_4)\dot{x}_4, \quad \ddot{x}_4 = -Tf'(\gamma x_4)\dot{x}_3 \quad (6.106b)$$

The  $x_3 - x_4$  subspace is unchanged due to the magnetic field, while the  $x_1 - x_2$  equations are solved by  $x_1 = x_2 = 0$ . This immediately means that the instanton action, the saddle point value for  $T$  and the second  $T$ -derivative stay the same. The fluctuation prefactor does change however, but since  $x_1$  and  $x_2$  do not mix with  $x_3$  and  $x_4$  in the action, the fluctuation operator is block-diagonal. This means that the  $x_3$ - $x_4$  part stays the same, while the  $x_1$ - $x_2$  components read

$$\Lambda^{(1,2)} = \begin{pmatrix} -\frac{\partial_u^2}{T} & -ib\partial_u \\ ib\partial & -\frac{\partial_u^2}{T} \end{pmatrix}. \quad (6.107)$$

The solutions satisfying the correct initial conditions are easily found

$$\begin{aligned} \eta_1^{(1)} &= \frac{\sinh(bTu)}{bT}, & \eta_2^{(1)} &= -\frac{\cosh(bTu) - 1}{ibT}, \\ \eta_1^{(2)} &= \frac{\cosh(bTu) - 1}{ibT}, & \eta_2^{(2)} &= \frac{\sinh(bTu)}{bT}, \end{aligned} \quad (6.108)$$

so the additional fluctuation determinant is

$$\det(\eta^{(1)}(1), \eta^{(2)}(1)) = \frac{2}{(bT)^2} (\cosh(bT) - 1) = \left(\frac{2}{bT}\right)^2 \sinh^2\left(\frac{bT}{2}\right). \quad (6.109)$$

For scalar QED the only change is then the additional factor

$$\frac{1}{\sqrt{\det(\cdot)}} = \frac{ab}{2} \frac{1}{\sinh\left(\frac{ab}{2}\right)}. \quad (6.110)$$

For spinor QED we have to calculate the spin factor. Now not only the term containing  $\sigma_{34}$  survives in the exponent, but also

$$\sigma_{12}iF_{12} + \sigma_{21}iF_{21} = 2ib\sigma_{12} = 2ib \begin{pmatrix} \sigma_1\sigma_2 & \mathbf{0} \\ \mathbf{0} & \sigma_1\sigma_2 \end{pmatrix} = 2ib \text{diag}(-1, 1, -1, 1). \quad (6.111)$$

Since this term is diagonal as well, everything in the exponent commutes again so we can proceed as before and perform the integral before exponentiating, so

$$\begin{aligned} \Phi &= \frac{1}{2} \text{tr} \exp\left(iT \text{diag}(1, -1, -1, 1) + \frac{ab}{2} \text{diag}(-1, 1, -1, 1)\right) \\ &= \frac{1}{2} \left(e^{iT-ab/2} + e^{-iT+ab/2} + e^{-iT-ab/2} + e^{iT+ab/2}\right) \\ &= 2 \cos(T) \cosh\left(\frac{ab}{2}\right). \end{aligned} \quad (6.112)$$

This gives the same factor of two and alternating sign expression as before, with the additional cosh term combining with the sinh from the fluctuation prefactor so for spinor QED we simply obtain an additional factor of

$$\frac{ab}{2} \frac{1}{\tanh\left(\frac{ab}{2}\right)}. \quad (6.113)$$

For the parallel combination of constant, homogeneous electric and magnetic fields we finally have

$$\frac{\Re\Gamma^{\text{Scalar}}}{V_4} = \frac{(qE)^2}{2(2\pi)^3} \sum_{n=1}^{\infty} \frac{(-1)^{n+1}}{n^2} \frac{n\pi b}{\sinh(n\pi b)} \exp\left(-n\pi \frac{m^2}{qE}\right), \quad (6.114a)$$

$$\frac{\Re\Gamma^{\text{Spinor}}}{V_4} = \frac{(qE)^2}{(2\pi)^3} \sum_{n=1}^{\infty} \frac{1}{n^2} \frac{n\pi b}{\tanh(n\pi b)} \exp\left(-n\pi \frac{m^2}{qE}\right). \quad (6.114b)$$



## 7

## Dynamically assisted Sauter-Schwinger effect

In this chapter we will examine the dynamically assisted Sauter-Schwinger effect in detail.

### 7.1. Introduction

One category of electric fields deserves special attention and thus warrants its own chapter, the *dynamically assisted* Sauter-Schwinger effect [SGD08]. The basic idea is to superimpose a strong, slowly varying (or static) field and a weak, time dependent pulse. As it turns out, the combined effect on pair production is much stronger than the individual contributions. A qualitative picture is shown in Figure 7.2. The additional time dependent field can give an electron in the lower continuum some additional energy, “raising” it into the forbidden region so the barrier it has to tunnel through is shortened. Thus one would expect an exponential enhancement compared to just the static, homogeneous electric field.

Using the worldline instanton formalism this can be calculated intuitively in a geometrical picture. As a concrete example, let us consider a constant, homogeneous strong field and a fast, weak Sauter pulse. Then the instanton equations are

$$\ddot{x}_3 = a(1 + \varepsilon \cos^{-2}(\gamma x_4))\dot{x}_4, \quad (7.1a)$$

$$\ddot{x}_4 = -a(1 + \varepsilon \cos^{-2}(\gamma x_4))\dot{x}_3, \quad (7.1b)$$

with  $\varepsilon = E_{\text{weak}}/E_{\text{strong}}$  a small parameter. When  $\varepsilon$  tends to zero the  $\cos^{-2}$ -terms are effectively zero almost everywhere, except when  $x_4 \rightarrow \pm\pi/2\gamma$  where  $\cos$  goes to zero. The idea is now to treat this term not explicitly in the equations of motion, but as a geometrical constraint, in the form of a perfectly reflecting barrier.

We know that the equations of motion without the time dependent field are solved by<sup>66</sup>

$$x_3(u) = -\cos(au), \quad x_4(u) = \sin(au), \quad (7.2)$$

so as long as  $\gamma < \gamma^{\text{crit}} := \pi/2$  the trajectory never “touches” the barriers and the time dependent field has no effect. However, as soon as  $\gamma > \gamma^{\text{crit}}$  only a part of the circular trajectory fits between the barriers. Since the instanton still has to have a periodicity of 1 this modifies the value of  $a$ . After a quarter of the period we demand that the trajectory touches the barrier at  $x_4 = x_4^*$  (see Figure 7.1), so

$$\sin\left(\frac{a}{4}\right) \stackrel{!}{=} x_4^* = \frac{\gamma^{\text{crit}}}{\gamma} \quad \leadsto \quad a = 4 \arcsin\left(\frac{\gamma^{\text{crit}}}{\gamma}\right). \quad (7.3)$$

[SGD08] Schützhold, Gies, and Dunne. *Phys. Rev. Lett.* (2008)

[A] = 1,  $x_i = x^i$   
(see page 13).

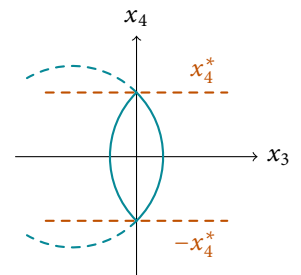
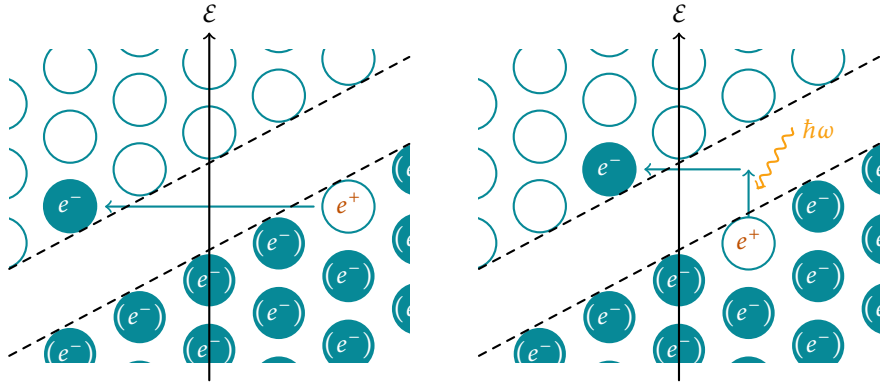


Figure 7.1.: The poles due to the time dependent pulse act as reflecting barriers at  $\pm x_4^*$  (red dashed lines), confining the trajectory in between. The dashed blue line depicts the trajectory without the barriers.

<sup>66</sup> We moved  $u_0$  so that  $x_4(0) = 0$  for convenience.

Figure 7.2.: Qualitative picture for the classic (left) and dynamically assisted (right) Sauter-Schwinger effect.



We can then piece together the trajectory using two circular arcs with this value of  $a$ . Obtaining the action is even easier, the upper limit in the integral formulation for  $g(\tilde{\gamma})$ <sup>67</sup> is the turning point of the trajectory,

<sup>67</sup> We use  $\tilde{\gamma}$  for the inhomogeneity of the background field and  $\gamma$  for the frequency of the weak, fast pulse.

$$g(\tilde{\gamma}) = \frac{4}{\pi} \int_0^{y^*} dy \frac{\sqrt{1-y^2}}{f'(f^{-1}(\tilde{\gamma}y))}, \quad (7.4)$$

with  $f(x) = x$  and thus  $f' = 1$  for the constant homogeneous field. We have defined  $y$  so that at the turning point  $y^* = x_4^* = 1$ , the barrier from the additional time dependent field now instead forces the turning point to be at  $y^*(\gamma) = x_4^* = \gamma^{\text{crit}}/\gamma$ . We immediately obtain  $g$  and thus the exponent of the pair production rate

$$\begin{aligned} \mathcal{A} = \pi g(\gamma) &= 4 \int_0^{y^*(\gamma)} dy \sqrt{1-y^2} \\ &= 2 \left( \frac{\gamma^{\text{crit}}}{\gamma} \sqrt{1 - \left( \frac{\gamma^{\text{crit}}}{\gamma} \right)^2} + \arcsin \left( \frac{\gamma^{\text{crit}}}{\gamma} \right) \right). \end{aligned} \quad (7.5)$$

Nothing about this discussion explicitly needed the weak pulse to be of Sauter type. The only important property is that the (Euclidean) electric field diverges for some  $x_4 = \gamma^{\text{crit}}/\gamma$ , for example a Lorentzian with  $f'(x) = 1/(1-x^2)$  where we would have the same result with  $\gamma^{\text{crit}} = 1$ .

Figure 7.3 compares the geometrical,  $\varepsilon \rightarrow 0$  expression (7.5) to the full numerical instanton result with  $\varepsilon = 1/100$ . As expected, for finite  $\varepsilon$  the threshold is “softened,” but the overall agreement is excellent.

## 7.2. Inhomogeneous background field

[SS16a]

An interesting generalization results from allowing the strong field to be spatially inhomogeneous. We already know that spatial inhomogeneity makes the instantons grow, so the trajectory reaches the barriers for smaller frequencies and we expect to find effects when

$$\gamma_\omega > \gamma_\omega^{\text{crit}}(\gamma_k) \quad (7.6)$$

where  $\gamma_\omega^{\text{crit}}(0) = \pi/2$  when the time dependent field is a Sauter pulse and  $\gamma_\omega^{\text{crit}}(\gamma_k)$  decreasing for stronger inhomogeneity.

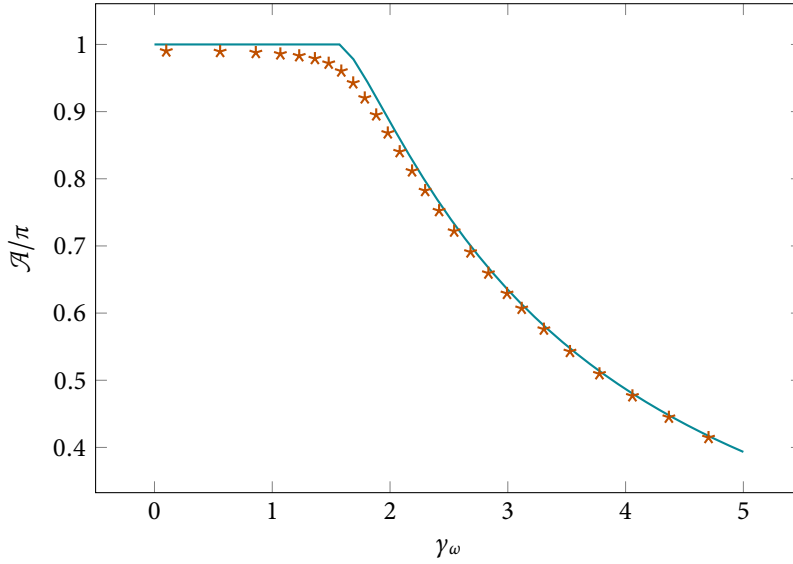


Figure 7.3.: Instanton action for a static, homogeneous background field with a weak temporal Sauter pulse. The lines show the geometrical estimate (7.5), the markers the discrete instanton result with  $\varepsilon = 1/100$ .

We choose the potential  $iA_4 = f(\gamma_k x_3)/\gamma_k$  for the strong background field. In the region where the time dependent pulse is negligible the instanton equations are

$$\ddot{x}_3 = a f'(\gamma_k x_3) \dot{x}_4 \quad (7.7)$$

$$\ddot{x}_4 = -a f'(\gamma_k x_3) \dot{x}_3 \quad \leadsto \quad \dot{x}_4 = -a (f(\gamma_k x_3)/\gamma_k + b).$$

The integration constant  $ab = \dot{x}_4(x_3 = 0)$  is needed because the trajectory has a velocity component in  $x_4$ -direction immediately after the reflection, in contrast to the “smooth” turning point when no barrier is present. We can again find an expression closed in  $x_3$  by using that  $a$  is constant, so

$$\dot{x}_3 = \pm a \sqrt{1 - \left( \frac{f(\gamma_k x_3)}{\gamma_k} + b \right)^2}. \quad (7.8)$$

The value of  $b$  is fixed by demanding that after a quarter of the trajectory (that is after  $x_3$  ranged from 0 to its turning point  $x_3^*$ ) the  $x_4$  component exactly reaches the barrier at  $x_4^*$ .

Choosing a quarter where  $\dot{x}_3 > 0$  and  $\dot{x}_4 > 0$  we have

$$\frac{dx_4}{dx_3} = \frac{dx_4}{du} \left( \frac{dx_3}{du} \right)^{-1}, \quad (7.9)$$

and since the right hand side can be given entirely as a function of  $x_3$  we can integrate it from 0 to  $x_3^*$ ,

$$\begin{aligned} x_4^* &\stackrel{!}{=} \int_0^{x_3^*} dx_3 \frac{f(\gamma_k x_3)/\gamma_k + b}{\sqrt{1 - (f(\gamma_k x_3)/\gamma_k + b)^2}} \\ &= \int_b^1 dy \frac{y}{\sqrt{1 - y^2}} \frac{1}{f'(f^{-1}(\gamma_k(y - b)))}, \end{aligned} \quad (7.10)$$

**[A] = 1,  $x_i = x^i$**   
(see page 13).

where we have substituted  $y := f(\gamma_k x_3)/\gamma_k + b$ . This integral can usually not be performed analytically for finite  $b$ , but the limit  $b \rightarrow 0$  gives the size of the unperturbed instanton in the background field in  $x_4$ -direction, and thus the minimum frequency the time dependent pulse needs to have any effect.

Of course this includes the result of last section, for a homogeneous background field  $f' = 1$ , and for a fast Sauter pulse as the time dependent field  $x_4^* = \pi/2\gamma_\omega$ , then

$$\frac{\pi}{2\gamma_\omega} = \int_b^1 dy \frac{y}{\sqrt{1-y^2}} = \sqrt{1-b^2} \quad \leadsto \quad b = \sqrt{1 - \left(\frac{\pi}{2\gamma_\omega}\right)^2}. \quad (7.11)$$

The threshold  $b = 0$  thus translates again to  $\gamma_\omega = \pi/2 =: \gamma_\omega^{\text{crit}}(0)$ .

For a spatial Sauter profile as the background field we have  $f'(f^{-1}(y)) = 1 - y^2$ , and we can no longer perform the integral with finite  $b$ . For  $b = 0$ , so the critical threshold, we have

$$\begin{aligned} \frac{\gamma_\omega^{\text{crit}}(0)}{\gamma_\omega^{\text{crit}}(\gamma_k)} &= \int_b^1 dy \frac{y}{\sqrt{1-y^2}} \frac{1}{1-(\gamma_k y)^2} = \frac{\arcsin \gamma_k}{\gamma_k \sqrt{1-\gamma_k^2}}. \\ &\leadsto \quad \gamma_\omega^{\text{crit}}(\gamma_k) = \gamma_\omega^{\text{crit}}(0) \frac{\gamma_k \sqrt{1-\gamma_k^2}}{\arcsin \gamma_k}. \end{aligned} \quad (7.12)$$

This also reduces to  $\gamma_\omega^{\text{crit}}(\gamma_k \rightarrow 0) = \gamma_\omega^{\text{crit}}(0)$ , which justifies the notation, and reduces the critical frequency with increasing inhomogeneity, as expected. For a different example, consider a sinusoidal background field,  $f = \sin$ , then  $f'(f^{-1}(y)) = \sqrt{1-y^2}$  and

$$\begin{aligned} \frac{\gamma_\omega^{\text{crit}}(0)}{\gamma_\omega^{\text{crit}}(\gamma_k)} &= \int_b^1 dy \frac{y}{\sqrt{1-y^2}} \frac{1}{\sqrt{1-(\gamma_k y)^2}} = \frac{1}{\gamma_k} \operatorname{arsinh} \left( \frac{\gamma_k}{\sqrt{1-\gamma_k^2}} \right). \\ &\leadsto \quad \gamma_\omega^{\text{crit}}(\gamma_k) = \gamma_\omega^{\text{crit}}(0) \gamma_k \operatorname{arsinh} \left( \frac{\gamma_k}{\sqrt{1-\gamma_k^2}} \right)^{-1}, \end{aligned} \quad (7.13)$$

which has the same qualitative behavior. In both cases  $\gamma_\omega^{\text{crit}}(\gamma_k \rightarrow 1) \rightarrow 0$ , so when the inhomogeneity gets so strong that the static field alone would produce no pairs at all, any time dependent addition immediately has an effect.

The next step is now to compute the instanton action. We can not directly reuse the integral expression for  $g(\gamma_k)$ , since it assumed that  $\dot{x}_4(x_3 = 0) = 0$  which is not true anymore. We can however perform the derivation again, we get

$$\begin{aligned} \mathcal{A} &= a + 4 \int_0^1 du \dot{x}_4 f(\gamma_k x_3)/\gamma_k = a - 4 \int_0^1 du \dot{x}_4 \left( \frac{\dot{x}_4}{a} - b \right) \\ &= 4 \int_b^1 dy \frac{1-y(y-b)}{\sqrt{1-y^2}} \frac{1}{f'(f^{-1}(\gamma_k(y-b)))} =: \pi g(\gamma_k, b). \end{aligned} \quad (7.14)$$

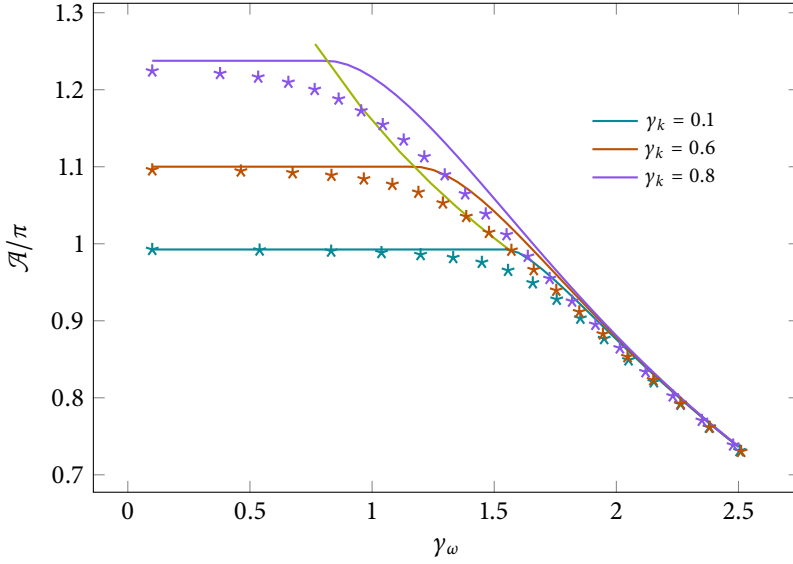


Figure 7.4.: Instanton action for a static, inhomogeneous Sauter profile with a weak temporal Sauter pulse. The lines show the geometrical estimate  $g(\gamma_k, b)$ , the markers the discrete instanton result with  $\varepsilon = 1/100$ . The green line marks the critical threshold  $\gamma_\omega^{\text{crit}}(\gamma_k)$ .

For  $b \rightarrow 0$  this reduces to the expression for  $g(\gamma_k)$  from before. Let us first check that it correctly includes the  $\gamma_k \rightarrow 0$  case, then

$$\begin{aligned} \pi g(0, b) &= 4 \int_b^1 dy \frac{1 - y(y - b)}{\sqrt{1 - y^2}} = 4 \int_b^1 dy \sqrt{1 - y^2} + 4b \int_b^1 dy \frac{1}{\sqrt{1 - y^2}} \\ &= 2 \left( \arccos(b) - b\sqrt{1 - b^2} \right) + 4b\sqrt{1 - b^2}, \end{aligned} \quad (7.15)$$

and inserting the value of  $b$  we know for the homogeneous case,

$$\begin{aligned} b &= \sqrt{1 - \left( \frac{\gamma_\omega^{\text{crit}}(0)}{\gamma_\omega} \right)^2} \\ \simeq \pi g(0, b) &= 2 \left( \frac{\gamma_\omega^{\text{crit}}(0)}{\gamma_\omega} \sqrt{1 - \left( \frac{\gamma_\omega^{\text{crit}}(0)}{\gamma_\omega} \right)^2} + \arcsin \left( \frac{\gamma_\omega^{\text{crit}}(0)}{\gamma_\omega} \right) \right). \end{aligned} \quad (7.16)$$

In the generic case where the background field is inhomogeneous and the time dependent pulse fast enough to have an effect, we have to resort to numerical integration. The implicit equation (7.10) can be inverted numerically to obtain  $b(\gamma_k, x_4^*(\gamma_\omega))$ , which we can insert into (7.14) and numerically perform the integration.

In Figure 7.4 this procedure is compared to a full numerical instanton treatment of the combinations of a strong, inhomogeneous Sauter field for different values of  $\gamma_k$  and the fast pulse with relative strength  $\varepsilon = 1/100$ . Again the region around the threshold is softened compared to the geometrical estimate, but the approaches agree reasonably well. For  $\gamma_\omega$  well above threshold the action for different values of  $\gamma_k$  converge to the  $\gamma_k \rightarrow 0$  limit. This is intuitively clear, higher  $\gamma_\omega$  confines the instantons into a smaller region, so they “notice” less of the inhomogeneous

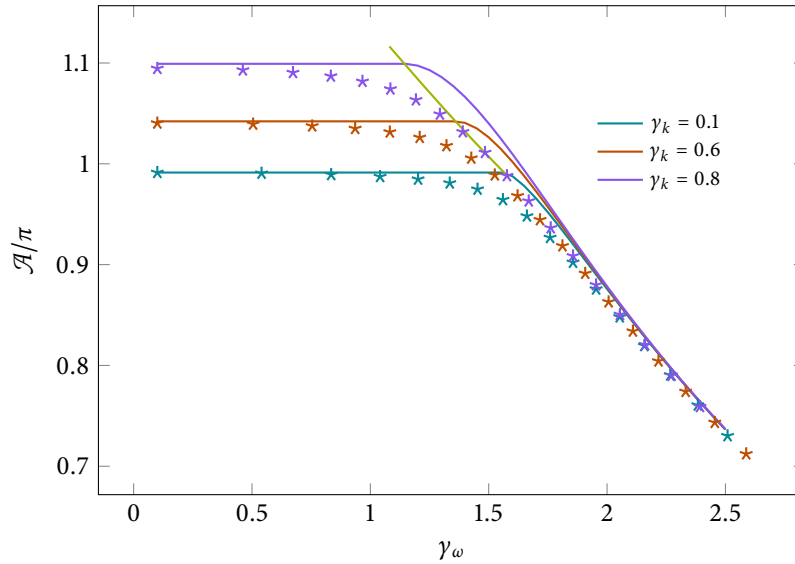


Figure 7.5.: Instanton action for a static, inhomogeneous Cosine profile with a weak temporal Sauter pulse. The lines show the geometrical estimate  $g(\gamma_k, b)$ , the markers the discrete instanton result with  $\varepsilon = 1/100$ . The green line marks the critical threshold  $\gamma_\omega^{\text{crit}}(\gamma_k)$ .

generality of the background field. Figure 7.5 shows the same for a Cosine profile as the strong field.

### 7.3. Pulse shape dependence

[Lin+15]

The geometrical picture of the last two chapters works as long as the time dependent pulse diverges for some imaginary time  $x_4 = x_4^*$  and we choose the relative strength  $\varepsilon$  of the weak pulse to be very small. If the time dependent field is sinusoidal however, it is still smooth after analytic continuation, giving a term  $\sim \varepsilon \cosh(\gamma x_4)$  in the equations of motion. The qualitative behavior should be similar, for small  $\varepsilon$  we need large enough  $\gamma x_4$  to see an effect, but now we expect the (soft) threshold to depend on the strength of the weak field, that is  $\gamma^{\text{crit}}(\varepsilon)$ .

[A] = 1,  $\mathbf{x}_i = \mathbf{x}^i$   
(see page 13).

Instead of approximating the slow field as static we keep it explicitly time dependent. This is important if we want to evaluate the prefactor as well, for a static background field without the additional pulse translation in  $x_4$ -direction is a zero mode that makes the result diverge for  $\varepsilon \rightarrow 0$ . We choose

$$f(\gamma x_4) = f_0(\rho \gamma x_4)/\rho + \varepsilon f_1(\gamma x_4) \tag{7.17}$$

with  $\rho = \gamma_{\text{slow}}/\gamma$ .<sup>68</sup> We can now approximate the integral expression for  $g(\gamma)$  for small  $\varepsilon$  and  $\rho$ .

The  $\varepsilon \rightarrow 0$  limit just gives the instanton action for the strong field only. For the term linear in  $\varepsilon$  we need

$$\left. \frac{d}{d\varepsilon} g(\gamma, \varepsilon) \right|_{\varepsilon=0} = \frac{4}{\pi} \int_0^1 dy \sqrt{1-y^2} \left. \frac{d}{d\varepsilon} \frac{1}{f'(f^{-1}(\gamma y))} \right|_{\varepsilon=0}. \tag{7.18}$$

Since both  $\varepsilon$  and  $\rho$  are supposed to be small, we neglect the  $\rho$ -dependence in the

<sup>68</sup> We have to express the frequency of the slow field in relation to the fast frequency because the scaling with  $\gamma$  is built into the formalism. In this case this is slightly inconvenient, however it enables us to express the prefactor using  $\gamma$ -derivatives, for example.

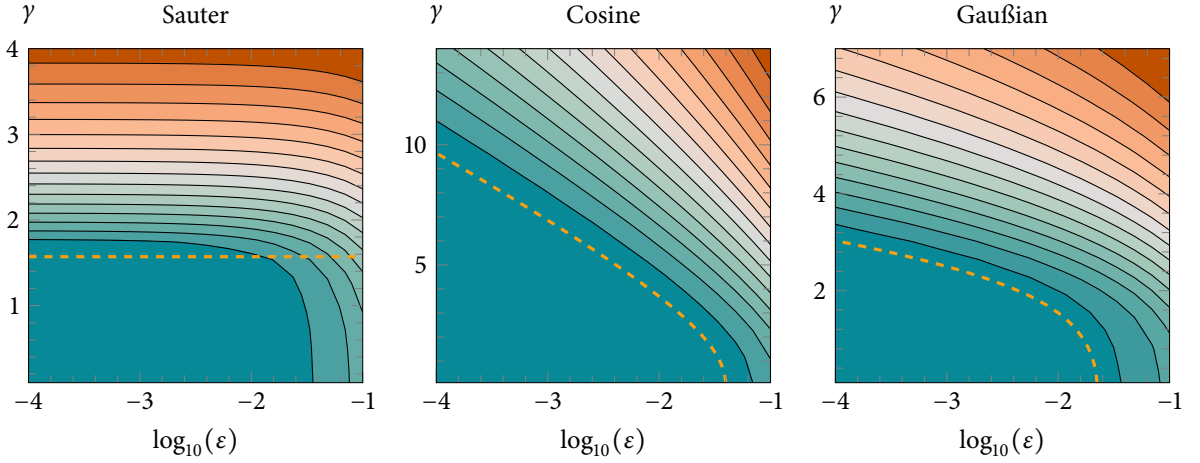


Figure 7.6.: Imaginary part of the effective action for a static field with  $E_{\text{strong}} = 0.033m^2/q$  and different time dependent pulses of varying relative strength and frequency. The orange dashed line marks the critical threshold  $\gamma_{\omega}^{\text{crit}}(\epsilon)$ .

linear term, so  $f_0$  is the identity. Then

$$\frac{d}{d\epsilon} \frac{1}{f'(f^{-1}(\gamma y))} = - \frac{\left( \frac{\partial f'}{\partial \epsilon}(f^{-1}(\gamma y)) + f''(f^{-1}(\gamma y)) \frac{\partial f^{-1}}{\partial \epsilon}(\gamma y) \right)}{(f'(f^{-1}(\gamma y)))^2} \quad (7.19)$$

$$\stackrel{\epsilon=0}{=} -f_1'(\gamma y),$$

so for the exponent we have

$$g(\gamma, \epsilon) \approx g_0(\rho y) - \epsilon g_1(\gamma) \quad (7.20)$$

with  $g_0(\rho y)$  the result for the strong, slow field only and

$$g_1(\gamma) = \frac{4}{\pi} \int_0^1 dy \sqrt{1-y^2} h'(\gamma y). \quad (7.21)$$

The function  $g_1(\gamma)$  carries the information how, to leading order in  $\epsilon$ , the additional time dependent pulse increases pair production.

For a sinusoidal weak field we have

$$g_1(\gamma) = \frac{4}{\pi} \int_0^1 dy \sqrt{1-y^2} \cosh(\gamma y) = \frac{2}{\pi} \int_{-1}^1 dy \sqrt{1-y^2} \exp(\gamma y) \quad (7.22)$$

$$= \frac{2}{\pi} \int_0^\pi d\theta \sin(\theta)^2 \exp(\gamma \cos(\theta)) = \frac{2}{\pi} \frac{\sqrt{\pi} \Gamma(1+1/2)}{(y/2)^1} I_1(\gamma) = \frac{2}{\gamma} I_1(\gamma),$$

where  $I_\nu$  denotes the modified Bessel functions of the first kind [Olv+10]. Similarly, for a Gaussian pulse we get

$$g_1(\gamma) = \frac{4}{\pi} \int_0^1 dy \sqrt{1-y^2} \exp(\gamma^2 y^2) = e^{\gamma^2/2} \left( I_0\left(\frac{\gamma^2}{2}\right) - I_1\left(\frac{\gamma^2}{2}\right) \right). \quad (7.23)$$

[Olv+10] Olver, Lozier, Boisvert, and Clark. *Cambridge University Press* (2010)

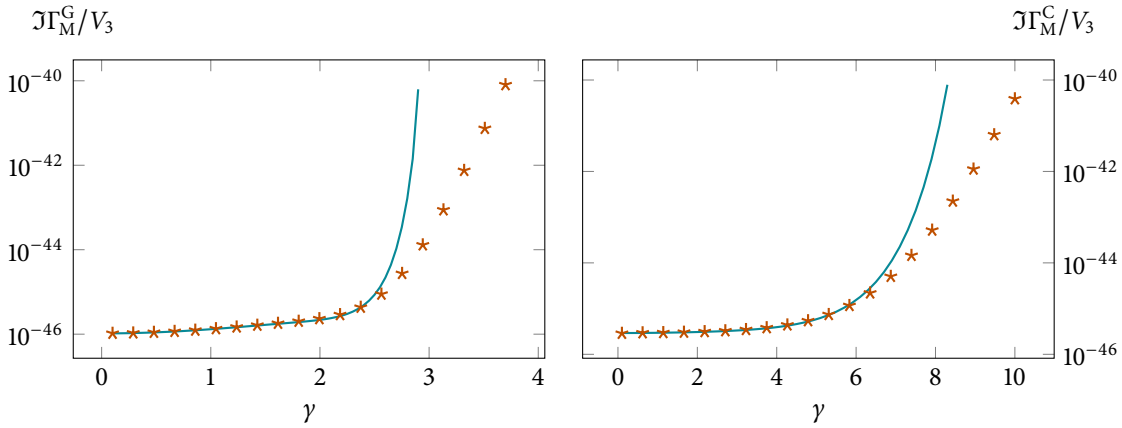


Figure 7.7.: Imaginary part of the Minkowskian effective action for  $E_{\text{strong}} = 0.033m^2/q$  and a Gaußian (left) or Cosine (right) pulse with  $\epsilon = 10^{-3}$  at the onset of dynamical assistance. The points are obtained by numerically integrating  $g(y)$ , the lines are the approximation linear in  $\epsilon$ . The approximation works well up to the threshold, above  $\epsilon g_1$  is not small anymore.

Although it belongs to the class of fields that have poles on the imaginary axis, we can also calculate  $g_1$  for a Lorentzian pulse,

$$g_1(\gamma) = \frac{4}{\pi} \int_0^1 dy \sqrt{1-y^2} \frac{1}{1-\gamma^2 y^2} = 2 \frac{1-\sqrt{1-\gamma^2}}{\gamma^2}, \quad (7.24)$$

but this is only possible below threshold, otherwise the expansion we performed would not be valid.

A very important point we can extract from  $g_1(\gamma)$  is the minimum value of  $\gamma$  that we need to see a sizable effect due to the time dependent field. For the fields with poles on the imaginary axis it is just some value  $\gamma_{\text{crit}}$ , independent of  $\epsilon$ . For the Sauter and Cosine profiles however, we can demand a decrease in action by  $\delta$ , then

$$\delta^{\frac{1}{2}} \epsilon g_1(\gamma) \quad \simeq \quad \gamma_{\text{crit}}(\epsilon) = g_1^{-1}\left(\frac{\delta}{\epsilon}\right). \quad (7.25)$$

Figure 7.6 shows the full pair production rate including the prefactor for  $E_{\text{strong}} = 0.033m^2/q$  by numerically integrating the exact expression for  $g(\gamma, \epsilon)$  and its derivatives for weak Sauter, Gaußian and Cosine pulses. We also included the thresholds, just  $\pi/2$  for the Sauter case and numerical evaluations of  $g_1^{-1}(\delta/\epsilon)$  with  $\delta \approx 1/50$ . For the Sauter pulse the geometrical estimate works for  $\epsilon \lesssim 1/100$ , for the other two fields the first order estimate using  $g_1$  shows the scaling between  $\gamma_{\text{crit}}$  and  $\epsilon$  perfectly.

We can also express the prefactor for small  $\epsilon$  using  $g_0$  and  $g_1$  by inserting (7.20) into (6.65). Assuming a slow Sauter pulse for the background field, so  $f_0 = \tan$ , we have

$$\frac{d}{dy^2} \gamma^2 g_0(\gamma^2) = \frac{1}{\sqrt{1+\rho^2 \gamma^2}}, \quad -\frac{d^2}{d(\gamma^2)^2} \gamma^2 g_0(\gamma^2) = \frac{\rho^2}{2(1+\rho^2 \gamma^2)^{3/2}}. \quad (7.26)$$

For the Gaußian and Cosine fast pulse the derivatives have rather simple forms as

well, due to relations between derivatives of the Bessel functions,

$$\begin{aligned} \frac{d}{dy^2} \gamma^2 g_1^G(\gamma^2) &= e^{\frac{\gamma^2}{2}} \left( I_0 \left( \frac{\gamma^2}{2} \right) - I_1 \left( \frac{\gamma^2}{2} \right) \right), & \frac{d}{dy^2} \gamma^2 g_1^C(\gamma^2) &= I_0(\gamma), \\ -\frac{d^2}{d(\gamma^2)^2} \gamma^2 g_1^G(\gamma^2) &= e^{\frac{\gamma^2}{2}} I_0 \left( \frac{\gamma^2}{2} \right), & -\frac{d^2}{d(\gamma^2)^2} \gamma^2 g_1^C(\gamma^2) &= -\frac{I_1(\gamma)}{2\gamma}, \end{aligned} \quad (7.27)$$

which we can use to assemble the effective action (6.65). Figure 7.7 compares this approach to an exact numerical evaluation of (6.65) for the total field.

## 7.4. Momentum spectra and dominant order [Tor+17]

The results of last section show that in the dynamically assisted Sauter-Schwinger effect two visually very similar temporal field profiles (the Gaußian and the Sauter pulse) can lead to qualitatively different behavior. We traced this to the different analytical structure after rotating to imaginary times. In this section we provide a second, related explanation in terms of the Fourier transform of the weak field.

The analytical derivation in [Tor+17] does not use the formalism of this thesis, but the numerical results were obtained using the numerical scheme for the Riccati equation introduced in Section 3.3. We will thus only sketch the derivation of the analytical result, for details refer to [Tor+17].

The idea is to approach the process of pair creation using perturbation theory. Of course we can not take the free theory and treat the whole electric background field as a perturbation – the Sauter-Schwinger effect is still nonperturbative. We can however treat the constant field exactly and then expand the pair production amplitude in orders of the relative strength  $\varepsilon = E_{\text{weak}}/E$  of the additional weak pulse. We consider the combination

$$\mathbf{E} = E(f_0(t) + \varepsilon f_1(t)) \hat{\mathbf{e}}_z, \quad (7.28)$$

the full pair production probability is then

$$\frac{P_{e^+e^-}}{V_3} = \int d^3 p \left| \mathfrak{A}_0(\mathbf{p}) + \varepsilon \mathfrak{A}_1(\mathbf{p}) + \dots \right|^2. \quad (7.29)$$

The zero-order amplitude contains just the effect of the strong field, which can be calculated analytically for a constant field or a single Sauter pulse. The first order amplitude can be given as a frequency integral over the Fourier transform of the weak field  $\tilde{f}_1$ ,

$$\mathfrak{A}_1(\mathbf{p}) = \int d\omega \tilde{f}_1(\omega) W_1(\omega, \mathbf{p}), \quad (7.30)$$

where the form of  $W_1$  depends on the strong field profile. In general,  $W_1$  is exponentially suppressed for small frequencies, increasing for larger values of  $\omega$ . The Fourier transform of the weak field  $\tilde{f}_1$  on the other hand decreases for larger  $\omega$ , so the integral (7.30) is dominated by some  $\omega_{\text{dom}}$  depending on  $\tilde{f}_1$ .

For a weak, fast Sauter pulse  $f_1(t) = 1/\cosh^2(\omega_{\text{fast}} t)$  the Fourier transform reads

$$\tilde{f}_1(\omega) = \frac{\pi}{\omega_{\text{fast}}^2} \frac{\omega}{\sinh(\pi\omega/(2\omega_{\text{fast}}))} \sim \exp\left(-\frac{\pi}{2} \frac{\omega}{\omega_{\text{fast}}}\right), \quad (7.31)$$

[Tor+17] Torgrimsson, Schneider, Oertel, and Schützhold. *JHEP* (2017)

[A] =  $\mathbf{L}^{-1}$ ,  $\mathbf{x}_i = -\mathbf{x}^i$   
(see page 13).

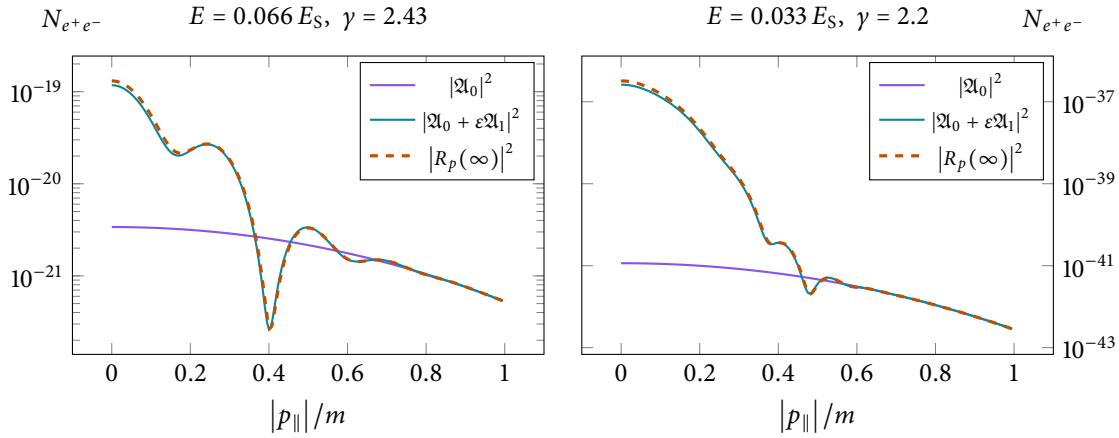


Figure 7.8.: First order perturbative expansion for a slow + a fast Sauter pulse compared to a numerical evaluation of the Riccati equation. In both cases  $\varepsilon = 10^{-3}$ ,  $\gamma_{\text{slow}} = 0.2$ .

for  $\omega \gg \omega_{\text{fast}}$ . As it turns out, the exponential decay of the Fourier transform for large frequencies is essential here. Calculating (7.30) with the saddle point method we find, just as with the instanton method, that the frequency of the weak field has to exceed the critical threshold  $\gamma = m\omega_{\text{fast}}/qE > \pi/2$ . Then, inserting into the integrand the saddle point value

$$\omega_{\text{dom}} = 2m_{\perp} \sqrt{1 - \left( \frac{1}{\gamma_{\perp}} + i \frac{p_{\parallel}}{m_{\perp}} \right)^2} \quad (7.32)$$

we find

$$\mathfrak{A}_1(\mathbf{p}) = 4\pi \frac{qE}{\omega_{\text{fast}}^2} \frac{m_{\perp}}{\omega_{\text{dom}}} \exp \left( -i \frac{m_{\perp}^2}{qE} \left( \phi \left[ \frac{p_{\parallel}}{m_{\perp}} - i \frac{1}{\gamma_{\perp}} \right] - \phi \left[ \frac{p_{\parallel}}{m_{\perp}} \right] \right) \right), \quad (7.33)$$

with the function

$$\phi(z) = z\sqrt{1+z^2} + \text{arsinh}(z), \quad (7.34)$$

and the definitions

$$p_{\parallel} = p_z, \quad \mathbf{p}_{\perp} = p_x \hat{\mathbf{e}}_x + p_y \hat{\mathbf{e}}_y, \quad m_{\perp}^2 = m^2 + \mathbf{p}_{\perp}^2, \quad \gamma_{\perp} = \frac{2}{\pi} \sqrt{1 + \frac{\mathbf{p}_{\perp}^2}{m^2}}. \quad (7.35)$$

With this first order term we already get good agreement with a numerical integration of the Riccati equation. Figure 7.8 shows the zero order “background”  $|\mathfrak{A}_0|^2$ , the first order approximation  $|\mathfrak{A}_0 + \varepsilon \mathfrak{A}_1|^2$  and the numerical result  $|R_p(\infty)|^2$  for  $\gamma_{\text{slow}} = 0.2$ ,  $\varepsilon = 10^{-3}$  and two different values of the strong field strength and Keldysh parameter  $\gamma$ . The oscillations in the spectrum arise due to interference between  $\mathfrak{A}_0$  and  $\mathfrak{A}_1$ .

As mentioned above, the important point is the exponential decay of the Fourier transform of the weak field. We can construct a visually quite different field with

$$f_1(t) = -\frac{\sinh(\omega_{\text{fast}} t)}{\cosh^2(\omega_{\text{fast}} t)}, \quad (7.36)$$

see Figure 7.9. Its Fourier transform is then

$$\tilde{f}_1(\omega) = -i \frac{\pi}{\omega_{\text{fast}}^2} \frac{\omega}{\sinh(\pi\omega/(2\omega_{\text{fast}}))} \sim -i \exp \left( -\frac{\pi}{2} \frac{\omega}{\omega_{\text{fast}}} \right), \quad (7.37)$$

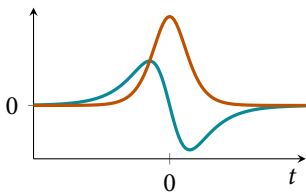


Figure 7.9.: The electric field (7.36) (blue) compared to a Sauter pulse (red).

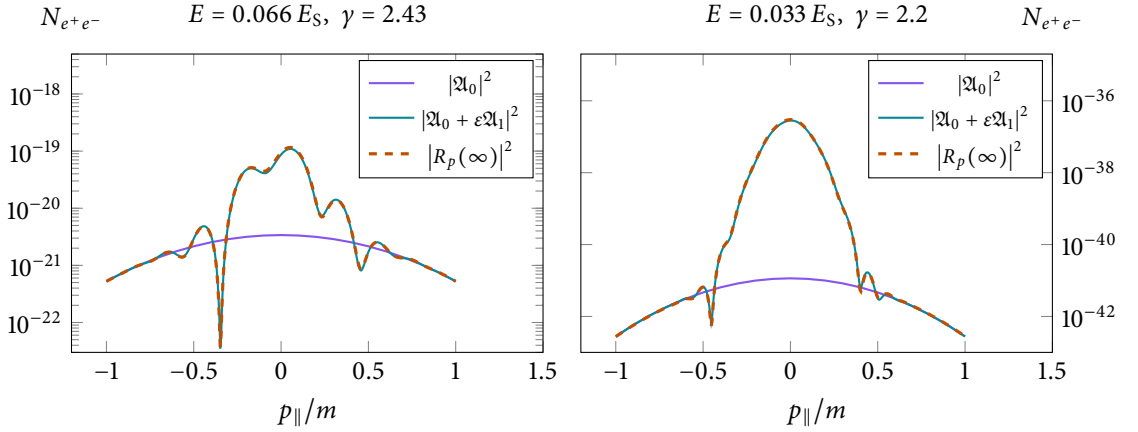


Figure 7.10.: First order perturbative expansion for a slow Sauter pulse + a weak field given by (7.36). Again,  $\varepsilon = 10^{-3}$ ,  $\gamma_{\text{slow}} = 0.2$ .

simply  $-i$  times the Fourier transform of the Sauter pulse. This means we immediately obtain the first order term with  $\mathfrak{Q}_1 = -i\mathfrak{Q}_1^{\text{Sauter}}$ , see Figure 7.10. Due to interference with the slow Sauter pulse the momentum spectrum looks quite different though, and since the field is not an even function of  $t$  anymore the spectrum loses its  $p_{||} \rightarrow -p_{||}$  - symmetry. Still we again obtain a very good approximation to the full numerical result.

The story changes substantially when we instead consider a Gaussian weak pulse  $f_1(t) = \exp(-\omega_{\text{fast}}^2 t^2)$ , with the Gaussian Fourier transform

$$\tilde{f}_1(\omega) = \frac{\sqrt{\pi}}{\omega_{\text{fast}}} \exp\left(-\frac{\omega^2}{4\omega_{\text{fast}}^2}\right). \quad (7.38)$$

Performing the saddle point approximation for the frequency integral again, we find

$$\omega_{\text{dom}} = \frac{2m}{\sqrt{1 + (qE/\omega_{\text{fast}}^2)^2}}, \quad (7.39)$$

with no threshold condition. Calculating the first order amplitude we get a factor of  $\varepsilon^2$  in the prefactor, so instead of the clear-cut threshold at  $\gamma = \pi/2$  for the other two fields, the first order term gradually starts to dominate when  $\gamma \approx \sqrt{|\log \varepsilon|}$ , as we saw in Section 7.3.

We can also obtain the momentum spectrum for the Gaussian weak pulse and compare it to a numerical evaluation of the Riccati equation for two sets of parameters, see Figure 7.11. For  $E = 0.066E_S$  we again see good agreement between the approximation and the numerical data. For  $E = 0.033E_S$  however, something goes very wrong, the analytical spectrum looks qualitatively different.

The reason for this is that higher order terms become important. These higher order contributions have been found in [Tor+17] using the worldline formalism, so only the integrated pair production probability is accessible, not the momentum spectrum. The probabilities are expanded in orders  $N$ ,

$$\frac{P^{e^+e^-}}{V_3} = \sum_N \varepsilon^N P_N. \quad (7.40)$$

The qualitative difference between the field profiles is that for the Sauter pulse

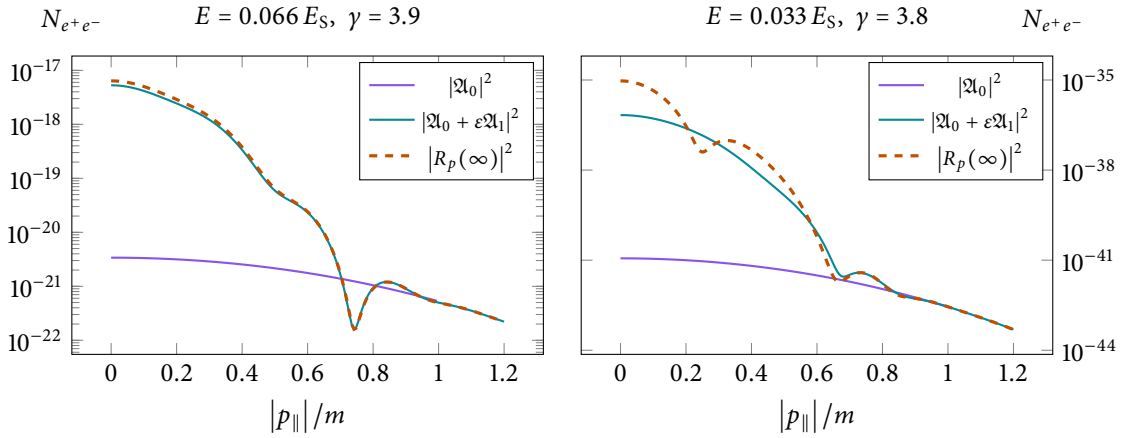


Figure 7.11.: First order perturbative result and full numeric simulation for a slow Sauter + a fast, weak Gaussian. For  $E = 0.066E_S$  the spectra agree well, but for  $E = 0.033E_S$  there are strong, qualitative differences. This can be explained by higher order contributions.

all orders  $P_N$  have the same,  $N$ -independent exponential dependence,

$$P_N \sim \exp\left(-2 \frac{m^2}{qE} \left(\frac{\sqrt{\gamma_*^2 - 1}}{\gamma_*^2} + \arcsin \frac{1}{\gamma_*}\right)\right). \quad (7.41)$$

This explains why the first order results for the spectrum agree well with the full simulation already, for the higher orders the exponentials are of the same magnitude, but the prefactor is smaller by a factor of  $\varepsilon$  for each order.

For the Gaussian pulse, however, the exponential does depend on  $N$ ,

$$P_N \sim \begin{cases} \exp\left(-\frac{2m^2}{qE} \arctan\left(\frac{2}{N} \frac{qE}{\omega_{\text{fast}}^2}\right)\right) & \text{for } N \text{ even,} \\ \exp\left(-\frac{2m^2}{qE} \arctan\left(\frac{2N}{N^2-1} \frac{qE}{\omega_{\text{fast}}^2}\right)\right) & \text{for } N \text{ odd.} \end{cases} \quad (7.42)$$

For higher  $N$  the exponential suppression decreases, while the prefactor gets smaller with higher orders of  $\varepsilon$ . In general, some order  $N$  dominates for given values of the field parameters. Estimating this dominant order by treating  $N$  as a continuous variable we find

$$N_{\text{dom}}^{\text{Gauß}} \sim \frac{2m^2}{qE} \frac{1}{|\log \varepsilon|} \frac{\sqrt{\chi^2 - 1}}{\chi^2}, \quad \text{with } \chi \sim \frac{\gamma}{\gamma_{\text{crit}}}. \quad (7.43)$$

For the parameters in the left plot of Figure 7.11 we have  $N_{\text{dom}} \approx 2$ , which corresponds to first order in the amplitude, while it is  $N_{\text{dom}} \approx 4$  for the parameters in the right plot, so we would need to include the second order amplitude as well to expect good agreement.

## 7.5. Assistance by a plane wave

[TSS18]

The last sections considered spatially homogeneous fast pulses for the dynamically assisted Sauter-Schwinger effect. The electromagnetic field of a high-energy laser might be better approximated by a propagating plane wave however, as even extremely short pulses still contain many wavelengths<sup>69</sup>.

Using a propagating plane wave for the assisting field is also interesting because, no matter the energy, it could never produce electron-positron pairs on its

<sup>69</sup> A femtosecond pulse at 1 keV contains several hundred oscillations

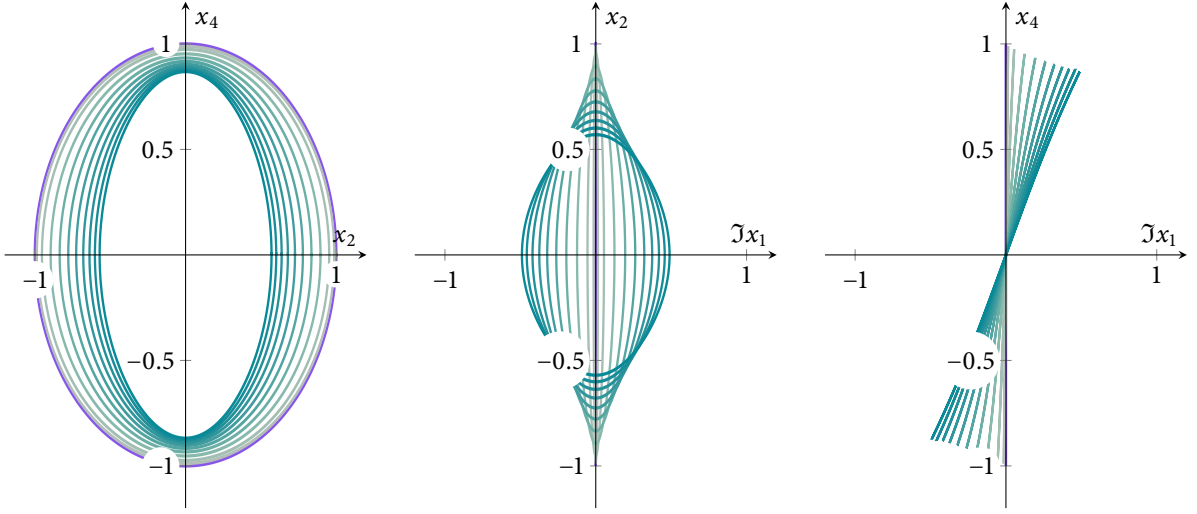


Figure 7.12.: Worldline instantons in the plane wave field (7.48), projected onto the coordinate planes.

own<sup>70</sup>. For the dynamically assisted Sauter-Schwinger effect this means that there is no transition to perturbative multi-photon pair creation at high energies, the production mechanism stays non-perturbative.

We consider the superposition of a strong, constant electric field and a weak plane wave propagating perpendicularly to the strong field but polarized in the same direction, i.e.

$$\mathbf{E} = E(1 + \varepsilon \cos(\omega(t - x)))\hat{\mathbf{e}}_z, \quad \mathbf{B} = -E\varepsilon \cos(\omega(t - x))\hat{\mathbf{e}}_y \quad (7.44)$$

This scenario has already been considered in [DGS09], in terms of a single high-energy photon added to the strong, static field. This corresponds to a first-order approximation of the amplitude in the sense of last section, while [TSS18] includes both an estimate for higher order contributions and fully nonperturbative results using discrete worldline instantons.

The  $N$ -th order contribution to the pair production probability is<sup>71</sup>

$$P_N \sim \exp\left(-\frac{2m_\perp^2}{qE} \left(\arccos \Sigma - \Sigma\sqrt{1 - \Sigma^2}\right)\right), \quad (7.45)$$

with

$$m_\perp = \sqrt{m^2 + (N\omega/4)^2}, \quad \Sigma = \frac{N\omega/2}{2m_\perp} = \frac{N\omega}{4\sqrt{m^2 + (N\omega/4)^2}}. \quad (7.46)$$

Estimating the dominant order by taking the derivative with regard to  $N$  we obtain a transcendental equation that has solutions for  $\gamma > \gamma_{\text{crit}} = |\log \varepsilon|$ . For  $\gamma \gg \gamma_{\text{crit}}$  we can approximate the solution of this equation and substitute the saddle point value for  $N$  into (7.45), yielding

$$P_{e^+e^-} \sim \exp\left(-8\frac{m^2}{qE}\sqrt{\frac{\gamma_{\text{crit}}}{3\gamma}}\right). \quad (7.47)$$

This, in contrast to the high frequency limit for purely time dependent weak fields, is still nonperturbative in the strong field  $E$ .

<sup>70</sup> This has been shown by Schwinger already in [Sch51] and can be quickly proved as both field invariants are zero.

[DGS09] Dunne, Gies, and Schützhold. *Phys. Rev. D* (2009)

<sup>71</sup> We again only briefly state the results of the perturbative approach.

[A] =  $\mathbf{L}^{-1}$ ,  $\mathbf{x}_i = -\mathbf{x}^i$   
(see page 13).

Figure 7.13.: Imaginary part of the effective action for the plane wave field (7.44) for  $E = 0.033m^2/q$ .

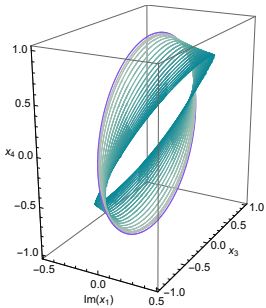
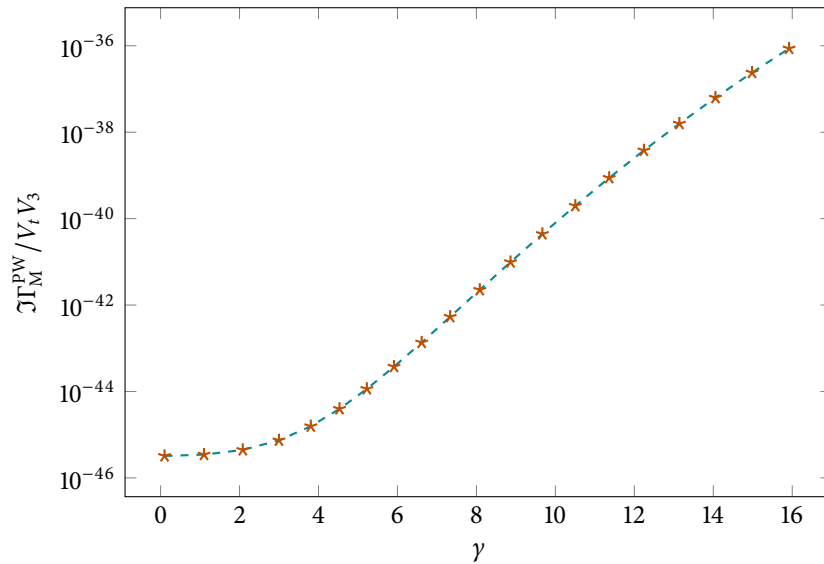


Figure 7.14.: The same worldline instantons as in Figure 7.12.

For the discrete instanton approach we use the Euclidean four-potential

$$iA_4 = Ex_3, \quad iA_3 = iE \frac{\varepsilon}{\omega} \sin(\omega(x_1 - ix_4)). \quad (7.48)$$

If the field did not have the spatial dependence we would have real, planar instantons and could again use the formalism of Section 7.3. Although the  $x_1$  dependence is transversal to the polarization direction, we can not use the results of Section 6.4 either, because the field does not have maxima in  $x_1$  *not depending on time*. We thus need to solve the full equations of motion, obtaining three dimensional instantons. They are also not purely real, the  $x_1$ -component of the solutions is imaginary.

Starting from the limit  $\gamma \rightarrow 0$  we find a family of instantons using numerical continuation, shown in figures 7.12 and 7.14. The qualitative behavior is similar to other assisting weak fields, the instantons shrink from their circular shape for increasing frequencies, in this case additionally tilting into the imaginary  $x_1$  direction.

To find the full pair production probability we have to deal with multiple zero modes. Since the field does not depend on  $x_2$  and  $x_3$  this trivially gives a two-volume factor  $V_2$ . The field also does not depend on one lightfront coordinate which is not that intuitive in an experimental setup. For the prefactor in our discrete instanton approach we just need to hold *something* constant that fixes the zero mode. We choose to keep  $x_1$  fixed, yielding an additional spatial volume factor. We interpret the resulting three-volume  $V_3$  as the fixed spatial region where the strong field is active through which the plane wave travels, but this is simply a matter of viewpoint. Additionally, there is one instanton for each oscillation of the plane wave at the fixed spatial location. If we assume the background field is active for a time period of  $V_t$ , there are  $n = V_t \omega / 2\pi$  instantons, effectively giving an additional temporal volume factor. The full pair creation rate is shown in Figure 7.13.

It also possible to consider other polarization directions of the plane wave,

i.e. perpendicular both to the propagation direction and the direction of the strong background field or any angle in between. This, however, leads to four-dimensional instantons that are cumbersome to visualize<sup>72</sup>, and the case of parallel polarization gives the highest pair production probability.

<sup>72</sup> The frontispiece and back cover of the thesis show different two-dimensional projections of these instantons.



# 8

## Code user's manual

*This chapter includes practical guides on how to use the computer programs that produced the numerical results of this thesis.*

### 8.1. Riccati equation

The programs to numerically solve the Riccati equation consist of multiple interacting parts. The overall workflow is as follows:

1. Define the field profile of interest in Mathematica,
2. Generate the C code that performs the integration,
3. Tweak the main `.c`-file to set parameters,
4. Compile and run the program.

A set of tools to simplify this process has been developed. These work together by adhering to some conventions concerning parameter order and directory structure, so we will now outline how to define two fields (a single Sauter pulse and a superposition of a strong, slow and a weak, fast pulse) and obtain pair production results for them.

To generate the files, we assume an initially empty working directory, where we first save a Mathematica notebook file, say `codeGeneration.nb`. In it, we load the prepared package `Riccati`` and set the working directory to the one the notebook resides in:

```
<< Riccati`
```

```
SetDirectory[NotebookDirectory[]]
```

The package includes a helper function to perform operations in a subdirectory (without changing the current, global working directory) which we use to prepare and compile the two fields in different directories. For the single Sauter field the file generation is simply:

```
InSubDir["single", WriteRiccatiFiles["sauter_fun", Tanh]]
```

The first argument to `WriteRiccatiFiles` is the name of the generated files (with extensions `.c` and `.h`), where the suffix `"_fun"` is one of the conventions mentioned earlier. These files contain the function definition of the ODE, we still need to supply the *driver*-program to actually call the integration. We can generate a driver template by passing the option `GenDriver`  $\rightarrow$  `True` to the call to

`WriteRiccatiFiles`. This outputs a file with placeholder marks for initial values and values of parameters that need to be filled in. While these can be substituted directly into the code, we prefer parsing command line arguments, as shown in the following snippet<sup>73</sup>

<sup>73</sup> An example of a complete driver file is given in the appendix.

```
/* --- CHECK PARAMETERS ----- */
    if(argc < 6) {
        fprintf(stderr, "Usage: %s E gamma p tmax prec\n",
            argv[0]);
        return -1;
    }

    int prec = atoi(argv[5]);

    char acc[16];
    sprintf(acc, "1.e-%i\n", prec-1);

/* --- SET PRECISION ----- */
    set_precision_digits(prec);

/* --- PARAMETERS ----- */
    int npar = 3;
    mpfr_t p[npar];
    for(i=0; i<npar; i++) mpfr_init2(p[i], TIDES_PREC);
    mpfr_set_str(p[0], argv[1], 10, TIDES_RND);
    mpfr_set_str(p[1], argv[2], 10, TIDES_RND);
    mpfr_set_str(p[2], argv[3], 10, TIDES_RND);
```

The practice of ordering the parameters as  $E$  first,  $p$ ,  $T_{\max}$  and the precision  $N_d$  (number of digits) last, is again (an arbitrary, but consistent) convention.

At the end of the driver file after performing the integration, we need to obtain the pair production probability and add a print statement for it:

```
/* --- PAIR PRODUCTION RATE ----- */
    mpfr_sqr(v[0], v[0], TIDES_RND);
    mpfr_sqr(v[1], v[1], TIDES_RND);
    mpfr_add(v[0], v[0], v[1], TIDES_RND);

    mpfr_printf("%Re\n", v[0]);
```

After completing the driver file and saving it as `sauter.c` in the subdirectory `single`, we can compile it in the Mathematica notebook using

```
InSubDir["single", CompileRiccati["sauter"]]
```

and run it from the subdirectory:

```
~/single> ./sauter 0.01 2.0 0 30 50
4.752284376670175288077739079816429164004122217553328e-85
```

This is already very close to the analytical value (a relative deviation of about  $10^{-6}$ ), but took only a few seconds to calculate. The only limiting factor in `TIDES` is the time we are willing to wait,<sup>74</sup> so we can do the calculation again using more digits and larger  $T_{\max}$ :

```
~/single> ./sauter 0.01 2.0 0 60 100
4.7523015234281739239560575129327559236370653135717853747
↳ 0972480084069779268805744590857109367568485785e-85
```

which has a relative deviation of about  $10^{-57}$  and still took just below one minute. So let's try more:

```
~/single> ./sauter 0.01 2.0 0 120 200
4.7523015234281739239560575129327559236370653135717853747
↳ 27139795119192809488935026697311386209853324761690694
↳ 33680696928618991460909334290162037484508539007807179
↳ 1097282507772516313229055265273697514171e-85
```

This time, after about five minutes of waiting, the deviation is only  $10^{-85}$ .

To see an example with more parameters, let's implement the setup for dynamical assistance, i.e. a superposition of two Sauter pulses.

```
fAssistedSauter[ε_, Ωω_][γτ] = 1/Ωω Tanh[Ωω γτ] + ε
↳ Tanh[γτ]
InSubDir["assisted", WriteRiccatiFiles["sauter_fun",
↳ fAssistedSauter[ε, Ωω], {ε, Ωω}]]
```

in this definition  $\varepsilon$  is the ratio of the weak and strong field strength, while  $\Omega\omega$  is the ratio of the frequencies. The additional parameters are added to the call to `WriteRiccatiFiles` and subsequently made known to `TIDES`. Again, we parse the arguments in the driver program, where we also set  $\Omega\omega$  from the two frequencies specified separately (for convenience)

```
/* --- CHECK PARAMETERS ----- */
if(argc < 8) {
    fprintf(stderr, "Usage: %s E Gamma eps gamma p tmax
↳ prec\n", argv[0]);
    return -1;
}

int prec = atoi(argv[7]);

char acc[16];
sprintf(acc, "1.e-%i\n", prec-1);

/* --- SET PRECISION ----- */
set_precision_digits(prec);

/* --- PARAMETERS ----- */
int npar = 5;
```

<sup>74</sup> And computer memory, but it is completely negligible in this case.

```

mpfr_t p[npar];
for(i=0; i<npar; i++) mpfr_init2(p[i], TIDES_PREC);
mpfr_set_str(p[0], argv[1], 10, TIDES_RND); // E
mpfr_set_str(p[1], argv[4], 10, TIDES_RND); // gamma
mpfr_set_str(p[2], argv[5], 10, TIDES_RND); // p
mpfr_set_str(p[3], argv[3], 10, TIDES_RND); // eps
mpfr_set_str(p[4], argv[2], 10, TIDES_RND); // Gamma

// Divide Gamma by gamma
mpfr_div(p[4], p[4], p[1], TIDES_RND);

```

Compiling this from the notebook again,

```
InSubDir["assisted", compile["sauter"]]
```

we can execute the resulting binary just as before

```
~/assisted> ./sauter 0.066 0.2 0.001 2.43 0 120 40
1.30891335120099744848899821395829524940226e-19
```

To simplify the calling of different fields with different parameter sets in different directory structures, we use a python script named `riccati.py`. It contains a list of available fields, where the binaries are located (relative to the script) and how many parameters need to be specified, for our two examples it looks like

```
fields = {
  'sauter': ['single/sauter', 1],
  'assisted_sauter': ['assisted/sauter', 3]
}
```

We can then call the script like

```
~> riccati.py assisted_sauter 0.2 0.001 2.43 -E 0.066 -T 120
1.3076599108682783533e-19
```

## 8.2. Discrete worldline instantons

The approach derived in Chapter 5, finding discrete instantons and performing numerical continuation to trace families of solutions, are all implemented in a single Mathematica package, called `Instantons``. General trajectories and instantons are represented as lists of  $N$  points, with  $d$  dimensions each. Electromagnetic background fields are represented via ( $i$  times) the Euclidean four-potential, as functions of one parameter (a  $d$ -dimensional list) returning the  $d$ -dimensional potential. The number of points  $N$  and dimension  $d$  do not have to be supplied explicitly in any function, they are always derived from supplied trajectories and four-potentials.

Let us begin with the simplest example, a constant homogeneous electric field. We import the package, and define the potential

```
<< Instantons`

iAconst = {0, -#[1]}&
```

Note that we have taken the potential to be two-dimensional. All of the code is completely independent of the dimension of spacetime,<sup>75</sup> so we do not need to include coordinates that are irrelevant to the field. The minimum is of course two, the electric field has to have a direction, and to represent it using the corresponding component of the “vector” potential the latter has to depend on time. The same argument holds when we use the scalar potential, which depends on the spatial coordinate, as for our `iAconst` above.<sup>76</sup> In Euclidean space there is no difference between spatial and temporal coordinates, by convention we designate the last component to be the temporal one.

To find the instanton for this field, we first have to provide some initial guess. This can be any list of two-dimensional points, but we already expect the instanton to be circular in this case, so we can construct a circular trajectory using, for example, `Table[]`. Because circular initial guesses are very convenient, especially for continuation, a helper method `Circular[n, d]` is provided which returns a circle between the first and last component with `n` points.

Equipped with a background field and an initial guess we can start the root finding procedure, which is as simple as

```
inst = FindInstanton[iAconst, Circular[500, 2]];
```

Note that we did not need to specify that the loop position has to be held fixed, this is detected automatically. Which coordinates to fix can also be given as an option (in this case `Fixed`  $\rightarrow$  `{1, 2}`), the default being `Fixed`  $\rightarrow$  `Automatic`. For fields where a lightfront coordinate like  $x \pm t$  is a zero mode (as is the case for the plane wave in Section 7.5),  $x_1$  or  $x_4$  have to be manually specified to be fixed as the code can not make this decision automatically.

The instanton can then be inspected using `ListPlot[]` or similar methods, and we can evaluate its action using

```
Action[iAconst, inst] (* returns 3.14163 *)
```

For scalar QED we only need the fluctuation prefactor now,

```
Fluctuation[iAconst, inst, e]
(* returns (0. + 0.00199611 I) e^2 *)
```

The parameter `e` (the reference field strength) is supplied here because depending on the number of fixed directions its power changes. The result is imaginary which might seem strange, but there is a temporal volume factor that is also imaginary, so the overall prefactor is real as expected for the Euclidean effective action. The numeric factor is reasonably close, the exact result would be  $1/2(2\pi)^3 \approx 0.00201572$ .

To make the switch to spinor QED we have to include the spin factor, and a global factor of  $-\frac{1}{2}$ . The formulation of the spin factor needs a four-dimensional trajectory and potential though, so we redefine

```
iAconst = {0, 0, 0, -#[1]}&;
inst = FindInstanton[iAconst, Circular[500, 4]];
```

Both the action and the fluctuation still return the same values, but we can now evaluate the spin factor

<sup>75</sup> Except for the spin factor, which needs a four-dimensional potential.

<sup>76</sup> There is no maximum number of components, so instantons in a spacetime of arbitrary dimensions can be found.

```
Spinfactor[iAconst, inst] (* returns -4.03968 *)
```

Together with the factor of  $-\frac{1}{2}$  this brings the overall prefactor close to the exact value of  $1/(2\pi)^3 \approx 0.00403144$ . For convenience there is a combined function that includes the spin factor if given as an option

```
Prefactor[iAconst, inst, e, Spin → True]
(* returns (0. + 0.00403182 I) e^2 *)
```

We can also immediately obtain the full effective action

```
EffectiveAction[iAconst, inst, e, Spin → True]
(* returns (0. + 0.00403182 I) e^2 E^(-3.14163/e) *)
```

This result can then be evaluated for different values of  $e$ , without any significant computation.

Let us now consider a field with a parameter and find instantons for a whole range. A simple but interesting case is the spatial Sauter profile  $E = E \cosh^{-2}(kz)\hat{e}_z$ , represented by the potential<sup>77</sup>

```
iAsauter[γ_] = {0, -Tanh[γ #[1]]/γ}&
```

We first use the simpler natural parameter continuation. The parameter range specification works similarly to `Table`, `Range` and similar functions, so

```
instantons = NaturalContinuation[
  iAsauter[γ], {γ, 0.1, 0.9, 0.1}, Circular[500, 2]
]
```

The function `NaturalContinuation` uses the range specification to substitute the first value for the symbol in the potential given as the first argument and finds an instanton using the third argument as an initial guess. This is then used as initial guess for the next value of the parameter and so on until the maximum value is reached.

The instantons are returned in a list where each first element is the value of the parameter and the second is the instanton, that is

```
{{γ1, X1}, {γ2, X2}, ...}
```

To quickly inspect all instantons it is possible to only pick the trajectories out of the list, for example

```
ListPlot[instantons[All, 2]]
```

To plot any derived quantities like the action over the values of the parameter it is useful to introduce a helper function

```
mapper[f_][{λ_, X_}] := {λ, f[λ, X]}
```

```
ListPlot[mapper>Action[iAsauter[#1], #2]&]/@instantons]
```

For this field, the instantons for small  $\gamma$  hardly change, while they diverge for  $\gamma \rightarrow 1$ . This is a great opportunity to exploit the adaptive step control of arclength/Dauidenko continuation. The usage is very similar,

<sup>77</sup> Note that `iAsauter` is a *higher order* function now, given a value of  $\gamma$  it still returns the potential as a function.

```
instantons = DavidenkoContinuation[
  iAsauter[ $\gamma$ ], { $\gamma$ , 0.1, 0.9}, 2, Circular[500, 2]
]
```

Instead of a step width of the parameter, we provide a value for the overall step along the arclength. We can also supply an optional number of in-between steps, that provide an even better guess for the next instanton, for example 4 substeps using

```
instantons = DavidenkoContinuation[
  iAsauter[ $\gamma$ ], { $\gamma$ , 0.1, 0.9, 4}, 2, Circular[500, 2]
]
```

Now the parameter  $\gamma$  takes large steps at first that progressively shrink to counteract the diverging instantons. That makes values of  $\gamma$  much closer to 1 attainable without wasting many steps for smaller values.

This concludes the basic usage of the `Instantons`` package. There are more options (for example minimum and maximum step widths for Davidenko continuation) and useful functions available that are documented in the source code included in Section A.2.



**Part III.**

**Conclusions**



## Conclusions and outlook

Over the course of this thesis we have introduced several methods to compute pair production rates in the Sauter-Schwinger effect. Using the worldline instanton method we were able to build intuition on how different kinds of electromagnetic background fields affect pair creation, in particular the difference between spatial and temporal inhomogeneities.

In Part I we first gave some historical context and introduced the mathematical tools and conventions needed in the remaining chapters, most importantly the path integral, Laplace's method applied to the path integral including the fluctuation prefactor, and how to deal with zero modes using the Faddeev-Popov-method.

We then introduced the Riccati equation as an exact formulation of the pair production problem for fields that are spatially homogeneous but depend on time, and described a numerical scheme to solve it using arbitrary precision. This is an important tool, because it allows us to verify the accuracy of different approximations. A quick comparison to the analytically known result for a single Sauter pulse shows excellent agreement even for a rather weak field, which usually poses great problems for numerical methods.

In Chapter 4 we introduced the physical models we use, scalar and spinor quantum electrodynamics, and the worldline path integral representation of the vacuum persistence amplitude. The physical models were discussed in some detail, with a focus on *why* they describe the systems we are interested in (electrons and positrons interacting with electromagnetic fields). We then proceeded to derive the worldline instanton method, both in the usual continuous setting and in a discrete formulation that forms the basis for our novel numerical instanton finding approach. The discrete formulation has a number of benefits compared to the usual continuous approach, most prominently the fact that Laplace's method yields a prefactor that is a finite determinant, sparing us the complication of carefully regularizing a functional determinant and recovering the correct phase by finding the instanton's Morse index. Zero modes can be extracted very neatly using the Faddeev-Popov-method as well.

The last chapter of Part I introduced the algorithmic details of numerical instanton finding, most importantly *numerical continuation*. Numerical continuation is the collective term for a number of algorithms to map out the solution space of a system of nonlinear equations. In general,  $m$  equations in  $n$  unknowns describe a, possibly complicated,  $n - m$ -dimensional manifold. In our case,  $d$ -dimensional trajectories discretized into  $N$  points in a background field with one parameter can be seen as a  $N \times d + 1$ -dimensional parameter space, while we only get  $N \times d$  equations, so we expect a one-dimensional manifold of instantons. Continuation algorithms allow us to start off from one point (an instanton for a specific value of the field parameter) and step along the manifold. Apart from

finding *all* the solutions for a range of field parameters, this also allows us to find *any* solutions for more complicated scenarios, by starting with a simpler field and slowly deforming it into the configuration we want.

In Part II the methods introduced in Part I were applied to some example fields. First, we derived the well known constant field result by a direct evaluation of the vacuum persistence amplitude, analytically using the worldline instanton method, numerically employing discrete instantons and finally by numerically integrating the Riccati equation. For this case we also checked that the discretization error in the discrete instanton approach scales with  $N$  as expected. We then discussed in detail the case of a field depending on time or one spatial coordinate only, giving the full pair production rate including the prefactor in terms of a single function and its first two derivatives determined by the background field. The central qualitative result is that time dependent fields lead to smaller instantons, reduced action and increased pair production, while spatial inhomogeneity does the opposite.

To demonstrate the broad applicability of the discrete instanton method we then turned to more complicated, multidimensional fields, including a highly nontrivial  $e$ -dipole field depending on time and all spatial coordinates that is an actual vacuum solution of Maxwell's equations and might be seen as a model for a focused laser pulse. As a special case of multidimensional fields we also considered transversal field dependences, which do not affect the exponent of the pair production rate. We have also seen that the difference between scalar and spinor QED is a trivial factor of two in the case of a one dimensional inhomogeneity and the effect of an additional magnetic field in the scalar and spinor cases.

Finally, we focused on the *dynamically assisted* Sauter-Schwinger effect, the exponential enhancement from superimposing a strong static field by a weak time dependent pulse. This setup has many interesting properties, especially concerning the dependence on the weak field's temporal profile. A lot of intuition can be gained from the worldline instanton approach here, which provides a geometrical picture of dynamical assistance – additional time dependent fields add “barriers” that reflect the instanton trajectory. The critical threshold for assistance occurs when the barriers move close enough to the origin to touch the instanton.

First, we quickly recalled the result for a constant homogeneous background field with a weak, Sauter-type pulse, which follows immediately using the formalism developed for one-dimensional field inhomogeneities and the geometrical approach. We then extended it to spatially inhomogeneous background fields, which lower the critical threshold. This is again intuitively clear, we know that inhomogeneity leads to larger instantons, so they first hit the barriers for smaller assisting frequencies. We then investigated how different temporal profiles for the assisting field affect pair production. We found that the strong qualitative difference between, for example, a Sauter pulse and a Gaussian can be traced to the different analytic structure after rotating to imaginary times. We have also seen how these differences manifest themselves in a perturbative approach, where we used the Riccati equation to check analytical estimates of the momentum spectrum of produced pairs. Finally, we have found discrete worldline instantons in the superposition of a strong, static field and a propagating plane wave.

This thesis can only be seen as a starting point, there are still a lot of things to

be done. The discrete worldline instanton method, and especially the Mathematica implementation, is very general and can now easily be used for further investigations. These could be motivated by experimental considerations, for example realistic background fields that model experimentally realizable laser pulses. On the other hand it might be possible to investigate situations that yield interesting instantons. In some fields instantons can be found that are not continuously connected to the circular constant field limit, but diverge for small  $\gamma$  instead. We would expect the instanton connected to the circular one to be dominant, but it's not clear if other instantons might become important in some regime. Furthermore, multiple instantons can produce interference effects, it would be particularly interesting to see how collections of instantons with nontrivial topology interact.

Hopefully, the exposition in this thesis and the description of the algorithms will be of some use in future endeavors to shed light on the Sauter-Schwinger effect.



**Part IV.**

**Appendix**



# A

## Source code listings

*This chapter includes annotated source code listings of the programs developed for, and used in the preparation of this thesis.*

### A.1. Riccati equation

The code to find pair production probabilities using the Riccati equation consists of multiple parts,

1. a Mathematica package to generate C sources for a particular field profile,
2. a C driver file that numerically integrates the Riccati equation for this field,
3. a Python script to simplify calling the compiled executables.

The Mathematica package `Riccati`` implements the Riccati ODE as defined in Section 3.3 and uses functions of the `MathTIDES`` package to generate C code that integrates the ODE using the Taylor method.

#### `Riccati.m`

```

1 Numerical integration of the Riccati equation
2 mathTIDESVersion$="2.00"
3 BeginPackage["Riccati`"]
4 Get["MathTIDES`"]
5
6 Public exports
7
8 Usage messages
9 InSubDir::usage = "InSubDir[dir, e] runs expression e after changing to (and creating if
  ↳ necessary) the subdirectory 'dir'."
10 WriteRiccatiFiles::usage = "WriteRiccatiFiles[name, f, params] creates the C files for field
  ↳ described by f with params."
11 GenDriver::usage = "Option to WriteRiccatiFiles that decides whether to include an example
  ↳ driver in the output."
12 CompileRiccati::usage = "Helper function to call the C compiler with necessary arguments."
13
14 Private implementation
15 Begin["`Private`"]
16 InSubDir[dir_, exp_] := CheckAbort[Block[{ret},
17   If[!DirectoryQ[dir], CreateDirectory[dir]];
18   SetDirectory[dir];
19   ret=exp;
20   ResetDirectory[];
21   ret

```

```

22  ],
23  ResetDirectory[];
24  ];
25  SetAttributes[InSubDir, HoldAll];
26
27  Definitions to use in the Riccati equation
28  Ω[f_,p_,γ_][t_] = Sqrt[1 + (p + f[γ t]/γ)^2];
29  Ξ[f_,p_,γ_][t_] = f'[γ t]/(1 + (p + f[γ t]/γ)^2);
30
31  Define ODE to use with TIDES
32  riccatiODE[f_, params_:{}] := FirstOrderODE[{
33  1/2 Ξ[f,p,γ][t] (Cos[2/e Φ] +ComplexExpand@Re[(reR+I imR)^2 Exp[-2I/e Φ]]),
34  1/2 Ξ[f,p,γ][t] (Sin[2/e Φ] +ComplexExpand@Im[(reR+I imR)^2 Exp[-2I/e Φ]]),
35  Ω[f,p,γ][t]
36  },t,{reR,imR,Φ},Join[{e,γ,p},params]]
37
38  Special version of the ODE that finds f[γ t] by integrating
39  riccatiODEintf[df_, params_:{}] := FirstOrderODE[{
40  1/2 Ξ[f,p,γ][t] (Cos[2/e Φ] +ComplexExpand@Re[(reR+I imR)^2 Exp[-2I/e Φ]]),
41  1/2 Ξ[f,p,γ][t] (Sin[2/e Φ] +ComplexExpand@Im[(reR+I imR)^2 Exp[-2I/e Φ]]),
42  Ω[f,p,γ][t],
43  γ df[γ t]
44  }/.{f'[e_]→df[e],f[_]→f},t,{reR,imR,Φ,f},Join[{e,γ,p},params]]
45
46  Command to compile TIDES code
47  compileString=StringTemplate["gcc -o `1` -I$HOME/include/ -L$HOME/lib/ `1`.c `1`_fun.c -lTIDES
48  → -lm -lmpfr -lgmp"];
49  CompileRiccati=If[#!= 0,$Failed,Null]&@*Run@*compileString;
50
51  Merge options with defaults
52  mergeOpts[opt1_,opt2_] := Sequence@@Normal@Merge[{opt1, opt2},First]
53
54  Generate the necessary files
55  WriteRiccatiFiles[name_String, f_, params_:{}, opts:OptionsPattern[]]:= TSMCodeFiles[
56  riccatiODE[f, params],
57  name, Precision → Multiple, If[OptionValue[GenDriver], Driver → True, Driver → False]]
58  Options[WriteRiccatiFiles] = {GenDriver → False}
59
60  Epilog
61  End[]
62  EndPackage[]

```

After creating the necessary files using the `Riccati`` package we have to supply some details to the generated driver file. Below is an example of a driver file for the superposition of two Sauter pulses with field parameters passed on the command line.

### `assisted_sauter.c`

```

1  #include "mpfr.h"
2  #include "mp_tides.h"
3  #include "assisted_sauter_fun.h"
4
5  int main(int argc, char* argv[]) {
6
7      int i;
8
9      /* --- CHECK PARAMETERS ----- */
10     if(argc < 8) {

```

```

11     fprintf(stderr, "Usage: %s E Gamma eps gamma p tmax prec\n", argv[0]);
12     return -1;
13 }
14
15 int prec = atoi(argv[7]);
16
17 char acc[16];
18 sprintf(acc, "1.e-%i\n", prec-1);
19
20
21 /* --- SET PRECISION ----- */
22 set_precision_digits(prec);
23
24 /* --- PARAMETERS ----- */
25 int npar = 5;
26 mpfr_t p[npar];
27 for(i=0; i<npar; i++) mpfr_init2(p[i], TIDES_PREC);
28 mpfr_set_str(p[0], argv[1], 10, TIDES_RND); // E
29 mpfr_set_str(p[1], argv[4], 10, TIDES_RND); // gamma
30 mpfr_set_str(p[2], argv[5], 10, TIDES_RND); // p
31 mpfr_set_str(p[3], argv[3], 10, TIDES_RND); // eps
32 mpfr_set_str(p[4], argv[2], 10, TIDES_RND); // Gamma
33
34 // Divide Gamma by gamma
35 mpfr_div(p[4], p[4], p[1], TIDES_RND);
36
37 /* --- VARIABLES ----- */
38 int nvar = 3;
39 mpfr_t v[nvar];
40 for(i=0; i<nvar; i++) mpfr_init2(v[i], TIDES_PREC);
41 mpfr_set_str(v[0], "0", 10, TIDES_RND);
42 mpfr_set_str(v[1], "0", 10, TIDES_RND);
43 mpfr_set_str(v[2], "0", 10, TIDES_RND);
44
45 /* --- NUMBER OF FUNCTIONS ----- */
46 int nfun = 0;
47
48 /* --- TOLERANCES ----- */
49 mpfr_t tolrel, tolabs;
50 mpfr_init2(tolrel, TIDES_PREC);
51 mpfr_init2(tolabs, TIDES_PREC);
52 mpfr_set_str(tolrel, acc, 10, TIDES_RND);
53 mpfr_set_str(tolabs, acc, 10, TIDES_RND);
54
55 /* --- INTEGRATION POINTS ----- */
56 mpfr_t tini, dt, tend;
57 mpfr_init2(tini, TIDES_PREC);
58 mpfr_init2(dt, TIDES_PREC);
59 mpfr_init2(tend, TIDES_PREC);
60 mpfr_set_str(tend, argv[6], 10, TIDES_RND);
61 mpfr_neg(tini, tend, TIDES_RND);
62 int nipt = 1;
63 mpfr_set(dt, tend, TIDES_RND);
64 mpfr_sub(dt, dt, tini, TIDES_RND);
65 mpfr_div_si(dt, dt, nipt, TIDES_RND);
66
67 /* --- INTEGRATOR ----- */
68 mp_tides_delta(assisted_sauter_fun, NULL, nvar, npar, nfun, v, p, tini, dt, nipt, tolrel,
69 ↪ tolabs, NULL, NULL);

```

```

69
70 /* --- PAIR PRODUCTION RATE ----- */
71     mpfr_sqr(v[0], v[0], TIDES_RND);
72     mpfr_sqr(v[1], v[1], TIDES_RND);
73     mpfr_add(v[0], v[0], v[1], TIDES_RND);
74
75     mpfr_printf("%Re\n", v[0]);
76
77 /* --- END ----- */
78     return 0;
79 }

```

To keep track of the compiled executables we use a small python script that includes a list of fields and the number of their physical parameters. Then all prepared fields can be called using a single script instead of having to directly execute the C binaries.

### riccati.py

```

1  #!/usr/bin/env python2
2  from __future__ import print_function
3
4  import sys
5  import os
6
7  def eprint(*args, **kwargs):
8      print(*args, file=sys.stderr, **kwargs)
9
10 import argparse
11 import subprocess
12
13 fields = {
14     'sauter': ['single/sauter', 1],
15     'assisted_sauter': ['assisted/sauter', 3],
16     '...': '...'
17 }
18
19 parser = argparse.ArgumentParser(description='Run Riccati equation.')
20 parser.add_argument('field', help='Identifier of the field to run',
21                    choices=[k for k in fields])
22 parser.add_argument('-E', help='Reference field strength', required=True)
23 parser.add_argument('params', help='Field parameters (depend on chosen field, Gamma eps gamma
24     ↪ for assisted types)', nargs='*')
25 parser.add_argument('-T', '--Tmax', help='Time period to integrate', required=True)
26 parser.add_argument('-q', '--momentum', help='Longitudinal momentum (default 0)',
27     ↪ default='0.0')
28 parser.add_argument('-p', '--precision', help='Number of digits of precision to use (default
29     ↪ 18)', default='18')
30
31 args = parser.parse_args()
32
33 if len(args.params) != fields[args.field][1]:
34     eprint('Exactly %d parameter(s) needed for field "%s"' % (fields[args.field][1],
35     ↪ args.field))
36     sys.exit(-1)
37
38 path = os.path.join(os.path.dirname(os.path.realpath(__file__)), fields[args.field][0])
39
40 subprocess.call([path, args.E] + args.params + [args.momentum, args.Tmax, args.precision])

```

## A.2. Discrete worldline instantons

Mathematica uses special symbols to encode some functionality, which makes the following code rather expressive. For example, this allows us to directly use Greek letters and operators as in  $\delta \neq \lambda \geq 0$  as opposed to `delta != lambda >= 0`. Some notation that may not be immediately obvious, especially in this typeface, are:

<code>a → b</code>	replacement rule	<code>a-&gt;b</code>
<code>x ⇒ f(x)</code>	anonymous function	<code>Function[{x}, f(x)]</code>
<code>z†</code>	complex conjugation	<code>Conjugate[z]</code>
<code>ı</code>	imaginary unit	<code>I</code>
<code>l[i]</code>	list indexing	<code>l[[i]]</code>

The listing that begins below is the Mathematica package `Instantons``. The first part defines all the functions and options that are visible when the package is imported, while the rest defines the implementation. As a guideline, all identifiers that begin with a capital letter are exported, the others are local helper functions only.

### `Instantons.m`

```

1  Instanton finding, action and prefactor evaluation
2  BeginPackage["Instantons`"]
3
4  Public exports
5
6  Usage messages
7  Action::usage = "Action[jA, X] gives the action of Trajectory X in the field potential jA."
8  Circular::usage = "Circular[n, d] generates a circular trajectory in d dimensions with n
   → points."
9  FindInstanton::usage = "FindInstanton[jA, X0, Fixed→{μ, ...}] tries to find an instanton close
   → to initial guess X0, optionally keeping coordinates μ... of one point fixed."
10 Fixed::usage = "Option to FindInstanton to specify which coordinates are to be held fixed
   → (default: Automatic)."
11 FieldTensor::usage = "FieldTensor[jA] prints (j times) the Euclidean field strength tensor
   → corresponding to jA."
12 Enhance::usage = "Enhance[jA, X0, n, Fixed→{μ, ...}] interpolates X0 and uses that as starting
   → point to find an instanton."
13 ActionHessian::usage = "ActionHessian[jA, X, Fixed→{μ, ...}] gives the Hessian for the given
   → field at X."
14 Fluctuation::usage = "Fluctuation[jA, X, E, Fixed→{μ, ...}] gives the fluctuation prefactor for
   → the given field at X."
15 Spinfactor::usage = "Spinfactor[jA, X] gives the Polyakov spin factor in the given Field."
16 Spinfactorτ::usage = "Spinfactorτ[jA, X] gives all intermediates of the integration."
17 Spinσ::usage = "The tensor σ^μν."
18 Prefactor::usage = "Prefactor[jA, X, E, Fixed→{μ, ...}, Spin→(True|False)] gives the complete
   → prefactor for spinor/scalar QED."
19 EffectiveAction::usage = "EffectiveAction[jA, X, E, Fixed→{μ, ...}, Spin→(True|False)] gives
   → the full effective Action."
20 Spin::usage = "Option to PairProduction to switch between spinor and scalar QED."
21 NaturalContinuation::usage = "NaturalContinuation[jA, {λ, λ0, λ1, Δλ}, X0, Fixed→{...}] varies a
   → parameter λ and finds the instanton at each step."
22 DavidenkoDerivative::usage = "DavidenkoDerivative[jA, {λ, λ0}, X, Fixed→{μ, ...}] gives the
   → derivative of an instanton by a parameter."

```

```

23 DavidenkoPredict::usage = "DavidenkoPredict[jA, λ, dx, {λ0, X}, options] predicts the next
  → instanton that is at most dx away."
24 DavidenkoContinuation::usage = "DavidenkoContinuation[A, {λ, λ0, λmax, m:1}, dx, X0, options]
  → varies λ to keep fixed step dx (with m intermediate derivatives)."
25 MaxStep::usage = "Option to DavidenkoPredict that determines the maximum value Δλ to step the
  → parameter (default: ∞)."
26 MinStep::usage = "Option to DavidenkoPredict, abort if suggested step length is below this
  → value (default: 0)"
27 StepScale::usage = "Option to DavidenkoPredict that sets a factor by which the steplength is
  → scaled (default: 1)"
28 InstantonPlot3D::usage = ""
29 InstantonModel::usage = ""
30 instMon::usage= ""
31 dA::usage=""
32
33 Error messages
34 Spinfactor::"dim" = "dim(A)≠4, Spin factor ignored";
35 DavidenkoContinuation::FindInstanton = "Finding an Instanton at `1`=`2` produced a message,
  → aborting continuation."
36 DavidenkoContinuation::StepSize = "Step size at `1`=`2` is smaller than MinStep (`3` < `4`),
  → aborting continuation."
37
38 Private implementation
39 Begin["`Private`"]
40
41 Helper functions
42
43 Give the dimensionality of field A (Quiet is necessary because we do not know the number of
  → dimensions yet and A will complain).
44 dimOf[A_Function]:= Quiet@Length@A[{}]
45
46 Generate a list of variables (for analytical derivatives)
47 makeVars[d_, sym_:"x$"]:= Table[Symbol[sym <> ToString[i]], {i, d}]
48
49 The field strength tensor (as a function)
50 F[A_]:= Module[{f, vars = makeVars[dimOf[A]]},
51   f = Function@@{vars, (#^t-#)&@Outer[D, A[vars], vars]};
52   f@@#&
53 ]
54 FieldTensor[A_]:= F[A][makeVars[dimOf[A],"x"]]
55
56 Generate a circular Instanton with n points in d dimensions (between first and last dimension)
57 Circular[n_, d_Integer?(# ≥ 2&)]:= Table[
58   {Cos[2.π θ],
59     Sequence@@ConstantArray[0, d-2],
60     Sin[2.π θ]}, {θ, 0, 1-1/n, 1/n}]
61
62 Analytically take the derivative of the field
63 dA[A_]:= Module[{f, d = dimOf[A], vs},
64   vs = makeVars[d];
65   f = Function@@{vs, D[A[vs], {vs}]^t};
66   f@@#&
67 ]
68
69 Find the velocity a along the trajectory
70 calcA[X_?MatrixQ]:= Sqrt[Length[X]] Sqrt[#.#&@Flatten[X - RotateRight[X]]]
71
72 Action, root function and root finding
73

```

```

74 Evaluate the action functional for a given trajectory in the field A
75 Action[A_Function, X_?MatrixQ]:=
76   calcA[X] + Flatten[(A/@X + RotateRight[A/@X])/2].Flatten[X - RotateRight[X]]
77
78 Local average velocity, helps convergence in root finding a lot.
79 locA[X_?MatrixQ]:= 1/2 Sqrt[#.#]&/@(RotateLeft[X] - RotateRight[X])
80
81 Root function, any X so that rootFun[A, X] == 0 is a discretized instanton.
82 rootFun[A_Function, X_?MatrixQ]:=
83   (2X - RotateLeft[X] - RotateRight[X]) +
84   locA[X](- ((RotateLeft[A/@X] - RotateRight[A/@X])/2)
85     + 1/2 MapThread[Dot, {dA[A]/@X, RotateLeft[X] - RotateRight[X]}]
86   )
87
88 Wrapper that keeps a list of coordinates fixed.
89 rootFunFixed[A_Function, X_?MatrixQ, X0_?MatrixQ, fix:{_Integer...}] :=
90   Fold[{l, μ}=>MapAt[X[1, \[Mu]] - X0[1, \[Mu]]&, l, {1, μ}],
91     rootFun[A, X],
92     fix]
93
94 Sparsity pattern of the Jacobian for above root Function (only works because of the locA
  ↳ cheat).
95 jacSparsity[n_,d_]:= SparseArray[{
96   Band[{1, 1}] → ConstantArray[_ , {n,d,d}],
97   Band[{1, 1+d}] → ConstantArray[_ , {n-1, d, d}],
98   Band[{1+d, 1}] → ConstantArray[_ , {n-1, d, d}],
99   Band[{1, n d+1-d}] → ConstantArray[_ , {d, d}],
100  Band[{n d+1-d, 1}] → ConstantArray[_ , {d, d}]
101 ], {n d, n d}]
102
103 Find an instanton close to initial guess X0 in field A. The option Fixed specifies a list of
  ↳ coordinates which should be held fixed, or the value Automatic which checks the field
  ↳ tensor for dependence on coordinates. If any coordinate is held fixed, Center means the
  ↳ average position is translated in the end.
104 Options[FindInstanton] = Join[
105   {Fixed → Automatic, Center → True},
106   Options[FindRoot]
107 ]
108 autoFixed[A_]:= Block[{d = dimOf[A], v},
109   v = makeVars[d];
110   MapIndexed[
111     If[#1 === ConstantArray[0, {d, d}], First[#2], Nothing]&,
112     Transpose[D[F[A][v], {v}], {3, 2, 1}]
113   ]
114 ]
115 centerInstanton[fix_, X_]:= Block[{m = Total[UnitVector[Length@First@X, #]&/@fix]},
116   Transpose[MapThread[#1 - #2 Mean[#1]&, {Transpose@X, m}]]
117 ]
118 centerInstanton[{}, X_]:= X
119 FindInstanton[A_Function, X0_?(MatrixQ[#, NumericQ]&), opts:OptionsPattern[]]:=
120   Block[{Xs},
121     Xs = X/.FindRoot[
122       rootFunFixed[A, X, X0, OptionValue[Fixed]/.Automatic → autoFixed[A]],
123       {X, X0}, Jacobian → {"FiniteDifference", Sparse → jacSparsity[Length[X0], dimOf[A]]},
124       AccuracyGoal → 6, PrecisionGoal → Infinity, StepMonitor :> (instMon=X;);
125     If[OptionValue[Center],
126       centerInstanton[OptionValue[Fixed]/.Automatic → autoFixed[A], Xs],
127     Xs]
128 ]

```

```

129
130 Number enhancement
131
132 Interpolate and resample trajectory
133 enhanceTraj[X_?MatrixQ, n_Integer]:= Transpose[
134   Table[Interpolation[Transpose[{Range[0, 1, 1./Length[X]], #}]]][u],
135   {u, 0, 1-1/n, 1/n}]&
136   /@Transpose@Append[#, First[#]]&@X
137 ]
138
139 Find instanton using enhanced trajectory
140 Enhance[A_Function, X0_?(MatrixQ[#, NumericQ]&), n_Integer, opts:OptionsPattern[]]:=
141   FindInstanton[A, enhanceTraj[X0, n], opts]
142
143 Hessian and Prefactor
144
145 Analytical second derivative of the potential
146 ddA[A_]:= Module[{f, d = dimOf[A], vs},
147   vs = makeVars[d];
148   f = Function@@{vs, Transpose[D[D[A[vs]], {vs}], {vs}], {3, 2, 1}}];
149   f@@#&
150 ]
151
152 Hessian of a
153 dda[Y_]:= Block[{d = Length@First@Y, n = Length@Y, M, X = Flatten[Y], a = calcA[Y]},
154   M = -#[-1] + 2 #[0] - #[1]&[RotateRight[IdentityMatrix[d n], d #]&];
155   -(n^2/a^3) Outer[Times, M.X, M.X] + n/a M
156 ]
157
158 Hessian of the remaining action
159 ddr[A_, Y_]:= Block[{d = Length@First@Y, n = Length@Y, X = Flatten[Y], d1, d2},
160   d1 = (# - RotateLeft[Transpose/@#])&[dA[A]/@Y];
161   SparseArray[Band[{1,1}] → MapThread[Dot, {ddA[A]/@Y, Y-RotateRight[Y]}]]+
162   Symmetrize[SparseArray[{
163     Band[{1, 1+d}] → Most[d1],
164     Band[{1+(n-1)d, 1}] → Last[d1]
165   }], Symmetric]
166 ]
167
168 Additional Faddeev-Popov terms to the hessian to fix zero modes
169 fpt[Y_]:= Block[{a = calcA[Y]},
170   (8π)/(a^4) Outer[Times, #, #]&[Flatten[RotateRight[Y] - Y]]]
171 fpx[n_, d_][μ_]:= KroneckerProduct[
172   ConstantArray[(2.π)/(n)^2, {n, n}],
173   DiagonalMatrix@UnitVector[d, μ]
174 ]
175
176 Function to evaluate the Hessian, optionally adding F.P.-terms to hold coordinates fixed
177 ActionHessian[A_, Y_, OptionsPattern[]]:=
178   ddr[A,Y] + dda[Y] + fpt[Y] +
179   Total[fpx[Length[Y], Length[First[Y]]]/@{OptionValue[Fixed]/.Automatic → autoFixed[A]}]
180 Options[ActionHessian] = {Fixed → Automatic}
181
182 Use Hessian to evaluate the prefactor
183 Fluctuation[A_, X_, e_, opts:OptionsPattern[]]:=
184   Block[{n = Length[X], d = Length[First[X]], a = calcA[X]},
185     (1/Sqrt[2 π a/e])^(4-d) e^(Length[OptionValue[Fixed]/.Automatic → autoFixed[A]])/2)
186     Sqrt[2 π/a] (n/a)^(n/2 d) Sqrt[1/Det@ActionHessian[A, X, opts]]
187 ]

```

```

188 Options[Fluctuation] = Options[ActionHessian]
189
190 Spin factor
191
192 Vector of  $\gamma$  matrices
193  $\gamma$  = Table[
194   KroneckerProduct[Reverse@DiagonalMatrix[{-1, 1}], I PauliMatrix[k]], {k, 3}
195 ]~Append~KroneckerProduct[Reverse@IdentityMatrix[2], IdentityMatrix[2]];
196
197 Spin generators
198  $\text{Spin}\sigma = -1/2$  (Outer[Dot,  $\gamma$ ,  $\gamma$ , 1] - Transpose[Outer[Dot,  $\gamma$ ,  $\gamma$ , 1], {2, 1}]);
199
200 Spin factor  $\Phi$ 
201 Spinfactor[A_, X_] := Tr@Apply[Dot,
202   (1.0 IdentityMatrix[4] + calcA[X]/2 TensorContract[
203     Spin $\sigma$   $\otimes$  F[A][#], {{1, 5}, {2, 6}}
204   ]/(2 Length[X]))&/@X
205 ];dimOf[A] == 4
206 Spinfactor $\tau$ [A_, X_] := Tr/@FoldList[Dot,
207   IdentityMatrix[4],
208   (1.0 IdentityMatrix[4] + calcA[X]/2 TensorContract[
209     Spin $\sigma$   $\otimes$  F[A][#], {{1, 5}, {2, 6}}
210   ]/(2 Length[X]))&/@X
211 ];dimOf[A] == 4
212 Spinfactor[_, _] := (Message[Spinfactor::"dim"]; 1)
213 Spinfactor $\tau$ [_, _] := (Message[Spinfactor::"dim"]; 1)
214
215 Combine the fluctuation- and spinfactor into the overall prefactor
216 Prefactor[A_, X_, e_, opts:OptionsPattern[]]:=
217   If[OptionValue[Spin], -(1/2) Spinfactor[A,X], 1] Fluctuation[A, X, e, FilterRules[{opts},
218      $\leftarrow$  Options[Fluctuation]]]
219
220 Options[Prefactor] = Append[Options[Fluctuation], Spin  $\rightarrow$  True]
221
222 All combined
223
224 Combine action, prefactor and spin factor
225 EffectiveAction[A_Function, X_List, e_, opts:OptionsPattern[]]:=
226   Prefactor[A, X, e, opts] Exp[-(1/e)Action[A,X]]
227 Options[EffectiveAction] = Options[Prefactor]
228
229 Numerical continuation
230
231 Natural parameter continuation in a parameter  $\lambda$  with different method signatures
232 Options[NaturalContinuation] = Options[FindInstanton];
233 NaturalContinuation[A_Function, { $\lambda$ _Symbol,  $\lambda$ s_List}, X0_, opts:OptionsPattern[]]:= Block[{m},
234   Monitor[Transpose[{ $\lambda$ s,
235     Rest@FoldList[(m = #2; FindInstanton[A/. $\lambda$   $\rightarrow$  #2, #1, opts])&, X0,  $\lambda$ s]
236   }], m]
237 ]
238 NaturalContinuation[A_Function, { $\lambda$ _Symbol,  $\lambda$ 0_,  $\lambda$ 1_?NumericQ,  $\Delta\lambda$ ?NumericQ}, X0_,
239    $\leftarrow$  opts:OptionsPattern[]]:=
240   NaturalContinuation[A, { $\lambda$ , Range[ $\lambda$ 0,  $\lambda$ 1,  $\Delta\lambda$ ]}, X0, opts]
241 NaturalContinuation[A_Function, { $\lambda$ _Symbol,  $\lambda$ 0_, s:{_,_}..}, X0_, opts:OptionsPattern[]]:=
242   NaturalContinuation[A, { $\lambda$ ,
243     Join@@(Range@@Rest[#]&/@FoldList[
244       Join[{#1[1], #1[3] + #2[2]}, #2]&,
245       Join[{ $\lambda$ ,  $\lambda$ 0}, First[{s}], Rest[{s}]
246     ])]
247   }, X0, opts]

```

```

245 NaturalContinuation[A_Function, {λ_Symbol, λ0_, λ1_, Δλ_}, {η_Symbol, η0_, η1_, Δη_}, X0_,
  ↳ opts:OptionsPattern[]]:=
246   Transpose[{
247     Flatten[Table[{λ, η}, {λ, λ0, λ1, Δλ}, {η, η0, η1, Δη}],1],
248     Flatten[
249       Map[res⇒Rest@FoldList[
250         FindInstanton[A/.{λ → res[1], η → #2}, #1, opts]&,
251         res[2], Range[η0,η1,Δη]
252       ], Transpose[{Range[λ0, λ1, Δλ],
253         Rest@FoldList[FindInstanton[A/.{λ → #2, η → η0}, #1, opts]&,
254         X0, Range[λ0, λ1, Δλ]]}]
255     ], 1]
256   }]
257
258 Continuation by Davidenko's ODE
259
260 Partial derivative of the root function by a parameter λ (at a specific value λ0)
261 dλf[A_, {λ_Symbol, λ0_}, X_] := Block[{dλA = Quiet[D[A,λ]/.λ → λ0, {Part::partw}]},
262   (- ((RotateLeft[dλA/@X] - RotateRight[dλA/@X])/2
263     + 1/2 MapThread[Dot, {dA[dλA]/@X, RotateLeft[X] - RotateRight[X]}]
264   )
265 ]
266
267 Given an instanton, find the derivative of the instanton by a parameter λ (at a specific value
  ↳ λ0)
268 DavidenkoDerivative[A_, {λ_Symbol, λ0_}, X_, opts:OptionsPattern[]]:=
269   Partition[
270     LinearSolve[ActionHessian[A/.λ → λ0, X, opts],
271     -Flatten@dλf[A, {λ, λ0}, X]
272   ], Length@First@X
273 ]
274 Options[DavidenkoDerivative] = Options[ActionHessian];
275
276 Predict an instanton that is at most dx away (effectively giving adaptive step width control)
277 DavidenkoPredict[A_, λ_Symbol, dx_, {λ0_, X_}, opts:OptionsPattern[]]:= Block[{dx, dλ},
278   dx = If[OptionValue[Center],
279     centerInstanton[OptionValue[Fixed]/.Automatic → autoFixed[A], #],
280     #
281   ]&[DavidenkoDerivative[A, {λ, λ0}, X,
282     FilterRules[{opts},Options[DavidenkoDerivative]]
283   ]];
284   dλ = Min[dx/Sqrt[Chop[#†.#&@Flatten[dx] + 1]], OptionValue[MaxStep]];
285   If[dλ < OptionValue[MinStep],
286     Message[DavidenkoContinuation::StepSize, λ, λ0, dλ, OptionValue[MinStep]]; $Failed,
287     {λ0 + dλ, X + OptionValue[StepScale] dλ dx}]
288 ]
289 Options[DavidenkoPredict] = Join[Options[DavidenkoDerivative], {Fixed → Automatic, MaxStep → ∞,
  ↳ MinStep → 0, StepScale → 1, Center → True}];
290
291 Perform continuation using n*m steps of Davidenko prediction, adding a root finding correction
  ↳ every m steps.
292 davidenkoPredictions[A_, λ_Symbol, dx_, {λ0_, X0_}, m_, opts:OptionsPattern[]]:=
293   Rest@NestWhileList[DavidenkoPredict[A, λ, dx, #, opts]&, {λ0, X0}, !FailureQ[#]&, 1, m]
294 correct[A_, λ_, opts:OptionsPattern[]][{λ0_, X0_}] := {λ0, FindInstanton[A/.λ → λ0, X0, opts]}
295 correct[_, _, OptionsPattern[]][e_?FailureQ] = e
296 Options[correct] = Options[FindInstanton];
297 DavidenkoContinuation[A_, {λ_, λ0_, λmax_, m_:1}, dx_, X0_, opts:OptionsPattern[]]:=
  ↳ Block[{mon}, Monitor[
298   NestWhileList[Check[mon = #[1];

```

```

299     correct[A, λ, FilterRules[{opts}, Options[FindInstanton]]
300     ]@Last@davidenkoPredictions[A, λ, dx/m, #, m, FilterRules[{opts},
↪ Options[DavidenkoPredict]]],
301     Message[DavidenkoContinuation::FindInstanton, λ, #[1]]; $Failed, {FindRoot::cvmit,
↪ FindRoot::lstol}&,
302     correct[A, λ, FilterRules[{opts}, Options[FindInstanton]]][{λ0, X0}],
303     ((!FailureQ[#]) && #[1] ≤ λmax)&, 1, ∞],
304 mon]]
305 Options[DavidenkoContinuation] = Join[Options[DavidenkoPredict], Options[FindInstanton]];
306

```

## Visualization

```

307 InstantonPlot3D[A_, λX_, opts:OptionsPattern[]]:=Block[
308     {v=(sol⇒(Append[#, sol[1]]&/@sol[2]))/@λX, ni, nj, act},
309     act=Rescale[Action[A#[1]], #[2]]&/@λX;
310     ni=Length[v];
311     nj=Length[First[v]];
312     Graphics3D[{Opacity[0.8],
313         Flatten[Table[{ColorData["ThermometerColors"][act[i]], Polygon[
314             {v[i, j], v[i, Mod[j+1, nj, 1]], v[i+1, Mod[j+1, nj, 1]], v[i+1, j]}],
315             {i, ni-1}, {j, nj}], 1]
316         }, opts]
317     ]
318 ]
319 Options[InstantonPlot3D] = Options[Graphics3D]
320 InstantonModel[v_]:=Block[{ni, nj},
321     ni=Length[v];
322     nj=Length[First[v]];
323     Flatten[Table[{Polygon[
324         {v[i, j], v[i, Mod[j+1, nj, 1]], v[i+1, Mod[j+1, nj, 1]], v[i+1, j]}],
325         {i, ni-1}, {j, nj}], 1]
326     ]
327 ]
328 Epilog
329 End[]
330 EndPackage[]

```



## Bibliography

- [Aba+12] Alberto Abad, Roberto Barrio, Fernando Blesa, and Marcos Rodríguez. “TIDES, a Taylor Series Integrator for Differential Equations.” In: *ACM Transactions on Mathematical Software* 39.1 (2012), pp. 1–28.
- [ABD11] Alberto Abad, Roberto Barrio, and Ángeles Dena. “Computing periodic orbits with arbitrary precision.” In: *Physical Review E* 84.1 (July 2011).
- [AAM82] Ian K. Affleck, Orlando Alvarez, and Nicholas S. Manton. “Pair production at strong coupling in weak external fields.” In: *Nuclear Physics B* 197.3 (1982), pp. 509–519.
- [AG03] Eugene L. Allgower and Kurt Georg. *Introduction to Numerical Continuation Methods*. Society for Industrial and Applied Mathematics, 2003.
- [And32] Carl D. Anderson. “The apparent existence of easily deflectable positives.” In: *Science* 76.1967 (1932), pp. 238–239.
- [And33] Carl D. Anderson. “The positive electron.” In: *Physical Review* 43.6 (1933), pp. 491–494.
- [Bas86] Ian M. Bassett. “Limit to Concentration by Focusing.” In: *Optica Acta: International Journal of Optics* 33.3 (Mar. 1986), pp. 279–286.
- [BP77] Aleksandr A. Belavin and Aleksandr M. Polyakov. “Quantum fluctuations of pseudoparticles.” In: *Nuclear Physics B* 123.3 (1977), pp. 429–444.
- [Bel+75] Aleksandr A. Belavin, Aleksandr M. Polyakov, Albert S. Schwartz, and Yu S. Tyupkin. “Pseudoparticle solutions of the Yang-Mills equations.” In: *Physics Letters B* 59.1 (1975), pp. 85–87.
- [BO99] C.M. Bender and S.A. Orszag. *Advanced Mathematical Methods for Scientists and Engineers I: Asymptotic Methods and Perturbation Theory*. Advanced Mathematical Methods for Scientists and Engineers. Springer, 1999.
- [Ber66] Felix Berezin. *The Method of Second Quantization*. Vol. 24. Monographs and Textbooks in Pure and Applied Physics. Academic Press, 1966.
- [Boh21] Nils Bohr. “Atomic Structure.” In: *Nature* 107.2682 (Mar. 1921), pp. 104–107.
- [Boh13] Nils Bohr. “On the constitution of atoms and molecules.” In: *The London, Edinburgh, and Dublin Philosophical Magazine and Journal of Science* 26.155 (1913), pp. 857–875.

- [BHJ26] Max Born, Werner Heisenberg, and Pascual Jordan. “Zur Quantenmechanik. II.” In: *Zeitschrift für Physik* 35.8-9 (1926), pp. 557–615.
- [BJ25] Max Born and Pascual Jordan. “Zur Quantenmechanik.” In: *Zeitschrift für Physik* 34.1 (Dec. 1925), pp. 858–888.
- [BI70] Édouard Brézin and Claude Itzykson. “Pair Production in Vacuum by an Alternating Field.” In: *Physical Review D* 2.7 (1970).
- [CM08] Thomas D. Cohen and David A. McGady. “The Schwinger mechanism revisited.” In: *Physical Review D* 78 (2008), p. 036008.
- [Dav53] D. F. Davidenko. “On a new method of numerically integrating a system of nonlinear equations (Russian).” In: *Doklady Akademii Nauk SSSR* 88 (1953), pp. 601–604.
- [Den+12] Ángeles Dena, Marcos Rodríguez, Sergio Serrano, and Roberto Barrio. “High-Precision Continuation of Periodic Orbits.” In: *Abstract and Applied Analysis* 2012 (2012), pp. 1–12.
- [Dir30a] Paul A. M. Dirac. “A Theory of Electrons and Protons.” In: *Proceedings of the Royal Society A* 126.801 (Jan. 1930), pp. 360–365.
- [Dir45] Paul A. M. Dirac. “On the analogy between classical and quantum mechanics.” In: *Reviews of Modern Physics* 17.2-3 (1945), pp. 195–199.
- [Dir30b] Paul A. M. Dirac. “On the annihilation of electrons and protons.” In: *Proceedings of the Royal Society A* 26.3 (1930), pp. 361–375.
- [Dir26] Paul A. M. Dirac. “On the Theory of Quantum Mechanics.” In: *Proceedings of the Royal Society A* 112.762 (Oct. 1926), pp. 661–677.
- [Dir31] Paul A. M. Dirac. “Quantised Singularities in the Electromagnetic Field.” In: *Proceedings of the Royal Society A* 133.821 (1931).
- [Dir25] Paul A. M. Dirac. “The Fundamental Equations of Quantum Mechanics.” In: *Proceedings of the Royal Society A* 109.752 (Dec. 1925), pp. 642–653.
- [Dir33] Paul A. M. Dirac. “The Lagrangian in Quantum Mechanics.” In: *Physikalische Zeitschrift der Sowjetunion* 3.1 (1933), pp. 64–72.
- [Dir27] Paul A. M. Dirac. “The Physical Interpretation of the Quantum Dynamics.” In: *Proceedings of the Royal Society A* 113.765 (Jan. 1927), pp. 621–641.
- [Dir28] Paul A. M. Dirac. “The Quantum Theory of the Electron.” In: *Proceedings of the Royal Society A* 117.778 (1928), pp. 610–624.
- [DD11] Cesim K. Dumlu and Gerald V. Dunne. “Interference effects in Schwinger vacuum pair production for time-dependent laser pulses.” In: *Physical Review D* 83.6 (2011), pp. 1–15.
- [DGS09] Gerald V. Dunne, Holger Gies, and Ralf Schützhold. “Catalysis of Schwinger vacuum pair production.” In: *Physical Review D* 80.11 (Dec. 2009), p. 111301.
- [DS05] Gerald V. Dunne and Christian Schubert. “Worldline instantons and pair production in inhomogenous fields.” In: *Physical Review D* 72.10 (Nov. 2005), p. 105004.

- [DW06] Gerald V. Dunne and Qing-hai Wang. “Multidimensional worldline instantons.” In: *Physical Review D* 74.6 (Sept. 2006), p. 065015.
- [Dun+06] Gerald V. Dunne, Qing-hai Wang, Holger Gies, and Christian Schubert. “Worldline instantons and the fluctuation prefactor.” In: *Physical Review D* 73.6 (Mar. 2006), p. 065028.
- [Ein05] Albert Einstein. “Über einen die Erzeugung und Verwandlung des Lichtes betreffenden heuristischen Gesichtspunkt.” In: *Annalen der Physik* 322.6 (1905), pp. 132–148.
- [FP67] Ludvig D. Faddeev and Victor N. Popov. “Feynman Diagrams for the Yang-Mills Field.” In: *Physics Letters* 25B.1 (1967), pp. 29–30.
- [Fer26a] Enrico Fermi. “Sulla quantizzazione del gas perfetto monoatomico.” In: *Rendiconti Lincei* 3 (1926), pp. 145–149.
- [Fer26b] Enrico Fermi. “Zur Quantelung des idealen einatomigen Gases.” In: *Zeitschrift für Physik* 36.11-12 (Nov. 1926), pp. 902–912.
- [Fey51] Richard Feynman. “An Operator Calculus Having Applications in Quantum Electrodynamics.” In: *Physical Review* 84.1 (Oct. 1951), pp. 108–128.
- [Fey50] Richard Feynman. “Mathematical Formulation of the Quantum Theory of Electromagnetic Interaction.” In: *Physical Review* 80.3 (Nov. 1950), pp. 440–457.
- [Fey48] Richard Feynman. “Space-time approach to non-relativistic quantum mechanics.” In: *Reviews of Modern Physics* 20.2 (1948), pp. 367–387.
- [Foc37] Vladimir Fock. “Die Eigenzeit in der klassischen und in der Quantenmechanik.” In: *Physikalische Zeitschrift der Sowjetunion* 12 (1937), pp. 404–425.
- [Foc26] Vladimir Fock. “Zur Schrödingerschen Wellenmechanik.” In: *Zeitschrift für Physik* 38.3 (1926), pp. 242–250.
- [Fou+07] Laurent Fousse, Guillaume Hanrot, Vincent Lefèvre, Patrick Pélicier, and Paul Zimmermann. “MPFR.” In: *ACM Transactions on Mathematical Software* 33.2 (2007), 13–es.
- [FGL73] Harald Fritzsch, Murray Gell-Mann, and Heinrich Leutwyler. “Advantages of the color octet gluon picture.” In: *Physics Letters B* 47.4 (1973), pp. 365–368.
- [Fru28] Giuliano Frullani. “Sopra Gli Integrali Definiti.” In: *Memorie di matematica e di fisica della Società Italiana delle Scienze, Modena* (1828), pp. 448–467.
- [Gav+04] Bernard Gaveau, Eva Mihóková, Marco Roncadelli, and Lawrence S. Schulman. “Path integral in a magnetic field using the Trotter product formula.” In: *American Journal of Physics* 72.3 (Mar. 2004), pp. 385–388.
- [GY60] Israel M. Gelfand and Akiva. M. Yaglom. “Integration in Functional Spaces and its Applications in Quantum Physics.” In: *Journal of Mathematical Physics* 1.1 (1960), p. 48.

- [GS22] Walther Gerlach and Otto Stern. “Der experimentelle Nachweis der Richtungsquantelung im Magnetfeld.” In: *Zeitschrift für Physik* 9.1 (1922), pp. 349–352.
- [GL02] Holger Gies and Kurt Langfeld. “Loops and loop clouds - a numerical approach to the worldline formalism.” In: *International Journal of Modern Physics A* 17.1 (2002), pp. 966–976.
- [GLM03] Holger Gies, Kurt Langfeld, and Laurent Moyaerts. “Casimir effect on the worldline.” In: *Journal of High Energy Physics* 2003.06 (2003), pp. 018–018.
- [Gon+13] Arkady Gonoskov et al. “Probing nonperturbative QED with optimally focused laser pulses.” In: *Physical Review Letters* 111.6 (2013), pp. 1–5.
- [Gon+12] Ivan Gonoskov, Andrea Aiello, Simon Heugel, and Gerd Leuchs. “Dipole pulse theory: Maximizing the field amplitude from 4?? focused laser pulses.” In: *Physical Review A* 86.5 (2012), pp. 1–11.
- [Gor26] Walter Gordon. “Der Comptoneffekt nach der Schrödingerschen Theorie.” In: *Zeitschrift für Physik* 40.1-2 (Jan. 1926), pp. 117–133.
- [Gou25] Samuel Goudsmit. “Über die Komplexstruktur der Spektren.” In: *Zeitschrift für Physik* 32.1 (Dec. 1925), pp. 794–798.
- [Gra44] Hermann Graßmann. *Die Lineale Ausdehnungslehre – ein neuer Zweig der Mathematik*. Otto Wigand, 1844.
- [Heb11] Florian Hebenstreit. “Schwinger effect in inhomogeneous electric fields.” PhD thesis. 2011.
- [Hei26] Werner Heisenberg. “Mehrkörperproblem und Resonanz in der Quantenmechanik.” In: *Zeitschrift für Physik* 38.6-7 (June 1926), pp. 411–426.
- [Hei25] Werner Heisenberg. “Über quantentheoretische Umdeutung kinematischer und mechanischer Beziehungen.” In: *Zeitschrift für Physik* 33.1 (1925), pp. 879–893.
- [HE36] Werner Heisenberg and Hans Euler. “Folgerungen aus der Diracschen Theorie des Positrons.” In: *Zeitschrift für Physik* 98.11-12 (Nov. 1936), pp. 714–732.
- [HJ26] Werner Heisenberg and Pascual Jordan. “Anwendung der Quantenmechanik auf das Problem der anomalen Zeemaneffekte.” In: *Zeitschrift für Physik* 37.4-5 (Apr. 1926), pp. 263–277.
- [Hun41] Friedrich Hund. “Materieerzeugung im anschaulichen und im gequantelten Wellenbild der Materie.” In: *Zeitschrift für Physik* 117.1-2 (1941), pp. 1–17.
- [Jor27] Pascual Jordan. “Über eine neue Begründung der Quantenmechanik.” In: *Zeitschrift für Physik* 40.11-12 (Nov. 1927), pp. 809–838.
- [Kel65] Leonid V. Keldysh. “Ionization in the field of a strong electromagnetic wave.” In: *Journal of Experimental and Theoretical Physics* 20 (1965), pp. 1307–1314.

- [KM03] Klaus Kirsten and Alan J. McKane. “Functional determinants by contour integration methods.” In: *Annals of Physics* 308.2 (2003), pp. 502–527.
- [KM04] Klaus Kirsten and Alan J. McKane. “Functional determinants for general Sturm-Liouville problems.” In: *Journal of Physics A* 4649 (2004), p. 28.
- [Kle29] Oskar Klein. “Die Reflexion von Elektronen an einem Potential-sprung nach der relativistischen Dynamik von Dirac.” In: *Zeitschrift für Physik* 53 (1929).
- [Kle27] Oskar Klein. “Elektrodynamik und Wellenmechanik vom Standpunkt des Korrespondenzprinzips.” In: *Zeitschrift für Physik* 41.10 (1927), pp. 407–442.
- [Kle09] Hagen Kleinert. *Path Integrals in Quantum Mechanics, Statistics, Polymer Physics, and Financial Markets*. EBL-Schweitzer. World Scientific, 2009.
- [Koh+13] Christian Kohlfürst, Mario Mitter, Gregory Von Winckel, Florian Hebenstreit, and Reinhard Alkofer. “Optimizing the pulse shape for Schwinger pair production.” In: *Physical Review D* 88.4 (2013), pp. 1–10.
- [Lan21] Alfred Landé. “Über den anomalen Zeemaneffekt (Teil I).” In: *Zeitschrift für Physik* 5.4 (July 1921), pp. 231–241.
- [Lin+15] Malte F. Linder, Christian Schneider, Joachim Sicking, Nikodem Szpak, and Ralf Schützhold. “Pulse shape dependence in the dynamically assisted Sauter-Schwinger effect.” In: *Physical Review D* 92 (Oct. 2015), p. 085009.
- [Lor09] Hendrik Antoon Lorentz. *The Theory of Electrons and Its Applications to the Phenomena of Light and Radiant Heat: A Course of Lectures Delivered in Columbia University, New York, in March and April, 1906*. Vol. 29. Columbia University Press, 1909.
- [Nam50] Yoichirō Nambu. “The Use of the Proper Time in Quantum Electrodynamics I.” In: *Progress of Theoretical Physics* 5.1 (1950), pp. 82–94.
- [Noe18] Emmy Noether. “Invariante Variationsprobleme.” In: *Nachrichten von der Gesellschaft der Wissenschaften zu Göttingen, Mathematisch-Physikalische Klasse* (1918), pp. 235–257.
- [Olv+10] Frank W. J. Olver, Daniel W. Lozier, Ronald F. Boisvert, and Charles W. Clark. *NIST Handbook of Mathematical Functions*. Cambridge University Press, 2010.
- [OHA11] Markus Orthaber, Florian Hebenstreit, and Reinhard Alkofer. “Momentum spectra for dynamically assisted Schwinger pair production.” In: *Physics Letters B* 698.1 (Mar. 2011), pp. 80–85.
- [Pau26] Wolfgang Pauli. “Über das Wasserstoffspektrum vom Standpunkt der neuen Quantenmechanik.” In: *Zeitschrift für Physik* 36.5 (1926), pp. 336–363.

- [Pau25] Wolfgang Pauli. “Über den Zusammenhang des Abschlusses der Elektronengruppen im Atom mit der Komplexstruktur der Spektren.” In: *Zeitschrift für Physik* 31.1 (1925), pp. 765–783.
- [Pau27] Wolfgang Pauli. “Zur Quantenmechanik des magnetischen Elektrons.” In: *Zeitschrift für Physik* 43 (1927).
- [PS95] Michael E. Peskin and Daniel V. Schroeder. *An Introduction to Quantum Field Theory*. 1995.
- [Pla00a] Max Planck. “Über irreversible Strahlungsvorgänge.” In: *Annalen der Physik* 306.1 (1900), pp. 69–122.
- [Pla00b] Max Planck. “Zur Theorie des Gesetzes der Energieverteilung im Normalspectrum.” In: *Verhandlungen der Deutschen Physikalischen Gesellschaft* 2.17 (1900), p. 237.
- [Pol77] Aleksandr M. Polyakov. “Quark confinement and topology of gauge theories.” In: *Nuclear Physics B* 120.3 (1977), pp. 429–458.
- [RF95] Silvio J. Rabello and Carlos Farina. “Gauge invariance and the path integral.” In: *Physical Review A* 51.3 (Mar. 1995), pp. 2614–2615.
- [Rie59] Bernhard Riemann. “Über die Anzahl der Primzahlen unter einer gegebenen Größe.” In: *Monatsberichte der Königlich Preussischen Akademie der Wissenschaften zu Berlin* (1859), pp. 671–680.
- [Sak94] Jun John Sakurai. *Modern quantum mechanics; rev. ed.* Reading, MA: Addison-Wesley, 1994.
- [Sau31] Fritz Sauter. “Über das Verhalten eines Elektrons im homogenen elektrischen Feld nach der relativistischen Theorie Diracs.” In: *Zeitschrift für Physik* 69.11-12 (1931), pp. 742–764.
- [Sau32] Fritz Sauter. “Zum Kleinschen Paradoxon.” In: *Zeitschrift für Physik* 73 (1932), pp. 547–552.
- [Sch+98] Sebastian Schmidt et al. “A Quantum Kinetic Equation for Particle Production in the Schwinger Mechanism.” In: *International Journal of Modern Physics E* 07.06 (1998), pp. 709–722.
- [SS16a] Christian Schneider and Ralf Schützhold. “Dynamically assisted Sauter-Schwinger effect in inhomogeneous electric fields.” In: *Journal of High Energy Physics* 2016.2 (2016).
- [SS16b] Christian Schneider and Ralf Schützhold. “Prefactor in the dynamically assisted Sauter-Schwinger effect.” In: *Phys. Rev. D* 94 (Oct. 2016), p. 085015.
- [STS19] Christian Schneider, Greger Torgrimsson, and Ralf Schützhold. “Discrete worldline instantons.” In: *Physical Review D* 98 (2019), p. 085009.
- [Sch26a] Erwin Schrödinger. “Quantisierung als Eigenwertproblem I.” In: *Annalen der Physik* 384.4 (1926), pp. 361–376.
- [Sch26b] Erwin Schrödinger. “Quantisierung als Eigenwertproblem II.” In: *Annalen der Physik* 384.6 (1926), pp. 489–527.

- [Sch26c] Erwin Schrödinger. “Quantisierung als Eigenwertproblem IV.” In: *Annalen der Physik* 386.18 (1926), pp. 109–139.
- [Sch26d] Erwin Schrödinger. “Über das Verhältnis der Heisenberg-Born-Jordanschen Quantenmechanik zu der meinen.” In: *Annalen der Physik* 384.8 (1926), pp. 734–756.
- [Sch01] Christian Schubert. “Perturbative quantum field theory in the string-inspired formalism.” In: *Physics Reports* 355.2 (2001), pp. 73–234.
- [SGD08] Ralf Schützhold, Holger Gies, and Gerald V. Dunne. “Dynamically assisted Schwinger mechanism.” In: *Physical Review Letters* 101 (2008), pp. 4–7.
- [Sch51] Julian Schwinger. “On Gauge Invariance and Vacuum Polarization.” In: *Physical Review* 82.5 (June 1951), pp. 664–679.
- [Shi80] Michael A. Shifman. “Wilson loop in vacuum fields.” In: *Nuclear Physics B* 173.1 (Oct. 1980), pp. 13–31.
- [Som16] Arnold Sommerfeld. “Zur Quantentheorie.” In: *Annalen der Physik* 51 (1916), pp. 1–94.
- [Ste21] Otto Stern. “Ein Weg zur experimentellen Prüfung der Richtungsquantelung im Magnetfeld.” In: *Zeitschrift für Physik* 7 (1921), pp. 249–253.
- [t H76] Gerard 't Hooft. “Symmetry Breaking through Bell-Jackiw Anomalies.” In: *Physical Review Letters* 37.1 (July 1976), pp. 8–11.
- [Tor+17] Greger Torgrimsson, Christian Schneider, Johannes Oertel, and Ralf Schützhold. “Dynamically assisted Sauter-Schwinger effect — non-perturbative versus perturbative aspects.” In: *Journal of High Energy Physics* 2017.6 (2017).
- [TSS18] Greger Torgrimsson, Christian Schneider, and Ralf Schützhold. “Sauter-Schwinger pair creation dynamically assisted by a plane wave.” In: *Physical Review D* 97 (2018), p. 096004.
- [UG25] George E. Uhlenbeck and Samuel Goudsmit. “Ersetzung der Hypothese vom unmechanischen Zwang durch eine Forderung bezüglich des inneren Verhaltens jedes einzelnen Elektrons.” In: *Die Naturwissenschaften* 13.47 (Nov. 1925), pp. 953–954.
- [UG26] George E. Uhlenbeck and Samuel Goudsmit. “Spinning Electrons and the Structure of Spectra.” In: *Nature* 117.2938 (Feb. 1926), pp. 264–265.
- [YM54] Chen N. Yang and Robert L. Mills. “Conservation of Isotopic Spin and Isotopic Gauge Invariance.” In: *Physical Review* 96.1 (Oct. 1954), pp. 191–195.
- [Zee10] Anthony Zee. *Quantum Field Theory in a Nutshell*. In a Nutshell. Princeton University Press, 2010.
- [Zee97] Pieter Zeeman. “On the influence of magnetism on the nature of the light emitted by a substance.” In: *The London, Edinburgh, and Dublin Philosophical Magazine and Journal of Science* 43.262 (1897), pp. 226–239.







# DuEPublico

Duisburg-Essen Publications online

UNIVERSITÄT  
DUISBURG  
ESSEN

*Offen im Denken*

ub

universitäts  
bibliothek

Diese Dissertation wird über DuEPublico, dem Dokumenten- und Publikationsserver der Universität Duisburg-Essen, zur Verfügung gestellt und liegt auch als Print-Version vor.

**DOI:** 10.17185/duepublico/70116

**URN:** urn:nbn:de:hbz:464-20190520-115145-2

Alle Rechte vorbehalten.